

© 2019 Seyed Saleh Yousefi

MODEL DEVELOPMENT AND VALIDATION OF BITUMINOUS-BASED CRACK
SEALANTS

BY

SEYED SALEH YOUSEFI

DISSERTATION

Submitted in partial fulfillment of the requirements
for the degree of Doctor of Philosophy in Civil Engineering
in the Graduate College of the
University of Illinois at Urbana-Champaign, 2019

Urbana, Illinois

Doctoral Committee:

Professor Imad Al-Qadi, Chair
Professor Marshall Thompson
Professor Erol Tutumluer
Research Assistant Professor Hasan Ozer
Senior Research Engineer Dr. B.K. Sharma

ABSTRACT

A wide spectrum of sealant types commonly used in the United States were installed in eight different test sites using two types of sealing treatment techniques. The performance of sealants was monitored after each winter for three years to determine a performance index (PI) consisting primarily of adhesive, cohesive, and overband wear. Field samples were collected from the sites to conduct laboratory testing and validate the sealant grading system. According to the field results, most sealants failed below a PI threshold of 70% after three years. In general, rout and seal sections performed better than the clean and seal sections. Field performance results highlighted the importance of test site selection, especially for clean and seal application.

Statistical correlations of tests parameters with the field performance were performed. A composite score approach, combining ranking and correlation, was used to develop a quantitative scale for determining the level of acceptance. Based on the composite score, a strong or acceptable correlation was obtained between field performance and laboratory test parameters for field test sites. After confirming the correlation between field performance and lab results, the thresholds for test method were selected or fine-tuned.

In addition to test methods validation, an investigation was also conducted to evaluate the short-term and long-term aging effects of hot-poured crack sealants through a differential aging test. Rheological and mechanical properties of sealants at different aging stages were monitored to characterize the aging effects. Laboratory aging of sealants was studied using three different aging methods: Kettle aging, melter aging, and vacuum oven aging (VOA). The aging index was used to evaluate the effect of these aging methods. Comparing the stiffness master curves obtained from the crack sealant bending beam rheometer (CSBBR) test for field-aged samples and laboratory-aged samples, VOA was validated as a reasonable aging method for simulating two-five years of field aging.

Finally, sealant rheological, mechanical and chemical properties were analyzed, implementing different performance-based tests and FTIR test to characterize sealants aging. A set of eight types of crack sealants was exposed to approximately four years of weathering conditions. Aging mechanisms were investigated by comparing the critical properties with those obtained at the time of installation inside a small kettle. Samples were collected every six months after installation for laboratory characterization. Laboratory characterization includes low temperature

stiffness, high temperature modulus, viscosity, and FTIR spectrum. According to the results of the experimental program, a consistent increase was observed in the low temperature stiffness and high temperature shear modulus of crack sealants due to weathering. The study showed that the low- and high-temperature properties of surface portion are significantly influenced by weathering effects even within a short period of life time. A superposition rule analogous to time-temperature superposition for viscoelastic materials was applied to develop master curves. A phenomenological aging model was developed as a function of aging time. Based on their aging potential, sealants were categorized into three groups at low and high temperatures with increasing aging potential: Type A, Type B, and Type C. FTIR analysis showed that rate of carbonyl index was significantly higher at the crust of crack sealants. On the other hand, the bottom part of field-aged crack sealants exhibited a higher sulfoxide index.

ACKNOWLEDGMENTS

I would like to thank Professor Al-Qadi, my supervisor and committee chair, for all his support, time and encouragement throughout the entire duration of this study. His guidance and professional style will remain with me as I continue my career.

I would like to thank my committee members: Professor Thompson, Professor Tutumluer, Dr. Sharma and Dr. Ozer for their valuable time and advices to this study.

I would like to express my special gratitude to Dr. Ozer for all his help, collaboration and friendship along this journey.

I would like to thank past and current research engineers at Illinois Center for Transportation: Jim Meister, Aaron Coenen, James Pforr, and Greg Renshaw for all their help and assistance in field and laboratory works.

I am also grateful to my industrial and state collaborators. This research is sponsored by the pooled-fund study TPF5 (225).

Friendship, support and encouragement from research team members and Prof. Al-Qadi's research group were the joy of this research and are highly appreciated.

Finally, I would like to express my deepest gratitude to my parents for their unconditional love and endless support all along. This dissertation would not have been possible without them.

Thanks Allah "who taught human what they did not know".

Dedication

To My Mother

TABLE OF CONTENTS

CHAPTER 1. INTRODUCTION	1
CHAPTER 2. BACKGROUND	6
CHAPTER 3. METHODOLOGY AND MATERIALS	18
CHAPTER 4. FIELD INSTALLATION AND PERFORMANCE.....	29
CHAPTER 5. RHEOLOGICAL CHARACTERISTICS AND VALIDATION OF TEST METHODS.....	108
CHAPTER 6. FIELD AND LABORATORY AGING OF CRACK SEALANTS	156
CHAPTER 7. SUMMARY, CONCLUSIONS, FINDINGS, AND RECOMMENDATIONS..	190
REFERENCES	197
APPENDIX A. TEST SITES TEMPERATURE VARIATION	205
APPENDIX B. DAILY LOW TEMPERATURE VARIATION	209
APPENDIX C. CRACK DISPLACEMENT AND SPACING	213
APPENDIX D. CRACK DISPLACEMENT AND COHESIVE FAILURE	214
APPENDIX E. CSBR STIFFNESS AND ACR AT 240S AT DIFFERENT AGING CONDITIONS	219
APPENDIX F. CSBBR STIFFNESS MASTER CURVES	223
APPENDIX G. CSBBR STIFFNESS AND ACR VARIATION WITH AGING TIME.....	227
APPENDIX H. CSBBR STIFFNESS CHANGING WITH THE SEALANT DEPTH	229

CHAPTER 1. INTRODUCTION

Crack sealing is widely accepted as a cost-effective, routine, and preventive maintenance practice that extends the service life of pavement life three to five years when properly installed (Chong and Phang, 1987). ASTM Standard D5535 defines crack sealant as a material that, possessing adhesive and cohesive properties, forms a seal to prevent liquid and solid materials from penetrating into the pavement system.

The selection of a proper crack sealant for a particular environment and pavement is essential to guarantee its performance. The standards and specifications currently used to select crack sealants were established based on material properties that are generally empirical and do not reflect the fundamental properties of sealants. Most state highway agencies have used these tests to select crack sealing materials; however, specification limits vary from one state to another. These differences create difficulties for crack sealant suppliers because several states with the same environmental conditions specify different limits for the measured properties. These standard tests are also reported to poorly characterize the rheological properties of bituminous-based crack sealants and often fail to predict sealant performance in the field.

Several researchers have observed poor correlation between laboratory test results and field performance (Masson, 2000; Belangie and Anderson, 1985; Masson and Lacasse, 1999; Smith and Romine, 1999; Al-Qadi et al., 2009). In addition, over the past two decades, a new generation of highly modified crack sealants has been introduced to the market. These sealants exhibit complex behavior compared with the behavior of traditional sealant materials (Belangie and Anderson, 1985). Hence, the need for a new set of specifications.

Recently, performance-based guidelines were developed as a systematic procedure to select hot-poured bituminous crack sealants (Al-Qadi et al, 2009). These guidelines are the outcome of the pooled-fund North American Consortium led by the University of Illinois at Urbana-Champaign and the National Research Council of Canada. The sponsoring consortium included 11 U.S. state departments of transportation, 13 Canadian transportation agencies, and industry. The U.S. contribution was made through pooled-fund research project TPF-5(045), led by the Virginia Department of Transportation (VDOT)/ Virginia Transportation Research Council (VTRC). The work proposed a “Sealant Grade” (SG) system to select hot-poured crack sealant based on environmental conditions. A special effort was made to use the equipment originally developed

by the Strategic Highway Research Program (SHRP), which was used to measure binder rheological behavior as part of the binder Performance Grade (PG) system. The equipment, specimen preparation, and testing procedure were modified in accordance with crack sealant behavior. In addition, new tests for sealant aging and sealant evaluation were introduced. The developed laboratory tests allow for measuring hot-poured asphalt crack sealants rheological and mechanical properties over a wide range of service temperatures. Preliminary thresholds for each test were identified to ensure desirable field performance. Then, the preliminary thresholds were used in the SG system based on extensive laboratory testing, limited between-laboratory testing, and limited field validation.

1.1 Problem statement

Laboratory tests were developed to measure hot-poured bituminous-based crack sealants rheological and mechanical properties over a wide range of service temperatures (Al-Qadi et. al. 2009). Preliminary thresholds for each test were identified to ensure desirable field performance. According to the SG system, for example, SG 52-34 suggests that the sealant can be used at a high-service temperature of 52°C and a low-service temperature of -34°C. The high temperature for a specific site is obtained by averaging the seven-day maximum pavement temperature (°C), and the low temperature comes from the minimum pavement design temperature likely to be experienced (°C). Hence, using the developed laboratory tests, a proper crack sealant can be selected systematically based on the expected service temperature.

The Preliminary thresholds utilized in the SG system are based on extensive laboratory testing and limited field performance data—mainly from Canada. Therefore, a field study was needed to validate and fine-tune the present threshold values. Furthermore, the developed guidelines should be validated in several states under various climate zones.

In addition, the mechanical properties of sealants can be significantly altered by heating during installation and by weathering during the sealants service life. Different sealant types have different aging pathways. Oxidation and the loss of oils may affect the binder phase; whereas, cross-linking, degradation, and oxidation define the aging pathway for the polymer phase. It may be hypothesized that aging affects progress from the surface layer to the bottom of sealant treatment, which creates a gradation in sealants properties. Therefore, the crust layer of the

sample represents true aging effects where most types of failures, such as adhesive failure, are triggered and then propagate to full depth.

The chemical composition has a direct effect on sealants performance because it affects their free surface energy, glassy temperature, and viscoelastic properties. Various sealants exhibit unique aging characteristics even though they fall into the same ASTM or AASHTO classification categories. The effects of field aging on the mechanical and rheological properties of sealants may be better understood through chemical and mechanical characterizations of various types of sealants.

1.2 Objectives

An extensive field study is designed to validate and fine-tune the threshold values proposed in the crack sealant test development study by Al-Qadi et. al. (2009). The scope of this study includes installation of test sites, evaluation of the sealant field performance, and correlation to laboratory performance. The research aim was to chemically and mechanically characterize field aging of crack sealants and to develop practical, simple test procedures for intermediate and high temperature grading of hot-poured crack sealants. Ultimately, this study aimed to achieve the following goals:

- Validate developed laboratory tests through field-measured performance;
- Determine test thresholds using a diverse array of field performance data;
- Characterize the mechanical properties of aged crack sealant using the developed test methods; resulting parameters were used to develop a sealant phenomenological aging model; and
- Evaluate the aging effect on crack sealants chemical properties.

The aging model and coefficients provided for each category allowed prediction of changes in the properties of a sealant after its installation. This study captured the effects of aging for an extended time period (3-4 years). The scope of testing was expanded to various temperatures, but was limited to Central Illinois.

1.3 Scope

In this study, an extensive field study was designed to validate and fine-tune the threshold values. The scope of this study included installation of test sites, evaluation of field performance,

and correlation to laboratory performance. Finally, new guidelines were developed and validated for full implementation as AASHTO specifications.

To study aging, experimental tests were conducted at two different levels, rheological and chemical tests, for the purpose of testing the crust (the exposed portion of crack sealant to weathering and sunlight) and bottom of field-aged samples. Each test helps evaluate the fundamental properties of crack sealants and monitor their changes during aging. Aging indices were obtained for each property at each aging level for the crust and bottom portions of the field-aged samples.

This study is organized in seven chapters, starting with an introduction and a summary of performance-based specifications as follows:

- Chapter 1 – Introduction: A brief background of the problems, study objectives, and scope are introduced.
- Chapter 2 – Background: This chapter summarizes the current state of knowledge.
- Chapter 3 – Methodology and Material: This chapter introduces a brief summary of all tests used in this study and developed selection methods used for grading the sealants.
- Chapter 4 – Test Site Installation and Field Performance: This chapter summarizes the installation details and procedures for each test site. Also, the results of detailed annual field survey of crack sealants at each section were discussed.
- Chapter 5 – Rheological Characteristics and Validation of Test Methods: This chapter includes and summarizes the validation of the developed sealant laboratory tests using field performance data.
- Chapter 6 – Field and Laboratory Aging of Sealants: Results from different aging methods are presented in this chapter. Results on vacuum oven aged sealants were compared to those obtained on field aged crack sealants.
- Chapter 7 - Summary, Conclusions, and Recommendations: This chapter summaries the study and listed the findings and conclusions. In addition, recommendations for further studies are presented. .

Finally, additional results are presented in the appendixes.

1.4 Research Significance and Impact

The fewer the number of sealant applications, the more cost effective the sealing approach becomes and, conversely, the more frequent the number of sealant treatments, the greater the cost. A survey on pavement preventive maintenance programs from 18 transportation agencies in North America shows significant investments in these programs (Al-Qadi et al., 2009). Hence, if sealing cracks could prove to be a cost-effective technique, life-cycle savings could be realized. A study by Ponniah and Kennepohl (1996) concluded by monitoring pavement performance index that “sealing cracks is a viable and cost-effective preventive maintenance treatment and can extend the service life of asphalt pavements by at least 2 years.” A study by Sawalha et. al. (2018) showed that sealants with excellent performance (four years in service) need to extend the pavement life by at least 0.16 years to be a cost effective treatment. While this number increases to 0.34 years if the sealant service life was 2 years (fair performance). It was shown that even an incremental improvement in pavement life (less than 1 year) would be sufficient for sealing to be cost-effective. The adoption of the developed laboratory tests and new guidelines, validated through this study, and implementation of the new developed AASHTO specifications would results in significant improvement on the cost effectiveness of crack sealing and filling treatment for asphalt pavements. These tests and specification will help agencies to select the proper crack sealant for their crack treatments by lowering the application cost and saving money by extending the service life of asphalt pavements. As an example, the commonwealth of VDOT spends approximately \$20M/year on crack sealing (Al-Qadi et. al. 2009). If the sealant life is doubled, the savings by US transportation agencies would be in the hundreds of millions of dollars.

CHAPTER 2. BACKGROUND

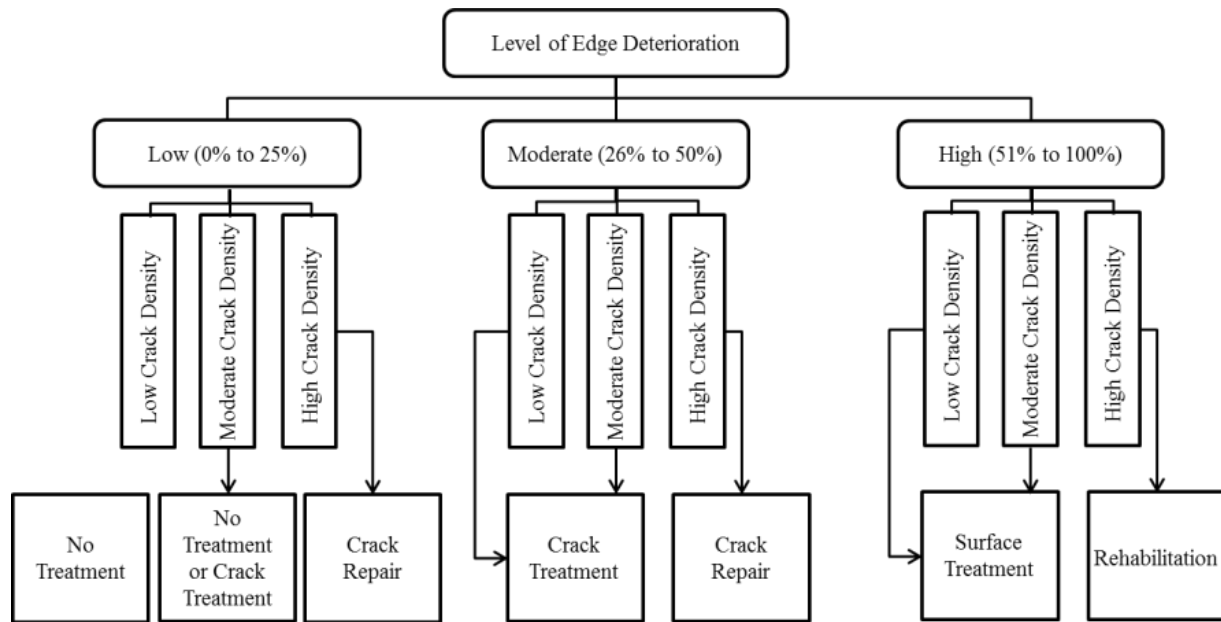
Hot-poured crack sealant maintains its shape as applied and hardens through chemical and/or physical processes to form a viscoelastic rubber-like material that withstands extension or compression (crack movement) and weathering (Al-Qadi et al., 2007). During its service life, crack sealant extends at low temperature and compresses at high temperature to accommodate pavement crack openings, which increase with falling temperature and decrease with rising temperature. At low-service temperature, the crack opening may increase from 10% to more than 90%, depending on the environmental location; hence, either cohesive failure inside the crack sealant or adhesive failure at the sealant–pavement crack wall occurs.

2.1 Crack Sealing Material

Crack sealants are elastomeric asphaltic composites. This type of material generally consists of asphalt binder, polymers, crumb rubber, and mineral filler. The purpose of including polymer modifiers is to increase the elasticity and melting point of sealants. Some of the essential properties of sealants, such as extendibility, cohesiveness, and adhesive properties, are needed to ensure good performance. Several types of hot-applied thermoplastic bituminous-based materials are available for crack sealing, including asphalt emulsion, asphalt cement, fiberized asphalt, polymer-modified emulsion, and rubberized asphalt.

2.2 Crack Sealing

Crack treatment strategies are selected based on crack density and the average level of crack deterioration (percentage of crack length) as presented by the SHRP study (Smith and Romine 1999). Figure 2.1 presents various maintenance strategies adopted by the SHRP study based on the average level of edge deterioration, which consists of spalls and secondary cracking. According to that study, crack sealing is recommended for cracks that have less than 50% edge deterioration.



*Low Crack Density: Linear crack length per 100m pavement section to be less than 10m

*Moderate Crack Density: Linear crack length per 100m pavement section to be from 10 to 135m

*High Crack Density: Linear crack length per 100m pavement section to be more than 135m

Figure 2.1. Guidelines to select the type of maintenance (after Smith and Romine, 1999).

Crack sealant treatment is suitable for pavements with transverse and longitudinal cracking and must be applied to cracks with little or no branching. Cracks shall not be a part of web cracks.

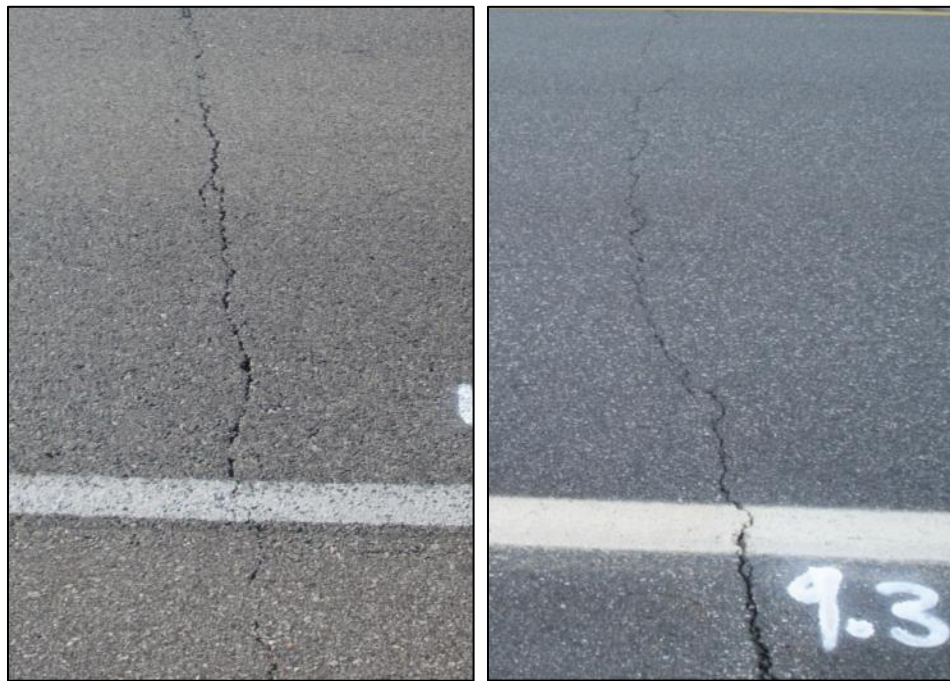
Crack sealant treatments are not recommended for cracks wider than 25mm. Figure 2.2 illustrates some examples of acceptable and unacceptable crack patterns. In addition, pavements exhibiting severe fatigue cracking are not recommended for crack sealing.

Once a decision is made to perform crack sealant treatment, two types of crack sealant treatment are available for selection, based on the initial condition of pavement and crack type. These treatment types are described below and are summarized in Table 2.1.

Crack Sealing: This method is defined as the application of hot-poured crack sealant in pre-routed and cleaned crack. The routing operation creates a rectangular reservoir (25mm x 20mm x 20mm) of sealant over the crack. This method is recommended for cracks exhibiting significant vertical and horizontal movements, often referred to as working cracks. The reservoir above the crack helps accommodating crack movement. Working cracks are defined as cracks with annual horizontal movement of more than 3mm. Transverse thermal cracks, transverse reflective cracks, longitudinal reflective cracks, and longitudinal cold-joint cracks are considered as working cracks



(a)



(b)

Figure 2.2. Various crack patterns usually considered in the selection of surface or crack treatments: (a) Cracks with severe branching and spalling, not recommended for crack sealing or filling; (b) Cracks with no branching and no spalling are appropriate for crack sealing or filling.

Crack Filling: This method is defined as the direct injection of hot-poured crack sealant in a cleaned crack. This method is recommended for non-working cracks. Non-working cracks are defined as cracks with annual horizontal movement of 3mm or less. Longitudinal reflective cracks, longitudinal cold-joint cracks, longitudinal edge cracks, and thermal or reflective transverse cracks with minimal movement are considered non-working cracks.

Table 2.1. Recommended Criteria for Treatment Selection (after Smith and Romine, 1999).

Crack Characteristics	Crack Treatment Activity	
	Crack Sealing	Crack Filling
Width, mm	5 to 19	5 to 25
Edge Deterioration (i.e., spalls, secondary cracks)	Minimal to None (≤ 25 percent of crack length)	Moderate to none (≤ 50 percent of crack length)
Annual Horizontal Movement, mm	≥ 3	< 3
Type of Crack	Transverse Thermal Transverse Reflective Longitudinal Reflective Longitudinal Cold-Joint	Longitudinal Reflective Longitudinal Cold-Joint Longitudinal Edge Distantly Spaced Block

Following the aforementioned procedures in preparation of cracks for sealant treatment, sealant is installed in the routs or directly in the cracks. The configuration for sealant installation will not only dictate the amount of materials used in a sealing job but also the lifetime of sealant treatment. The commonly applied configurations for sealant placement are shown in Figure 2.3 and Figure 2.4 and listed below:

- Flush fill
- Reservoir
- Overband
- Combination (reservoir and overband)

Several factors need to be considered for selection of sealant placement configuration. Based on the SHRP study (Smith and Romine, 1999) and field evaluations of the pooled fund study (TPF-5 (225) - *Validation of Hot-Poured Crack Sealant Performance-Based Guideline*), Table 2.2 is recommended to be used to select the placement configuration for sealant materials.

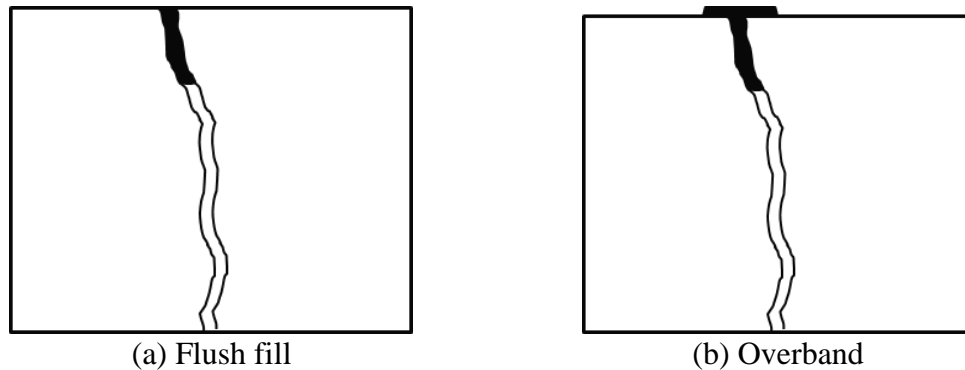


Figure 2.3. Crack filling common configurations

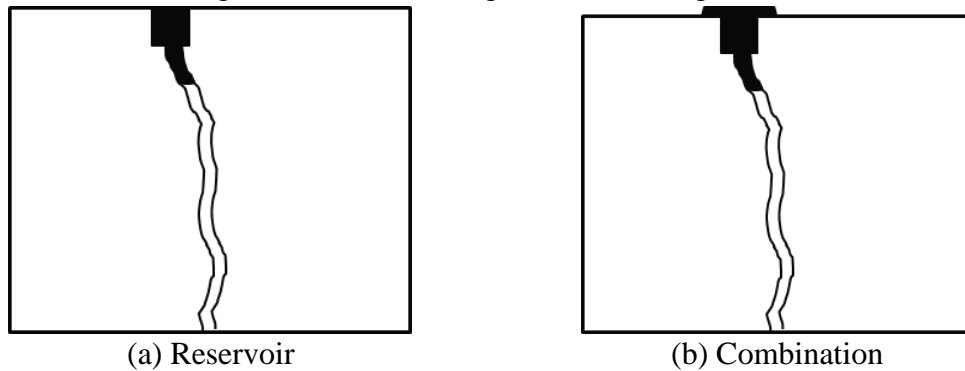


Figure 2.4. Crack sealing common configurations

Table 2.2. Considerations for Sealant Placement Configuration.

Consideration	Crack Filling	Crack Sealing
Type and Extent of Operation	No crack cutting operation; hence, duration of operation can be shorter. Can be preferable when traffic closures are a concern.	Duration of operation is greater due to routing and cleaning. Requires more traffic closure time.
Traffic	Overband wear is similar to crack seal configurations; however, the impact on sealant in the crack is less severe.	Overband configurations experience wear and, subsequently, high tensile stresses directly above the crack edge, leading to internal rupture.
Crack Characteristics	Overband configurations are more appropriate for cracks having a considerable amount of edge deterioration (>10% of crack length), because the overband simultaneously fills and covers the deterioration segments in the same pass.	
Material Type	Material such as emulsion, asphalt cement, and silicone must be placed unexposed to traffic due to serious tracking or abrasion problems.	
Desired Performance	For long-term sealant performance, flush, reservoir, and recessed band-aid configurations should be considered.	
Cost	Filling configurations require less material than reservoir configurations, resulting in lower costs.	Combination configurations require significantly more material than reservoir configurations, resulting in higher costs.

2.3 Crack Sealant Performance

The primary modes of failure for sealants vary depending on application and climatic conditions (Figure 2.5). A general classification of sealant failures as related to sealants properties are described as follows:

- Premature failure of crack sealants occurs when the viscosity of the sealant is either too high or too low during sealant installation. Highly viscous crack sealant might not fill the cracks properly causing incomplete bonding, while low viscous crack sealant might flow out of the cracks leading to improper installation.
- During its service life, crack sealant extends at low temperature and compresses at high temperature to accommodate pavement crack openings which increase with falling temperature and decrease with rising temperature.
- The third type of failure is associated with sealants resistance to pull-out and wear. Sealant pull-out occurs when a vehicle passes and pulls the sealant out from a crack because the sealant is not properly set or not viscous enough to resist vehicle movements at high temperatures. Sealant wear develops with every pass of vehicles at intermediate to high temperatures and as a result of snow plowing in winter. Prematurely worn sealants are exposed to weathering which accelerates debonding at the crack walls.

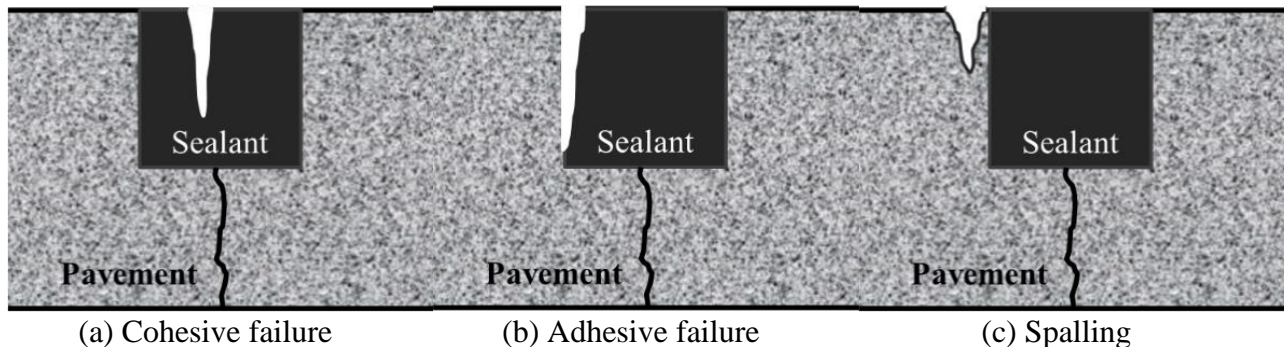


Figure 2.5. Primary modes of failure for sealants during field performance.

2.4 Test Specification for Hot-poured Crack Sealants

A summary of hot-applied thermoplastic materials available for crack sealing and filling is listed in Table 2.3. Currently, most agencies prefer to follow ASTM standards for material selection. Most agencies and industries use ASTM Standard D5329 (Standard Test Methods for Sealants and Fillers, Hot-Applied, for Joints and Cracks in Asphaltic and Portland Cement Concrete

Pavements) for material characterization and selection. Tests included in this specification are the following:

- Cone penetration
- Softening point
- Flow test
- Non-immersed bond test
- Water-immersed bond test
- Resilience test
- Oven-aged resilience test
- Asphalt compatibility test
- Artificial weathering test
- Tensile adhesion test, and
- Flexibility test.

Table 2.3. Summary of Asphalt Concrete Crack Treatment Materials.

Material Type	Application Specification	Recommended Application
Asphalt Emulsion	ASTM D 977, AASHTO M 140, ASTM D 2397, AASHTO M 208	Filling
Asphalt Cement	ASTM D 3381, AASHTO M 20, AASHTO M 226	Filling
Fiberized Asphalt	Manufacturer's recommended specification	Filling
Polymer-Modified Emulsion	ASTM D 977, AASHTO M 140, ASTM D 2397, AASHTO M 208	Filling (possibly sealing)
Asphalt Rubber	State specifications, ASTM D 5078	Sealing (possibly filling)
Rubberized Modified Asphalt	ASTM D 6690	Sealing
Low Modulus Rubberized Asphalt	State-modified ASTM D 6690 specifications	Sealing

According to ASTM standard D6690, crack sealants can be categorized in four groups: Types I through IV. ASTM classifications are related to penetration resistance, softening point, bonding strength, and asphalt compatibility. Agencies often make a decision on material choice based on the modulus characteristics of sealants. Low modulus sealants (likely to be ASTM Type II to IV) are often preferred in wet-freeze zones; whereas, high modulus products (likely to be ASTM

Type I to II) are preferred for dry no-freeze climatic regions. The recommended application for each sealant type is noted in Table 2.3. Generally, crack filling requires selection of a product with slightly higher modulus for the same climatic region.

However, these standard tests were reported to poorly characterize the rheological properties of bituminous-based crack sealants and often fail to predict sealant performance in the field (Masson, 2000; Belangie and Anderson, 1985; Masson and Lacasse, 1999; Smith and Romine, 1999; Al-Qadi et al., 2009). Performance-based tests and specifications have been introduced for asphalt materials to assist with the selection of appropriate materials for a given pavement section. For example, Superpave binder specifications are performance-based specifications introduced in 1990s. The tests make use of asphalt binder fundamental rheological concepts. The use of performance-based tests for sealant selection for different applications under various climatic conditions would improve consistency. Even though failure modes of sealants and performance expectations differ from those of asphalt binders, similar ideas and concepts could be adapted.

As part of a pooled-fund study conducted between 2003 and 2009 with participation from 11 state departments of transportation and industry, a series of sealant tests were developed based on the performance of sealants widely used in North America (Al-Qadi et. al. 2009). The newly developed sealant tests (Figure 2.6) predict fundamental sealant properties related to field failure mechanisms, including the apparent viscosity test at recommended installation temperature; vacuum oven aging procedure for simulating sealant aging in the field; dynamic shear rheometer (DSR) test for the assessment of sealants tracking resistance at high service temperatures; crack sealant bending beam rheometer (CSBBR) test to evaluate sealants creep properties at low temperature; crack sealant direct tension test (CSDTT) to characterize sealant's low-temperature extendibility; and low-temperature adhesive (surface energy, direct adhesion, and blister) tests to evaluate the bonding between sealants and their substrate. Performance parameters for the aforementioned tests were developed based on extensive laboratory testing and limited field performance data. The developed tests were practical, repeatable, and reproducible. The developed standards are as follows:

- AASHTO MP 25, Performance-Graded Hot-Poured Asphalt Crack Sealant
- AASHTO PP 85, Grading or Verifying the Sealant Grade (SG) of a Hot-Poured Asphalt Crack Sealants
- AASHTO T 366, Apparent Viscosity of Hot-Poured Asphalt Crack Sealant Using Rotational Viscometer
- AASHTO T 367, Accelerated Aging of Hot-Poured Asphalt Crack Sealants Using a Vacuum Oven
- AASHTO T 368, Measure Low-Temperature Flexural Creep Stiffness of Hot-Poured Asphalt Crack Sealants by BBR
- AASHTO T 369, Evaluation of the Low-Temperature Tensile Property of Hot-Poured Asphalt Crack Sealants by Direct Tension Test
- AASHTO T 370, Measuring Adhesion of Hot-Poured Asphalt Crack Sealant Using Direct Adhesion Tester
- AASHTO T 371, Measuring Interfacial Fracture Energy of Hot-Poured Crack Sealant Using a Blister Test
- AASHTO TP 126, Evaluation of the Tracking Resistance of Hot-Poured Asphalt Crack Sealants by Dynamic Shear Rheometer (DSR)

The aforementioned laboratory tests allow for measuring hot-poured bituminous-based crack sealants rheological and mechanical properties over a wide range of service temperatures.

Thresholds for each test were identified to ensure desirable field performance. For example, Sealant Grade (SG) 52-34 suggests that sealant can be used at a high service temperature of 52°C and a low-service temperature of -34°C. Hence, using the developed laboratory tests, a proper crack sealant can be selected systematically based on expected service temperature. Figure 2.7 shows different zones for the pavement low temperature in North America that may be used to select the proper sealant based on its SG.

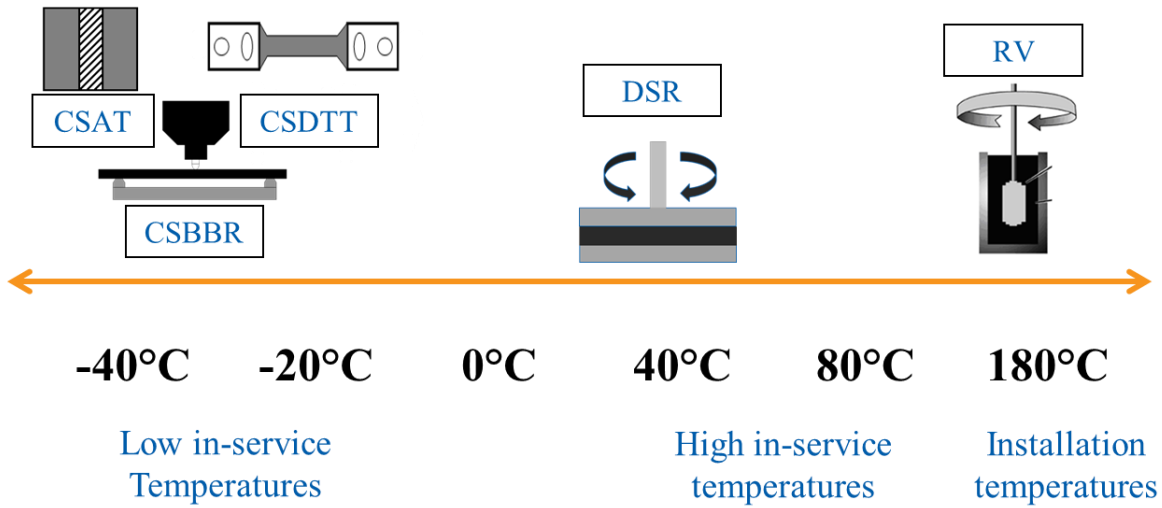


Figure 2.6. Schematics of developed AASHTO tests for crack sealant selection and spectrum of their performance temperature.

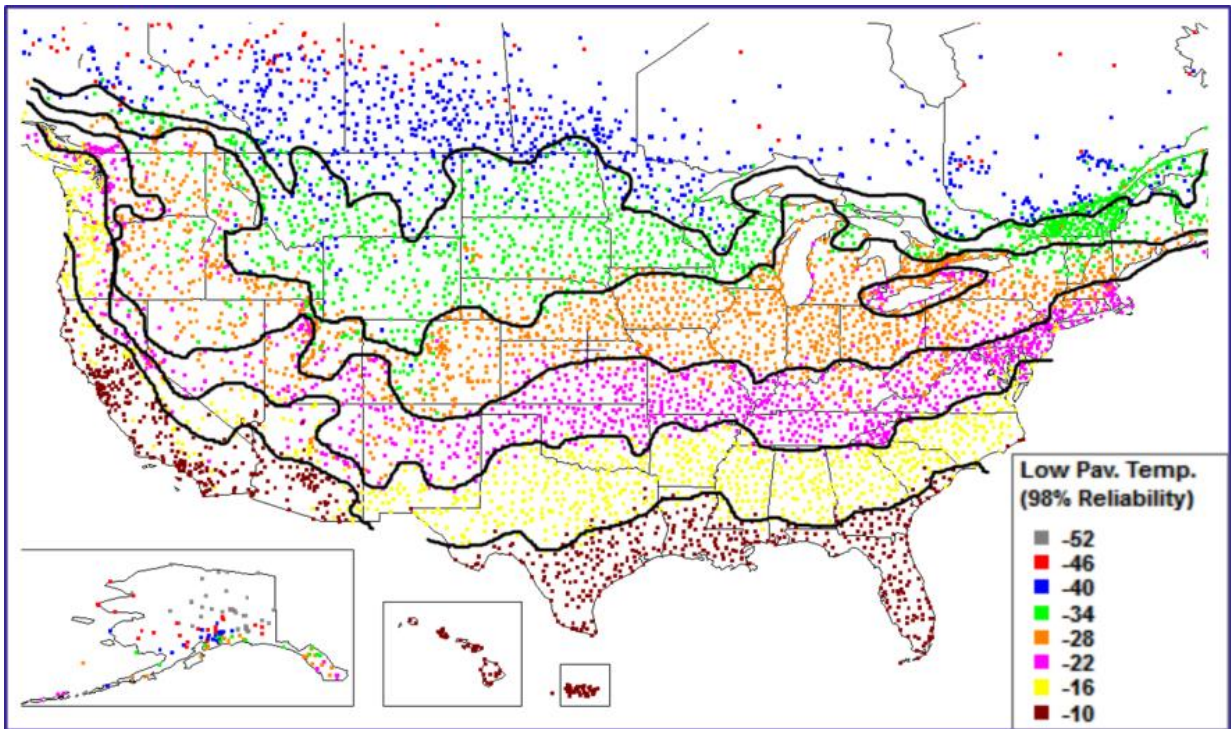


Figure 2.7. North America low pavement temperature zones (according to LTPP Bind V3.1).

2.5 Aging Mechanisms of Crack Sealants

Potential aging pathways for sealants differ for each component of the sealant. Oxidation and loss of oils affect the binder phase whereas cross-linking, degradation, and oxidation characterize polymeric phase aging. Installation activities, weathering, and trafficking during the service life

of sealants can significantly alter the sealant physical and chemical properties by triggering a combination of these aging mechanisms. Masson, et al. (2007) studied the short-term aging of crack sealants and found that sealant aging is divided into two categories: short-term aging, which refers to aging during the installation process; and long-term aging, which reflects the changes in material properties as a result of weathering and loading. The study revealed that the materials in effect change when heated for long periods of time. These changes include degradation of elastomers in the sealants, loss of volatile oils, and degradation of mechanical properties, which mostly occurs prior to sealant installation.

According to Masson et al. (2007), sealant aging is a physico-chemical process that modifies the structure of hot-poured crack sealants causing detrimental and irrecoverable effects on its fundamental properties. This process was described by Al-Qadi et al. (2003). The following four aging mechanisms have a significant impact on crack sealant performance:

- Fuming or loss of bitumen oils due to evaporation
- Gelling in the form of polymer cross-linking
- Breaking or polymer scission
- Oxidation

These mechanisms are triggered during installation of sealant, as a result of heating in a kettle at the recommended pouring temperature, and during service life of a sealant installed for crack treatment. In the former, kettle temperatures range from 160-200°C as recommended by sealant manufacturers. Sealants are heated in the kettle for five to eight hours in a typical installation procedure. Although all aforementioned four aging mechanisms might take place during the installation process, the loss of oils due to evaporation is considered the dominant mechanism in this phase. The second phase of aging occurs after installation, when sealants are subject to weathering, temperature variations, and traffic. These factors define the long-term aging phase and influence the physical and chemical properties of sealants. Ultraviolet rays and high temperatures can degrade the structure of polymers, while temperature variations induce thermal stresses within the material. Oxidation of the bituminous component hardens the material, thus increasing the stiffness and reducing the elasticity of sealants.

There are several ways to identify the effects of the damage resulting from aging during installation (short-term) and during the service life (long-term) of crack sealants. One of the

commonly used methods is molecular weight or size measurements. The reduction in molecular mass due to scission decreases mechanical strength and increases brittleness. Al-Qadi et al. (2003) conducted gel permeation chromatography (GPC) and Fourier-transform infrared spectroscopy (FTIR) analysis to support this hypothesis. They found that weathering does not contribute significantly to polymer degradation. Conversely, it was observed that high carbon oxidation had a predominant effect on the chemical composition of sealants. Moreover, according to another study by Masson (2004), the degree of stiffening caused by aging is mainly dependent on the chemical composition of sealants.

Crack sealants undergo field aging as a result of weathering, oxidation, exposure to UV rays, and loading. Based on conclusions drawn from previous studies (Al-Qadi et al. 2003 and Masson et al. 2004 and 2006), the reasons mentioned above motivated a broad study of crack sealant aging mechanisms.

Next chapter illustrates the plans for a field testing program to evaluate the performance of crack sealant material. In addition, laboratory tests, including mechanical tests developed by Al-Qadi et al. (2009) and chemical tests are presented. The selection of a wide range of commercial crack sealants used in North America is discussed in the next chapter.

CHAPTER 3. METHODOLOGY AND MATERIALS

The performance-based guidelines developed for the selection of hot-poured crack sealants were validated and fine-tuned in this study. While the between-laboratory test variations had been successfully verified, test precision was examined, in this study, so the developed laboratory tests and new guidelines could be validated for full implementation as AASHTO specifications. Field performance of crack sealants was evaluated to fine-tune the preliminary thresholds. To meet the objectives of this study, the methodology shown in Figure 3.1 was implemented.

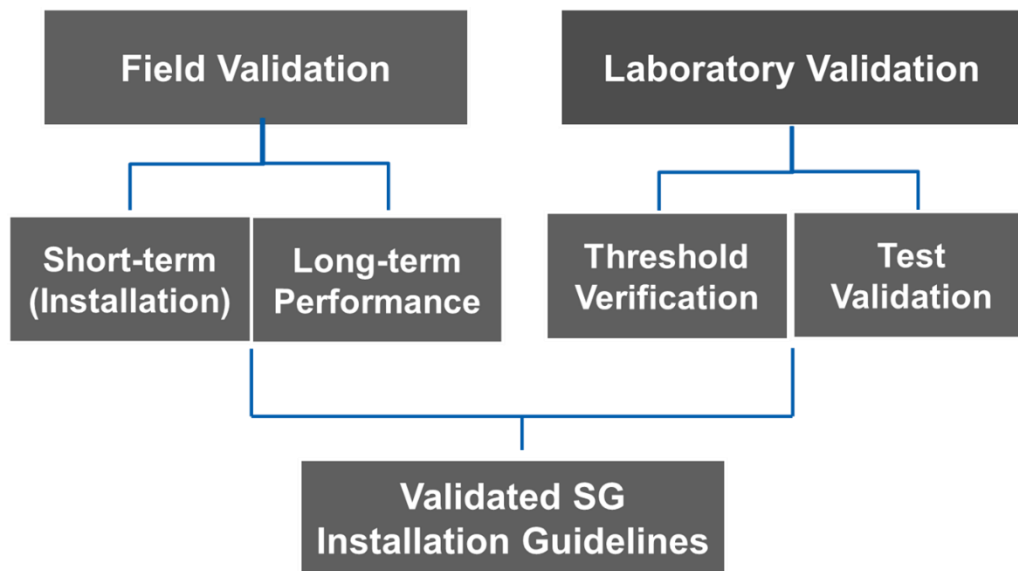


Figure 3.1. Experimental program used to validate and fine-tune provisional AASHTO test method for selection of hot-poured crack sealants.

Following the tests validation, the aging study combined experimental tests at two levels: Mechanical and rheological tests and a chemical test. These tests were used to examine the crust (the exposed portion of crack sealant to weathering and sunlight) and bottom of the field-aged samples. Each test helped evaluate a fundamental property of crack sealants and monitor their changes during aging. Therefore, an aging index was developed and used at each aging level for the crust and bottom portions of field-aged samples.

To characterize different types of crack sealants based on their chemical and mechanical properties, a laboratory experimental plan was developed. Details of the adopted laboratory experimental approach are discussed in this chapter.

3.1 Crack Sealant Materials

A list of products used in the field and lab experiments was determined based on the recommendations of the pooled-fund participants and the outcome of pool fund results (first phase). A wide spectrum of stiffness properties was targeted for field experiments to accomplish the study objectives. Table 3.1 shows the final list of materials selected for this study, including remarks about the reasoning for its selection. The laboratory performance of sealants, based on ASTM specifications, is also summarized in Table 3.2.

Sufficient quantities of the recommended products were requested from the manufacturers to ensure that materials from the same batch are used in different test sites. The products were stored at Advanced Transportation Research and Engineering Laboratory (ATREL) facilities. Pallets of each product were delivered to each test site 1-2 weeks prior to installation.

Table 3.1. Sealant Products with ASTM Type Used in the Study.

Product ID	ASTM Type	Remarks	
1	Ad	IV	Available performance data from SHRP H106 and used in previous study ¹
2	Bb	II	Same manufacturer product with different stiffness
3	Ca	I	Same manufacturer product with different stiffness
4	Da	I	SHRP Field Data and used in previous study ¹ and best performing in the field
5	Ed	IV	Suggested by MNDOT. Best performing product in Manitoba field study. Also used in Phase-I
6	Fb	II	SHRP field data available. Used in previous study ¹ . Best performing in the Manitoba field study
7	Gd	IV	Field data available (SHRP and others)
8	Hb	II	Added per MNDOT request
9	Ib	II	Same manufacturer product with different stiffness
10	Lb	II	Same manufacturer product with different stiffness
11	Jd	IV	Approved product by MNDOT and MIDOT
12	Kc	III	Used in previous study ¹ ; field data available
13	Mb	II	Suggested by MNDOT
14	Nb	II	Same manufacturer product with different stiffness
15	Ob	II	Used in previous study ¹ ; field data available (Manitoba)
16	Pd	IV	Same manufacturer product with different stiffness
17	Rb	II	Used in previous study ¹ ; field data available (Manitoba)
18	Sd	IV	A product commonly used in Ontario. ASTM designation close to Type IV

¹ Development of Performance-Based Guidelines for Selection Of Bituminous-Based Hot-Poured Pavement Crack Sealant: An Executive Summary Report. Al-Qadi et. al. (2009)

Table 3.2. List of Sealants Based on their ASTM Performance Data Provided by Manufacturers.

ID		ASTM Type	Lot #	Cone Penetration at 77°F (dmm)	Cone Penetration at 0°F (dmm)	Flow at 140°F (mm)	Resilience at 77°F (% recovery)	Ductility at 77°F (cm)	Bond at 0°F, 100% ext. passing cycles)	Bond at -20°F, 200% ext. (passing cycles)	Softening Point (°F)	Asphalt Compatibility	Flexibility at -13°F, 90 degree bend
1	Ad	IV											
2	Bb	II											
3	Ca	I											
4	Da	I	T2679	63		0	48	45	5				
5	Ed	IV	T9112	123	25	1	60			3		Pass	
6	Fb	II	T4407	71		2	46			3	181		Pass
7	Gd	IV	T2673	107			72			3	206	Pass	
8	Hb	II	T4398	70		0			5		204		
9	Ib	II	T3931	39	16					3	189		
10	Jd	IV	7HE106	110			70			3	181		
11	Kc	III	1HF032	70			64			3 (50%)	180		
12	Mb	II	1002402	78		0.3	66			3 (50%)	209	Pass	
13	Nb	II											
14	Ob	II	0018811	78			67			3 (100%)			
15	Pd	IV	0018847	135		0	56				185		
16	Sd	IV	Y1082	102		1	75				197		Pass

Eight different sealants were selected from various manufacturers spanning low and high modulus materials for the aging study. The list of materials used of raging study is presented in Table 3.3. The sealants were installed in a pavement section at the ATREL facilities. In order to observe the effects of pure aging caused by weathering, a pavement test section, free of working cracks and traffic loading, was selected for the installation of crack sealants in the field. The section was prepared by routing the pavement surface. A router machine was used to create 25x25mm reservoirs. Eight to 12 routs were created for each sealant product. Once the routs were done, they were cleaned with an air compressor and filled by the remaining sealant in the kettle.

Field-aged samples were collected from the sealed routs installed at a controlled pavement section without any traffic. Differential aging was evaluated throughout the depth of the weather-aged samples using the same experimental program. The field-aged samples were separated into field-aged crust (FAC) and field-aged bottom (FAB) layers to measure the effects of differential aging.

Sampling was conducted every six months after installation. Differential aging was investigated throughout the depth of the samples. Dissection of the sample into FAC (3mm – 5mm from surface) and FAB (remaining depth of material) layers would allow for measurement of changes in the properties of the material relative to crack depth. The results from different test methods were used to develop an aging model for crack sealants at various test levels based on aging potentials. This study captures the effects of aging for an extended time period (3-4 years).

Table 3.3. Crack Sealant Material Used in the Aging Study.

Sealant ID		ASTM Type
1	Ca	I
2	Da	I
3	Ed	IV
4	Fb	II
5	Jd	IV
6	Kc	III
7	Mb	II
8	Ob	II

3.2 Laboratory Tests

A summary of the performance-based test specifications used in this study is summarized in this chapter. Each method was validated using a detailed testing protocol.

3.2.1 Vacuum Oven Aging (VOA)

The vacuum oven aging procedure proved to be the most appropriate method for simulating the effects of weathering on sealant properties (Figure 3.2). According to AASHTO T367, sealants are cut into slices and placed on a stainless steel pan; each pan contains 35g of sealant. The pan is transferred into a conventional temperature controlled oven which is preheated to 180°C for approximately 5min to allow the sealant to melt and form an approximately 2mm film. The sealant is then removed from the oven and cooled to room temperature. Once it cools, the sealant is placed in a vacuum oven preheated to 115°C for 16hrs. Then, the vacuum is released and the sealant is placed in an oven at 180°C for 5min or until the sealant is fluid enough to be poured.



Figure 3.2. Vacuum oven used in aging of sealants.

3.2.2 Crack Sealant Bending Beam Rheometer (CSBBR)

The CSBBR (Figure 3.3), a binder modified bending beam rheometer (BBR) test, was introduced to measure the flexural creep of crack sealants at temperatures as low as -40°C . This procedure was adopted as an AASHTO standard (AASHTO T368). Two performance parameters were suggested: stiffness at 240s (S240) and average creep rate (ACR). The crack sealant specimen dimensions are $127 \times 12.7 \times 12.7\text{mm}$ and a clear span length of 102mm is used when tested under a point load. The crack sealant beam specimen is conditioned at test temperature in the CSBBR chamber for one hr before testing. A contact load and test load of

35±10mN and 980±50mN are applied, respectively; loading lasted for 240s and is followed by an unload period of 480s. Midpoint deflection is measured during loading and unloading.

$$S(t) = \frac{PL^3}{4bh^3\delta(t)} \quad (3.1)$$

where:

$S(t)$ = time-dependent stiffness (MPa);

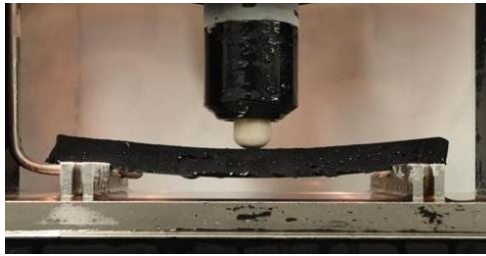
P = constant applied load (N);

L = span length (102mm);

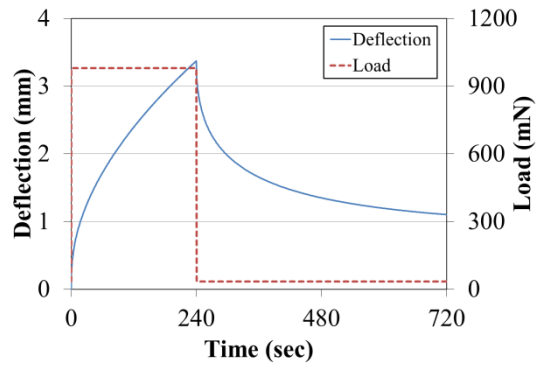
δ = deflection of the beam at mid-span (mm);

b = beam width (12.7mm); and

h = beam thickness (12.7mm).



(a) Sealant specimen



(b) Typical load-displacement curve



(c) Modified specimen supports



(d) CSBBR supports

Figure 3.3. Crack sealant bending beam rheometer (CSBBR) test.

3.2.3 Crack Sealant Direct Adhesion Test (CSAT)

The direct adhesion test, AASHTO T370, was developed to determine the adhesive strength of hot-poured crack sealants, as shown in Figure 3.4. The test is conducted by applying monotonic displacement rate until the sample is separated from the substrate, thus indicating interfacial failure. A minimum of six replicates is used for each material. The specification recommends using aluminum as substrate material; however, aluminum substrate can be replaced by other materials such as rock or asphalt mixture. Applied forces and displacements are also recorded to calculate the energy needed for breaking the bond between sealant and mold. The interfacial failure energy is the area extending from under the load-displacement curve to the peak point. The maximum loading force is considered as adhesive strength and is selected as the test performance parameter. The selected threshold is greater than 50 N for adhesion load to ensure good field performance. Figure 3.4 illustrates typical test results conducted for one material, showing the calculation of adhesive strength and interfacial fracture energy.

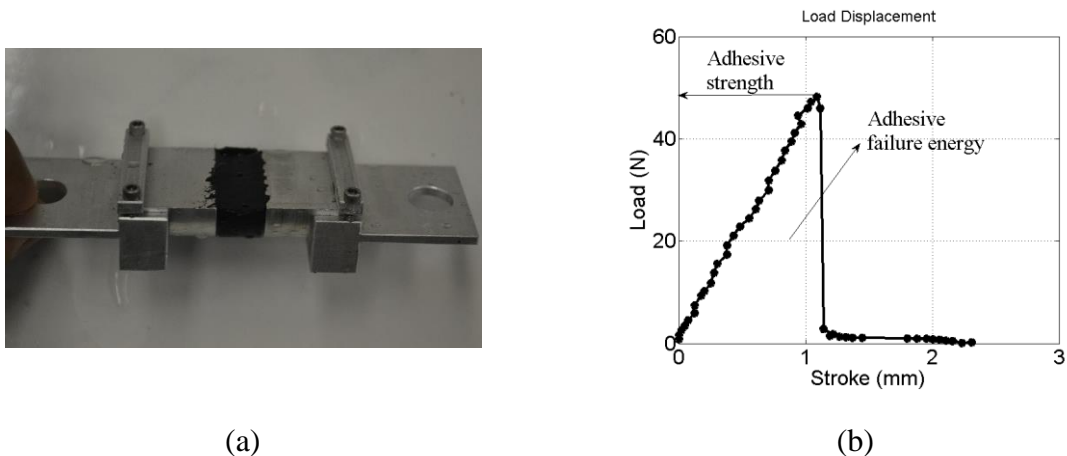


Figure 3.4. Crack sealant adhesion test (a) test specimen (b) typical maximum adhesive strength and interfacial energy results.

3.2.4 Crack Sealant Direct Tension Test (CSDTT)

The CSDTT as shown in Figure 3.5 is a modified direct tension test introduced to measure the extendibility of crack sealants at temperatures as low as -40°C under a monotonically displacement controlled test condition. This procedure was adopted as an AASHTO standard (AASHTO 369). Extendibility at test temperature is suggested as a performance parameter.

$$\lambda = \frac{\Delta L}{L_e} \times 100 \quad (3.2)$$

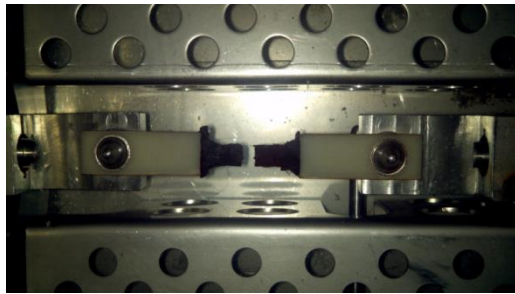
where:

λ = extendibility (%);

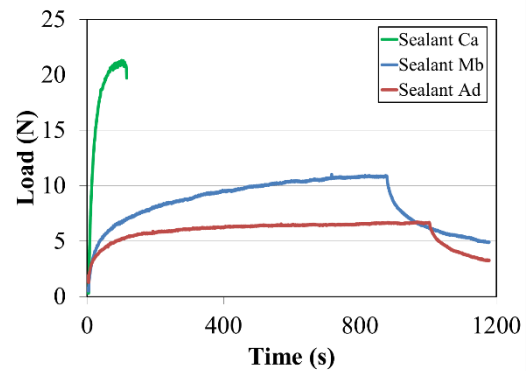
ΔL = tensile elongation (mm); and

L_e = effective length (20.3 mm).

The threshold for the extendibility depends on the sealants lowest application temperature, as shown in Table 3.4. This test was designated to evaluate sealants resistance to cohesive failure. The test can also be performed to confirm the lower temperature grade of crack sealant as defined by the CSBBR test. Based on the CSDTT, a tensile force at a deformation rate of 1.2mm/min is applied to elongate a dog-bone shape specimen with its effective gauge length of 20.3mm (AASHTO T369). Failure extension of the specimen on a stress-strain curve is defined at the maximum load taken by the specimen.



(a) Sealant specimen



(b) Typical test results

Figure 3.5. Crack sealant direct tension test (CSDTT).

Table 3.4. Thresholds for Crack Sealant Extendibility at Various Temperatures

Temperature (°C)	-4	-10	-16	-22	-28	-34	-40
Extendibility (%)	10	25	40	55	70	85	85

3.2.5 Dynamic Shear Test

Bituminous hot-poured sealants might fail as a result of deformation under the combined action of shear stresses and high service temperatures (Masson et al., 2007). This phenomenon is also known as tracking of sealants under traffic loading. This test method (AASHTO TP126) describes the procedure of measuring the flow coefficient and shear thinning exponent of a

bituminous sealant or filler by means of a crack sealant tracking test using DSR. The material is placed between two parallel plates and subjected to eight cycles of creep and recovery at increasing stresses and fixed temperature. The test is typically conducted at a temperature ranging between 46°C and 82°C; while the applied shear stress varies from 25Pa to 3200Pa. The limiting shear rate is obtained from the end of the creep phase for each stress level. Following the eight cycles, the stresses are plotted against the limiting shear rates, and a power law fit of the data provides characteristics of two parameters of the sealant flow properties: flow coefficient (C); and shear thinning exponent (P).

$$\sigma = C\dot{\gamma}^P \quad (3.3)$$

where:

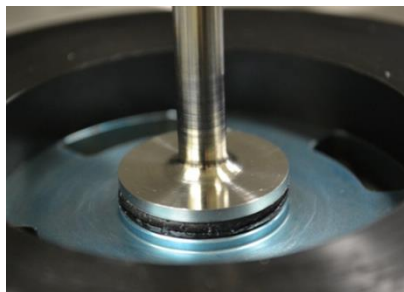
σ = stress (Pa);

$\dot{\gamma}$ = shear rate (1/s);

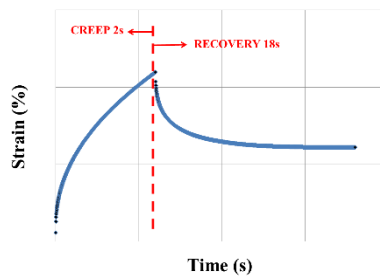
C = flow coefficient (Pa.s); and

P = shear thinning coefficient.

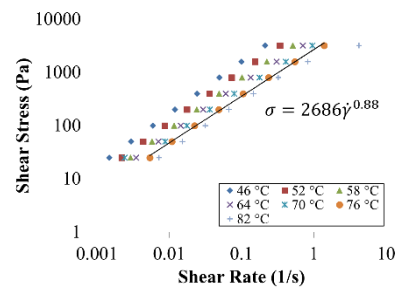
Plots of σ vs $\dot{\gamma}$ are interpreted based on the Ostwald power law model. The flow coefficient (C) and shear thinning coefficient (P) correlated well with sealant pseudo-field performance as measured by tracking (Collins et al., 2007). Limits of C at 4000Pa.s and P at 0.70 are used to define the level of sealant performance.



(a) Parallel plate setup



(b) One creep-recovery cycle



(c) Ostwald model

Figure 3.6. Crack sealant tracking test.

DSR is also used to obtain their viscoelastic properties from low to intermediate temperatures and high temperatures. For this purpose, a frequency sweep test was developed to measure complex shear modulus at various loading frequencies. Samples were tested at an angular frequency range of 0.1-100 rad/s. To cover low temperature properties, the test was conducted at

a temperatures range of -40°C to 82°C . The test results are presented in a master curve in Chapter 6.

Table 3.5. Experimental Program for High-Temperature Grading.

Test	Parameter	Objective
MSCR	C and P	Find high-temperature grade with respect to the previous procedure
Complex Modulus	G^* and phase angle	Master curve will be needed for some calculations in yield tests
Yield	Yield stress	A potential new approach for high-temperature grading

3.2.6 Rotational Viscosity Test (RV)

A Brookfield rotational viscometer was used to measure apparent viscosity of the hot-poured crack sealants. This procedure was modified from the one adopted by Superpave for asphalt binders. The main difference is the change in spindle and hook configuration, in addition to changes in testing procedures, as shown in Figure 3.7. The viscosity test was designed to simulate installation conditions. Since viscosity can play an essential role in predicting the field performance of hot-poured crack sealants, upper and lower viscosity limits (1 to 3.5Pa.s) are recommended. Upper limit ensures the material is liquid so it can be poured. The lower limit helps avoid excessively liquid sealants which can create problems in the filling of cracks during installation. The test is conducted in accordance with AASHTO T366 at 60rpm at the installation temperatures recommended by the manufacturers.



(a) Apparatus (b) Modified spindle

Figure 3.7. Crack sealant viscosity test.

3.2.7 Fourier-Transform Infrared Spectroscopy

Fourier-transform infrared (FTIR) spectroscopy is a test method used to classify the chemical bonds in a molecular matrix. FTIR projects an infrared radiation (IR) which has longer wavelength than visible light through a molecule, and the frequencies absorbed by atoms vibration are obtained. These vibrations form a spectrum, available few minutes after radiating the sample, using a spectrometer. Hence, the absorbed frequencies can be identified using a Fourier transform. Figure 3.8 is an example of an FTIR spectrum for a sealant where the frequency of absorbance is expressed in reciprocal centimeters, cm^{-1} (Masson et. al., 2003). Furthermore, a list of bonds can be associated to their IR absorbance frequencies. FTIR spectrum is also known as a material fingerprint—in this study, a sealant fingerprint. Therefore, FTIR can be useful for identifying crack sealants, the type of bonds in a sealant, and changes in sealants due to aging (Masson et. al., 2003).

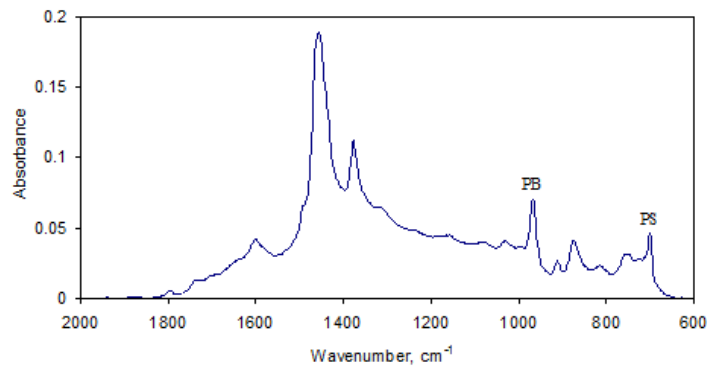


Figure 3.8. Example of an IR spectrum for a crack sealant.

After an introduction to sealant field evaluation and laboratory tests, details on test sites selection, sealant installation and data gathering are discussed in the next chapter. The development of an index sealant performance is discussed. Finally, the use of statistical methods to compare and categorize crack sealants, based on their performance, is presented. Beside sealant performance, different application and treatment methods are also assessed and compared in the next chapter.

CHAPTER 4. FIELD INSTALLATION AND PERFORMANCE

This chapter introduces the installation and field evaluation of sealants used at the experimental test sites. Seven sections were selected in collaboration with participating state departments of transportation in different environmental regions in North America. The test sites are introduced herein along with selection criteria, material selection and acquisition, and test site preparations. Field performance of crack sealants is also discussed in this chapter.

4.1 Test Site Selection

The selection of candidate pavements and the condition of cracks play an important role in successful sealant treatment and performance evaluation. Pavements with sufficient structural strength and good rideability were considered as candidate test sites. The typical pavement condition ratings used in the “Guidelines for Sealing and Filling Cracks in Asphalt Concrete Pavements (2003)” were used as guidelines for the selection of test sites. According to these guidelines, crack sealing applies to pavements in good condition with smooth riding. Therefore, pavements in good or fairly good conditions, i.e., with cracks in relatively good condition, were selected as test sites.

The candidate transverse cracks were full-lane wide cracks with minimal edge deterioration (i.e., spalls and secondary cracks). Cracks with some edge deterioration were evaluated using crack filling technique. The candidate longitudinal cracks, on the other hand, were at least 8 m long. Transverse and longitudinal cracks with minimal crack branching were also selected for field experiments. The criteria for selecting candidate test sections are similar to those presented by Masson (2001):

- Less than 15 mm wide cracks
- Cracks should not be a part of a web of cracks
- Crack should show little or no branching
- Cracks with no severe vertical distress, such as lipping or cupping

Climatic variability was also considered in the selection of test sections. Four test sections were identified in the first year of the project (2011) and installed thereafter. All sections are located in wet-freeze climatic zone. Two test sites were added to the experimental matrix in the second year (2012); one of the two test sections was located in a dry, no-freeze climatic zone. Table 4.1

summarizes all test sections and the relevant parameters considered in the selection of each. Installations were completed in six states between June 2011 and January 2013.

Table 4.1. Test Section Summary and Parameters Considered in the Selection of Field Experimental Plan.

Test Site Location	Climatic Region	Min/Max Temperature (°C)	Traffic	Initial Pavement Condition	Pavement Type	Installation Date
Belleville, Wisconsin	Wet-Freeze	-29/32	2,000 AADT with 6% Truck	11 years old ² in fair condition with longitudinal and transverse cracks	AC	7/19/2011
St Charles, Minnesota	Wet-Freeze	-31/31	13,055 ADT	2 years old in good condition with transverse reflective cracking	AC Overlay on Jointed PCC	9/11/2011
Lindsay, Ontario, CA	Wet-Freeze	-29/30	9,022 AADT with 7.5% Truck	13 years old in fair condition with transverse and some long. Cracks	AC	9/20/2011
Grantham, New Hampshire	Wet-Freeze	-29/32	9,500 AADT with 9% Truck	2 years old in good condition with transverse reflective cracking	AC over PCC	10/3/2011
Canandaigua, New York	Wet-Freeze	-24/31	6,600 AADT with 5% Truck	2 years old in very good condition with transverse reflective cracking	AC over PCC	9/11/2012
Roscommon County, Michigan	Wet-Freeze	-29/30	N.A	N.A	AC	10/11/2010
Salem, Virginia	Wet-Freeze	-16/34	N.A	N.A	AC	
Champaign, Illinois ¹	Wet-Freeze	-24/34	No Traffic	N.A	AC	09/15/2011

¹ This section was only designed and installed to investigate field aging mechanisms and weathering.

² Pavement age is calculated at the time of installation.

4.2 Field Test Matrix

Following the selection of sealants, a testing plan was prepared for each test site. The sealants were distributed to the test sites with approximately five to seven sealants installed at each test site. The distribution of sealants to each site was determined based on the following criteria: (1) installation of a sealant material at a minimum of two different sections for repeatability; (2) spectrum of material properties to ensure significant differences in field performance; and (3)

agencies request to include a specific product in the test matrix. Table 4.2 summarizes the final sealant-state matrix that was applied.

Table 4.2. Distribution of Materials to the Test Sites.

ID	Minnesota	New Hampshire	Wisconsin	New York	Ontario	Virginia	Total Repetitions
Ad	X		X				2
Bb	X		X		X		3
Ca				X			1
Da				X	X		2
Ed		X	X			X	3
Fb	X	X	X				3
Gd	X	X			X		3
Hb	X					X	2
Ib				X		X	2
Lb						X	1
Jd				X			1
Kc		X		X			2
Mb	X				X		2
Nb	X						1
Ob		X		X			2
Pd			X		X		2
Rb					X		1
Sd					X		1

Once the test sites was selected and materials were determined, and site-dependent test plans were proposed to the agencies considering site characteristics, such as pavement condition, number of transverse cracks available, crack spacing, availability of traffic control, and length of test section. A test matrix was prepared with the proposed sealants and the test parameters deemed critical for field performance, including sealant type, crack treatment type, rout geometry, and overbanding. An overview of the test plan for each test site is shown in Table 4.3.

Table 4.3. Experimental Plan for Field Investigation of Sealant Performance.

Test Site	Climatic Region	Crack Treatment Variables	Reservoir Geometry (mm)	Materials
Wisconsin	Wet-Freeze	Crack Seal only	20 x 20	Five materials from three different manufacturers
Minnesota	Wet-Freeze	Crack Seal & Fill, Variable Rout Size	12.5 x 12.5 20 x 20 30 x 15	Seven materials from three different manufacturers
Ontario	Wet-Freeze	Crack Seal & Fill, Variable Rout Size	20 x 20 12.5 x 12.5 30 x 15 40 x 10	Seven materials from four different manufacturers
New Hampshire	Wet-Freeze	Crack Seal & Fill, Variable Rout Size	12.5 x 12.5 20 x 20 30 x 15	Five materials from three different manufacturers
New York	Wet-Freeze	Crack Seal & Fill, Variable Rout Size	12.5 x 12.5 20 x 20 30 x 15	Eight materials from four different manufacturers
Virginia	Wet-Freeze	Crack Seal & Fill	20 x 20	Four materials from same manufacturer
Michigan	Wet-Freeze	Crack Fill only	NA	Sixteen materials from seven different manufacturers

4.3 Test Site Preparation

Prior to sealants installation, several tasks were performed, including preliminary detailed survey of the test site, installation of displacement pins, and finalization of the test plan based on site conditions. The preliminary tasks are summarized in detail hereafter.

4.3.1 Preliminary Survey

A preliminary survey was conducted at the test sites prior to installation collect information about the initial condition of pavement and cracks. Each test site was surveyed rigorously to determine crack spacing, number of cracks, crack rating, station numbering, and photo documentation. A rating system was developed to document the cracks initial condition. The rating system is a qualitative measurement based on visual inspection. The cracks were rated based on initial condition (partial- or full-length crack, branching severity, and cracks width and depth) and suitability for sealing. Ratings from 1 to 5 were assigned to cracks with 5 indicating best condition per the selection criteria (full-length crack, no branching, <10 mm opening) and 1 indicating worst condition. Crack ratings below 3 were not considered in this study; however, such ratings were considered for field sampling. Figure 4.1 shows pictures from two different test sites.



Figure 4.1. Initial survey and crack numbering of a test section.

Based on the preliminary survey, a summary of pavement and initial crack conditions is provided in Table 4.4. In general, the selected test sections were in favorable conditions for crack sealing and filling. The variation in crack spacing also allowed for the evaluation of the influence of crack displacements on sealant performance.

Table 4.4. A Summary of Preliminary Survey Results.

Test Site	Average Crack Spacing (m)	Number of Cracks	Average Crack Rating
Wisconsin	17.5	156	3.3
Minnesota	11.5	225	4.6
Ontario	30	276	3.5
New Hampshire	21.5	234	4.7
New York	39	181	3.7
Virginia	15.5	137	2.8

4.3.2 Crack Displacement Pin Installation

Crack displacement is one of the most critical parameters influencing sealant performance. Opening and closing of cracks can be a function of temperature, crack spacing, pavement structure, and materials. Crack displacements were measured at each test site using stainless steel pins driven on each side of the crack. Approximately 30 cracks were pinned at each test site to monitor displacements. Pins installation included drilling a 6 mm hole, filling the hole with rapid setting epoxy, and driving the pin in the hole. Measurements were taken using a conical-end calipers. Initial measurements were recorded right after installation.

Steel pins were installed at the edge, mid-lane, and center lane locations. Figure 4.2 shows two cracks at a test site with single- and triple-point displacement pins. Initial measurements were taken after installation.



Figure 4.2. Crack displacement pins: Single-point measurement (left) and three-point measurement (right).

4.4 Tasks Performed during Test Site Installations

Several tasks were performed at each test site during installation to collect as much data as possible for use in long-term performance analysis of installed sealants and to ensure repeatability between test sites. The main tasks performed during installation are summarized herein, including placement of sealants in kettles, sealant temperature recording, routing and cleaning, sampling, and photo documentation:

- Sealant placement in the kettle and heating – Installation starts with the placement of sealant blocks in the kettle and heating the sealant for two hrs. Initially, two blocks (approximately 20 to 40L of materials) were heated and flushed out to ensure cleanliness of the kettle and to reduce contamination from residual sealants in the kettle. Approximately 230L of sealant were then added to the kettle and heated up to recommended installation temperatures. Sealant temperature in the kettle was frequently checked to ensure that the sealant reached the target temperature and was not overheated. The information collected at this stage was recorded in journals prepared for each section.
- Sealant temperature measurements – The temperature of sealants is critical for ensuring proper installation and expected performance. Temperature readings were recorded at regular intervals from (1) panel readings (dial gage and heated hose); (2) inside the kettle using a 180 cm long probe that can record temperatures at three locations: at the tip and 12.5 and 25 cm above the tip of the probe; and (3) outside the kettle using infrared and T-type thermocouples. Figure 4.3 shows the various methods used to record temperature during installation.



Figure 4.3. Temperature measurement methods during test site installation.

- Pavement and ambient temperature measurements – Two wireless temperature nodes were installed at each test site to monitor pavement and air temperatures during the evaluation period. One of the nodes was installed in the proximity of test site, avoiding direct sun light, to monitor ambient temperature. Another node was buried in the pavement (25 mm below the surface) using epoxy, as shown in Figure 4.4, to measure pavement temperature.



Figure 4.4. Wireless temperature nodes for ambient temperature (left) and pavement temperature (right).

- Crack routing and cleaning – Cracks were routed in accordance with the testing plan prepared for each test site. Reservoir geometry was one of the test parameters considered in this study. Actual rout dimensions were verified at the site using specially prepared aluminum blocks as shown in Figure 4.5. Rout were cleaned with a leaf blower to ensure that no dust or debris are left in and around the rout. The slabs were also cleaned to prevent dust and debris carried by construction vehicles back to the rout. Figure 4.5 illustrates crack and rout preparation operations and shows a properly cleaned pavement after routing operation. The routs were then cleaned again using hot air lance and compressed air, which were consistently used at all of the test sites to ensure repeatability.

- Sealing and finishing – The routs were cleaned and dried using hot air lance and compressed air, and sealant was applied using the wand and overbanding with a squeegee as shown in Figure 4.6. The width of the overband varied from 7 to 10 cm. In some sites, crack filling and sealing operations were completed using horseshoe or disk adapter, as shown in Figure 4.7, which does not require a squeegee for overbanding. Some cracks were left without an overband to evaluate the effect of overband on crack sealant performance.
- Sampling – Two to three samples were obtained from each material at different times. The first sample was collected right before installation when the material was at the recommended temperature. The second and third samples were collected during installation. These samples were used to study the effect of kettle aging (short-term aging) on the rheological properties of crack sealants.
- Photo documentation – After installation was completed, a final survey was conducted and pictures of each crack were taken to document the condition of sealed cracks.
- Equipment list – A list of equipment and their models used during crack sealing and filling is summarized in Table 4.5.

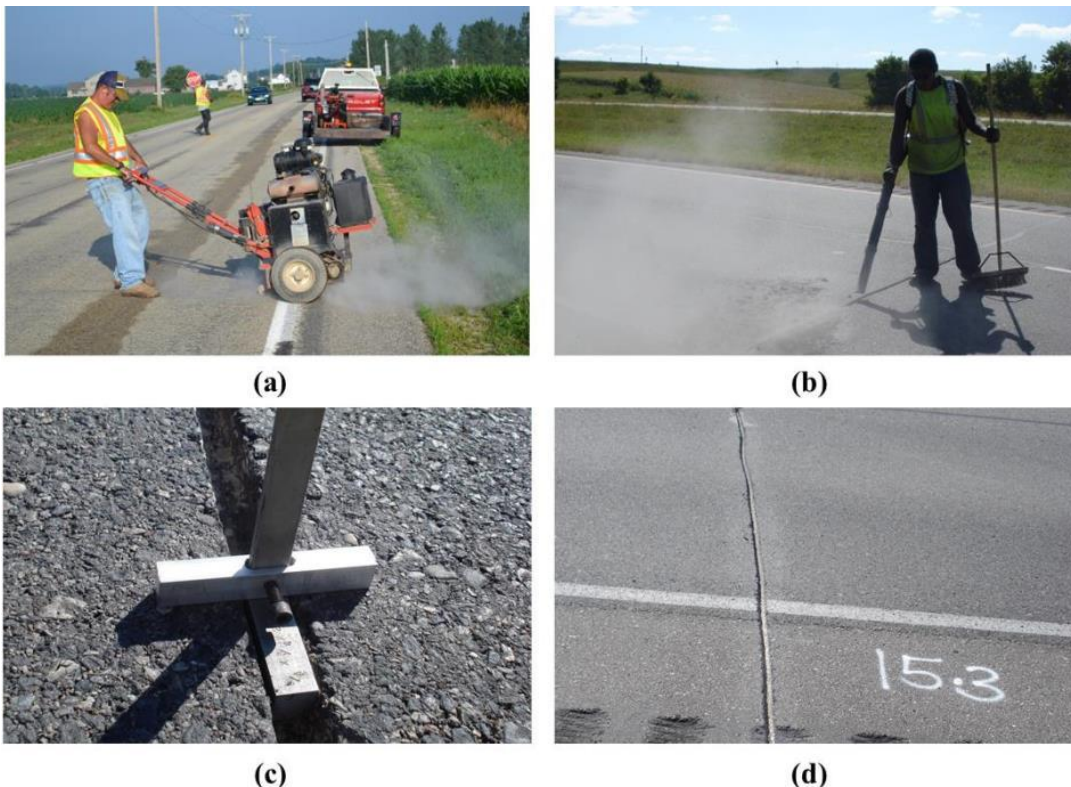


Figure 4.5. Typical operations prior to crack sealing: (a) routing; (b) pavement and crack cleaning; (c) route size checking; and (d) a properly finished rout and clean pavement surface.









Figure 4.6. Typical crack sealing operations: Drying and cleaning the rout using hot air lance and compressed air (left); sealant and overband application using squeegee (middle); and the finished product (right).



Figure 4.7. Various sealing adapters to apply sealant and overband: Horse shoe (left) Disk (right).

Table 4.5. List of Equipment Used during Crack Sealing and Filling.

Equipment	Primary Use	Picture
Router	Making reservoir at different size for sealant.	
Hot air lance	Drying the routs wall.	
Leaf Blower	Cleaning dust and debris out of the routs and pavement surface.	
Kettle	Heating and melting the sealant up to installation temperature.	
Applicator	Pouring the sealant into the routs.	
Squeegee	Overband application.	

4.5 Test Site Sealant Installations

This section summarizes the test site installations conducted between 2011 and 2014. A brief overview of each test site, data collected during installation, and highlights of the installation process are presented herein.

4.5.1 Wisconsin

Test Site Overview

The Wisconsin test site is located in Green County on State Highway 92. The test sections were selected from a 17.5 km pavement section between Brooklyn and Belleville. The total length of sections where test sealants were installed is 2.9 km. Figure 4.8 shows a map and an aerial picture of the test site. This pavement section was constructed in 2000 and consists of 10 cm AC overlay on 15 cm AC supported by crushed aggregate base. Shoulders were paved with 8 cm thick AC on 30 cm thick gravel base. The section is a two-lane highway; each lane is 3.5 m wide.



Figure 4.8. Wisconsin test site map and aerial view.

Test Section Layout

This test site was partitioned into five sections for installing five different sealants. Standard route geometry was used in the entire test site. A summary of the test sections is presented in Table 4.6.

Table 4.6. Wisconsin Site Test Matrix Illustrating Sealant Materials and Installation Method

Section #	Length (m)	# of Cracks	Sealant ID	Route Geometry (mm)
1	382	26	Fb	20 x 20
2	457	31	Ed	20 x 20
3	542	31	Pd	20 x 20
4	563	24	Ad	20 x 20
5	841	44	Bb	20 x 20

Pre-Installation Survey

Thermal transverse cracks were the main crack type present at this site. Surface rating and ride quality were reported as 7 (on a scale 1 to 10) and 130 by Wisconsin Department of Transportation. The sections were surveyed prior to installation to document the station number for each crack and to document photos. Figure 4.9 presents a selection of pictures from each section illustrating the initial condition of the cracks (cracks' pictures are labeled with the section and the crack number at each test site. For example Crack 4.18 is the 18th crack in section 4). In general, cracks were suitable for crack sealing. However, some sections exhibited medium to sever longitudinal cracking.



(a) Crack 1.1, Rating 4 (b) Crack 2.1, Rating 3 (c) Crack 3.25, Rating 4 (d) Crack 4.18, Rating 4.5

Figure 4.9. A selection of crack pictures prior to installation showing initial crack conditions.

A summary of the pre-installation survey is presented in Table 4.7, including average crack spacing and initial crack ratings. In general, cracks in Sections 1 and 2 were more favorable for crack sealing than other sections. Some longitudinal cracking in addition to transverse cracks were observed in Sections 3 to 5.

Table 4.7. A Summary of Pre-Installation Crack Ratings in Wisconsin Test Site.

Section #	Sealant ID	Average Rating	Average Crack Spacing (m)
1	Fb	3.5	14.5
2	Ed	3.5	14.5
3	Pd	3.4	17
4	Ad	3.2	23.5
5	Bb	3.2	19

Installation Notes

The sealants were installed on July 19–21, 2011. Green County Highway Department controlled traffic and installed the sealants. The driving lane was closed to traffic during the day of installation. Moving traffic control was maintained with the help of two flaggers. The crew consisted of eight personnel (One router, two flaggers, one cleaner, two drivers, one sealer, and one blotter). Two different Crafcro model kettles were used in this project: Crafcro EZ 500 (475 L capacity) and 1000 (985 L capacity). Figure 4.10 shows the smaller capacity kettle and one of the adapters used during installation. Hot air lance and compressed air were used for cleaning the routs.



Figure 4.10. Kettle used in Wisconsin for heating sealant (left) and horse shoe adapter (right).

Sealant installation in the five sections was completed in two days. The time log for different activities in each section is shown in Table 4.8. In Sections 1, 2 and 3, transverse cracks were sealed in full width from edge to edge. On day 2, only cracks in one lane were routed and sealed to accelerate installation time for Sections 4 and 5.

Table 4.8. Wisconsin Test Site Installation Time Log.

	Section #	Start Heating	Start Routing/Sealing	End	Kettle Model
Day 1	1	6:40 AM	7:27 AM	8:25 AM	Crafcro EZ 1000
	2	7:45 AM	10:15 AM	11:15 AM	Crafcro EZ 500
	3	12:30 PM	2:10 PM	3:22 PM	Crafcro EZ 1000
Day 2	4	7:30 AM	8:40 AM	11:30 AM	Crafcro EZ 500
	5	9:50 AM	11:50 AM	1:45 PM	Crafcro EZ 1000

Sealant temperature was closely monitored during installation. Temperature measurements were taken using the kettle panel readings, temperature probe inside the kettle, and from the samples in the cans. Inside the kettle, the temperature was measured using a temperature probe while

outside-kettle temperatures were measured using an infrared gun. Temperature variations during installation of the five sections are shown in Figure 4.11.

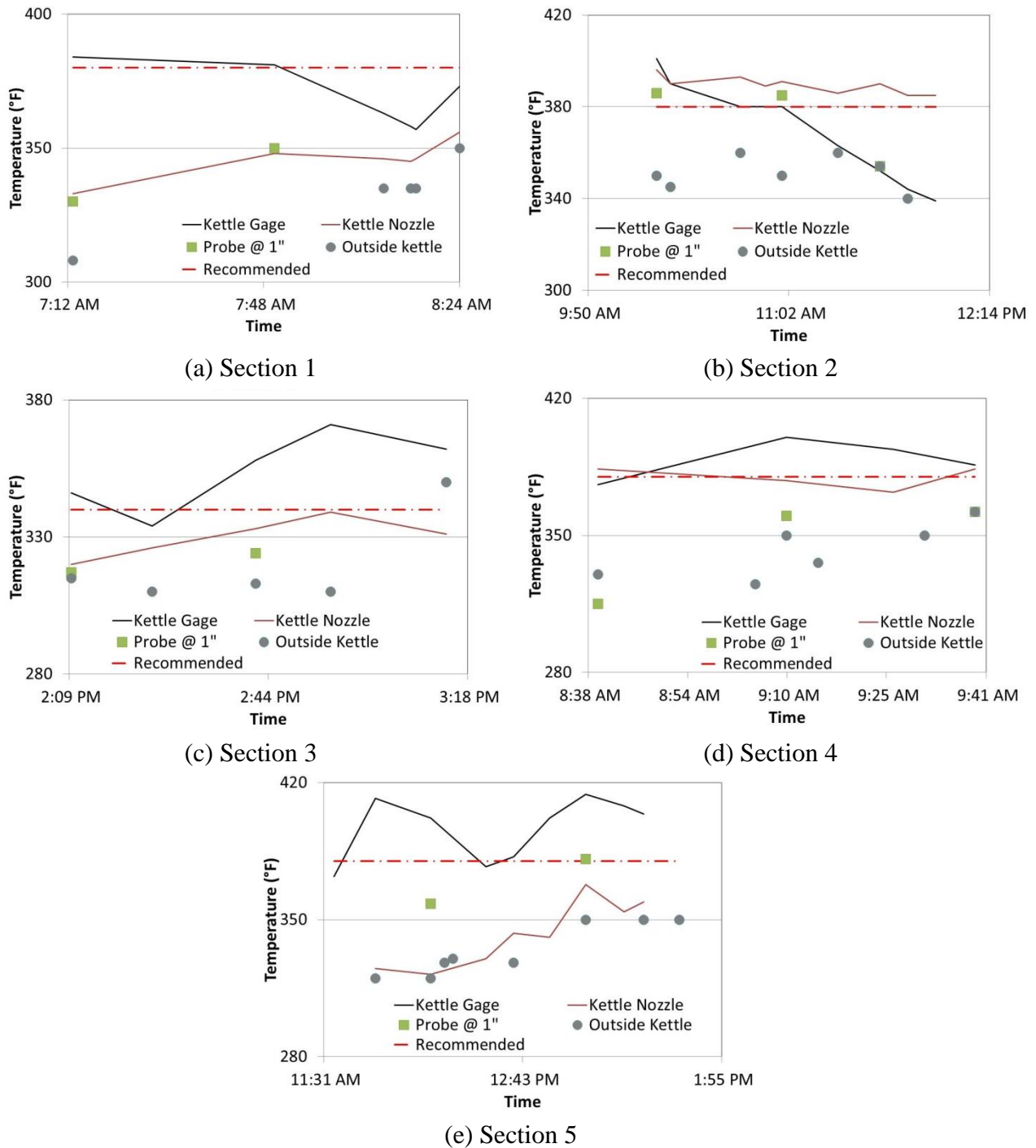


Figure 4.11. Temperature measurements during the installation of Sections 1 through 5 at the Wisconsin test site.

4.5.2 Minnesota

Test Site Overview

The Minnesota test site is located on Interstate-90 in St. Charles area. The test sections are on west bound I-90 between mileposts 235 and 238. The total length of the section is 2.9 km. The sections are located in the driving lane. A site map is shown in Figure 4.12.

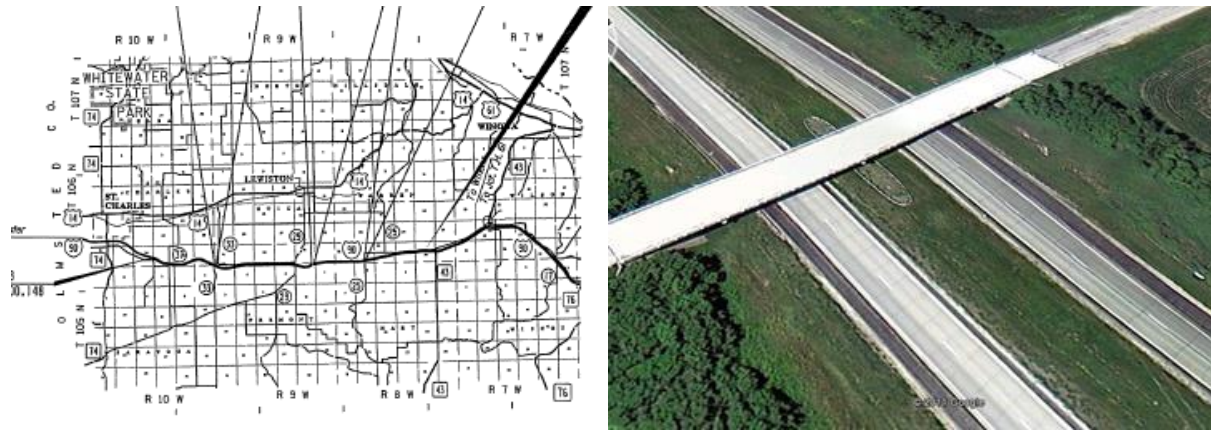


Figure 4.12. Minnesota test site map.

The section was overlaid in 2009 with 11 cm thick AC on a jointed PCC. It consists of two lanes in each direction, each is 3.6 m wide. Shoulder width is 3 m throughout the entire test section. A picture from the test site is shown in Figure 4.13.



Figure 4.13. Minnesota test site overview.

Test Section Layout

This test site consisted of 24 sections. Seven sealants were installed using various treatment methods. A summary of the test sections is presented in Table 4.9.

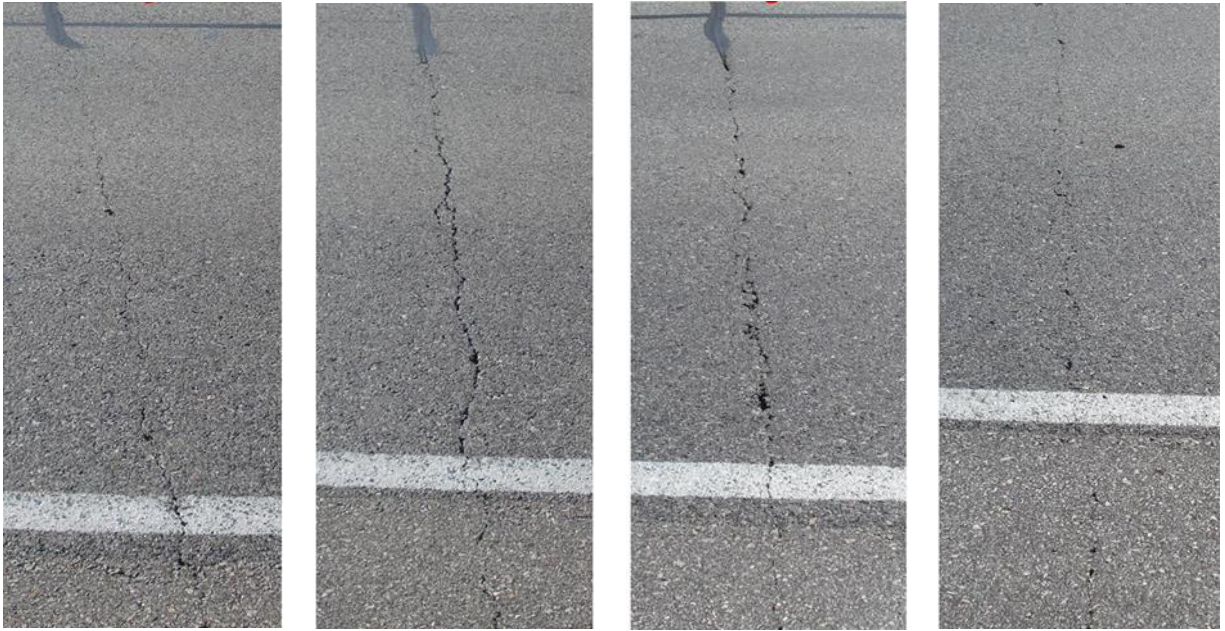
Table 4.9. Minnesota Test Section Layout.

Section #	Length (m)	# of Cracks	Sealant ID	Rout Geometry (mm)
Contractor # 1				
3 ¹	91	10	Gd	20 x 20
4	99	10		20 x 20
5	137	10		30 x 15
6	89	10		12.5 x 12.5
7	81	10	Fb	20 x 20
8	146	10		20 x 20
9	74	10		Clean & Seal
10	173	15	Hb	20 x 20
11	116	10		Clean & Seal
Contractor # 2				
12	272	15	Ad	25 x 25
13	183	15		25 x 25
14	176	15	Bb	25 x 25
15	192	15		25 x 25
16	147	15		Clean & Seal
17	157	15	Mb	25 x 25
18	99	10		25 x 25
19	128	10		30X15
20	123	10		Clean & Seal
21	123	10		12.5 x 12.5
22		10	Control	
23		15	Nb	25 x 25
24		10		25 x 25
25		20		Clean & Seal

¹ Section numbering starts with 3 in the test site.

Pre-Installation Survey

Reflective transverse cracking was found to be the main crack type in this test site. Figure 4.14 presents pictures taken during the initial survey of the project site, reflecting the general condition of pavement and cracks. A summary of crack ratings is presented in Table 4.10. The survey indicates that cracks were generally in a very favorable condition (ratings are in the range of 4 to 5) for sealing.



(a) Crack 4.1, Rating 4.5 (b) Crack 4.4, Rating 3 (c) Crack 5.9, Rating 3 (d) Crack 12.6, Rating 5

Figure 4.14. A selection of crack pictures prior to installation showing initial crack conditions.

Table 4.10. A Summary of Initial Crack Ratings at the Minnesota Test Site.

Section #	Sealant ID	Average Rating	Average Crack Spacing (m)
3	Gd	4.6	9
4		4.3	10
5		4.3	14
6		4.6	9
7	Fb	4.8	8
8		4.6	15
9		4.6	7
10	Hb	4.6	12
11		4.9	12
12	Ad	4.5	18
13		4.7	12
14	Bb	4.5	12
15		4.5	13
16		4.7	10
17	Mb	4.8	10
18		4.9	10
19		4.9	13
20		4.7	12
21		4.4	12

Installation Notes

Installation took place during the week of September 11, 2011. Traffic control was provided by MNDOT. The driving lane was closed to traffic during installation. Two contractors worked on the test site. The test site was also part of sealant verification trials conducted by MNDOT; the products were installed by contractors representing the manufacturers. The first contractor's crew consisted of five personnel (one sealer, one finisher, one router, one rout cleaner, and two truck drivers). The second contractor's crew consisted of six personnel (one sealer, one finisher, one router, one blower, one rout cleaner, and one truck driver). Two kettle types were used: Crafcro SuperShot 125 with 475 L capacity and Cimline Model 2009 with 870 L capacity. A squeegee finisher was used to apply sealant and overbanding. Figure 4.15 shows the kettle and adapter used by the second contractor. The second contractor used a leaf blower to clean the pavement after routing and followed a double-finishing approach to apply overbanding where routs had been recently filled. Both contractors used hot air lance and compressed air for cleaning cracks prior to sealing. After sealing all cracks in a section, the crew created overband by injecting more sealant and sweeping with a squeegee.



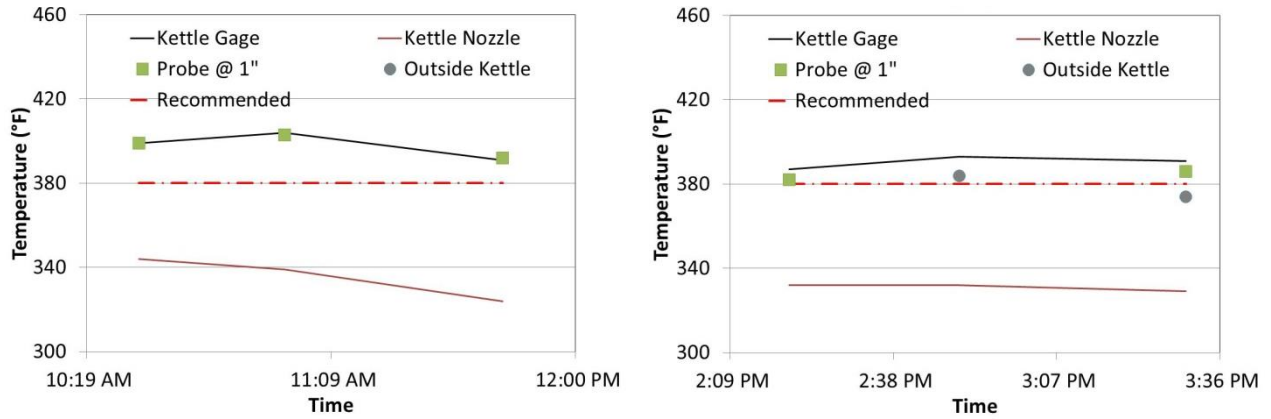
(a)



(b)

Figure 4.15. A kettle and sealant installation at the Minnesota test site (Section 13).

The temperature was closely monitored during installation and a probe was used to measure temperature inside the Cimline kettle. Outside the kettle, temperature measurements were taken by a T-type thermocouple. Panel readings (hose and dial gage) were also recorded during installation. The temperature records for some sections are presented in Figure 4.16.



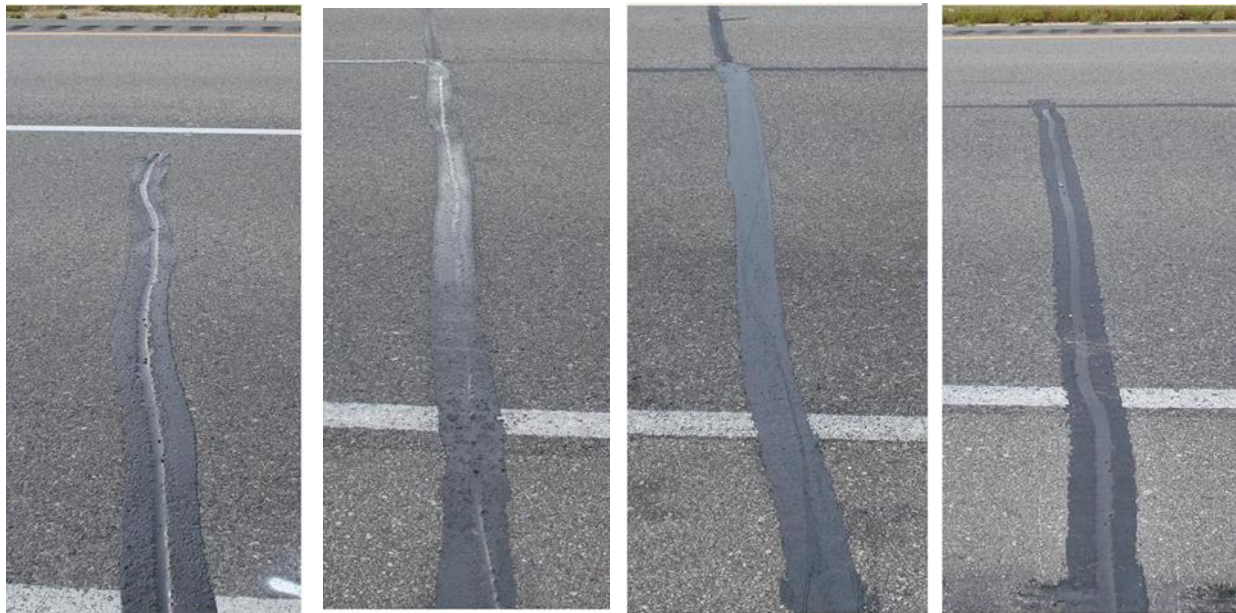
(a) Sections 12 and 13

(b) Sections 14, 15, and 16

Figure 4.16. Temperature measurements during sealant installation for five sections in Minnesota test site.

Post-Installation Notes

After sealant installation was completed, each crack was digitally documented as shown in Figure 4.17.



(a) Crack 3.3,
20x20 mm

(b) Crack 6.5,
12.5x12.5 mm

(c) Crack 16.5,
clean and seal

(d) Crack 19.3,
30x15 mm

Figure 4.17. Sealed routs at various test sections in Minnesota.

4.5.3 Ontario

Test Site Overview

Ontario test site is located on Highway 35 in Lindsay area. The test site starts 140 m south of Bethany Hills Rd on Highway 35 and ends at around 6.1 km south of Highway 7 junction. The total length of the section is 8.9 km. A map for the test site is shown in Figure 4.18.

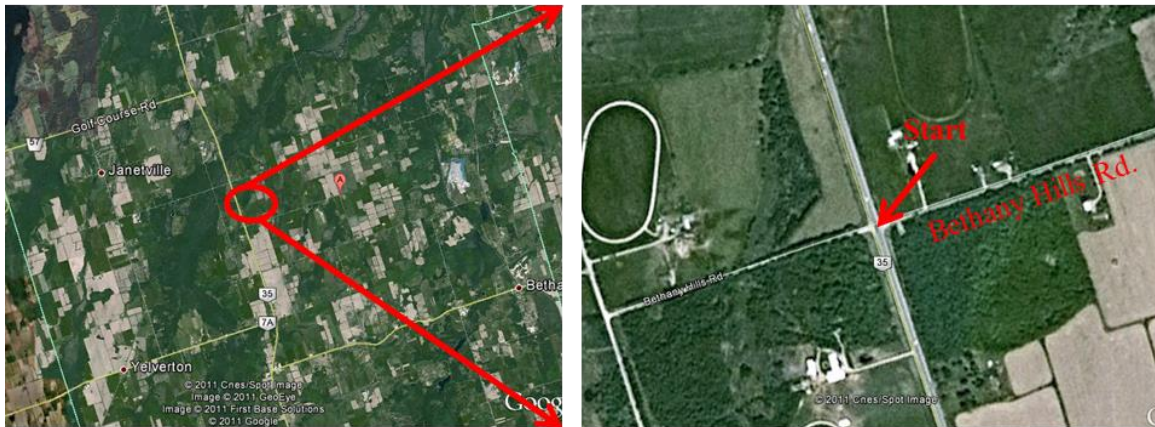


Figure 4.18. Ontario test site map.

The section was rehabilitated in 1998 using full-depth reclamation and 25mm thick AC overlay. It consists of two lanes; each lane is 3.2 m wide. The shoulders, 1 m wide, were partially paved. Figure 4.19 shows an overview of the Ontario test site.



Figure 4.19. An overview of the Ontario test site.

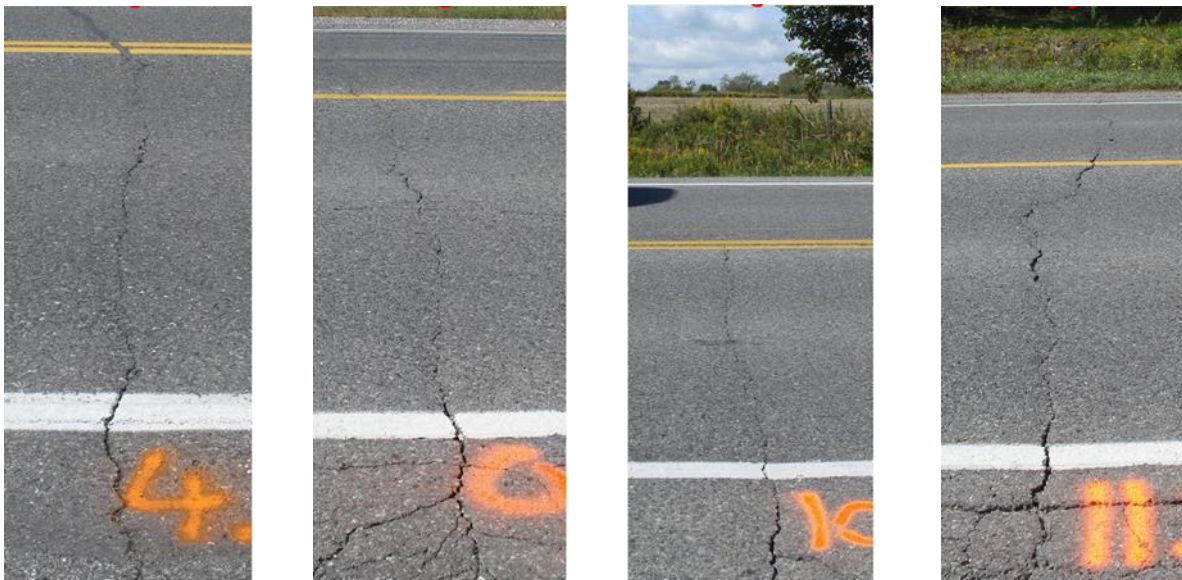
Test Section Layout

This test site consists of 16 sections. Seven sealants were installed using various treatment methods. A summary of the test sections is presented in Table 4.11.

Table 4.11. Ontario Test Section Layout.

Section #	Length (m)	# of cracks	Sealant ID	Rout Geometry (mm)
1	660	15	Rb ¹	20 x 20
2	467	10		30 x 15
3	322	10		40 x 10
4	1030	20	Pd	20 x 20
5	676	20	Gd	20 x 20
6	499	10		30 x 15
7	595	10		40 x 10
8	901	10		Clean & Seal
9	821	25	Bb	20 x 20
10	547	30	Mb	20 x 20
11	257	15		30 x 15
12	225	15		40 x 10
13	209	15		Clean & Seal
14	740	30	Sd	20 x 20
15	290	30	Da	20 x 20
16	129	11	Control	

¹ This product was not in the list of materials proposed for the pooled fund study.



(a) Crack 4.10, Rating 3 (b) Crack 9.24, Rating 4.5 (c) Crack 10.28, Rating 4.5 (d) Crack 11.3, Rating 2.5
 Figure 4.20. Initial condition of cracks at various sections at Ontario test site.

Table 4.12. A Summary of Pre-Installation Crack Ratings at Ontario Test Site.

Section #	Sealant ID	Avg. Crack Rating	Avg. Crack Spacing (m)
1	Rb	3.4	44
2		3.6	47
3		3.4	32
4	Pd	3.7	51
5	Gd	3.1	34
6		3.5	49
7		3.0	59
8		3.5	90
9	Bb	3.7	33
10	Mb	3.8	18
11		3.2	17
12		3.6	15
13		4.2	14
14	Sd	3.9	24
15	Da	3.8	10
16	Control	4.0	11

Installation Notes

The sealant was installed in the week of September 20, 2011. Traffic control was provided by the contractor. The driving lane was closed to traffic by flaggers on the north and south sides of the section, covering about 0.8 km each time. As the job progressed, flaggers moved with the crew to the next station. The contractor’s crew consisted of eight personnel (one finisher, one inspector, one router, one blower, one rout cleaner, one truck driver, two flaggers). A Cimline kettle (Model 2009) was used in the installation; and squeegee was used for overbanding. Figure 4.21 shows the kettle and adapter used at the test site. A CrafcO pavement cutter was used for routing. The routed crack and its surrounding was cleaned with a leaf blower after routing and, prior to sealing, a hot air lance and compressed air were used to clean the rout. Sealed cracks were sprayed by Glenzoil 20 Plus for traffic protection.

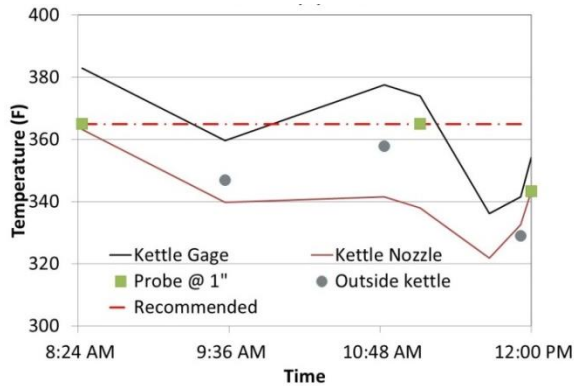
Procedures similar to those implemented in other project sites were followed for heating and sealant installation. Table 4.13 presents the time log for each activity. Installation was completed in three days. Temperature measurements were taken during installation from inside and outside the kettle. Figure 4.22 illustrates the temperature readings taken during installation. The panel readings were consistent with the inside- and outside-kettle temperature information.



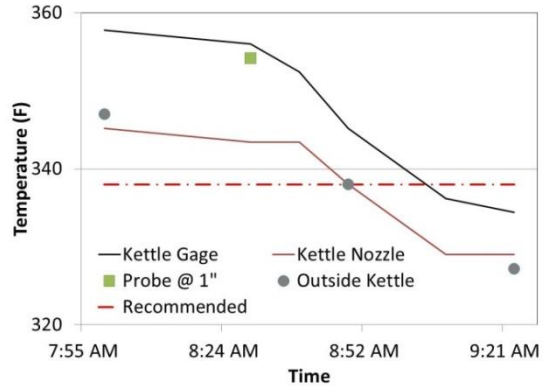
Figure 4.21. The kettle used at Ontario (left) test section and finishing with a squeegee (right).

Table 4.13. Ontario Test Site Installation Time Log.

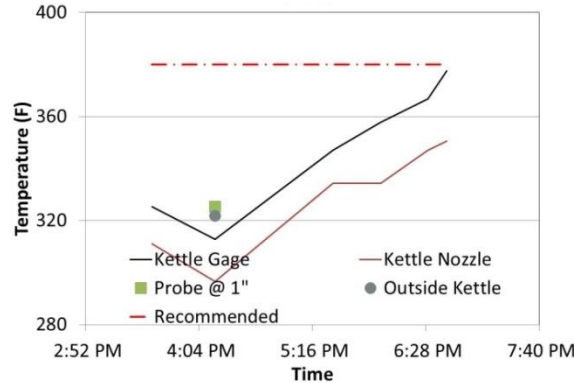
	Sections	Start Heating	Start Routing	Start Sealing	End
Day 1	1,2,3	5:15 AM	8:30 AM	9:00 AM	12:00 PM
	5,6,7,8	2:35 PM	3:35 PM	3:35 PM	6:45 PM
Day 2	10,11,12,13	5:15 AM	8:00 AM	8:10 AM	10:56 AM
	14	11:30 AM	12:40 PM	12:50 PM	1:48 PM
Day 3	15	2:30 PM	3:45 PM	3:55 PM	4:25 PM
	4	5:15 AM	8:00 AM	8:10 AM	9:25 AM
	9	10:15 AM	11:40 AM	11:50 AM	1:00 PM



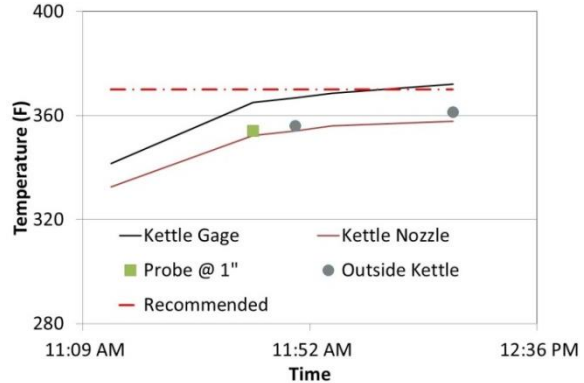
(a) Sections 1, 2, and 3



(b) Section 4



(c) Sections 5, 6, 7, and 8



(d) Section 9

Figure 4.22. Kettle temperature variations during Ontario test site installation.

Post-Installation Notes

After sealant installation was completed, each crack was digitally documented as shown in Figure 4.23. It was observed that the thickness of overbanding was relatively greater than that at other sections.



(a) Crack 10.5,
20x20 mm

(a) Crack 11.7,
30x15 mm

(a) Crack 12.8,
40x10 mm

(a) Crack 13.5,
clean and seal

Figure 4.23. Pictures after crack sealant treatment in Ontario (Sections 10 through 13).

4.5.4 New Hampshire

Test Site Overview

New Hampshire test site is located on Interstate-89 in the Grantham area. The test sections are on both south and northbound of I-89. The sections in the southbound start at milepost 48.0 and end at around milepost 46.2. The sections in the northbound extend from milepost 44 to milepost 45.6. The total test section is 5.7 km long. Installations took place in the driving lane. A map for the test site is shown in Figure 4.24.

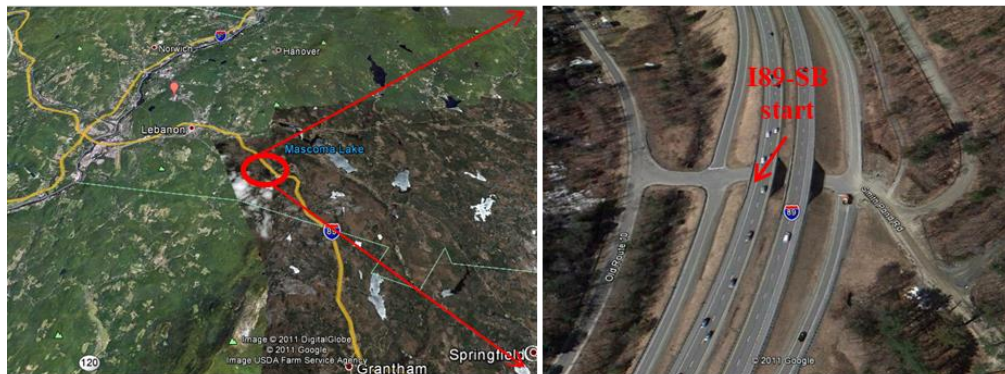


Figure 4.24. New Hampshire test section site map and aerial picture of the test site.

The pavement sections were originally constructed between 1958 and 1971. The sections were overlaid in 2009 with 2.5 cm thick AC. The sections consist of two 3.7 m wide lanes in each direction. The shoulder width is 3 m throughout the entire test sections. Figure 4.25 shows an overview picture from the southbound.



Figure 4.25. New Hampshire test site overview.

Test Section Layout

The test site consists of 19 sections. Five sealants were installed using various treatment methods. A summary of test sections is presented in Table 4.14.

Table 4.14. New Hampshire Test Section Layout.

Section #	Length (ft)	# of Cracks	Sealant ID	Rout Geometry (mm)
I89-SouthBound (starts at MP 48.0)				
1	557	30	Ob	20 x 20
2	211	10		20 x 20 (no overband)
3	458	25	Kc	20 x 20
4	213	9		12.5 x 12.5
6	135	10		30x15
7	222	10		30x15
8	403	20	Gd	20 x 20
9	152	10		12.5 x 12.5
10	275	12		30 x 15
I89-NorthBound (starts at MP 44.0)				
12	350	20	Fb	20 x 20
13	151	10		20 x 20 (no overband)
14	222	10		12.5 x 12.5
15	143	10		30 x 15
16	296	10		Clean & Seal
17	783	20	Ed	20 x 20
18	341	10		20 x 20 (no overband)
19	185	8	Control (No Sealant)	

¹ There are no sections with numbering 5 and 11.

Pre-installation Survey

Transverse reflective cracks were the main cracking type with a few longitudinal cracks developing in some sections. The rating system adopted in this study was used to evaluate cracks initial condition. Cracks generally met the criteria set in this study as shown in Figure 4.26. A summary of crack rating is presented in Table 4.15.



(a) Crack 12.1, Rating 4.5 (a) Crack 12.2, Rating 5 (a) Crack 12.3, Rating 4 (a) Crack 12.4, Rating 5
Figure 4.26. Initial crack condition in Section 12 of the New Hampshire test site.

Installation Notes

Sealant installation took place during the week of October 3, 2011. Traffic control was provided by the contractor. The driving lane was closed to traffic during installation. The contractor's crew consisted of eight personnel (one finisher, one inspector, one router, one blower, one rout cleaner, one truck driver, and two flaggers). Cimline Model 2009 and Cimline Model 1999 (without a heated hose) were used. Disk shape adapters (without swivel shoe) were used to apply sealant and overbanding, as shown in Figure 4.27. Routing was done using a Crafcro pavement cutter. Similar to the Minnesota and Ontario sections, the pavement was cleaned with a leaf blower after routing, and hot air lance and compressed air were applied before sealing.

Table 4.15. A Summary of Initial Crack Ratings at the New Hampshire Test Site.

Section #	Sealant ID	Average Rating	Average Crack Spacing (m)
1	Ob	4.5	19
2		4.6	21
3	Kc	4.7	18
4		4.8	24
6		5	13
7		4.9	22
8	Gd	4.9	20
9		4.8	15
10		4.7	23
12	Fb	4.8	17
13		4.8	15
14		4.5	22
15		4.5	14
16		5.0	30
17	Ed	4.8	39
18		4.7	34
19	Control (No Sealant)	4.3	23



Figure 4.27. Kettle and sealant installation using disk shape adapter in New Hampshire. After draining the kettle to achieve kettle cleanliness, 300-400kg of sealant blocks were added to the kettle for each section. A time log detailing all activities is presented in Table 4.16. Sealant installation was completed in two days.

Table 4.16. New Hampshire Test Site Sealant Installation Time Log.

	Sections	Start Heating	Start Routing/Sealing	End	Kettle
Day 1	1, 2	6:30 AM	10:15 AM	12:20 PM	Cimeline (2009)
	3,4,6,7	9:30 AM	1:40 PM	3:45 PM	Cimeline (1999)
	8,9,10	2:05 PM	4:10 PM	5:25 PM	Cimeline (2009)
Day 2	12 to 16	6:10 AM	8:45 AM	10:05 AM	Cimeline (2009)
	17, 18	8:00 AM	10:27 AM	11:17 AM	Cimeline (1999)

The sealant temperature was closely monitored during installation. Temperature measurements were taken from the kettle panel and during sampling in the cans using a T-type thermocouple. Panel temperature readings were recorded continuously; whereas, sample temperature measurements were taken only during sampling.

Post-Installation Notes

After sealant installation, each crack was digitally documented as shown in Figure 4.28.



(a) Crack 1.8, 20x20 mm
 (b) Crack 2.6, 20x20 mm (no overband)
 (c) Crack 3.4, 20x20 mm
 (d) Crack 16.7, clean and seal

Figure 4.28. Crack sealant treatment in Sections 1, 2, 3, and 16 in New Hampshire.

4.5.5 New York

Test Site Overview

The New York test site is located on Chaplin Road (road 21) in the Canandaigua area, located southeast of Rochester. The test sections are on both southbound and northbound of Chaplin Road. The sections in the southbound start at milepost 3003 and end at around milepost 3025. The test sections in the northbound extends from milepost 3025 to milepost 3003. The total test section length is 7.1 km. A map for the test site is shown in Figure 4.29.



Figure 4.29. New York test site map.

The section was milled and overlaid in 2010. It consists of one lane in each direction and the lane width is 3.7 m. Shoulder width is 1.8 m throughout the entire test section. A picture from the test site is shown in Figure 4.30.



Figure 4.30. New York test site overview.

Test Section Layout

The test site consists of 13 sections. Six sealants were installed using various treatment methods. A summary of the test sections is presented in Table 4.17.

Table 4.17. New York Test Section Layout.

Section #	Length (m)	# of Cracks	Sealant ID	Rout Geometry (mm)
Road 21-NorthBound (starts at MP 3003)				
1	483	10	Ob	20 x 20
		5		20 x 20 (No overband)
2	644	15		Clean & Seal
3	483	15	Ca	12.5 x 12.5
4	483	15		30x15
5	644	10	Kc	20 x 20
		5		20 x 20 (No overband)
6	644	10	Jd	20 x 20
		5		20 x 20 (No overband)
7	161	5		Clean & Seal
Road 21-SouthBound (starts at MP 3025)				
8	805	5	Ib	20 x 20
		5		20 x 20 (No overband)
		6		Clean & Seal
9	644	12	Kc	Clean & Seal
10	483	12	Da	20 x 20
		4		20 x 20 (No overband)
11	483	11		Clean & Seal
12	644	11	Ca	20 x 20
		6		20 x 20 (No overband)
13	483	14		Clean & Seal

Pre-installation Survey

Transverse cracks were the main cracking type at the site with a few longitudinal cracks. The initial condition of the cracks was evaluated in accordance with the study criteria and was found to meet the study parameters, as presented in Figure 4.31. A summary of crack rating is presented in Table 4.18.



a) Crack 2.6, Rating 4 (b) Crack 4.6, Rating 4.5 (c) Crack 5.6, Rating 5 (d) Crack 7.7, Rating 3.5
 Figure 4.31. Initial crack conditions in New York test site.

Table 4.18. A Summary of Initial Crack Ratings at New York Test Site.

Section #	Sealant ID	Average Rating	Average Crack Spacing (m)
1	Ob	3.7	37
2			39
3	Ca	3.9	33
4			32
5	Kc	3.9	36
6	Jd	3.3	46
7			55
8	Ib	3.3	53
9	Kc	3.9	45
10	Da	3.7	30
11			45
12	Ca	3.7	64
13			39

Installation Notes

Sealant installation took place during the week of September 11, 2012. Traffic control was provided by the contractor. Part of the working lane was closed to the traffic during installation and flaggers controlled the traffic in both directions through one lane. The contractor’s crew consisted of nine personnel (one finisher, one inspector, one router, one blower, one rout cleaner, two truck driver, two flaggers). Two different Crafcro model kettles were used in this project:

Crafco EZ 500 (125 gallon capacity) and 1000 (260 gallon capacity). Figure 4.32 shows the kettle and adapter used in most sections. Hot air lance and compressed air were used for cleaning the routs. Disk shape adapters (without swivel shoe) were used to apply sealant and a squeegee was used to apply overband. Routing was performed utilizing a pavement cutter.



Figure 4.32. Kettle (left) and disk shape adapter (right) used at New York test section sealant installation.

Similar to the other test sites, prior to heating sealants, the kettle was flushed out with approximately 25kg of the same sealants. After draining the kettle, 150kg to 250kg of sealant blocks were added to the kettle for each section. A time log detailing all activities is presented in Table 4.19. Sealant installation was completed in two days.

Table 4.19. New York Test Site Sealant Installation Time Log.

	Sections	Start Heating	Start Routing/Sealing	End	Kettle
Day 1	1,2	6:30 AM	9:10 AM	9:50 AM	Crafco SS250
	3,4,12,13	7:35 AM	10:00 AM	1:00 PM	Crafco SS125
	10,11	10:35 AM	1:10 PM	1:50 PM	Crafco SS250
	5,9	1:25 PM	2:22 PM	3:00 PM	Crafco SS125
Day 2	6,7	6:30 AM	7:30 AM	8:17 AM	Crafco SS250
	8	6:30 AM	8:35 AM	9:00 AM	Crafco SS125

The sealant temperature was closely monitored during installation. Temperature measurements were taken from the kettle panel and during sampling from the cans using a T-type thermocouple. Panel readings were recorded continuously; whereas, sample measurements were taken only during sampling.

Post-Installation Notes

After sealant installation, each crack was digitally documented as shown in Figure 4.33.

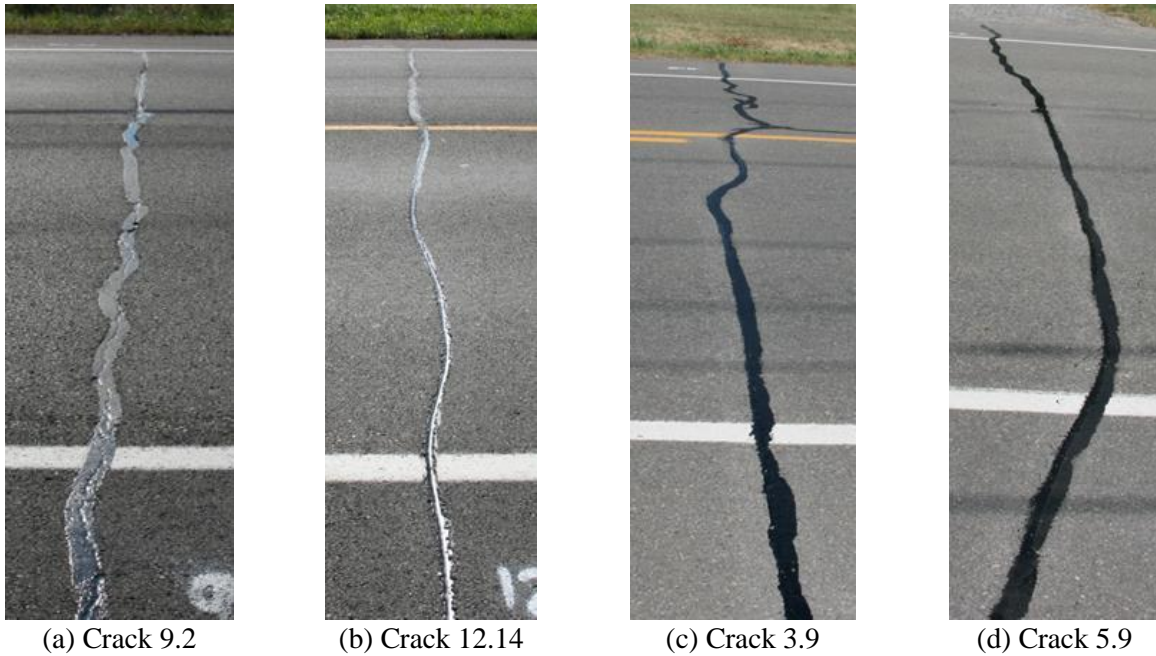


Figure 4.33. Crack sealant treatment in New York.

4.5.6 Virginia

Test Site Overview

The Virginia test site is located on Rte. 11 Northbound Lane at MP 7.51 to MP 9.04. The section is 2.5 km running from 1 km N NINT. A map for the test site is shown in Figure 4.34.

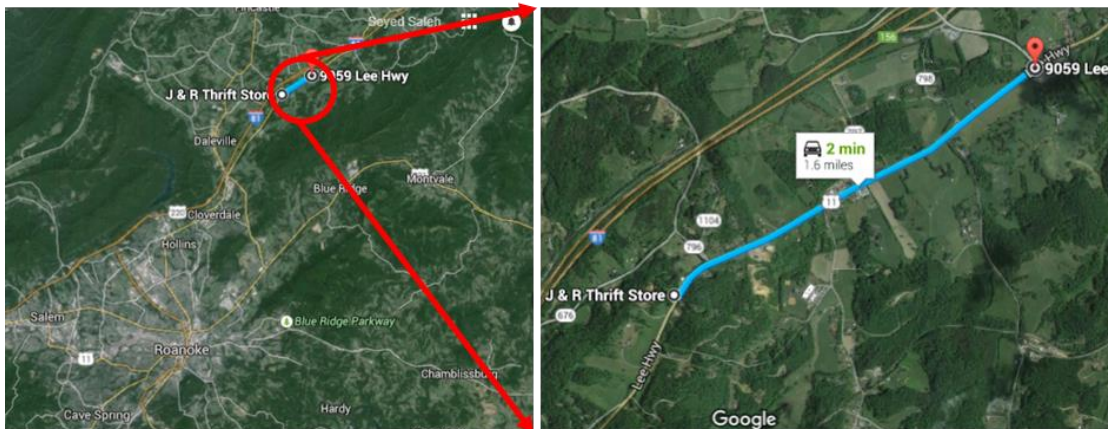


Figure 4.34. Virginia test site map.

The section consists of two 3.7 m wide lanes in each direction. A picture from the test site is shown in Figure 4.35.



Figure 4.35. Virginia test site overview.

Test Section Layout

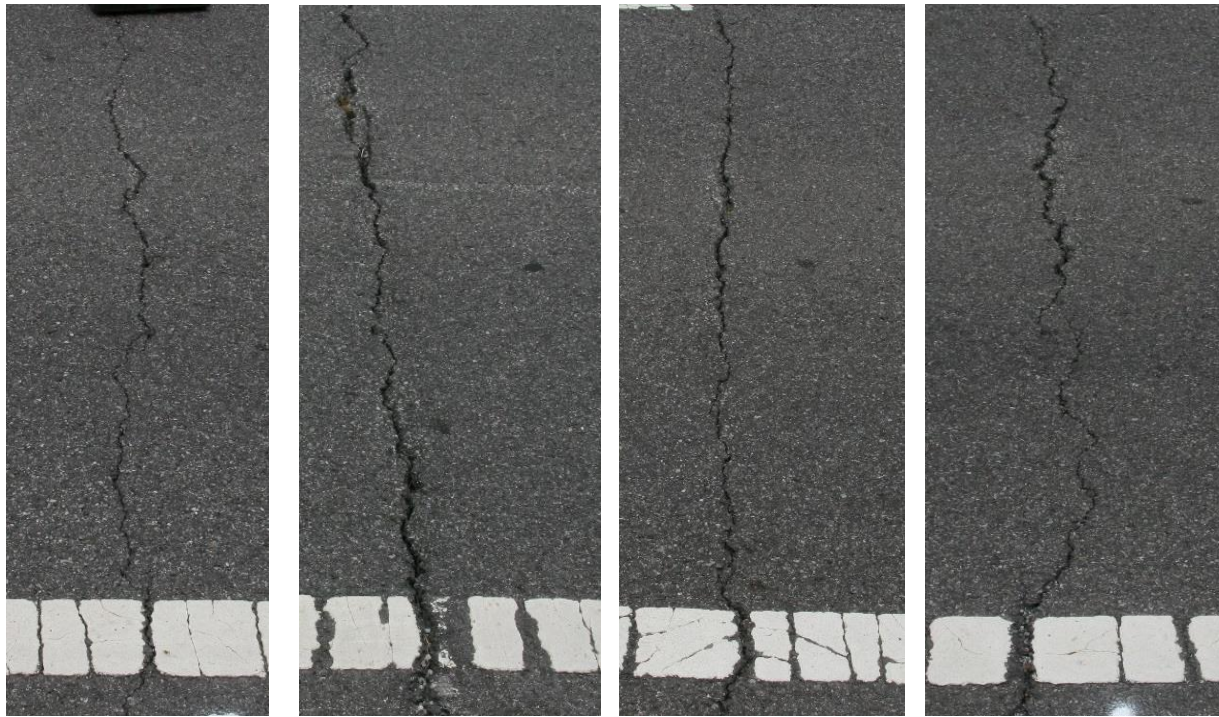
The test site consists of five sections. Four sealants were installed using a typical rout and seal treatment. A summary of the test sections is presented in Table 4.20.

Table 4.20. Virginia Test Section Layout.

Section #	Length (ft)	# of Cracks	Sealant ID	Rout Geometry (mm)
1	408	20	Lb	20 x 20
		10		Clean and Seal
2	502	20	Ed	20 x 20
		10		Clean and Seal
3	486	20	Ib	20 x 20
		10		Clean and Seal
4	412	20	Hb	20 x 20
		10		Clean and Seal
5	300	15	Hb	20 x 20
		10		Clean and Seal

Pre-installation Survey

Transverse cracks were the main cracking type at the site with a few longitudinal cracks. The cracks were evaluated in accordance with the study criteria and were found to meet the study's parameters, as shown in Figure 4.36. A summary of crack rating is presented in Table 4.18.



(a) Crack 2.13, Rating 4 (b) Crack 3.17, Rating 2 (c) Crack 3.29, Rating 4 (d) Crack 4.22, Rating 3
 Figure 4.36. Initial crack conditions in Virginia test site.

Table 4.21. A Summary of Initial Crack Ratings at Virginia Test Site.

Section #	Sealant ID	Average Rating	Average Crack Spacing (m)
1	Lb	2.9	14
2	Ed	2.7	17
3	Ib	2.5	16
4	Hb	3.0	14
5	Hb	3.0	18

Installation Notes

Sealant installation took place during the week of September 29, 2014. Traffic control was provided by the contractor. Part of the right lane was closed to the traffic during installation. The contractor’s crew consisted of five personnel (one finisher, one router, one blower, one rout cleaner, and one truck driver). Crafcro EZ 500 (475 L capacity) were used in this project, as shown in Figure 4.37. Hot air lance and compressed air were used for cleaning the routs. Disk shape adapters (without swivel shoe) were used to apply the sealant; overband was applied utilizing a squeegee; and a diamond saw pavement cutter was used for routing.



Figure 4.37. Kettle (left) and disk shape adapter (right) used at Virginia test section sealant installation.

Similar to the other test sites, prior to heating sealants, the kettle was flushed out with approximately 25kg of the same sealant. After draining the kettle, 150kg – 250kg of sealant blocks were added to the kettle for each section. The time log shown in Table 4.22 details the activities performed during sealant installation, which was completed in two days.

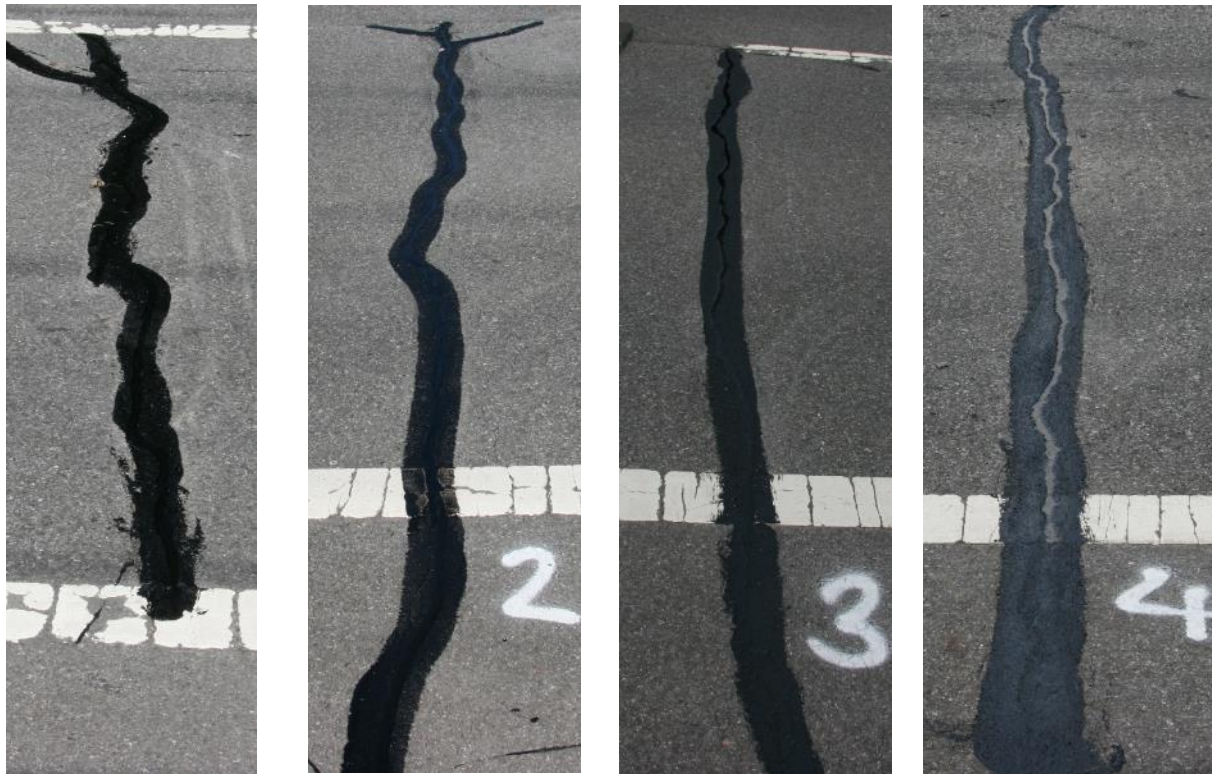
Table 4.22. Virginia Test Site Sealant Installation Time Log.

	Sections	Start Heating	Start Routing/Sealing	End	Kettle
Day 1	1	9:34 AM	10:00 AM	11:45 AM	Crafco SS125
	2	12:15 PM	12:40 PM	1:50 PM	Crafco SS125
Day 2	3	8:35 AM	8:45 AM	10:12 AM	Crafco SS125
	4, 5	10:55 AM	11:40 AM	12:40 PM	Crafco SS125

The sealant temperature was closely monitored during installation. Temperature measurements were taken from the kettle panel and during sampling from the cans using a T-type thermocouple. Panel readings were recorded continuously; whereas, sample measurements were taken only during sampling.

Post-Installation Notes

After sealant installation, each crack was digitally documented as shown in Figure 4.38.



(a) Crack 1.8

(b) Crack 2.14

(c) Crack 3.12

(d) Crack 4.18

Figure 4.38. Crack sealant treatment in Virginia.

4.5.7 Michigan

This test site was used for evaluating the performance of clean and seal treatment. The test site was installed and monitored by Michigan DOT. Failures associated with clean and seal treatment were mainly overband failure caused by low-tracking resistance in the summer or plow damage in the winter, and cohesive failure resulting from insufficient extendibility of sealant due to the crack opening during the cold season.

Crack Sealant Materials

Sixteen hot-pour sealants covering a wide spectrum of products were installed. The materials were mostly different from those used in the other test sites and were designed, installed, and monitored by the research team. However, since materials were collected at the time of installation and performance data were available, it was decided to add the test site to the test matrix. Table 4.23 presents a list of sealants, selected for this study. The selection of those sealants was in accordance with ASTM D6690 classifications and initial test results.

Table 4.23. List of Sealants Installed in Michigan Sections.

Section ID	Penetration @ 77°F (dmm)	Penetration @ 0°F (dmm)	Resilience
1	88	20	75%
2	68	9	32%
3	69	21	55%
4	58	13	70%
5	71	14	71%
6	69	25	70%
7	27	6	68%
8	68	15	60%
9	63	14	67%
10	83	11	55%
11	71	14	56%
12	65	16	70%
13	44	9	58%
14	95	4	106%
15	66	5	60%
16	63	12	62%

Test Site Overview

Michigan test site is located on the north and south bound lanes of US 127. The test sections are located between south Roscommon County line and Canoe Camp road. Total length of the section is 4.8 km. The test sections exist in the driving and passing lanes. The test site is located in the wet-freeze zone.



Figure 4.39. Pictorial view of a Michigan test site.

Two wireless temperature nodes were installed at the test site to monitor pavement and air temperature during the evaluation period. One of the nodes was installed in the proximity of the test site to avoid direct sunlight and to monitor the ambient temperature. Another node, shown in Figure 4.4, was buried in the pavement (2.5 cm below pavement surface) using an epoxy for measuring pavement temperature.



Figure 4.40. Wireless temperature nodes for ambient (left) and pavement (right) temperatures.

Cracks in this section were treated using clean and seal technique without routing. Figure 4.5 shows the crack and preparation operations.



Figure 4.41. Typical cleaning operation prior to crack filling.

A typical crack filling operation consists of cleaning and drying the cracks with compressed air, then applying the sealant using a wand and overbanding with a disk-shaped adaptor as shown in Figure 4.6. The width of the overband varied from 7 to 10 cm. Crack filling was completed using a disk adaptor that does not require a squeegee to apply an overband. After sealant installation, a final survey was conducted. Pictures of each crack were also taken to document the condition of sealed cracks.



Figure 4.42. Typical crack filling operations: Heating the material in a kettle (left), sealant and overband application using disk adaptor (middle), and the finished product (right).

4.6 Field Performance

Field inspection of crack sealant performance was conducted annually throughout the project: immediately after crack sealant installation and every winter season from February to March. Performance data were routinely collected, including visual distress identification, crack opening displacement, temperature measurements, and sampling for laboratory evaluation. This section summarizes the results obtained from the test section survey since 2011.

The sealants were also visually inspected for evaluating material failure, loss in bond, and failure within the pavement. Figure 4.43 shows the common types of failure observed during the service life of sealants. The distresses, considered in the performance monitoring process, are listed in Table 4.24. Pavement failure was recorded separately in the form of spalling in the routed cracks and hairline cracking developing near the routed and non-routed cracks.

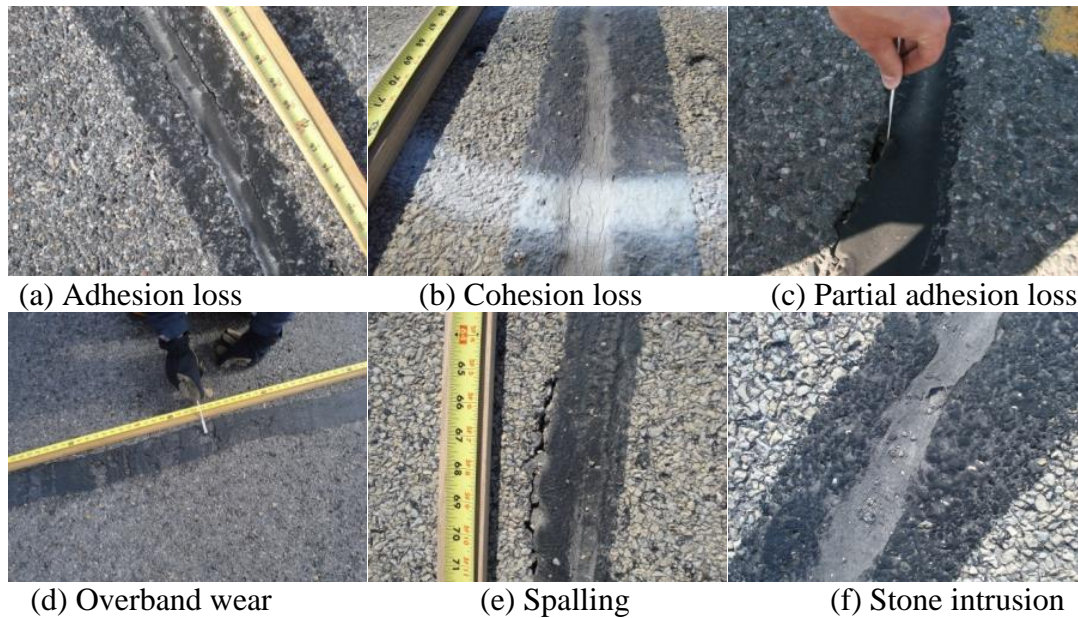


Figure 4.43. Commonly observed crack sealant distresses.

Table 4.24. Distress Types Considered in the Field Evaluation.

	Distress Type
Sealant material failure	Adhesion loss
	Cohesion loss
	Partial adhesion and cohesion loss
	Overband wear
	Tracking
	Stone intrusion
Pavement failure	Spalling
	Hairline cracking

4.6.1 Performance Data Collection

The field performance of sealants was evaluated by conducting a detailed field survey of crack sealants in accordance with National Transportation Product Evaluation Program (NTPEP) protocols. During each field survey, more than 200 cracks were evaluated and crack conditions were digitally documented. Specifically, each crack was quantitatively evaluated for percent length of full-depth adhesive/cohesive failure, percent length of partial-depth adhesive/cohesive failure, percent length of overband wear, percent length of spalling failure, and the amount of stone intrusion. Figure 4.44 illustrates a sample of the data collection procedure. An overview of each test site and a summary of collected data for the years 2012, 2013 and 2014 is presented hereafter.

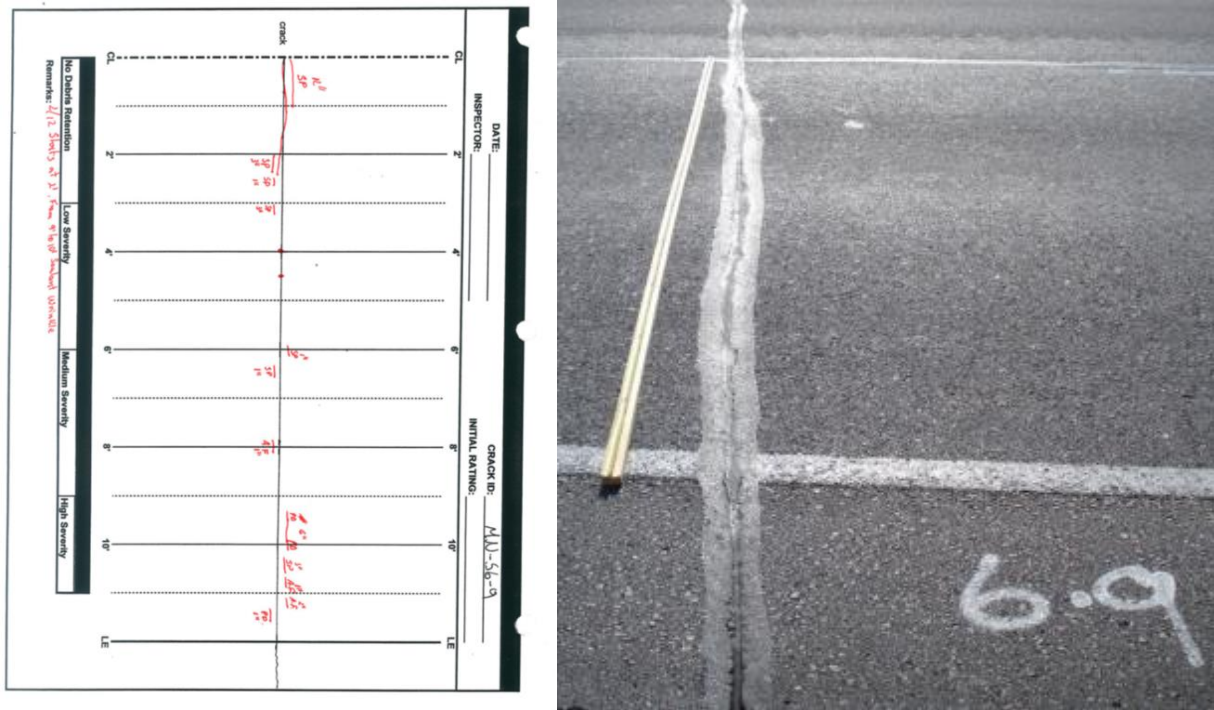


Figure 4.44. Data collection sheet for crack 6.9 at the Minnesota section (left) and a scale used to measure various distress lengths (right).

A weighted rating system known as the performance index (PI) is implemented to develop a sealant damage index. Earlier studies (Masson et al., 1999, Smith and Romine, 1999, and McGraw et al., 2007) are used as references to establish the rating system.

$$PI = 100 - (AC + PAC \times 0.5) \quad (4.1)$$

where, *AC* is the percentage of full adhesive and cohesive failures, and *PAC* is the percentage of partial adhesive and cohesive failure.

Sealant performance is summarized based on its PI. Statistical data are presented as boxplots (Figure 4.45) to allow for a comparison between different rout geometries. Performance data from each section are presented next, along with the statistical boxplots and overall yearly performance of each sealant.

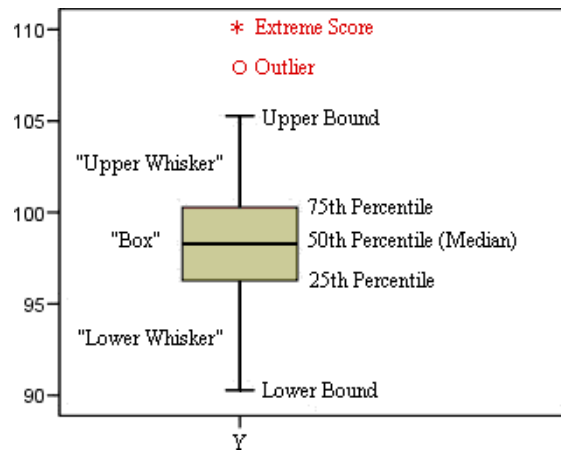


Figure 4.45. Boxplots example used in the analysis of survey data.

4.6.2 Test Sites Temperature and Displacement

During field installation, a wireless temperature node was installed at each test site to monitor the air temperature during the evaluation period (Figure 4.46). Ambient temperature data were used during test methods validation.

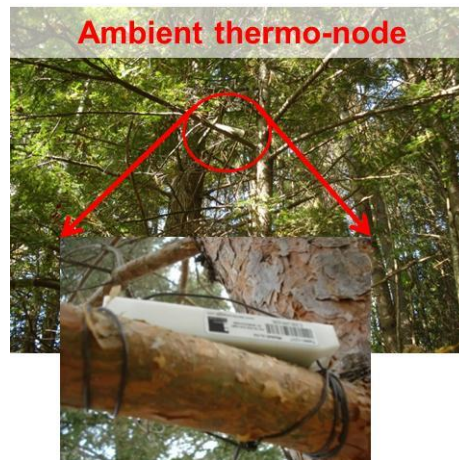


Figure 4.46. Wireless temperature node for ambient temperature.

The temperature log obtained from the Minnesota test site in the year following installation is presented in Figure 4.47. Detailed information for each test site is presented in Appendices A and B. Based on the temperature log, the minimum temperature during the second year was -24°C on February 1, 2013 and lasted for 2hrs. The detailed temperature log for the coldest day of the year is presented in Figure 4.48.

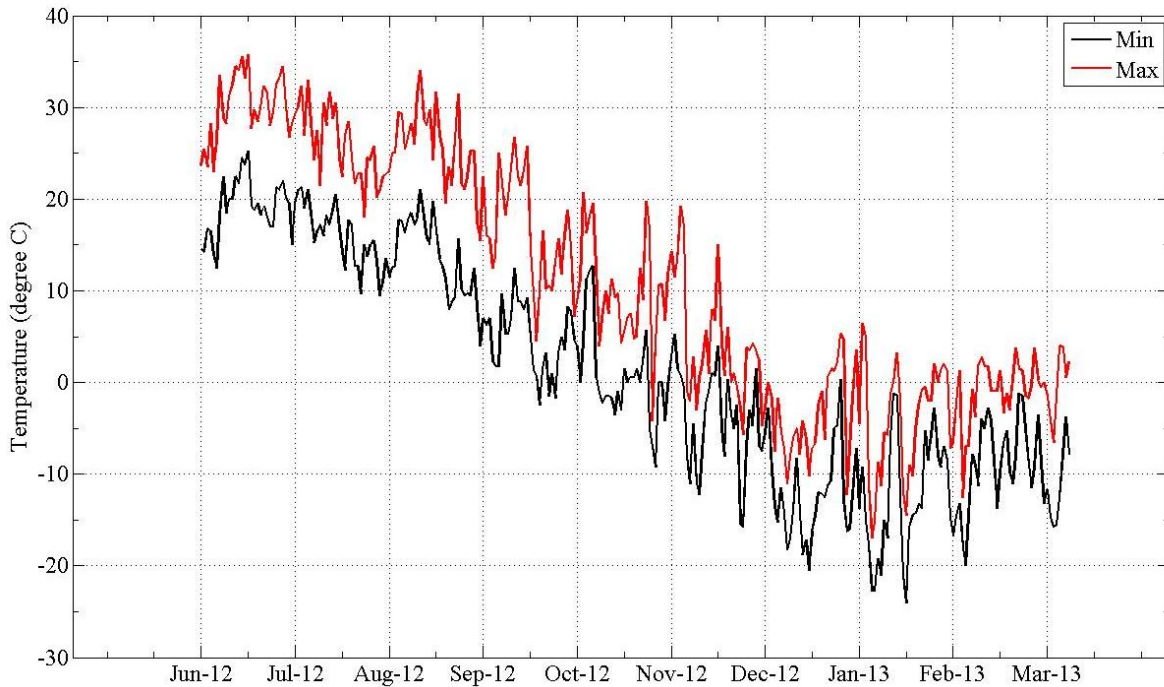


Figure 4.47. Ambient temperature for Minnesota test site in the year following installation.

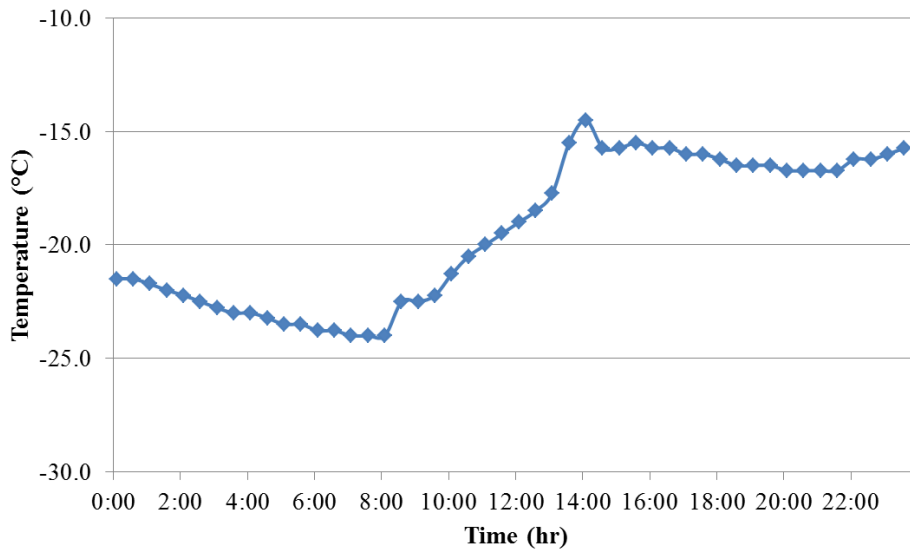


Figure 4.48. Daily variation of ambient temperature for the Minnesota test site.

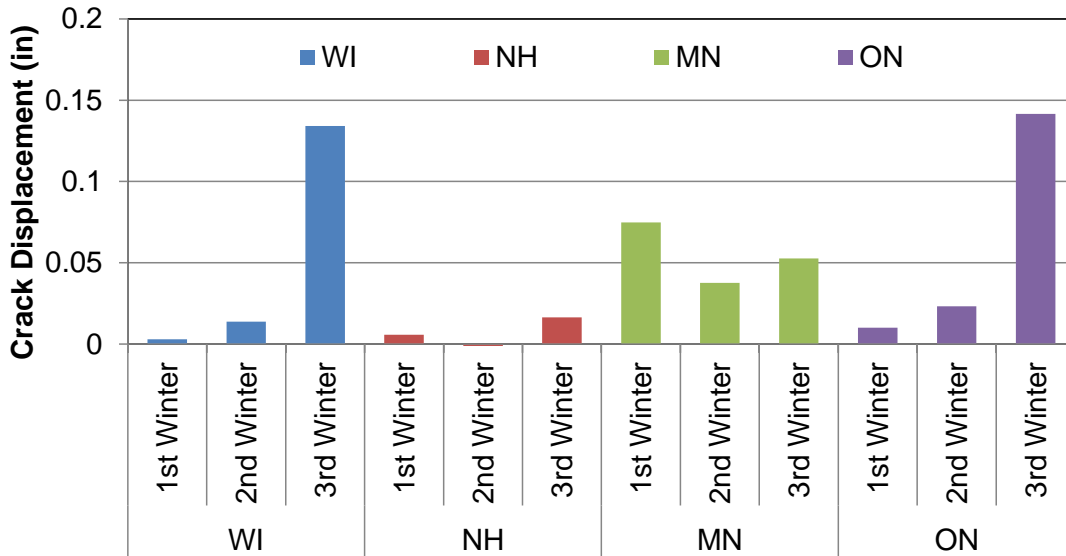
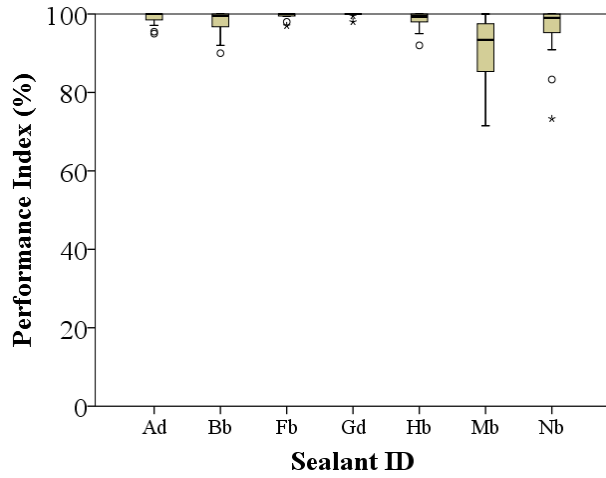


Figure 4.49. Average crack displacements measured at each test site.

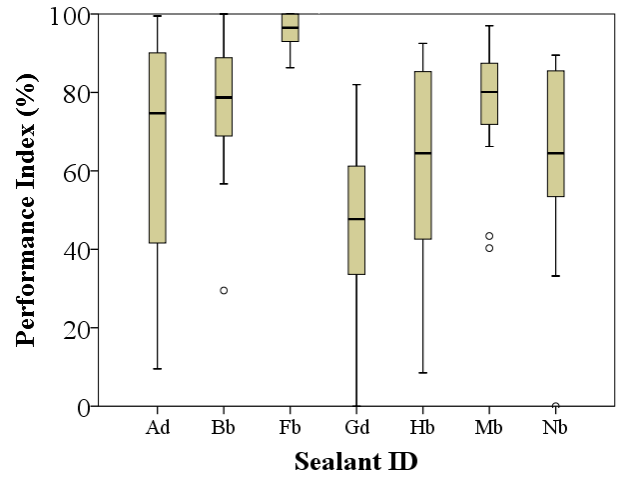
4.6.3 Minnesota Test Site

Overall, this test site consists of 24 sections installed with seven different sealants using various treatment methods. Each section had a replicate installed for field sampling. Replicate sections were not considered as part of the surveys. Therefore, field performance data from only 16 sections are used in this study.

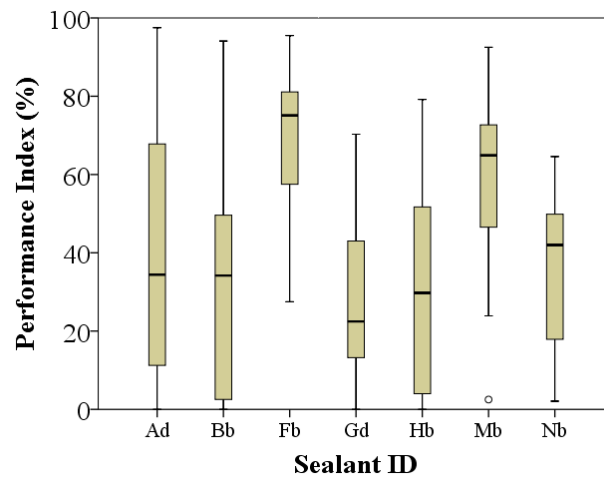
A summary of evaluation results in the Minnesota section is presented in Figure 4.50. Overall, significant changes in failures were observed from winter 2012 to winter 2014, mostly in adhesion loss, which allows water into pavement layers. The amount of adhesion loss was calculated based on the effective length of the crack, which is the total length of spalling along the crack subtracted from total crack length. Figure 4.51 shows that PI values dropped significantly in the second and third winters. Severe failure of the clean and seal sections was also observed. A sample of crack photos taken from each section in winter 2014 is presented in Figure 4.52. For clean and seal treated sections, it can be seen that the cracks are clearly visible through the sealant. Surface cohesive cracks were observed in the rout and seal sections, which could be related to sealant aging.



(a) Winter 2012

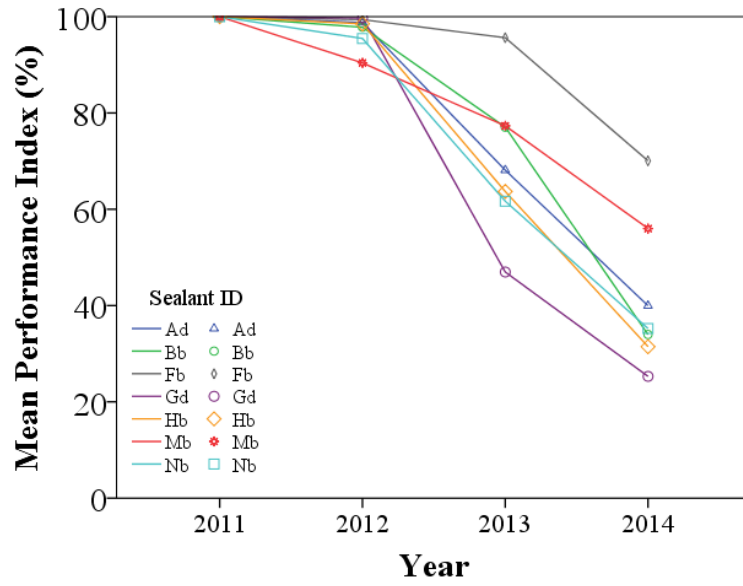


(b) Winter 2013

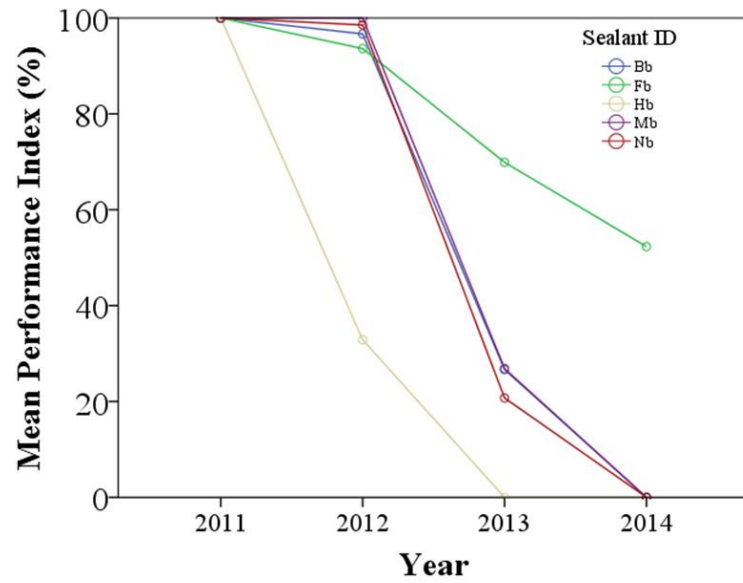


(c) Winter 2014

Figure 4.50. Statistical boxplots for the Minnesota test site in 2012-2014.



(a) Rout and seal sections



(b) Clean and Seal Sections

Figure 4.51. Overall performance of sealants in the Minnesota test site since 2011.



(a) Crack 3.9



(b) Crack 5.9



(c) Crack 6.1



(d) Crack 7.9



(e) Crack 9.5



(f) Crack 10.5



(g) Crack 11.3



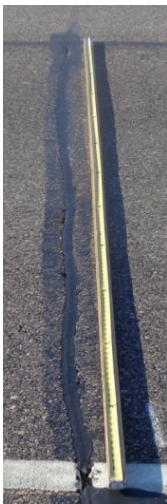
(h) Crack 12.1



(i) Crack 14.7



(j) Crack 16.9



(k) Crack 17.9



(l) Crack 20.1



(m) Crack 21.3



(n) Crack 23.7

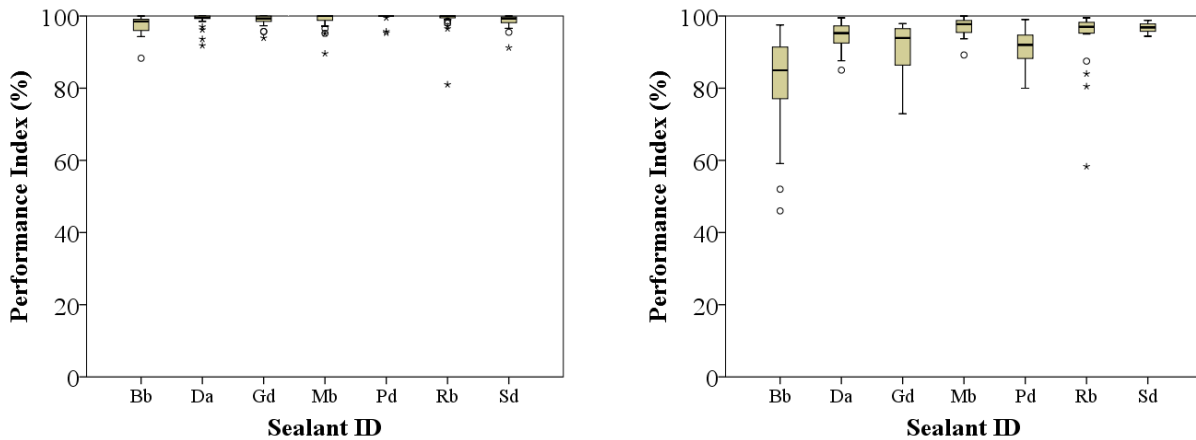


(o) Crack 25.19

Figure 4.52. Sample pictures from the Minnesota test sections in winter 2014.

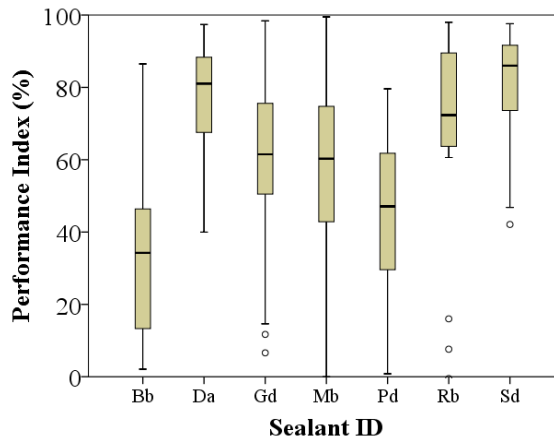
4.6.4 Ontario Test Site

The test site consists of 16 sections installed with seven different hot-poured sealants. A summary of evaluation results in the Ontario section is presented in Figure 4.53. Unlike the Minnesota test site, the sealants were still in good condition in winter 2013. However, significant failures occurred in winter 2014. Figure 4.54 shows that for the third winter; the PI value dropped significantly. A sample of crack pictures taken from each section in winter 2014 is presented in Figure 4.55. Similar to the Minnesota test site, sections treated with clean and seal failed earlier than other treatments primarily due to overband wear or cohesive loss.



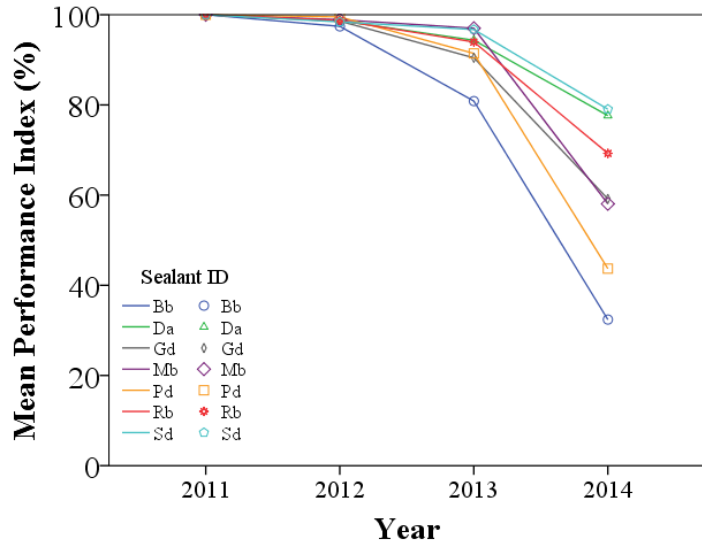
(a) Winter 2012

(b) Winter 2013

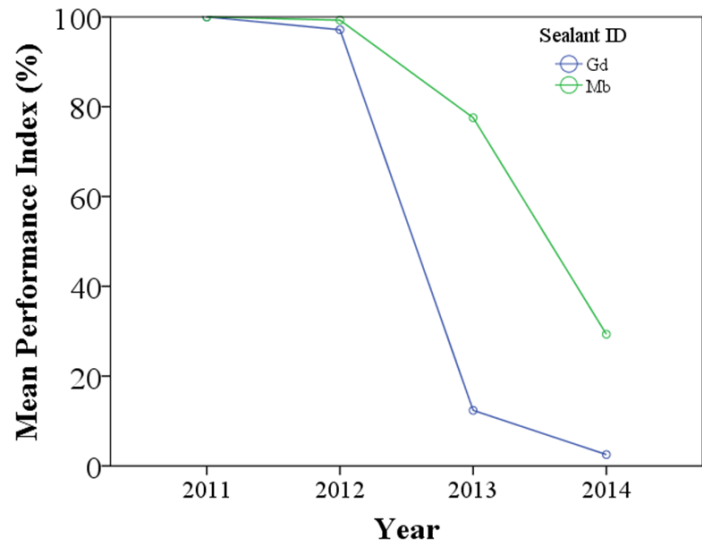


(c) Winter 2014

Figure 4.53. Statistical boxplots for the Ontario test site in 2012-2014.



(a) Rout and seal sections



(b) Clean and Seal sections

Figure 4.54. Overall performance of sealants in the Ontario test site since 2011.



(a) Crack 1.3



(b) Crack 2.8



(c) Crack 3.7



(d) Crack 4.9



(e) Crack 5.2



(f) Crack 6.3



(g) Crack 7.2



(h) Crack 8.8



(i) Crack 9.2



(j) Crack 10.2



(k) Crack 11.9



(l) Crack 12.5



(m) Crack 13.3



(n) Crack 14.3



(o) Crack 15.8

Figure 4.55. Sample photos from the Ontario test sections in winter 2014.

4.6.5 New Hampshire Test Site

The test site consists of 19 sections. A summary of evaluation results in New Hampshire section is presented in Figure 4.56 for different years. Similar to the Minnesota test site, sealant failures started to become visible in 2013 and accelerated in winter 2014. Figure 4.57 shows that the PI values dropped significantly in the second and third years. A sample of crack pictures taken from each section in winter 2014 is presented in Figure 4.58. Sections treated with clean and seal were again among the first to fail. Another observation was the wearing of the overband for almost all sealants.

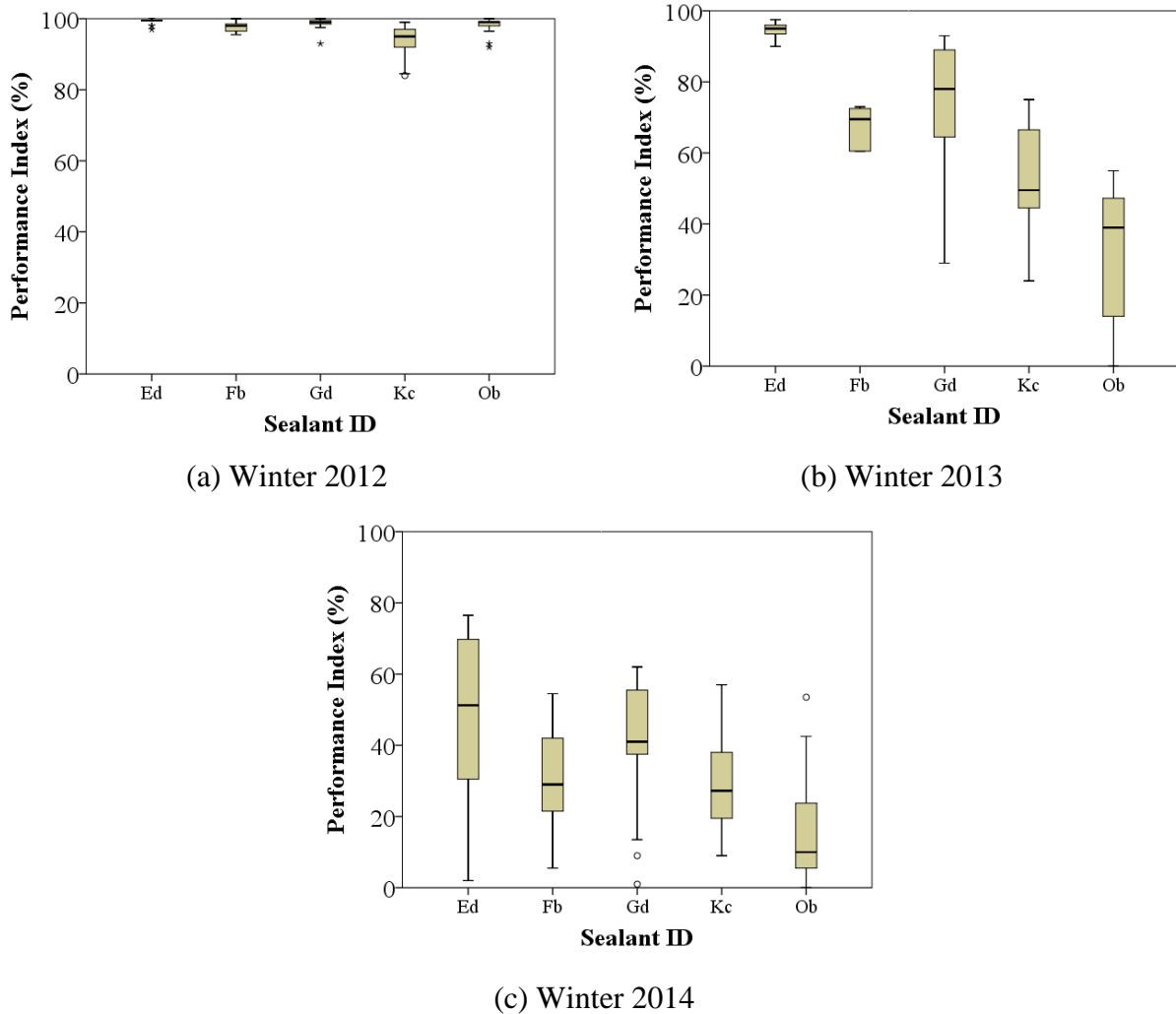
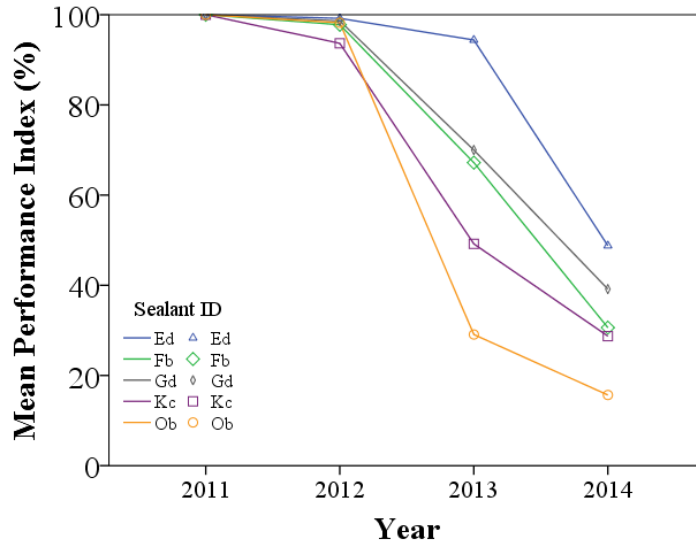
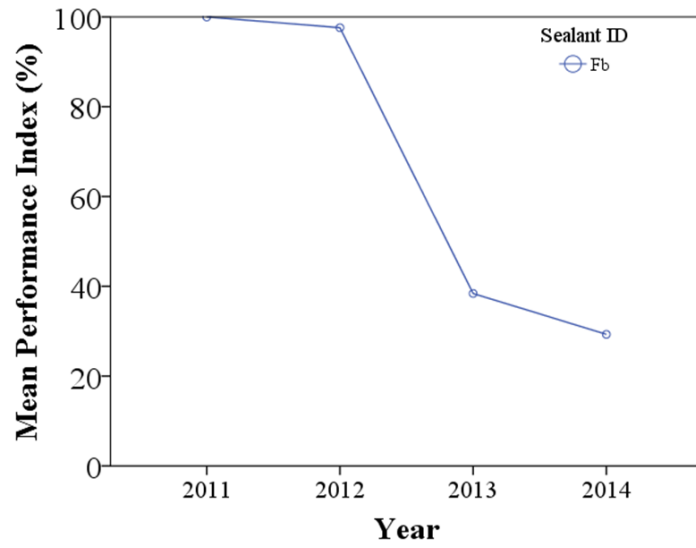


Figure 4.56. Statistical boxplots for the New Hampshire test site in 2012-2014.



(a) Rout and seal sections



(b) Clean and seal Sections

Figure 4.57. Overall performance of sealants in the New Hampshire test site since 2011.



(a) Crack 1.8



(b) Crack 2.5



(c) Crack 3.3



(d) Crack 4.7



(e) Crack 6.6



(f) Crack 8.8



(g) Crack 9.8



(h) Crack 10.9



(i) Crack 12.9



(j) Crack 13.4



(k) Crack 14.7



(l) Crack 15.4



(m) Crack 16.2



(n) Crack 17.8



(o) Crack 18.9

Figure 4.58. Sample photos from the New Hampshire test sections in winter 2014.

4.6.6 New York Test Site

The test site consists of 13 sections. A summary of evaluation results in New York section is presented in Figure 4.59 for winters 2013 and 2014. The New York test site was subject to two winters due to one-year late installation. In winter 2013, most sealants were performing well except sealant Ca. However, after the second winter, the performance of most of sealants changed significantly. It was expected to see a complete failure for some of the sealants after winter 2015. The drop in PI values can easily be seen in Figure 4.60. A sample crack picture taken from each section in winter 2014 is presented in Figure 4.61. Sections treated with clean and seal failed entirely within a year and a half following installation.

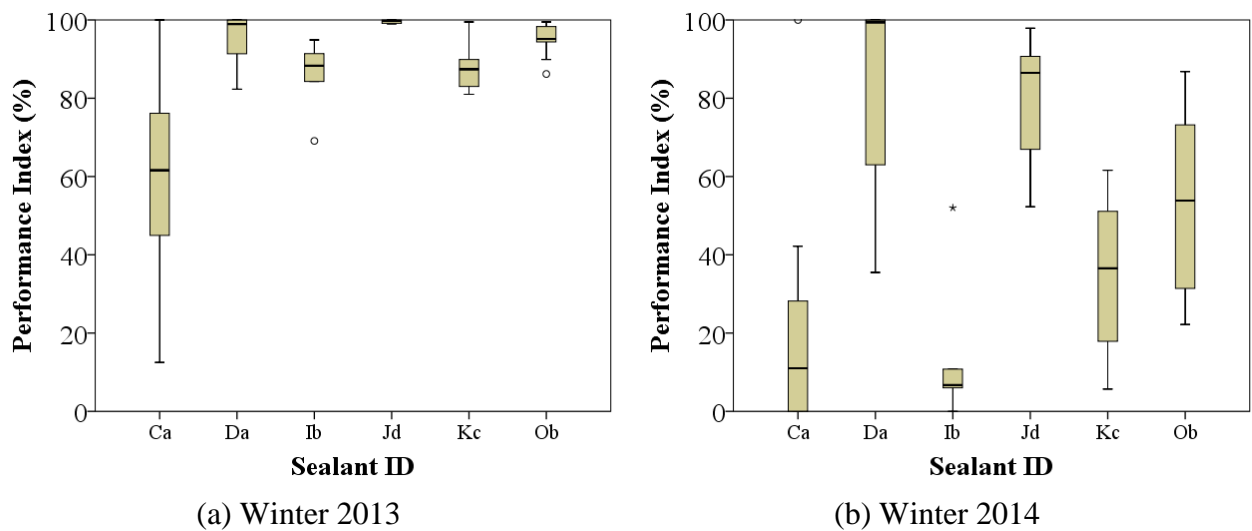
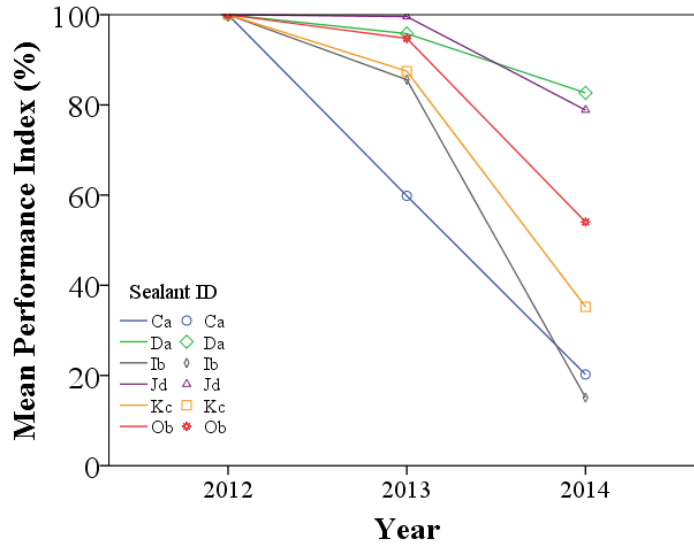
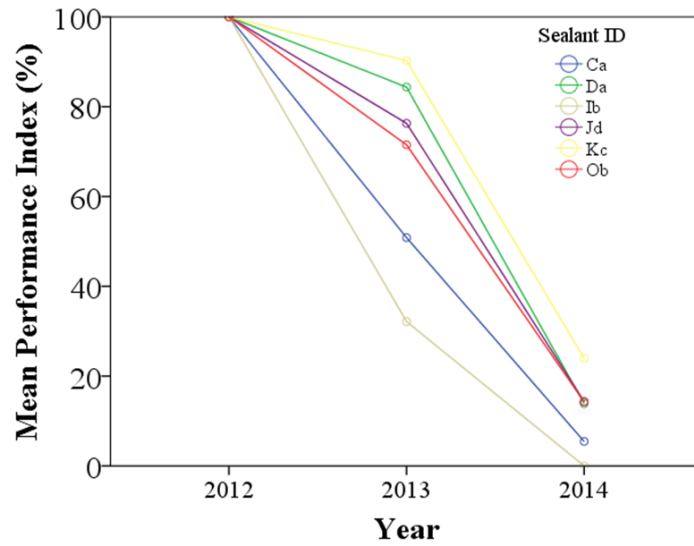


Figure 4.59. Statistical boxplots for the New York test site in 2013-2014.



(a) Rout and Seal sections



(b) Clean and Seal sections

Figure 4.60. Overall performance of sealants performance in New York test site since 2012.



(a) Crack 1.1



(b) Crack 2.8



(c) Crack 3.7



(d) Crack 4.13



(e) Crack 5.8



(f) Crack 6.5



(g) Crack 7.2



(h) Crack 8.4



(i) Crack 8.12



(j) Crack 9.4



(k) Crack 10.9



(l) Crack 11.2



(m) Crack 12.6



(n) Crack 13.2

Figure 4.61. Sample photos from the New York test sections in Winter 2014.

4.6.7 Wisconsin Test Site

This test site was partitioned into five sections for installing five different sealants. All sections on this test site had standard rout geometry of 20 × 20 mm. A summary of evaluation results for the Wisconsin test site for winters 2012, 2013, and 2014 is presented in Figure 4.62. Similar to most other test sites, the site underwent three winters. Until winter 2013, most sealants were performing well except Pb, which was in fair condition and sealant Fb which was in poor condition. However, after the third winter, only two out of five sealants were performing well (PI higher than 70). It was expected to see some sealants fail completely after winter 2015. The drop in PI values can easily be seen in Figure 4.63. A sample crack picture taken from each section in winter 2014 is presented in Figure 4.64.

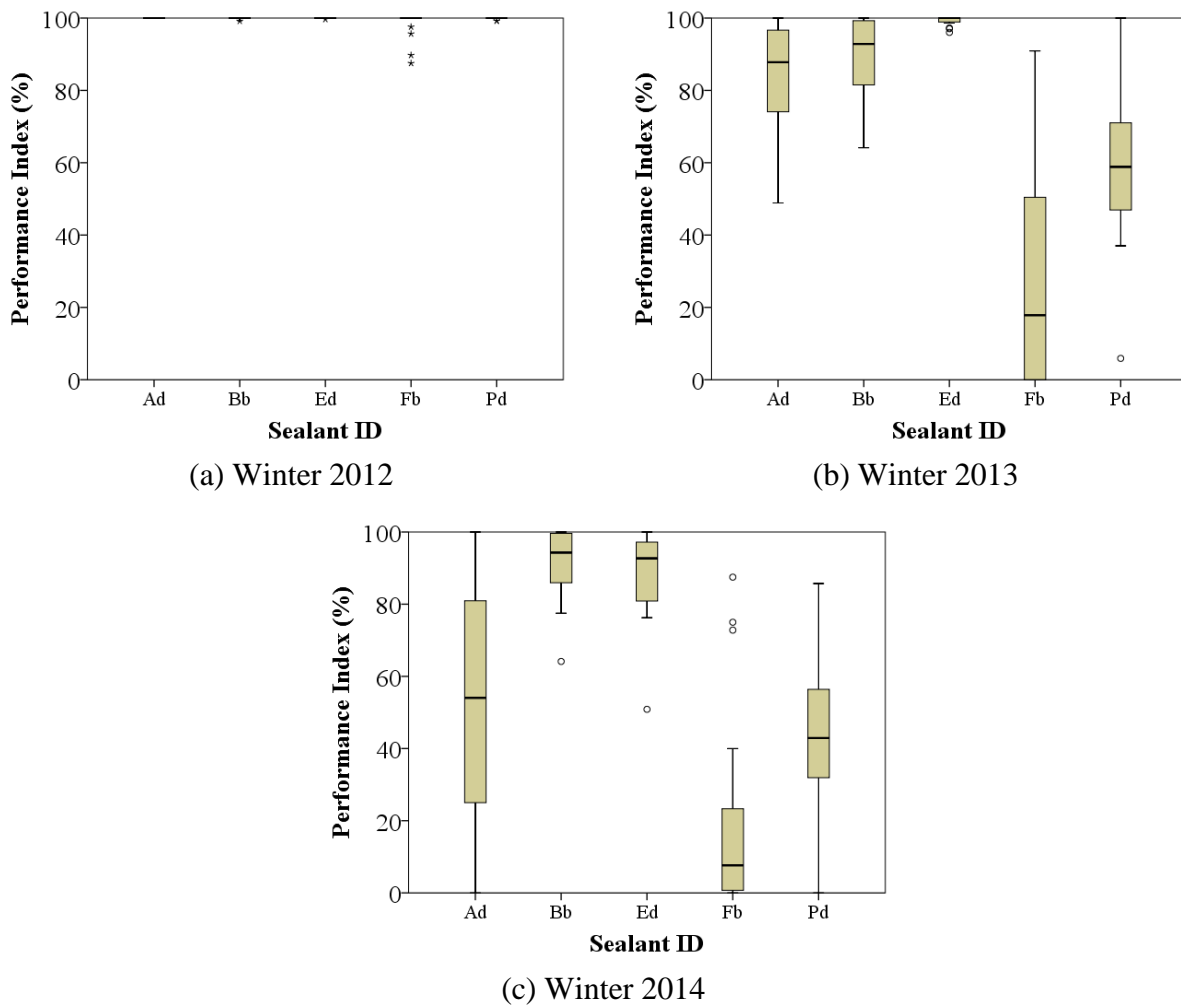


Figure 4.62. Statistical boxplots for the Wisconsin test site in 2012-2014.

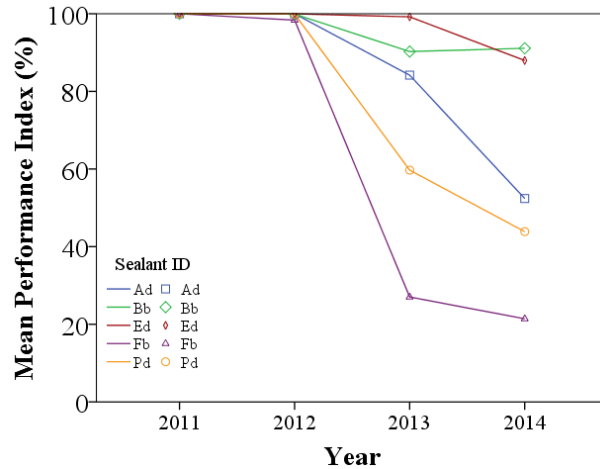


Figure 4.63. Overall performance of sealants in Wisconsin test site since 2011.



(a) Crack 1.17 (b) Crack 2.5 (c) Crack 3.27 (d) Crack 4.8 (e) Crack 5.13

Figure 4.64. Sample photos from the Wisconsin test sections in winter 2014.

4.6.8 Virginia Test Site

Four different sealants were installed in the Virginia test site. Each test section contains both clean and seal and rout and seal treatments. A standard rout geometry of 20×20 mm was used for rout and seal sections. A summary of evaluation results in the Virginia test site for winters 2015 and 2016 is presented in Figure 4.65. The Virginia test site was subject to two winters due to late installation (Fall 2014). All sealants were performing well after the first winter, and only one sealant (Ed) was performing well (with average PI higher than 70%) after the second winter. It was expected to see a significant failure for most sealants after winter 2017. A significant drop in PI values after two winters is clear in Figure 4.66. A sample crack picture taken from each section in winter 2014 is presented in Figure 4.67.

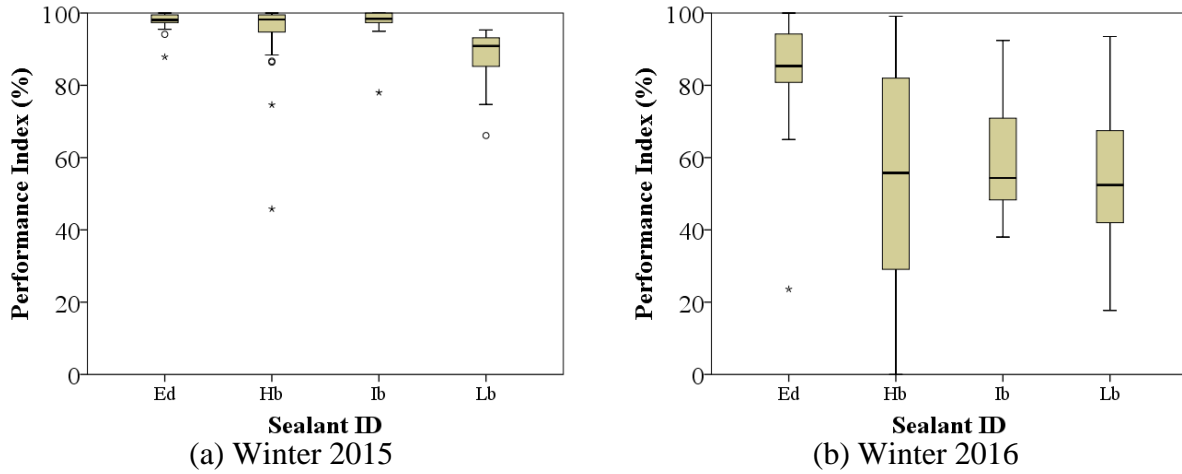


Figure 4.65. Statistical boxplots for the Virginia test site in 2015-2016.

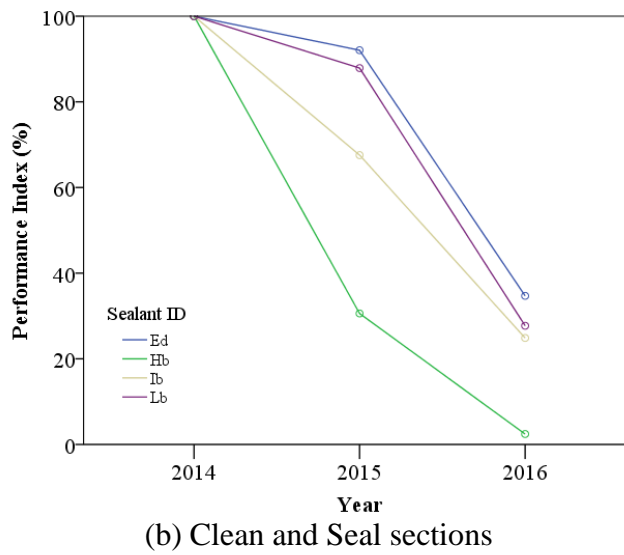
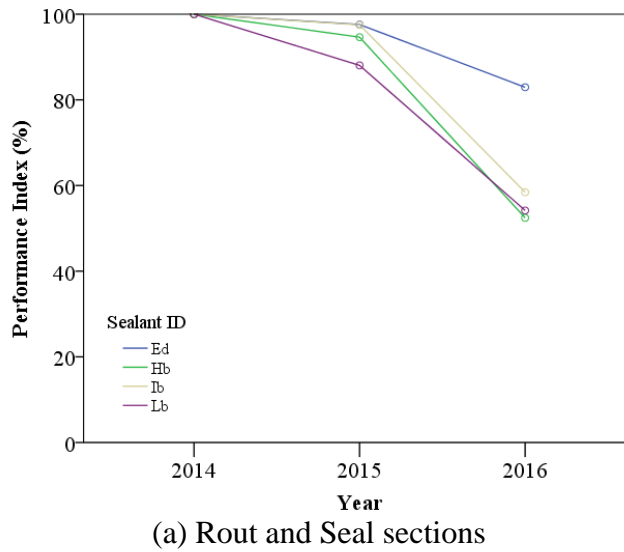


Figure 4.66. Overall performance of sealants in the Virginia test site since 2014.

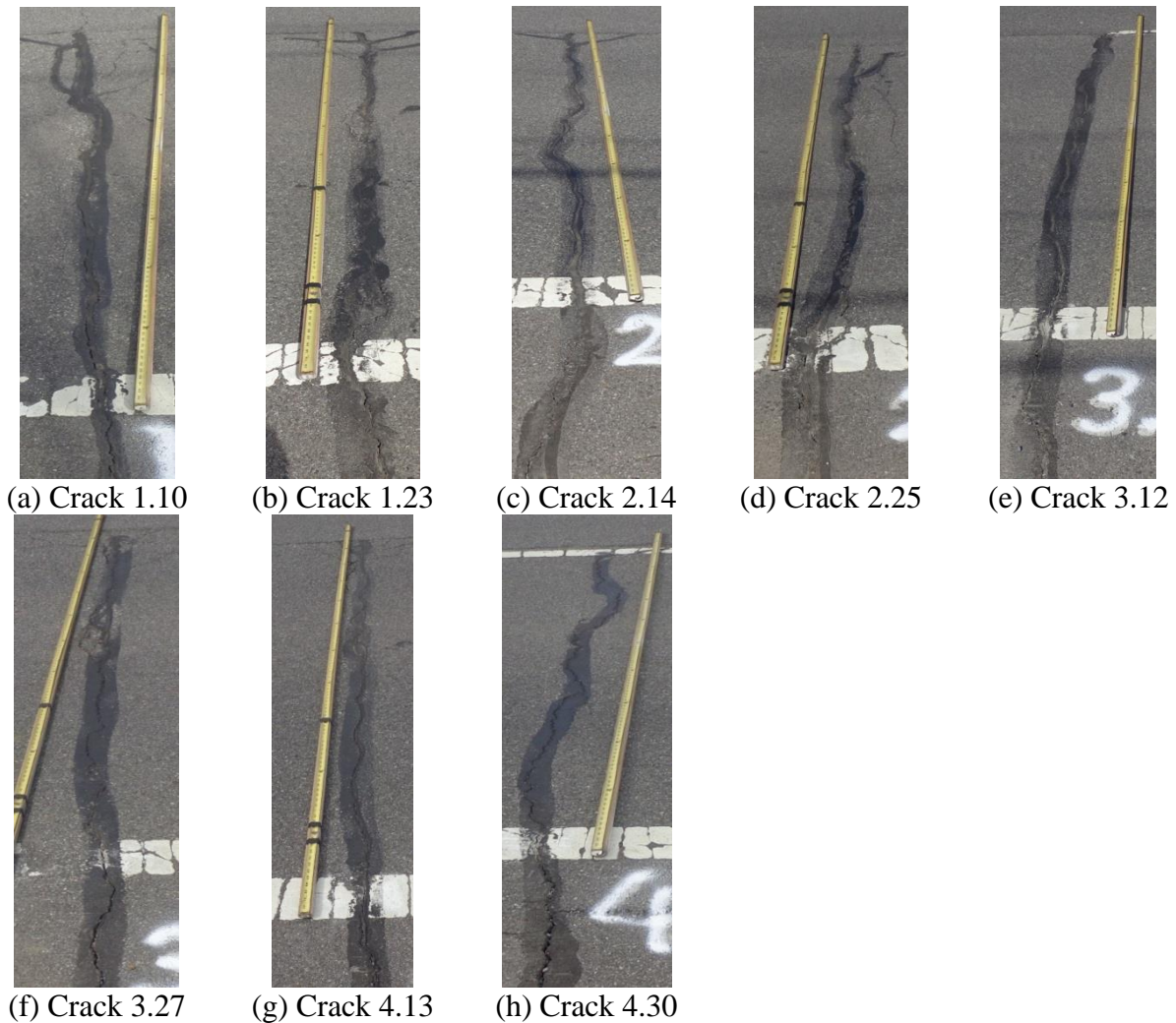


Figure 4.67. Sample photos from the Virginia test sections in winter 2016.

4.6.9 Michigan Test Site

Field performance data were obtained from the Michigan test site installed in 2010. Crack sealant field performance was inspected twice per year, at the end of every summer and during each winter season. Performance data were collected during site visits, including visual distress identification, crack opening displacement, temperature measurements. This report includes the results obtained from the survey data for the test section since 2011. The common crack filling failures as observed from the site were cohesive failures resulting from crack movements and overband failure due to tire tracking and plows (Figure 4.68). The sample pictures from sealants field performance are presented in Figure 4.69. Sample pictures for sealants field performance: Good performance (first row) and poor performance (second row).

The sealant in crack 1.1 failed due to poor cohesive performance while the overband was still in contact; the sealant in cracks 14.9 and 16.6 failed due to poor cohesive and overband performance.



(a) Cohesive failure



(b) Overband failure

Figure 4.68. Common failure modes of clean and seal treatment.



(b) Crack 5.7



(c) Crack 9.8



(d) Crack 8.7



(e) Crack 1.1



(h) Crack 14.9



(g) Crack 16.6

Figure 4.69. Sample pictures for sealants field performance: Good performance (first row) and poor performance (second row).

Field Data Collection

The field performance of sealants was evaluated by MDOT by conducting a detailed field survey in accordance with NTPEP protocols. Field surveys were conducted twice every year (winter and summer) after clean and fill installation of hot-poured crack sealants. During each field survey, approximately 160 cracks were evaluated. Each crack was quantitatively evaluated for percent length of cohesive failure and percent length of over band wear as plow abrasion.

Ambient air temperature was also monitored continuously. A data acquisition system was installed in the site to collect and store temperature data. Temperature data were downloaded to a laptop during the site visits and an accumulative variation of temperature was recorded.

Figure 4.70 shows the maximum and the minimum average of site temperatures using a wireless thermonode as installed inside the pavement.

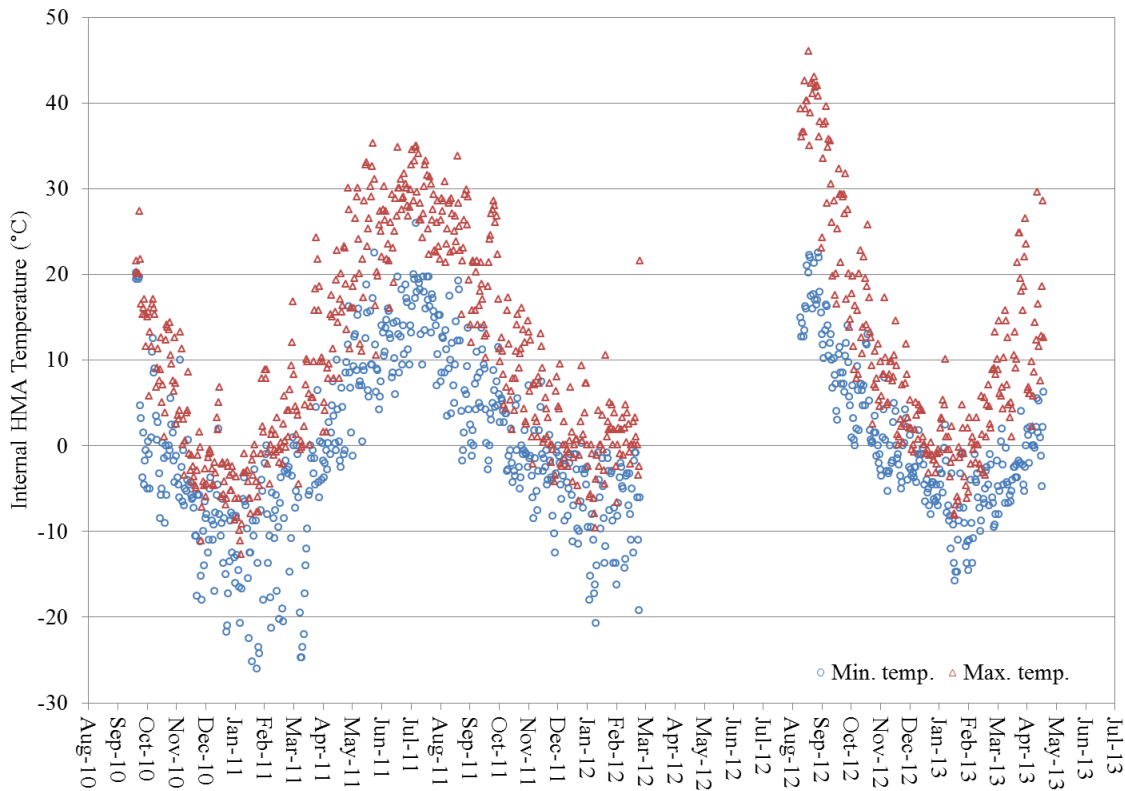


Figure 4.70. Maximum and minimum AC temperature history of the test site.

The main purpose of recording temperature readings was to investigate the effect of temperature on crack sealant cohesive and plow failure in the field and to study temperature performance ranges of the sealants.

Overall Performance of All Sealants

A weighted rating system known as performance index (PI) was implemented to develop a sealant damage index. Earlier studies (Masson et al., 1999, Smith and Romine, 1999, and McGraw et al., 2007, Ozer et. al. 2015) were used as references to establish the rating system.

$$PI = 100 - \%OBF \quad (4.2)$$

$$PI = 100 - \%CF \quad (4.3)$$

where *CF* is the percentage of cohesive failures and *OBF* is the percentage of overband failure caused by plow abrasion or sealant tracking. Unlike the NTPEP protocols, overband failure is added based on its significant effect on clean and fill treated cracks.

The overall performance of various sealants under prevailing climatic changes and actual traffic conditions was evaluated using PI. The PI used for both types of failures was simply determined by subtracting the percentage of corresponding failure value from a value of 100. The PI of all crack sealants installed in Michigan test site was calculated from 2010 onward based on overband and cohesive failure, respectively, as presented in Figure 29 and Figure 30.

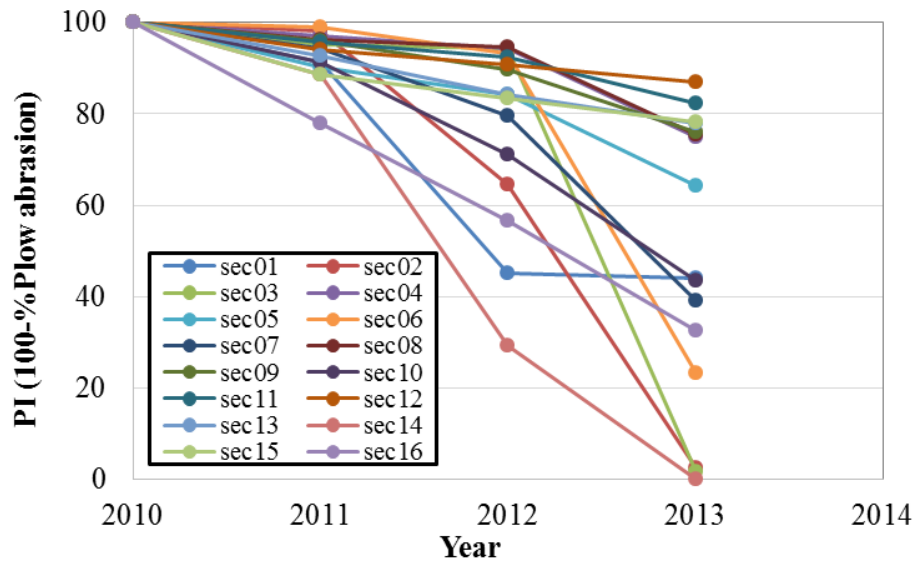


Figure 4.71. Performance index of all sealants based on overband failure.

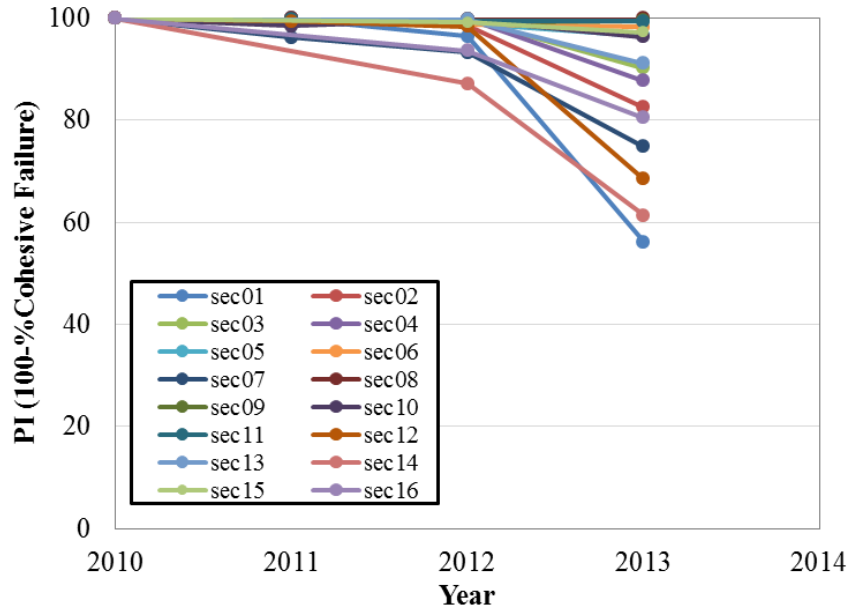


Figure 4.72. Performance index based on cohesive failure for different sealants.

Figure 4.71 presents PI of sealants based on the plow abrasion. By the end of 2013, three general groups of sealants were identified; Sections 2, 3 and 14 had the highest overband failure.

Field Performance of Selected Sealants

Six crack sealants were selected as reported in Table 4.25. The corresponding ASTM D6690 classification of each sealant is tabulated as provided by the manufacturer from Michigan test Deck (Sections 03, 04, 06, 07, 12, and 16). The selection criteria were based on the initial field performance of crack sealants (Figure 4.71 and Figure 4.72). Out of six hot-poured crack sealants selected in this study, three were Type I (section 04, 06, and 07), one was Type II (section 16), and two were Type IV (section 03 and 12). The sealants were classified per ASTM D 6690 based on effectiveness of the seal with respect to climatic conditions, low-temperature performance, and the percentage of extension. Based on the field performance and as a result of resistance against plows, sealants at Section 04 and 12 reflected good field performance; Sections 07 and 16 demonstrated fair performance; and Sections 03 and 06 had poor performance. Because of their cohesive properties, sealants at Sections 03, 04, and 06 had very good or good performance, while sealants at Sections 07, 12, and 16 had fair or poor performance. Table 4.25 shows consistent conditions during installation.

Table 4.25. ASTM Specification for the Selected Crack Sealants.

Section (ID)	ASTM D6690 Type	Installation Temperature (°C)	Melting Time (Min)	Field Performance	
				Plow Abrasion	Cohesive
03	IV	193	50	poor	good
04	I	193	45	good	good
06	I	193	45	poor	very good
07	I	193	45	fair	poor
12	IV	193	50	good	poor
16	II	193	45	fair	fair

Conventional ASTM D 5329 test properties of crack sealants are reported in Table 4.26. The sealant at Section 07 was made of relatively stiff material and offered zero flow value. Also, the sealant at Sections 04, 07, and 16 failed the bond test at -28°C and 50% extendibility. The sealants applied at Sections 06 and 12 showed excellent bond test results.

Table 4.26. Conventional ASTM Test Properties of Selected Crack Sealants.

Section (ID)	Properties of crack sealants as per ASTM D 5329-04						Resilience (%)
	Pen. at 21.1°C, 150g, 5sec, cone	Pen. at -17.8°C, 150g, 5sec, cone	Flow at 60°C, 5hr.s	Bond test at -28.9°C (50% extendibility)			
	(dmm)	(dmm)	(mm)	1st Cycle	2nd Cycle	3rd Cycle	
03	69	21	100	P	F	F	55
04	58	13	1.5	F	F	F	70
06	69	25	0.5	P	P	P	70
07	27	6	0	F	F	F	68
12	65	16	1	P	P	P	70
16	63	12	8	F	F	F	62

The performance of selected crack sealants was evaluated using SPSS (Statistical Package for the Social Science) software. Sealants were statistically analyzed based on their performance index as calculated from cohesive failure, overband failure, and overall performance. The main purpose of the statistical analysis was to find a relationship between laboratory results and field performance. The statistical data are presented as boxplots to allow for a comparison between different sealants.

Performance of Sealant Based on Overband Failure

The overband failure of sealants in winter was considered as plow abrasion although it happens due to insufficient tracking resistance during summer. In hot seasons, the shear strength of

sealants is reduced significantly, so they may be picked up or tracked. Summary of statistical results, shown in Figure 4.73, was produced for each year using boxplots to study data variations. It can be seen that the sealant at Section 12 shows the least amount of changes in the PI value, while the sealant at Section 3 shows a complete overband failure. Sealants at Sections 6, 7, and 16 exhibited similar PI values.

The PI based on plow abarasion of six sealants for the initial three years of field performance is shown in Figure 4.74. A gradual reduction in the PI value from 2011 to 2012 was observed for all sealants.

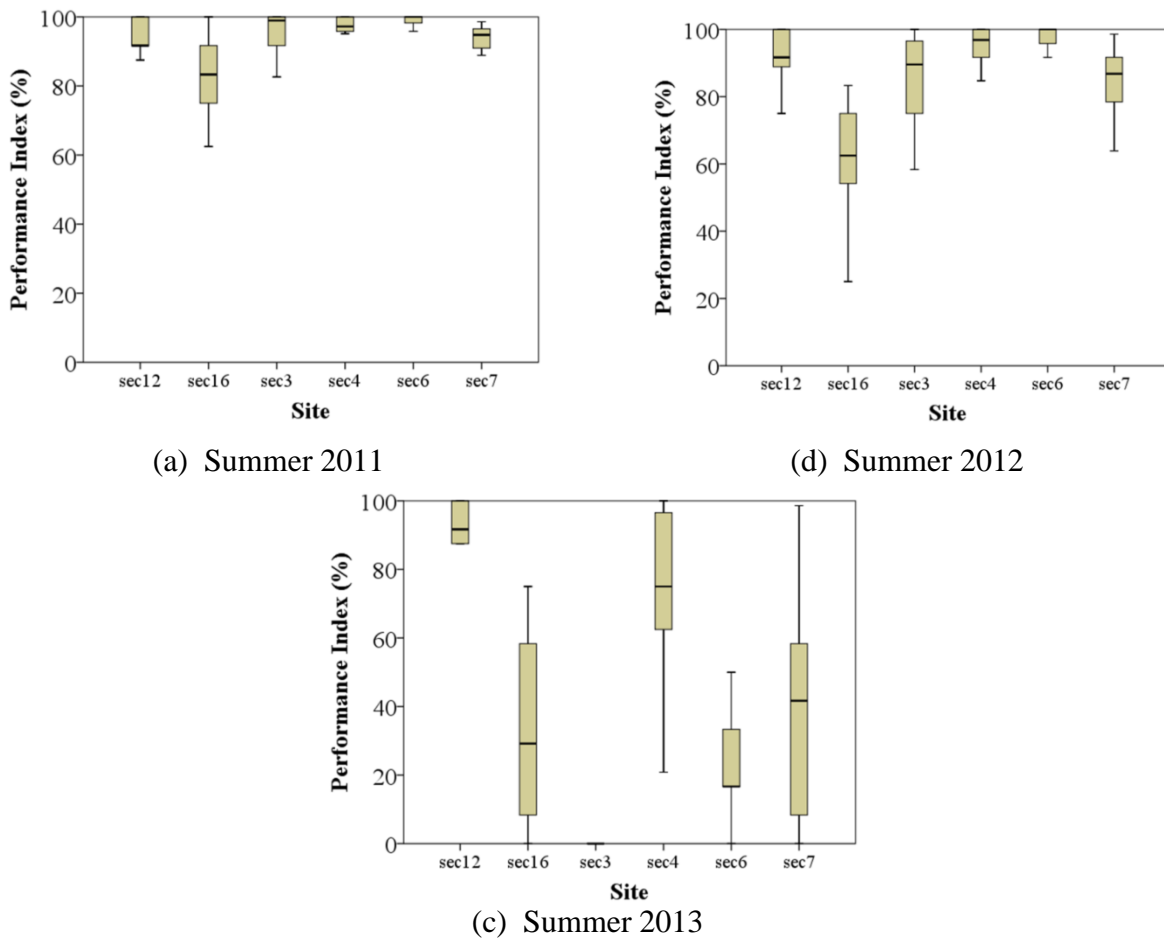


Figure 4.73. Boxplots based on overband failure since 2011.

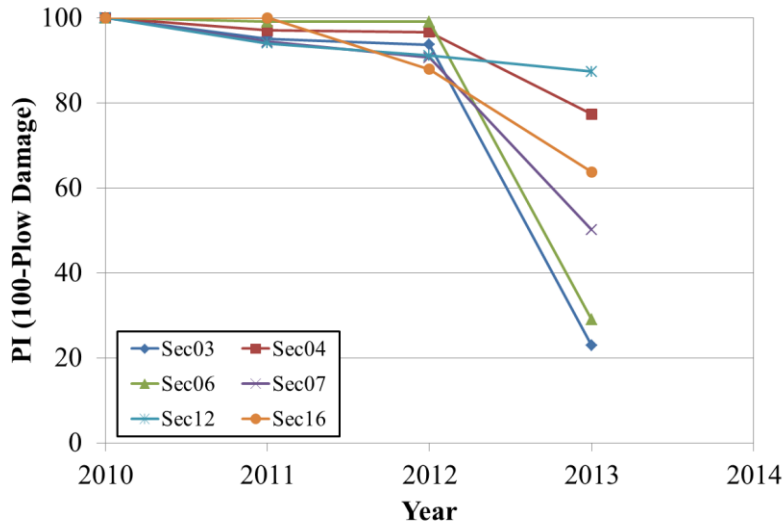


Figure 4.74. PI of selected sealants based on plow abrasion.

Performance of Sealant Based on Cohesive Failure

Similar to plow damage analysis, the PI of six sealants was calculated during the three years of service life based on cohesive failure, as shown in Figure 4.75. A reduction in PI was observed with the passage of time. All sealants showed a PI value higher than 50% by the end of 2013 (3 years of service life). However, a significant reduction in the PI value could be observed from 2012 to 2013. Sealants at Sections 12 and 6 showed relatively maximum and minimum reductions in PI value, respectively. Sealants at Sections 3 and 4 had almost a similar trend as sealants at Sections 7 and 16.

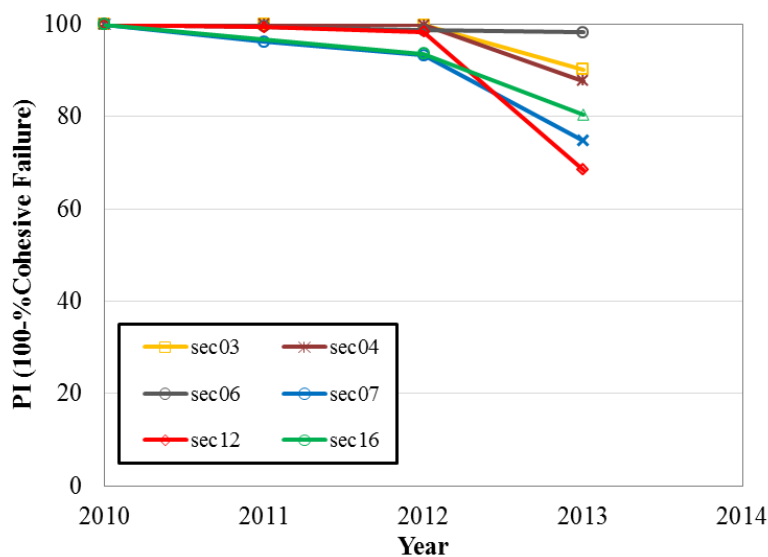


Figure 4.75. Performance index of selected sealants based on cohesive failure.

Boxplots as presented in Figure 4.76 show PI variation of sealants in each winter season. The sealant at Section 7 showed relatively higher sensitivity to winter, while the sealant at Section 6 showed relatively lower sensitivity to temperature. Sealants at Sections 3, 4, and 12 exhibited almost similar PI values by the end of 2013 winter season.

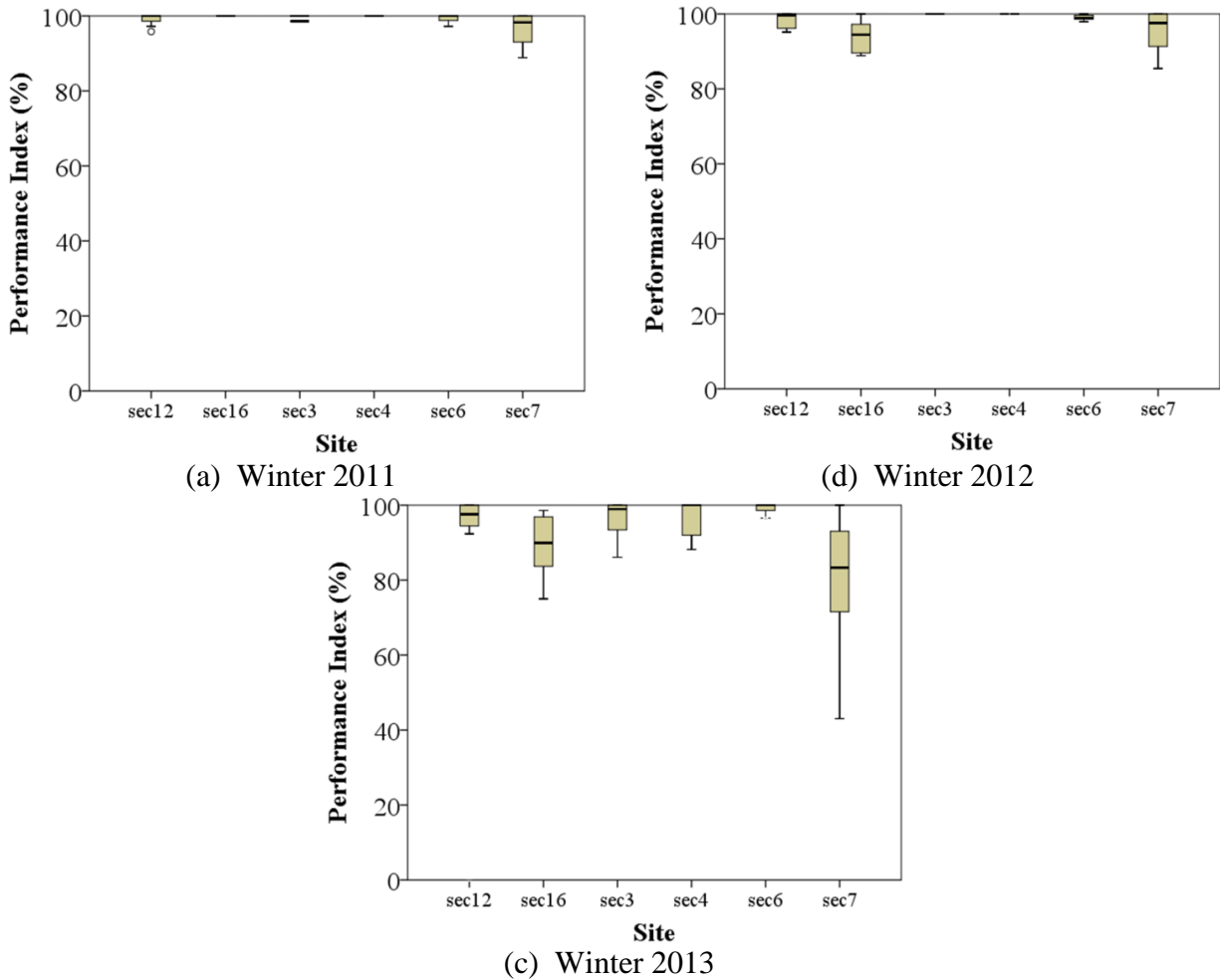


Figure 4.76. Boxplots based on cohesive failure since 2011.

Crack Movement and Displacement

During the seasonal surveys, the average pin reading representing crack displacement was obtained for specific sections to ascertain the effect of temperature on crack displacement and crack spacing. Average crack spacing and the net movement of ten consecutive cracks per section were measured based on the pin reading. Figure 4.77 presents the average crack displacement (bars) and spacing (line) from the field measurements during the winter surveys for the selected sections.

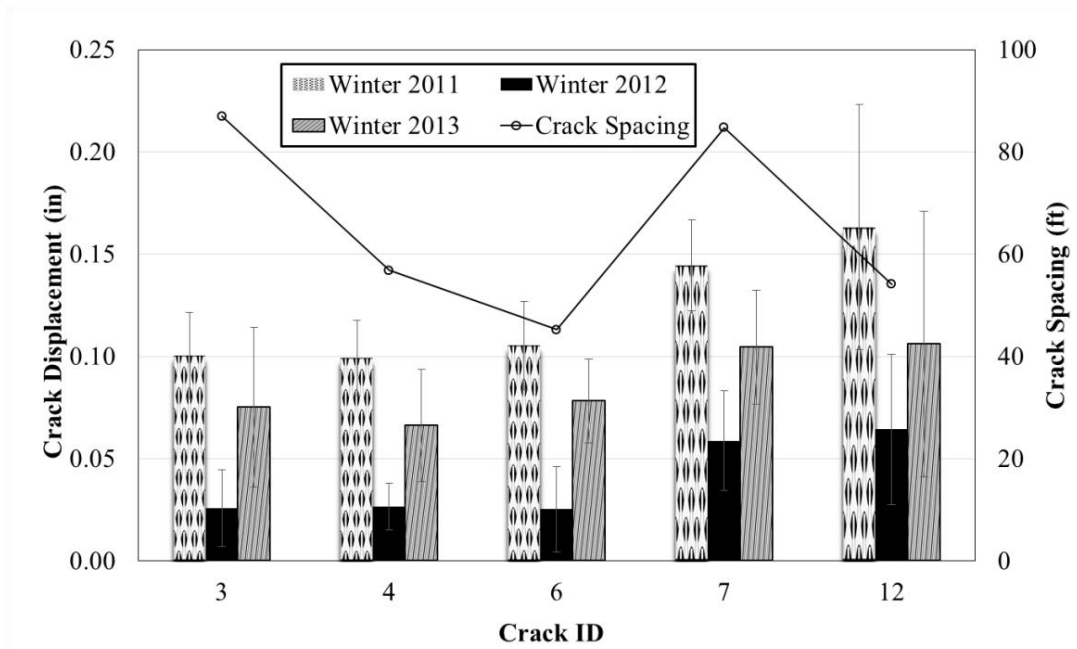


Figure 4.77. Average crack displacement and spacing.

It may be noted from Figure 4.77 that crack displacement during the winter of 2012 was lower than that of winter 2011 as shown in Figure 4.70. This may be attributed to the fact that the temperature was relatively lower in winter 2011 than winter 2012. Detailed crack spacing and displacement for each section are reported in Appendix C. Data are unavailable for the sealant at Section 16.

As previously mentioned, cohesive failures were caused by crack movements. Figure 4.78 presents the relationship between crack displacement and cohesive failure for each section after winter 2013. The plots for winter 2011 and 2012 are also presented in Appendix D. General trends in Sections 7 and 12 show that cohesive failure increases with the increase in crack displacement, but this assumption is not valid for Sections 3 and 4. It should also be mentioned that average displacement for Sections 7 and 12 are significantly higher than other sections. For Section 12, the cohesive failure for the last three cracks (12.8, 12.9, and 12.10) was not considered in the statistical analysis due to high crack displacements (almost two times more than other cracks). However, these cracks will be used for threshold determination.

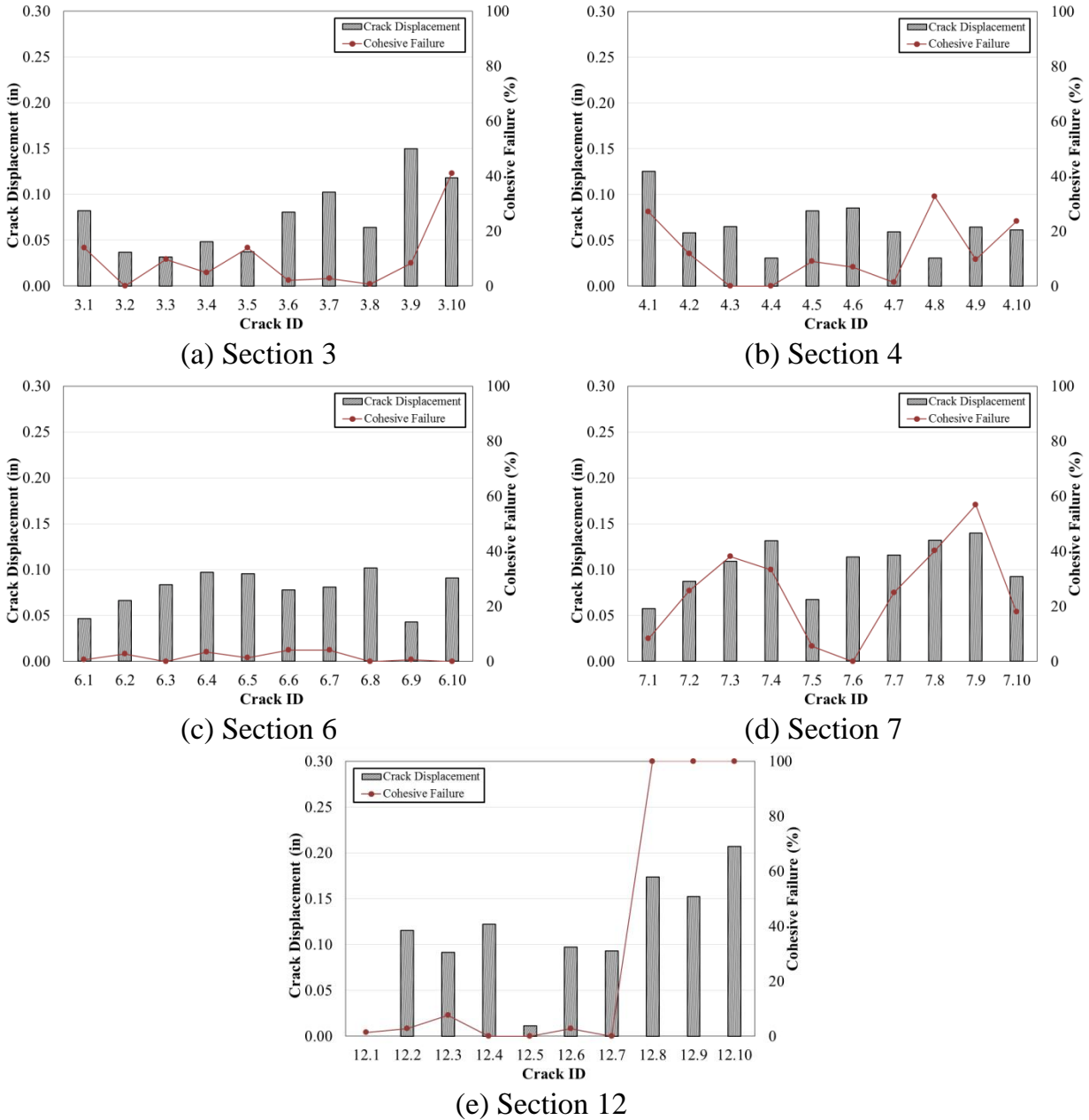


Figure 4.78. Cohesive failure for each section after winter 2013.

4.6.10 Effect of Treatment Type

To evaluate the effect of installation methods on sealants performance, cracks were treated by routing and sealing using different rout geometries and overbanding. Additionally, to evaluate the effect of the type of crack treatment, cracks of selected sections were cleaned and poured with sealant without any routing (uncut crack), referred to as clean and seal in this study (Table 4.27).

Table 4.27. Test Site Matrix Illustrating Treatment Method and Number of Cracks.

Sealant ID	Test Site	Rout Geometry (Number of Cracks ¹)						Clean & Seal
		12.5 x 12.5 mm	20 x 20 mm	20 x 20 mm ²	25 x 25 mm	30 x 15 mm	40 x 10 mm	
Bb	MN	-	-	-	15	-	-	15
	ON	-	25	-	-	-	-	-
Ca	NY	15	11	6	-	15	-	14
Da	ON	-	30	-	-	-	-	-
	NY	-	12	4	-	-	-	11
Ed	NH	-	20	10	-	-	-	-
Fb	MN	-	10	-	-	-	-	10
	NH	10	20	10	-	10	-	10
Gd	MN	10	10	-	-	10	-	10
	ON	-	20	-	-	10	10	10
	NH	10	20	-	-	12	-	-
Hb	MN	-	10	-	-	-	-	10
Ib	NY	-	5	5	-	-	-	6
Jd	NY	-	10	5	-	-	-	5
Kc	NH	9	25	-	-	10	-	12
	NY	-	10	5	-	-	-	-
Mb	MN	10	-	-	15	10	-	10
	ON	-	30	-	-	15	15	15
Nb	MN	-	-	-	15	-	-	20
Ob	NH	-	30	10	-	-	-	-
	NY	-	10	5	-	-	-	15
Rb	ON	-	15	-	-	10	10	-

¹ Number of cracks is provided in the table

² Rout geometry without any overband

According to Masson et al. (1999), wider sealants are subject to more weathering and age at a rapid rate. Sealants can lose a substantial amount of plasticizing oil within a single year, and the relative loss of oil may be greater in the more exposed sealant. This could lead to poor performance of sealants installed in wider rout geometry. Five rout geometries (12.5 × 12.5 mm, 20 × 20 mm, 25 × 25 mm, 30 × 15 mm, and 40 × 10 mm) were used in this study. For comparison purposes, selected sections with different rout geometries are presented in Figure 4.79, which shows that rout geometry influences the sealants PI values. For example, a small rout geometry, e.g., 12.5 × 12.5 mm or 20 × 20 mm, had the highest PI values in the MN and NH sites. The sealants used in these sections (Gd and Mb) were relatively soft sealants

(SG<-28°C). However, for stiff sealants such as Ca and Rb (SG>-28°C), wider rout geometries showed better performance, and for sealant Kc (SG=-28), the rout geometry did not have a significant effect on the sealant's performance. Overall, available performance data do not show a statistically significant trend between different rout geometries; however, observations were made during installation and surveys. For instance, it was noted that cutting narrow routs posed some challenges in following the crack, thus resulting in greater probability of missed cracks or spalling. On the other hand, wide and shallow routs (40 x 10 mm) can be adversely affected by additional exposure to weathering effects. Shallow routs with reduced wall area for bonding may increase the chance for adhesive failure.

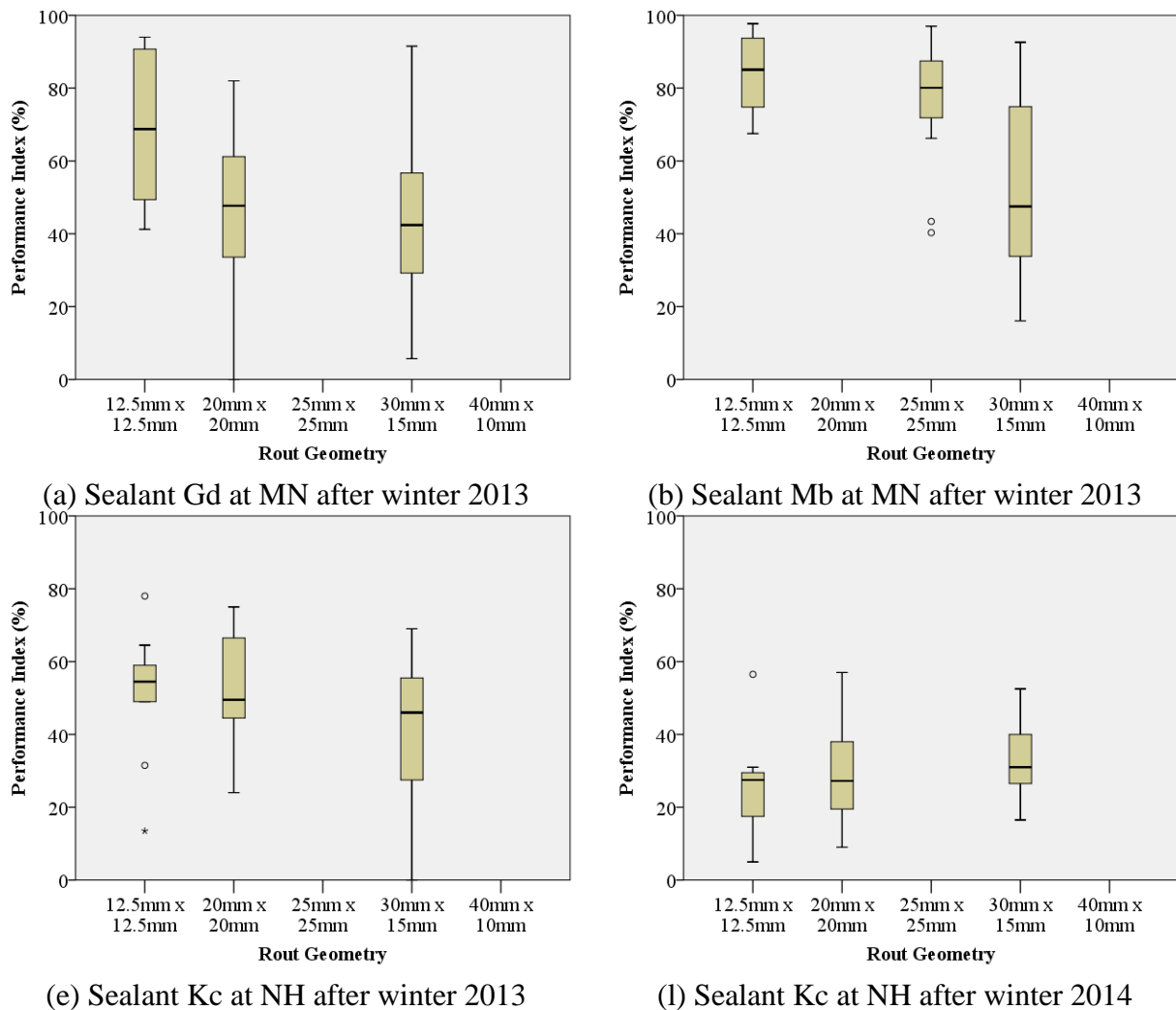
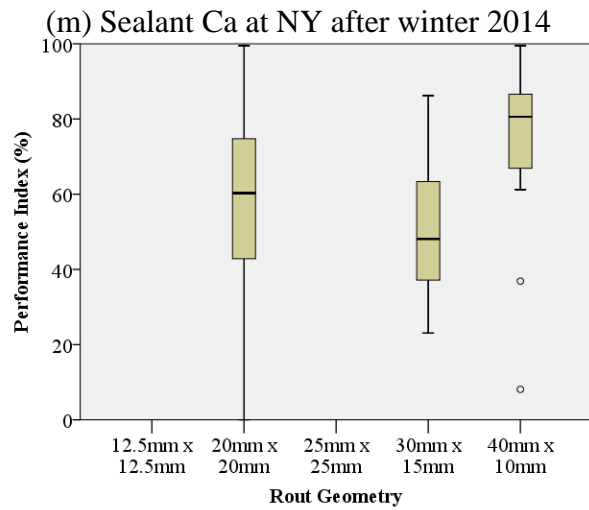
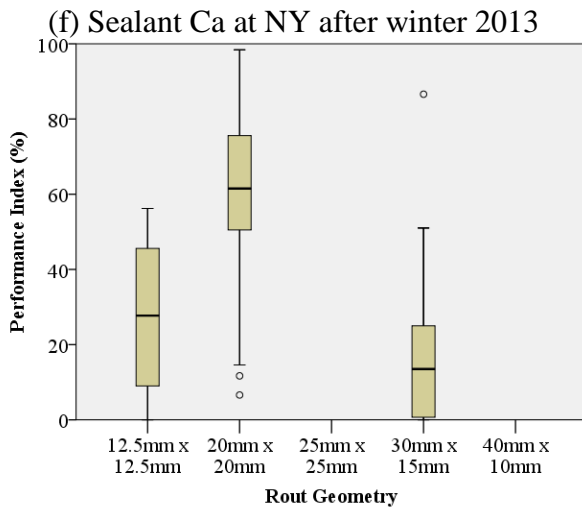
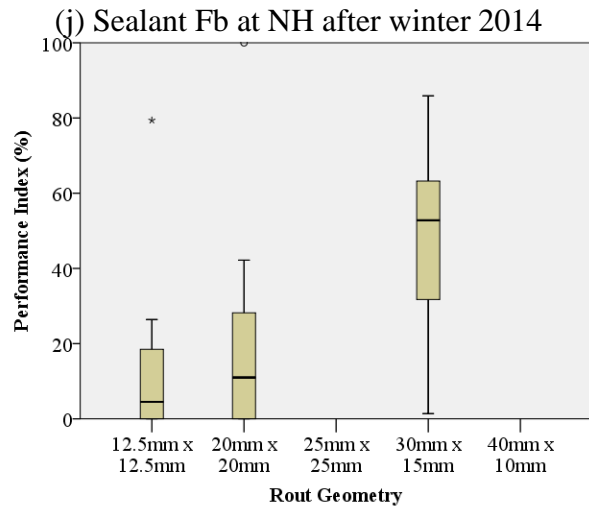
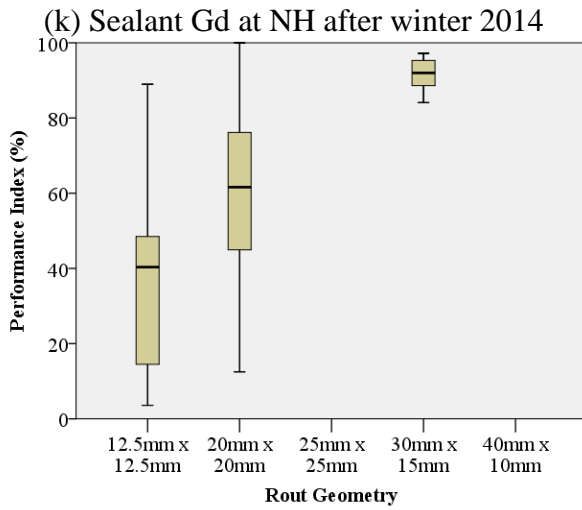
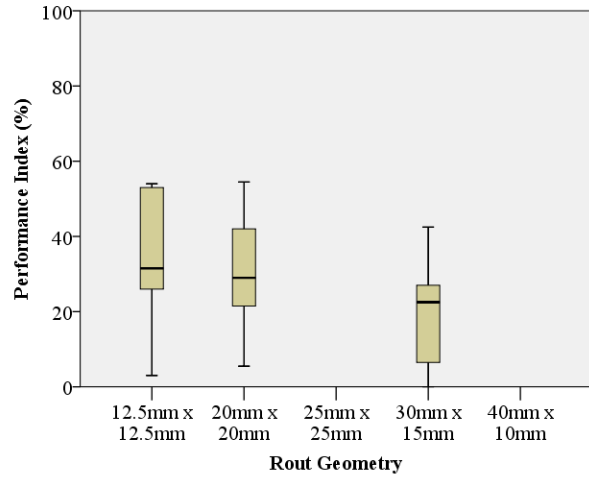
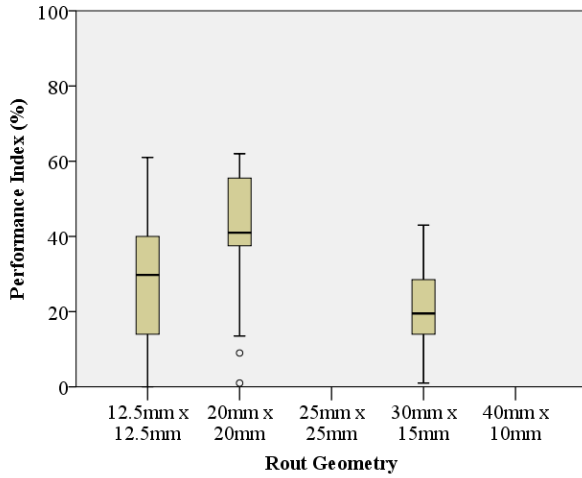


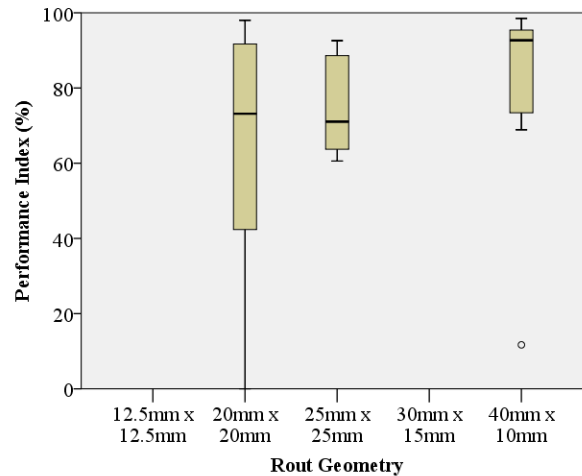
Figure 4.79. Boxplots for various rout geometry for different sealants regarding their test site and performance year.



(n) Sealant Gd at ON after winter 2014

(o) Sealant Mb at ON after winter 2014

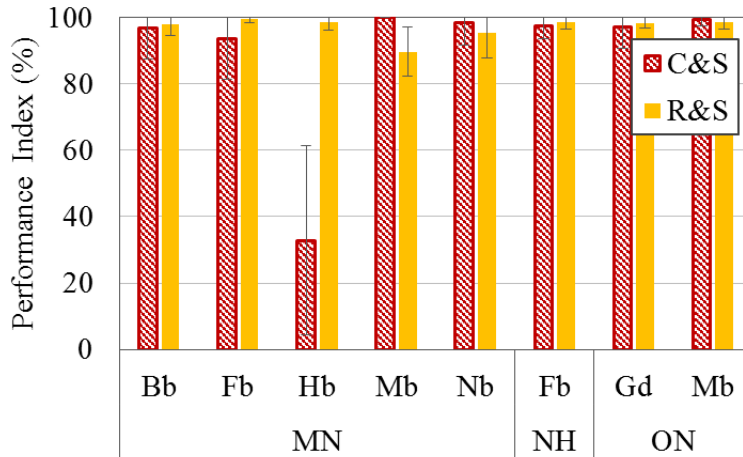
Figure 4.79 (continued)



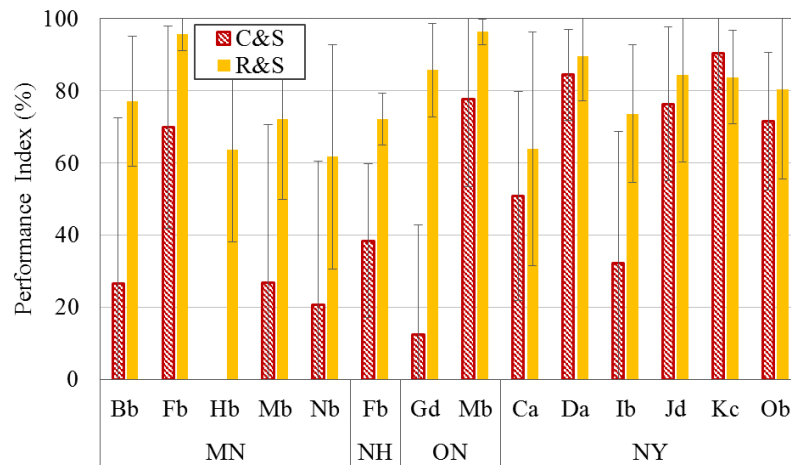
(p) Sealant Rb at ON after winter 2014
Figure 4.79 (continued)

The effect of different treatment methods on the performance of crack sealants is compared in Figure 4.80. After the first winter, except for one sealant (Hb in MN test site), both treatments were performing well. However, following the second winter at the MN, NH and ON test sites, there was a significant drop in the PI for clean and seal sections. The difference between crack filling sections (also called clean and seal (C&S) treatment) and crack sealing sections (also called rout and seal (R&S) treatment) after winter 2013 was approximately 30% in average and did not change after winter 2014. After winter 2014, almost all clean and seal sections failed.

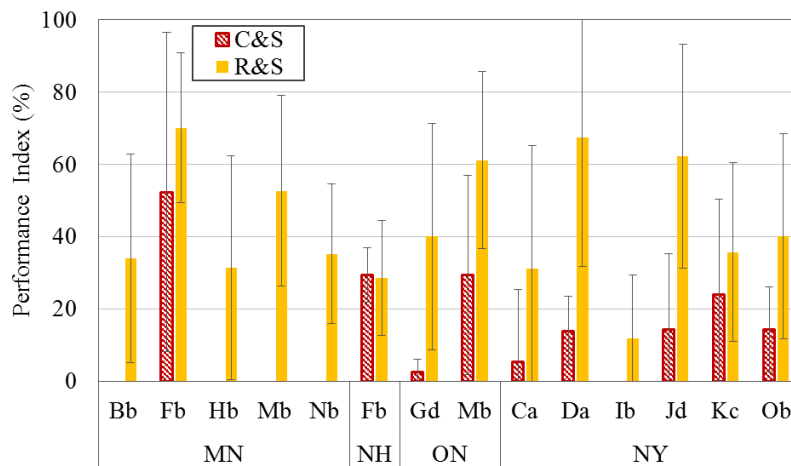
Overband application was also evaluated as another factor that affects the performance of crack sealants. The effect of overbanding is evident in Figure 4.81. Avoiding overbanding in NY test site caused a significant drop in the performance of sealants just after the first winter. The same trend was observed after the second winter for most sealants in NY and NH test sites. The average of differences between the sealants with overband and without overband after both winters is about 18% to 20%. Similar observations were reported in SHRP project H-106 (Smith and Romine, 1999).



(a) Winter 2012

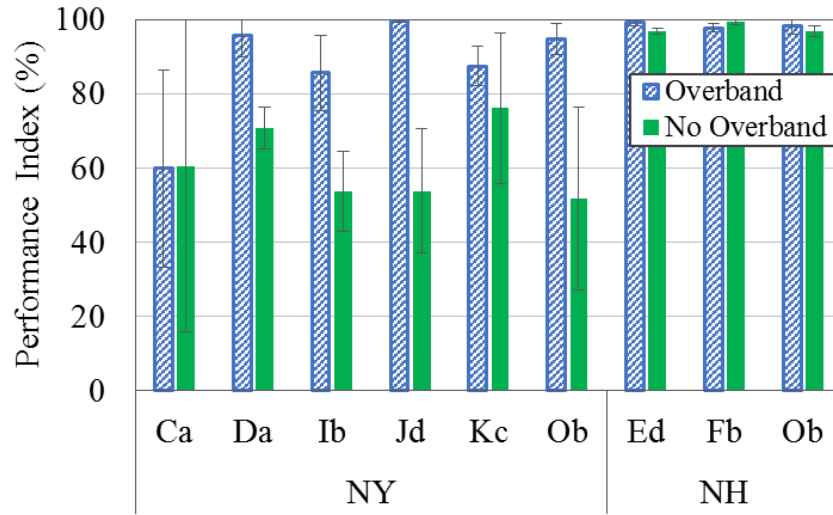


(b) Winter 2013

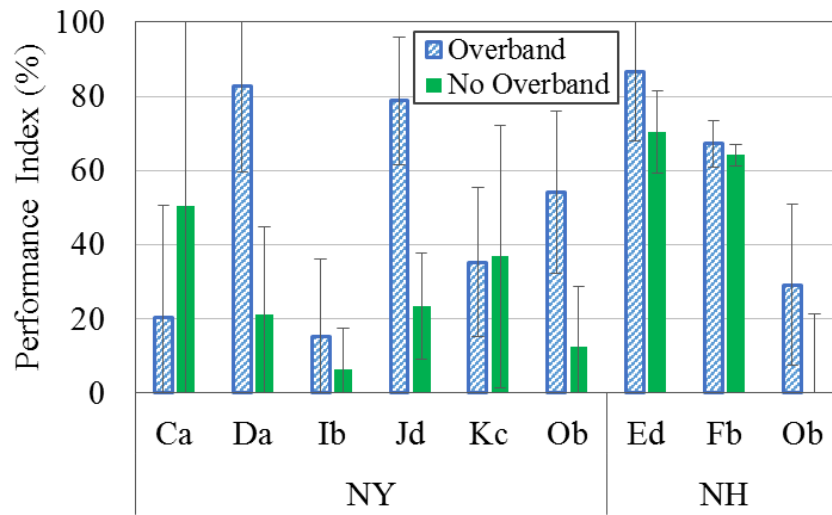


(c) Winter 2014

Figure 4.80. Effect of treatment type on crack sealants performance for different materials at different test sites during the surveys.



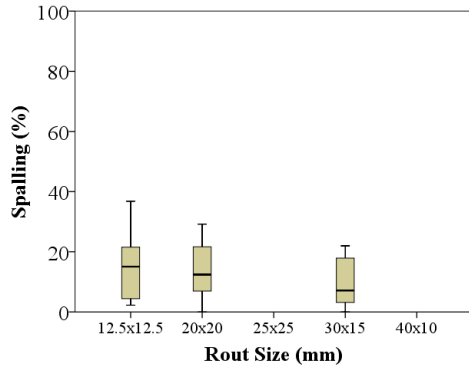
(a) After 1st winter



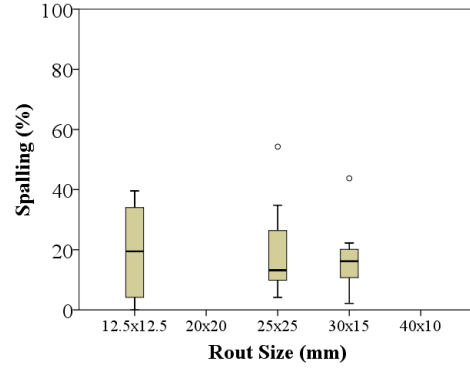
(b) After 2nd winter

Figure 4.81. Effect of overband application on crack sealants performance for different materials at different test sites during the surveys.

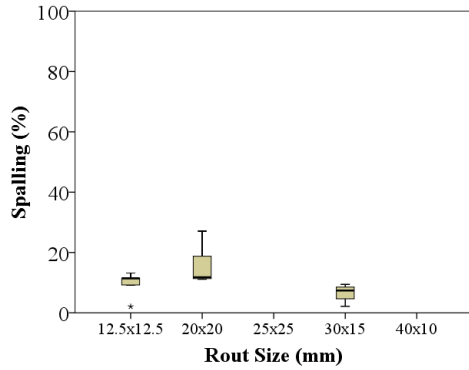
It is also interesting to investigate the effect of rout size on the amount of spalling. Figure 4.82 presents boxplots for the percentage of spalling for several sealants at different test sites with respect to the rout geometry. The variation of rout geometry had a minimal impact on the amount of spalling. For Minnesota and New Hampshire sites, average spalling ranged between 10% and 20% of the total crack length and was below 10% for the Ontario test site. This shows that the test site and better routing quality during the crack sealant treatment play a role in reducing the amount of spalling.



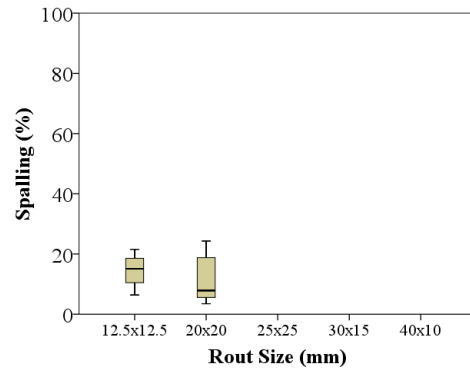
(a) Sealant Gd at MN test site



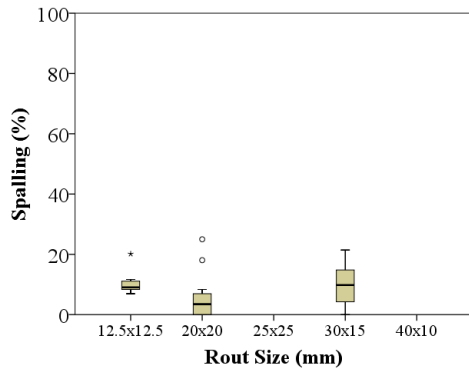
(a) Sealant Mb at MN test site



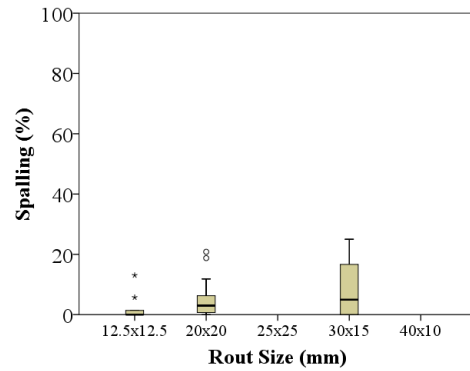
(a) Sealant Fb at NH test site



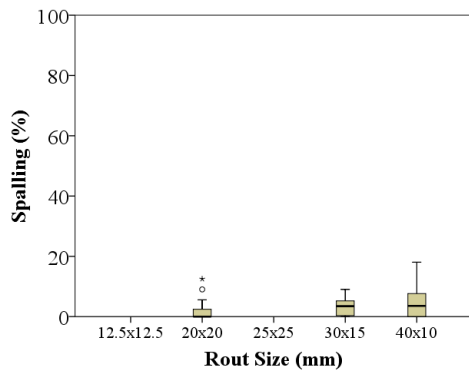
(a) Sealant Gd at NH test site



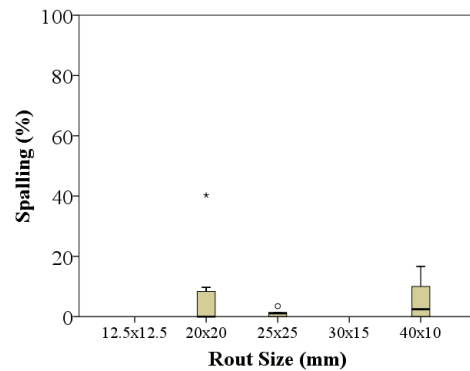
(a) Sealant Kc at NH test site



(a) Sealant Gd at ON test site



(a) Sealant Mb at ON test site



(a) Sealant Rb at ON test site

Figure 4.82. Effect of root size on spalling after the second winter.

4.7 Summary and Remarks

A summary of test sites, materials used, and installation are provided in this chapter. A wide spectrum of materials was installed in seven different test sites. It was expected to observe variations in performance correlated to laboratory performance tests, which would ultimately validate the test and threshold used in sealant grading. The test sites are located in wet-freeze climatic zones with some variations in temperature. The two commonly used sealing techniques (rout and seal and clean and seal) were implemented. Rout and seal treatments were applied with varying reservoir geometry. Clean and seal treatment were also applied at the same locations to compare the two techniques. Installations were monitored closely and data was recorded before, during, and after installation.

It was observed that, to achieve better installation quality, it is important to clean the pavement surface and routs. Moving vehicles may pick up the dust and debris during installation and transfer them to the clean cracks, thus causing loss of adhesive bond between sealant and rout walls which would eventually lead to a poor-performing sealant. In addition, it was noted that over- or under-heated sealants affect the sealants field performance. It is recommended to calibrate the kettle temperature frequently. If the kettle temperature is not well calibrated or adjusted, the sealants may be heated above the recommended temperature. The temperature may increase as the kettle gets empty during installation. It is also recommended to monitor the sealant temperature during installation to ensure that the sealant is installed at the recommended temperature. Also, using squeegees is recommended for proper overband application; a v-shaped squeegee can provide the required thickness as well as acceptable width to the overband.

The field performance of selected sealants installed at various test site locations was investigated. A PI was developed to monitor the performance of sealants. Percentage adhesive and cohesive failures were deducted from the index value representing the initial as-installed condition of the sealants. Test variables included material type, sealing technique, reservoir geometry (for rout and seal type), and overbanding. A summary of the observations is presented as follows:

- Most sealants failed below a PI threshold of 70% after three years. Seasonal effects played a role in the rate of deterioration. The 2013 and 2014 winters witnessed severe temperature drops that significantly affected sealants performance.

- Rout and seal sections performed much better than the clean and seal section. Most of clean and seal sections failed within two years except for the Michigan test site. This shows the importance of the test site selection for clean and seal applications and that transverse reflective cracks are not suitable candidates for clean and seal applications.
- Overband wear was commonly observed with a rapid rate of deterioration; especially low modulus sealants. Overband wear accelerated initiation and progression of adhesive failure.
- Adhesive failure is the predominant type of failure for rout and seal section; whereas, the clean and seal section failure was attributed either to complete loss of overband or to cohesive failure.
- Spalling was a commonly observed pavement failure. The percentage of spalling in the overall length of cracks was approximately 20%. In general, spalling occurred at the rout walls when crack and reservoir were not properly aligned. This was recorded as a pavement failure affecting the sealant's capacity and efficiency to perform its primary function (i.e., sealing the cracks).
- Several differences were observed in the performance of sealants when installed in different reservoir geometries. However, there was no clear trend between narrow and wide rout geometries. Due to the inability of routing practices to cut narrow reservoirs, narrow geometries are not recommended. On the other hand, wider routs may suffer due to greater exposure to weathering. Shallow depth is also not recommended as it may increase the probability of adhesive failure due to insufficient bonding.
- Overband application had a clear and positive impact on the performance of sealants.

Based on the chapter's findings, the following recommendations are made:

- Overband sealant application is recommended to increase sealant treatment life.
- For the same material, rout and seal treatment performs better than clean and seal. Therefore for longer treatment life, rout and seal treatment is recommended.
- Crew members should be trained on routing the cracks to avoid spalling during construction, which negates effective crack treatment.

CHAPTER 5. RHEOLOGICAL CHARACTERISTICS AND VALIDATION OF TEST METHODS

Since preliminary thresholds were established for each test based on extensive laboratory testing, and limited field and within-laboratory data, a field study was needed to validate and fine-tune the threshold values. This chapter summarizes test results and validation of the test methods. Development of the test procedures and grading specifications is described in details elsewhere (Al-Qadi et al, 2008) and the AASHTO test specifications (AASHTO T366, AASHTO T367, AASHTO T368, AASHTO T369, AASHTO T370 and, AASHTO TP126). Field performance data collected from the test sites were used to validate the low-temperature crack sealant grading test methods. Information collected from lab- and field-aged samples was used to establish correlation between laboratory and field performance and to validate the lab tests and fine-tune the thresholds. This chapter summarizes the field performance and laboratory data results and presents the correlation between the sets of data using statistical methods.

5.1 Crack Sealant Grading Specification

The method used to determine or verify the grade of a sealant is described by a provisional AASHTO specification (AASHTO PP85) similar to that of asphalt binders (AASHTO M320). Development of the grade selection was described in details elsewhere (Al-Qadi, et al., 2004; Al-Qadi et al., 2009; Yang et al., 2010). The sealant grade determination procedure is illustrated in Figure 5.1, which shows the steps necessary to obtain the sealant performance grade.

In this study, initial grading of sealants was conducted using existing specifications. However, changes were made to the specifications based on the findings of this study. To determine the sealant performance grade (SG) for each product, the following steps were followed:

1. Prepare samples and test specimens using the procedures specified for the required test methods. In case the grade of the sealant is unknown, approximately 550g of unaged sealant is required to complete the tests with the necessary replicates.
2. Homogenize the sealant according to ASTM D 5167.

Note 1: Vacuum oven aging (VOA) materials are needed for two DSR and four CSBBR beams at each test temperature. In addition, VOA materials are needed for at least six direct tension (DT) specimens and six adhesion test (AT) specimens at each test temperature. A minimum of two test temperatures is required. Approximately 300 g of homogenized material will be used.

3. Perform the DSR test (AASHTO TP 126) on VOA sealant at 64 °C, then increase or decrease the temperature at 6 °C increments until a value for flow coefficient ≤ 4 kPa.s and a value for shear thinning ≤ 0.7 are obtained. The highest test temperature where the

value for flow coefficient ≥ 4 kPa.s and the value for shear thinning ≥ 0.7 determine the high-temperature SG grade.

Note 2: If the flow coefficient is equal to 3.4 kPa.s and shear thinning is equal to 0.63 at 70 °C, and flow coefficient is equal to 4.1 kPa.s and shear thinning is equal to 0.84 at 64 °C, the sealant high-temperature grade is SG 64-xx.

4. Determine the viscosity of the homogenized sealant at installation temperature using AASHTO T366. The viscosity should be higher than 1.0 Pa.s and must not exceed 3.5 Pa.s.

Note 3: The installation temperature should be recommended by the sealant manufacturer.

5. If the homogenized sealant does not meet AASHTO T366 requirements for the test in Section 4, the sealant may not satisfy the specification for any SG, and no further testing is required.
6. Age a sufficient quantity of homogenized material in the vacuum oven (AASHTO T367). Quantities can be estimated based on the number of test samples specified in Note 1.
7. At the conclusion of the VOA procedure (AASHTO T367), including aging and combining the sealant, prepare four CSBBR specimens for each test temperature according to AASHTO T368. Retain sufficient residue to prepare at least six CSDT specimens and six CSAT specimens for each test temperature.
8. Perform the SCBBR test (AASHTO T368) on the VOA sealant beginning at -22 °C, and increase or decrease the temperature at 6 °C increments until a value for creep stiffness (S) ≥ 25 MPa and a value for ACR ≤ 0.31 is obtained. The lowest test temperature where the value for creep stiffness (S) ≤ 25 MPa and a value for ACR ≥ 0.31 determines the initial low temperature for SG grade.
9. Perform the CSDTT (AASHTO T369) on the VOA sealant beginning at the initial low-temperature SG grade determined by CSBBR test (AASHTO T368). The extendibility at the test temperature should meet the requirements of AASHTO MP 25. If the extendibility is lower than the threshold, then increase the temperature by 6 °C and test the VOA sample again using the SCDTT. Continue temperature increments until the extendibility is equal to or higher than the threshold defined by AASHTO MP 25.
10. Perform the CSAT test (AASHTO T370) on the VOA sealant beginning at the low-temperature SG grade confirmed by three CSDTT (AASHTO T369). The adhesion load should be higher than 50 N; otherwise, the sealant would not satisfy the requirements of low-temperature grade.
11. Using the results of aforementioned steps 8 through 10, determine the low-temperature sealant grade of the hot-poured bituminous crack sealant.
12. From steps 3 and 11, the sealant grade can be determined.

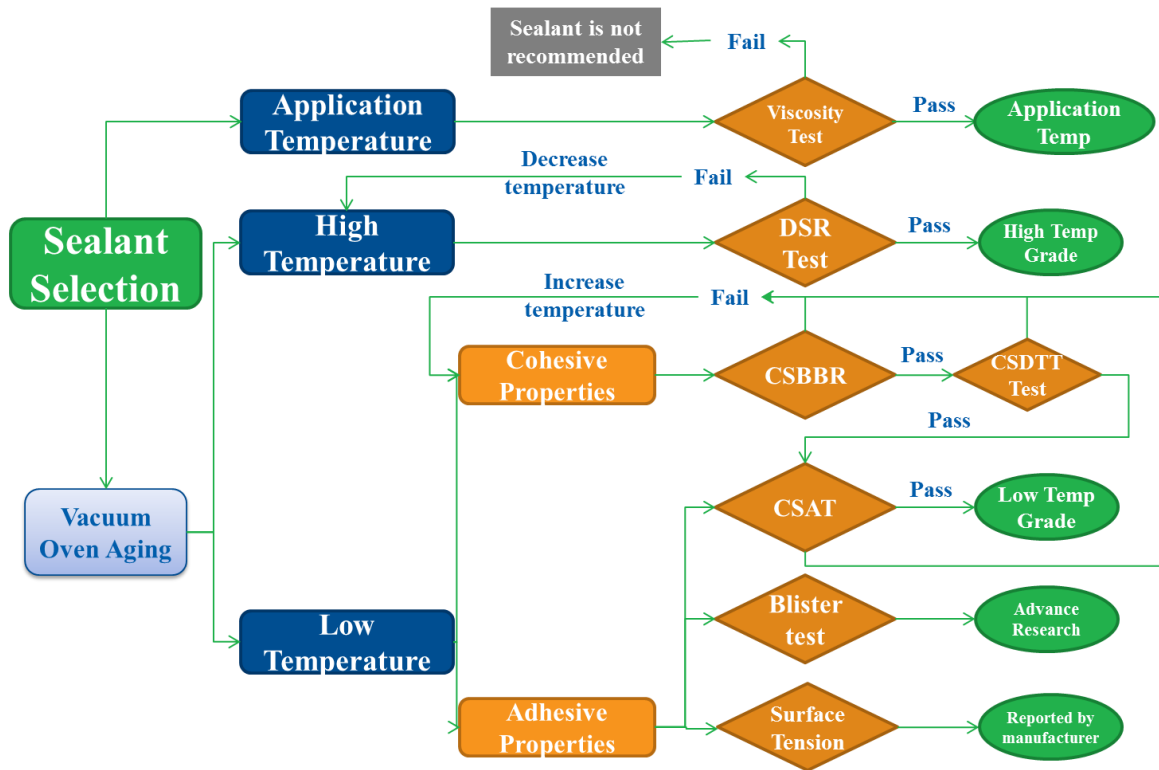


Figure 5.1. Illustration of steps necessary for determination of sealant performance grade.

5.2 Material Sealant Grade Determination

A summary of the test results used to obtain sealants grade is presented in this section. According to the procedures, the first low-temperature performance grade is determined using aged samples followed by high-temperature grade determination.

5.2.1 Determination of Sealant Low-Temperature Performance Grade

To obtain the sealants low-temperature performance grade, methods developed in previous studies were followed (Al-Qadi, et al., 2004; Al-Qadi et al., 2009; Yang et al., 2010). The sealant low-temperature grade determination procedure is illustrated in Figure 5.1. A summary of the results for CSBBR, CSDTT, and CSAT tests for all sealants is presented in Figure 5.3 through Figure 5.5.

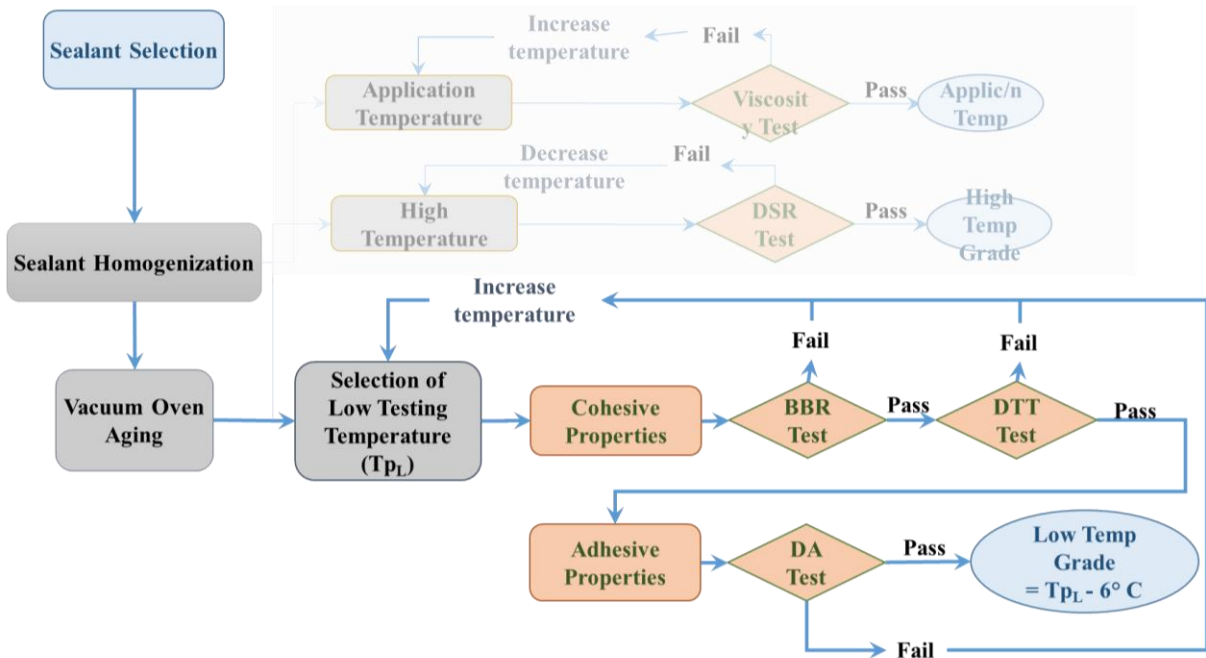


Figure 5.2. Illustration of steps necessary to determination sealant's low-temperature grade.

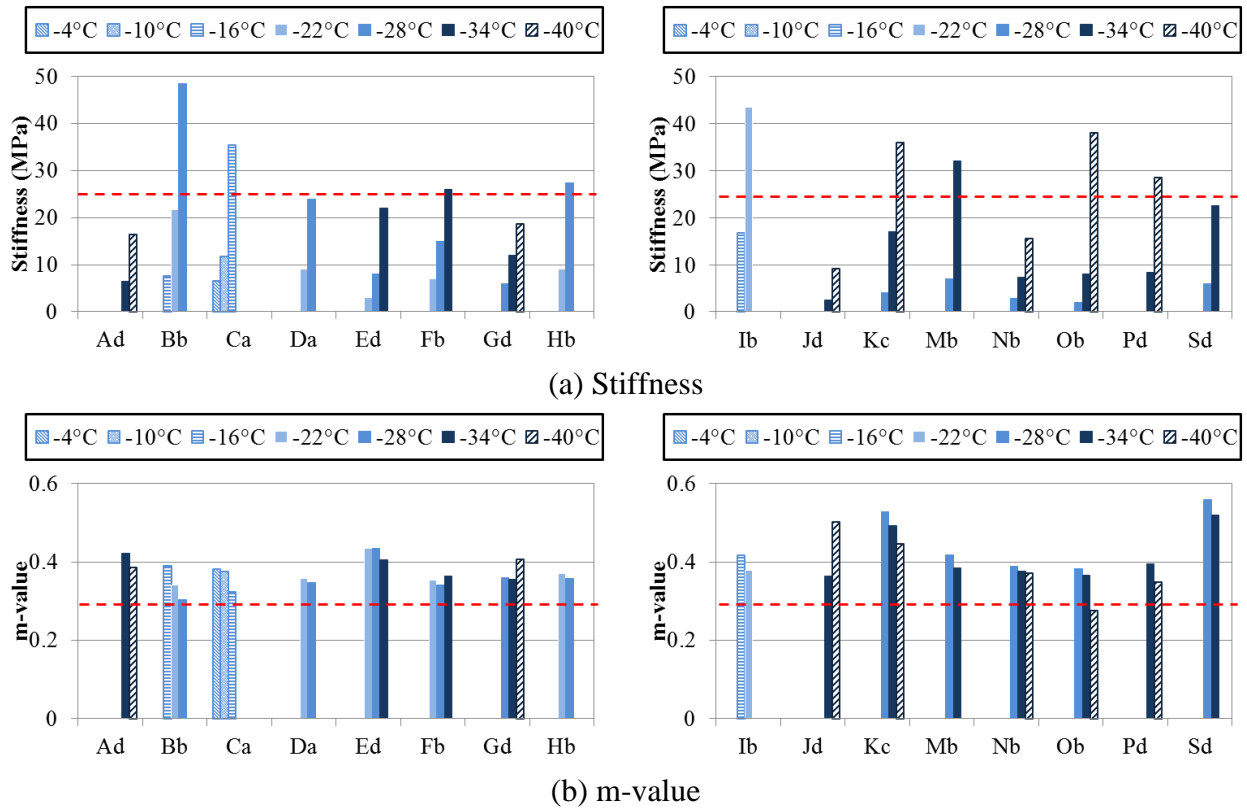


Figure 5.3. Test results summary for the CSBBR test.

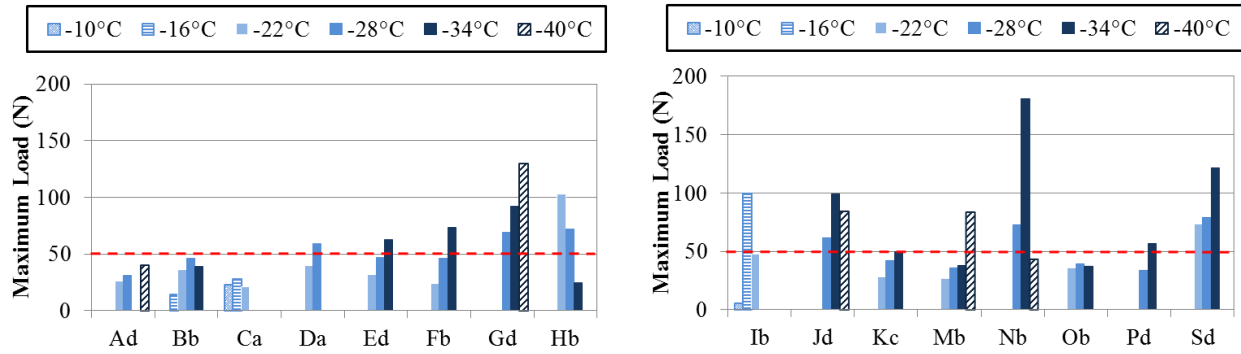


Figure 5.4. Test results summary for CSAT test.

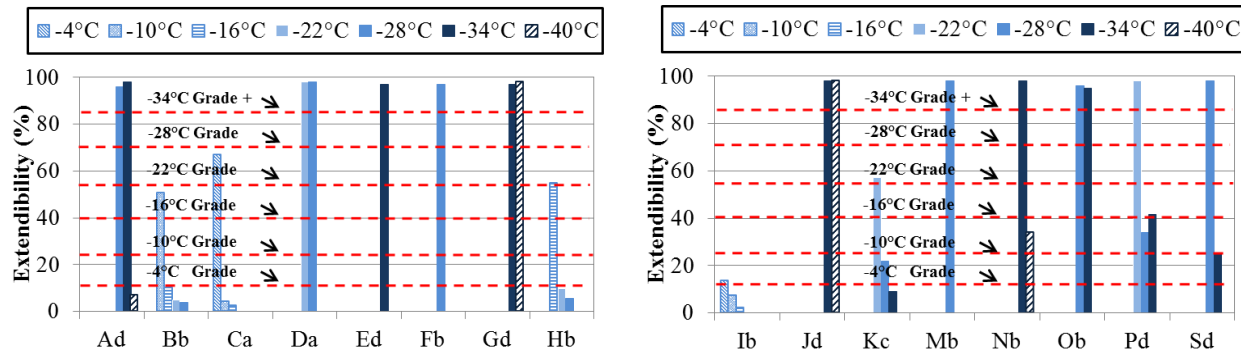


Figure 5.5. Test results summary for CSDTT test.

5.2.2 Determination of Sealant High-Temperature Performance Grade

The multiple-step creep recovery (MSCR) test was developed using DSR to determine high-temperature grading and tracking resistance. A shear creep stress of 25 Pa was applied for 2s to the sealant sample. Releasing the stress, the specimen was allowed to recover for 18s. The next loading step was applied after a 180s rest period. The stress was doubled and the same steps were followed until a stress of 3200 Pa was reached. A sample result for MSCR test for sealant Ad is shown in Figure 5.6, and the summary results for ten selected sealants are presented in Figure 5.7. According to the MSCR procedure, the sealants high-temperature grade is selected based on the C and P values obtained from Ostwald power law model, where C should be higher than 4 kPa and P should be higher than 0.7. Detailed information about obtaining MSCR parameters are discussed in Chapter 3.

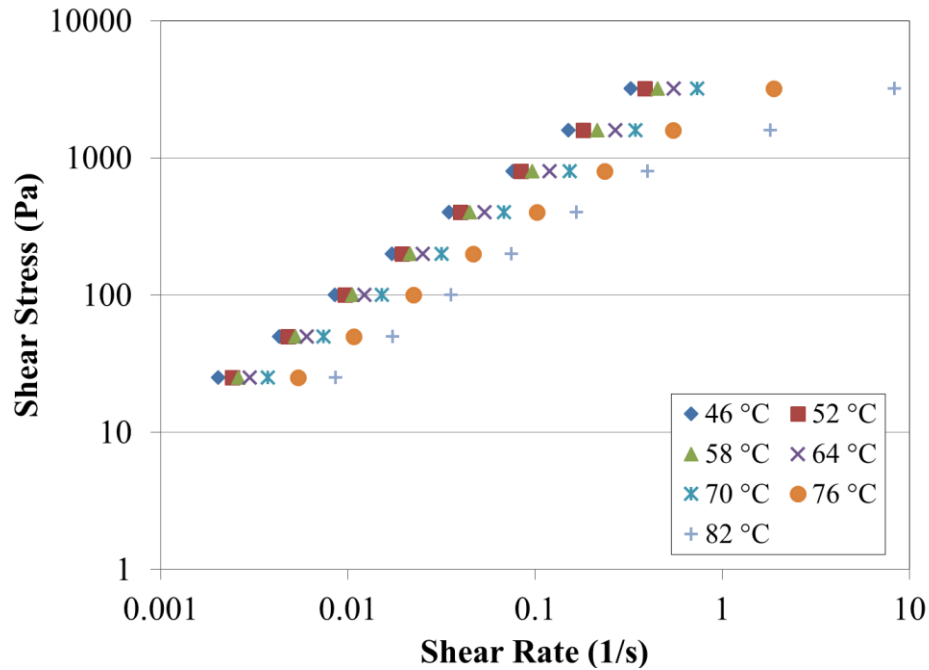


Figure 5.6. MSCR test results: shear stress vs. shear rate at different temperatures.

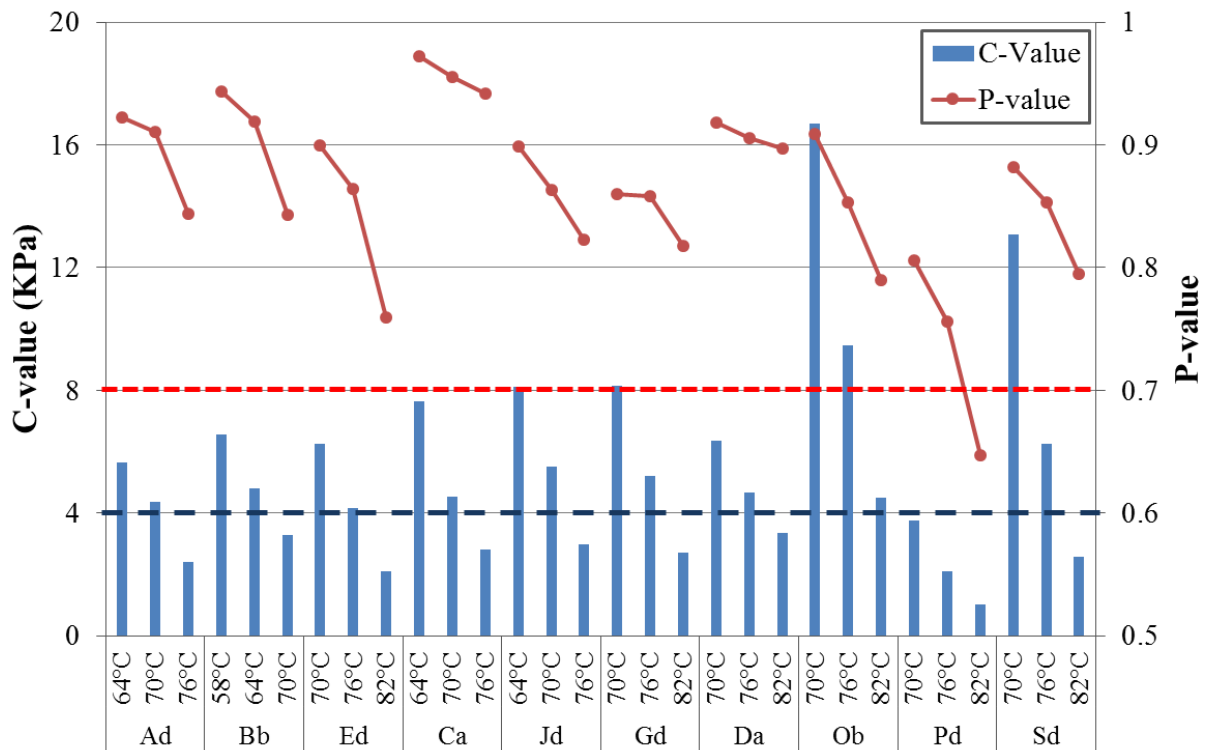


Figure 5.7. Summary of MSCR test results.

A summary of sealants grades based on all tests at low and high temperatures for each material is presented in Table 5.1.

Table 5.1. Summary of Low and High-Temperature Grade for All Sealants Used in This Study.

ID		SG (°C)				
		Low-Temperature Grade			High-Temperature Grade	Overall
		CSBBR	CSAT	CSDTT	DSR	
1	Ad	-46	NA	-40	70	70-40
2	Bb	-28	NA	-16	64	64-16
3	Ca	-16	NA	-10	70	70-10
4	Da	-34	-34	-34	76	76-34
5	Ed	-40	-40	-40	76	76-40
6	Fb	-34	-40	-34	-	-34
7	Gd	-46	-34	-46	76	76-34
8	Hb	-28	-28	-22	-	-22
9	Ib	-22	-22	-10	-	-10
10	Lb	NA	NA	NA	-	NA
11	Jd	-46	-46	-46	70	70-46
12	Kc	-40	-40	-28	-	-28
13	Mb	-34	-46	-34	-	-34
14	Nb	-46	-34	-40	-	-34
15	Ob	-40	NA	-40	82	82-40
16	Pd	-40	-40	-28	64	64-28
17	Rb ¹	NA	NA	NA	NA	NA
18	Sd	-40	-40	-34	76	76-34

¹Virgin material for sealant Rb was not available to be aged and graded in the laboratory

5.3 Validation of Low-Temperature Tests Methods

This study investigates correlations between laboratory results and field performance of crack sealants with an objective of validating the prediction potential of sealant grading system. Based on field performance, test parameter thresholds are adjusted and fine-tuned. Fine-tuning of the thresholds is discussed later in this chapter. The methodology adapted in this study for evaluating lab and field correlations is illustrated in Figure 5.8. The experimental program consists of two major tasks: field performance evaluation of crack sealants and laboratory characterization. Eighteen sealants were installed in six different test sites as discussed in details in Chapters 4. Field performance data collection was conducted annually to collect temperature log, performance data (types of crack sealant failure), and field-aged samples. Then, the field-aged samples were tested using laboratory test methods to characterize their low-temperature properties. Both field performance and lab results data were analyzed using statistical methods

and compared to one another. Once a satisfactory correlation was achieved, laboratory test results were converted to the actual test site temperature that the materials experienced. The results at the actual field temperature were used in fine-tuning the thresholds, if needed. The thresholds were selected by comparing the lab parameters with the field performance using an iterative approach that yielded consistent ranking and correlation between field and laboratory test results. The procedure, which was repeated for each test method, is presented in details in this chapter.

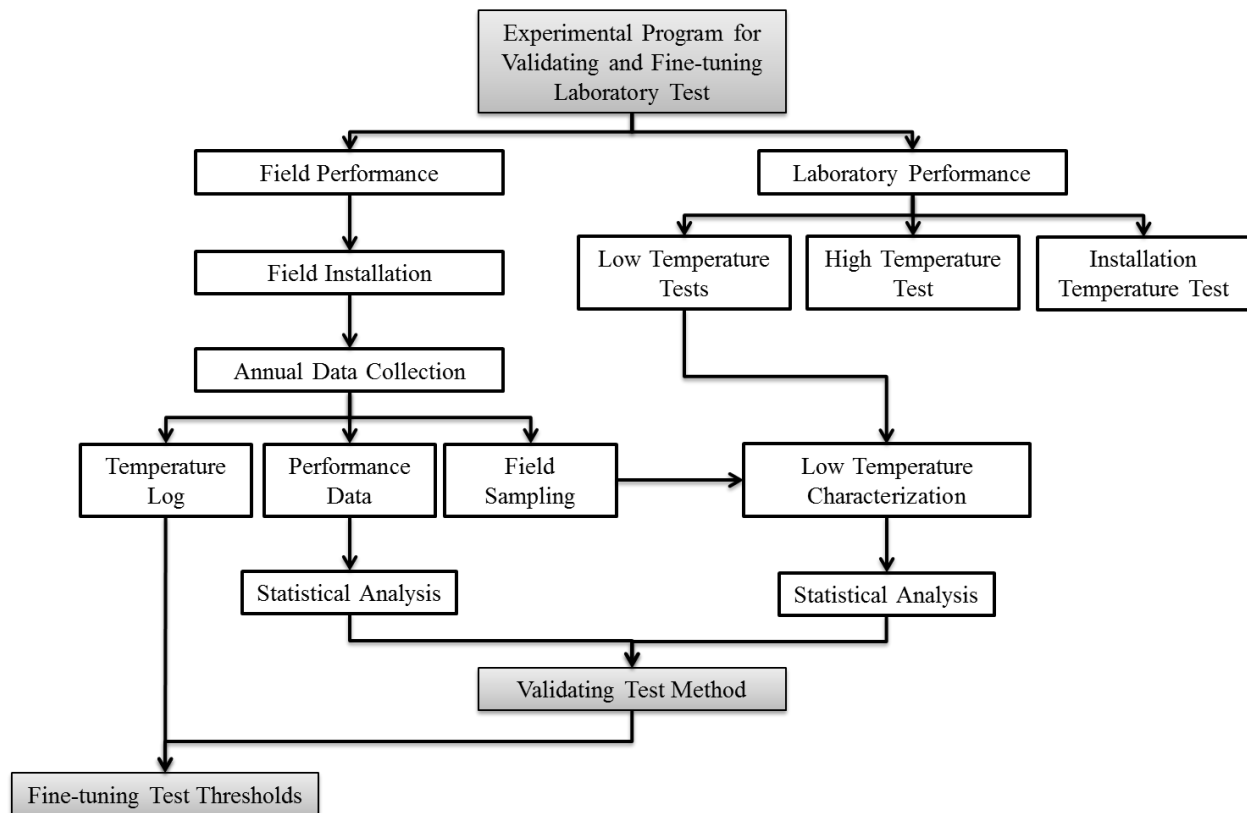


Figure 5.8. Experimental program for validating and fine-tuning Laboratory test method.

5.3.1 Crack Sealant Bending Beam Rheometer Test Validation

The hypothesis tested for validating laboratory tests is summarized hereafter. Sealants with similar field performance, according to their PIs, were grouped together based on a statistical testing. The sealants were evaluated based on their respective test results and grouped based on statistical tests. Groups with matching lab and field performance indicated that the laboratory test parameter provided positive correlation to field performance. Two separate statistical methods were used to determine groupings for the data collected from the lab and field. Field data were

statistically analyzed using the Games-Howell test and categorized in different subsets. Each subset presents a group of sealants with a similar field performance. Another statistical test was also applied to the test parameters obtained from the CSBBR test. Because of the normal distribution of laboratory test results, the Tukey test was used to categorize the sealants in different subsets. The subsets of field and lab data were compared separately for each test site.

Minnesota Test Site

Seven different sealants were installed in Minnesota (MN) test site. During the second and third evaluation periods (March and April 2013), field-aged samples (FA2 and FA3) were collected from the replicate section for each material to be tested in the lab. The results of CSBBR test for the sealants used in MN are summarized in Figure 5.9. The figure presents the master curve stiffness obtained from the test illustrating stiffness over a spectrum of testing time and temperature. The CSBBR results indicate a wide range of low-temperature stiffness of the materials used in the Minnesota test site. Based on the CSBBR master curves (Figure 5.9), it can be seen that sealants Bb and Fb have the highest stiffness followed by sealants Hb and Mb. The stiffness curves for the other three sealants (Ad, Nb and Gd) exhibited similar characteristics at short loading times.

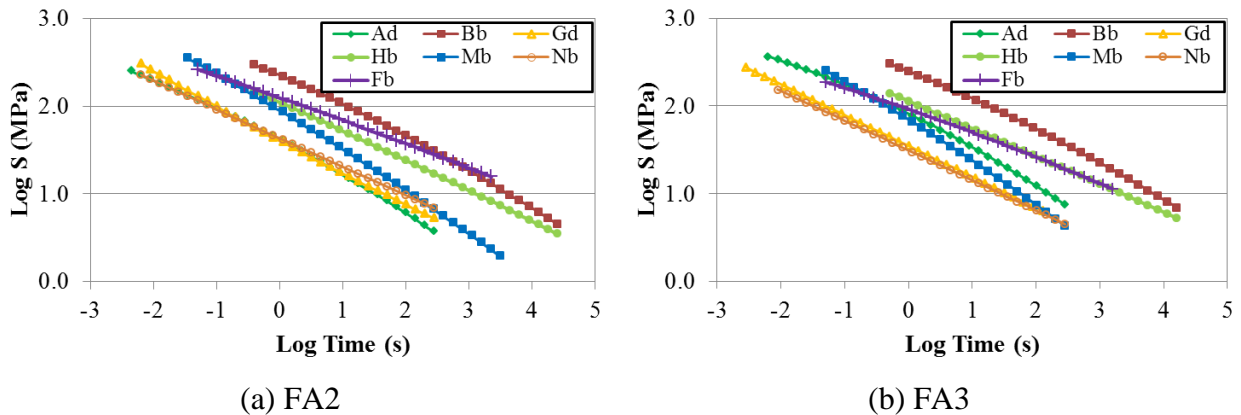


Figure 5.9. Stiffness master curves obtained from CSBBR test results at -28°C for sealants used in Minnesota test site.

The field performance and lab results of the seven sealants installed in Minnesota test site are compared in Table 5.2. The statistical subsets are defined by capital letters (i.e., A to C with increasing stiffness in the lab and increasing performance index in the field). Each subset represents the set of sealants with statistically similar lab or field performance characteristics. Materials with lower stiffness values (Gd, Nb and, Ad), as shown in Figure 5.9, are placed in the same subset for both field and lab performance. Subset A in the field performance table includes

sealants with a PI lower than the passing threshold ($PI < 70\%$). Sealants Fb and Bb with a significantly higher stiffness are placed in the field subsets with relatively high PI. It must be noted that the field performance of sealants is related to several factors including low-temperature stiffness, cohesive, and adhesive resistance as well as other on-site conditions (temperature, pavement condition and properties, crack spacing, etc.). Therefore, it was not expected to see a high correlation between field and CSBBR data. However, sealants with distinct lab behavior were expected to be grouped in the same field performance subsets in order to pass this initial test of validation. The same procedure of ranking and grouping was applied to data collected from other test sites.

Table 5.2. Statistical Grouping of the Sealants Installed in Minnesota Test Site Base on Their Field Performance and Lab Results.

Sealant ID	SG (°C)	Field Performance (FA2)		CSBBR	
		PI (%)	Statistical Subset ($\alpha=0.25$)	Stiffness (MPa)	Statistical Subset ($\alpha=0.05$)
Gd	-46	47.0	A	5.7	A
Nb	-46	61.7	A, B	7.1	A
Hb	-28	63.7	A, B	17.6	B
Ad	-46	68.1	A, B	4.0	A
Bb	-28	77.0	B	33.2	C
Mb	-34	77.3	B	7.0	A
Fb	-34	95.6	C	29.5	C

Ontario Test Site

Seven different sealants were installed in the Ontario (ON) test site. During the second and third evaluation periods (March and April 2013), field-aged samples (FA2 and FA3) were collected for each material to be tested in the lab. Results of CSBBR test for the sealants used in Ontario are summarized in Figure 5.10. Based on CSBBR master curves, sealant Bb had the highest stiffness while Sealant Pd had the lowest stiffness. Thus, a wide spectrum of low-temperature stiffness values was observed for the materials used in the Ontario test section.

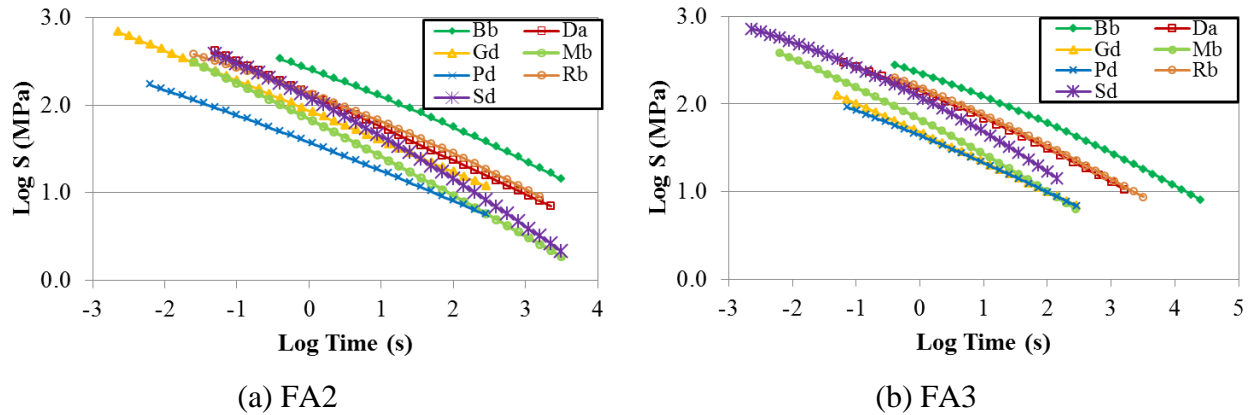


Figure 5.10. Stiffness master curves obtained from CSBBR test results at -28°C for sealants used in Ontario test site.

Similar to the Minnesota test site, seven different sealants, ranging from soft to stiff materials, were installed and surveyed in Ontario. The field performance and lab results of these sealants are presented in Table 5.3. Materials with lower stiffness (Gd, Pd and, Mb) are placed in the same subset (subset A). The three sealants also share the same subset based on their field performance (subset B). Sealants with high stiffness (Rb and Da), which appear in a different subset than soft sealants, are placed in the same group based on their field performance (subset B). Among these sealants, Bb had the highest stiffness and lowest PI. This important observation is later used to validate the maximum stiffness threshold to ensure field performance.

Table 5.3. Statistical Grouping of the Sealants Installed in Ontario Test Site Base on Their Field Performance and Lab Results.

Sealant ID	SG (°C)	Field Performance (FA3)		CSBBR	
		PI (%)	Statistical Subset ($\alpha=0.25$)	Stiffness (MPa)	Statistical Subset ($\alpha=0.05$)
Bb	-28	32.4	A	43.3	C
Pd	-40	43.7	A, B	7.1	A
Mb	-34	58.1	B, C	7.1	A
Gd	-46	59.2	B, C	7.3	A
Rb	NA	69.3	C, D	24.1	B
Da	-34	77.6	D	22.2	B
Sd	-40	79.1	D	10.8	A

Wisconsin Test Site

Five different sealants were installed in the Wisconsin (WI) test site. Similar to the Minnesota and Ontario test sites, during the second evaluation period (March and April 2013), a field-aged sample (FA2) was also collected from WI test site for each material to be tested in the lab. Here, the CSBBR test results for the sealants used in WI are summarized in Figure 5.11. Based on CSBBR stiffness master curves, it can be seen that sealants Fb and Bb had the highest stiffness while sealant Ad had the lowest stiffness.

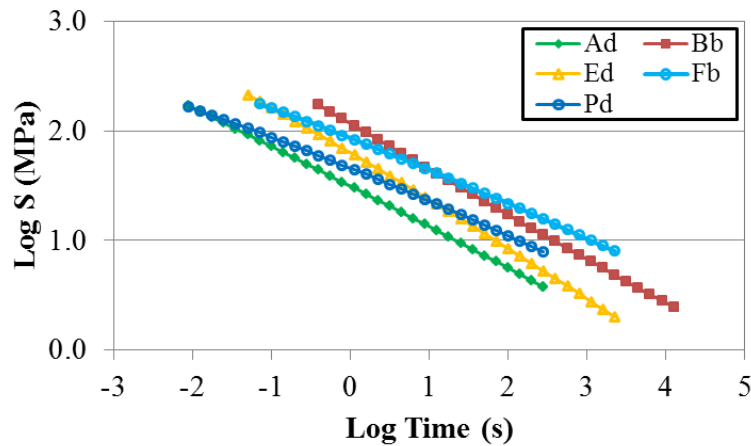


Figure 5.11. Stiffness master curves obtained from CSBBR test results at -28°C for sealants used in Wisconsin test site.

In general, there is no strong correlation between laboratory and field performance results for the materials tested from the Wisconsin test site, which hosted the first installation of sealants in this study. Pavement condition and cracks were not adequate for evaluating sealants performance. It has to be noted that consistency in sealant installation was observed.

Table 5.4. Statistical Grouping of the Sealants Installed in Wisconsin Test Site Base on their Field Performance and Lab Results.

Sealant ID	SG (°C)	Field Performance		CSBBR	
		PI (%)	Statistical Subset ($\alpha=0.25$)	Stiffness (MPa)	Statistical Subset ($\alpha=0.05$)
Fb	-34	28.9	A	16.5	D
Pd	-40	65.4	B	8.1	B, C
Ad	-46	86.2	C	4.0	A
Bb	-28	91.0	C	11.8	C
Ed	-40	99.3	D	5.8	A, B

New York Test Site

Six different sealants were installed in the New York (NY) test site. Similar to the other sites, during the second evaluation period (March 2014), a field-aged sample (FA2) was collected from the NY test site for each material to be tested in the lab. The CSBBR test results for the sealants used in NY are summarized in Figure 5.12. Based on CSBBR master curves, it can be seen that sealants Ca and Ib had the highest stiffness while sealants Ob and Jd demonstrated the lowest stiffness.

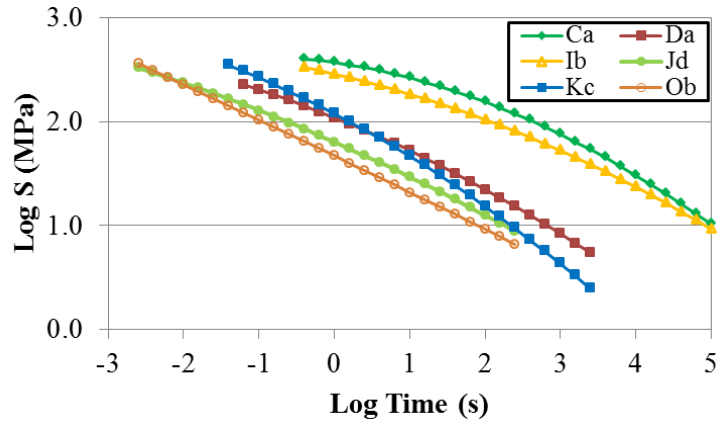


Figure 5.12. Stiffness master curves obtained from CSBBR test results at -28°C for sealants used in New York test site.

Six different sealants with a wide stiffness range were installed and surveyed in NY. The field and lab performance of all six sealants is presented in Table 5.5. It can be seen that two of three soft sealants (Kc and Ob) in subset A are placed in the same field performance group (subset B). Similar to the Minnesota and Ontario test sites, the sealants with high stiffness (Ib and Ca) appear in the same group based on their field performance (subset A).

Table 5.5. Statistical Grouping of the Sealants Installed in New York Test Site Base on Their Field Performance and Lab Results.

Sealant ID	SG (°C)	Field Performance		CSBBR	
		PI (%)	Statistical Subset ($\alpha=0.25$)	Stiffness (MPa)	Statistical Subset ($\alpha=0.05$)
Ib	-22	15.1	A	83.1	C
Ca	-16	20.2	A	119.5	D
Kc	-40	35.2	A, B	15.0	A, B
Ob	-40	54.0	B	6.6	A
Jd	-46	78.9	C	8.9	A, B
Da	-34	82.7	C	16.4	B

New Hampshire Test Site

Five different sealants were installed in the New Hampshire (NH) test site. For this specific test site, field-aged samples (FA3) were collected during the third evaluation period (March 2014) to be tested in the lab. The CSBBR test results for the sealants used in NH are summarized in Figure 5.13. Based on CSBBR master curves, it can be seen that sealants Fb and Ed had the highest stiffness while sealant Ob had the lowest stiffness.

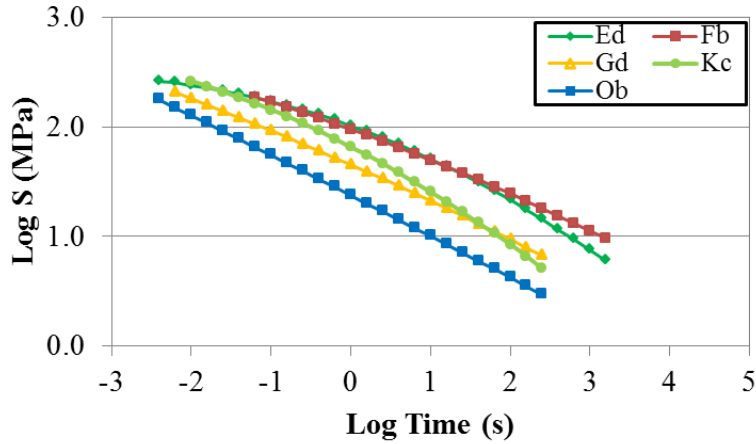


Figure 5.13. Stiffness master curves obtained from CSBBR test results at -28°C for sealants used in New Hampshire test site.

The field and lab performance of these five sealants is presented in Table 5.6. The soft sealants (Ob and Kc) in subset A also belong to the same field performance group (subset A). The other sealants with relatively high stiffness demonstrated better field performance than softer sealants and are, therefore, grouped differently.

Table 5.6. Statistical Grouping of the Sealants Installed in New Hampshire Test Site Base on Their Field Performance and Lab Results.

Sealant ID	SG (°C)	Field Performance		CSBBR	
		PI (%)	Statistical Subset ($\alpha=0.25$)	Stiffness (MPa)	Statistical Subset ($\alpha=0.05$)
Ob	-40	15.7	A	3.1	A
Kc	-40	28.7	A, B	5.6	A, B
Fb	-34	30.6	B	18.6	D
Gd	-46	39.2	B, C	7.1	B
Ed	-40	48.8	C	14.3	C

Summary of Lab-to-Field Comparison

In general, good correlation was observed between the low-temperature stiffness results and field performance of sealants, except for one test site. Statistical groups with similar stiffness and PI were consistent for these sites. A summary of the field PI from all test sites compared to sealants stiffness is presented in Figure 5.14. The sealants below the red line have a PI less than 70%, which is considered as a failure criterion in the field. Figure 5.14 shows three zones with distinctive performance characteristics of sealants:

- Zone 1: sealants with fair field performance ($50\% < PI < 70\%$) and low stiffness
- Zone 2: sealants with acceptable field performance ($PI > 70\%$) with moderate stiffness
- Zone 3: sealants with poor field performance ($PI < 50\%$) and high stiffness

The data provided in Figure 5.14 support the determination of stiffness threshold values to ensure good field performance. Based on the data presented in this figure, there is a need to define two threshold values to avoid using sealants that are either too soft or too stiff. It was observed that whenever sealants stiffness is too soft, premature overband failure could accelerate adhesive failure. On the other hand, sealants that are too stiff are not good candidates at low-temperature climates due to excessive stresses accumulating in the sealants. Stiffness variations could also result from formulations affecting the adhesive properties. These two hypotheses will be further discussed.

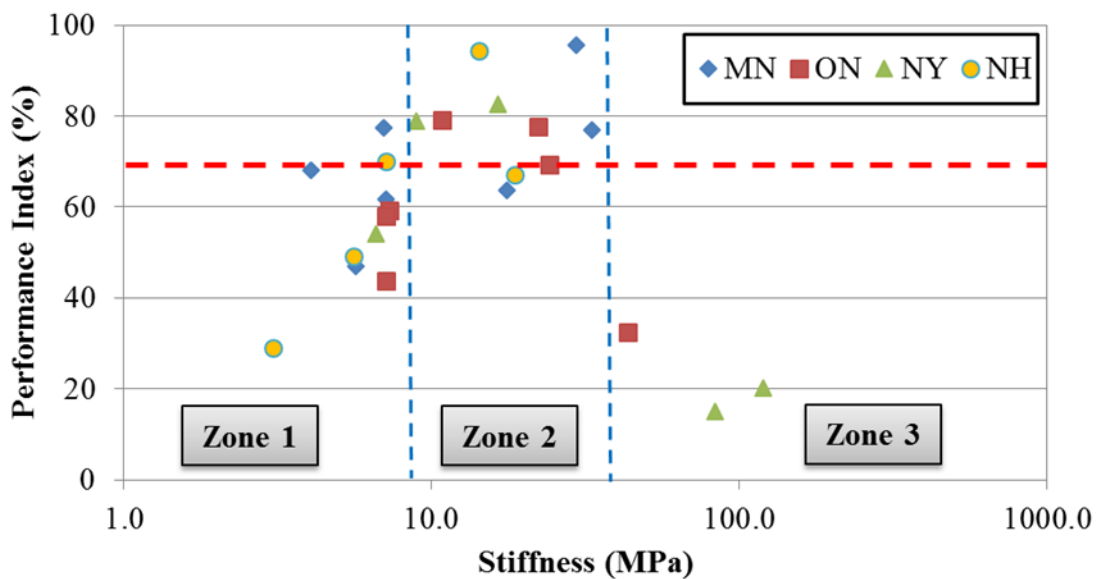


Figure 5.14. Summary of performance index compared to sealants stiffness.

Michigan Test Site (Case Study)

Following AASHTO T368 Standard, six selected sealants were aged and tested in the lab to obtain their CSBBR parameters (Table 5.7). Unlike the previously discussed test sites, Michigan (MI) test section consisted of only clean and seal treated cracks. Therefore, field-aged materials were not collected. Testing was conducted using laboratory-aged sealants only. This test site provided an opportunity to correlate low-temperature stiffness with clean and seal performance.

Table 5.7. Summary of CSBBR Test Parameters for Selected Sealants.

Section (ID)	CSBBR Test Parameters		SG (°C)
	Stiffness (MPa)	ACR	
3	13.7	0.42	≥ -40
4	23.0	0.48	≥ -34
6	20.4	0.41	≥ -46
7	12.5	0.39	≥ -16
12	10.0	0.44	≥ -40
16	14.1	0.37	≥ -34

Figure 5.15 shows the results of six selected crack sealants tested by CSBBR. According to AASHTO T368, two preliminary performance parameters, 25MPa for stiffness at 240s and 0.31 mm/mm/s for average creep rate, are recommended as selection criteria for sealants. The recommended selection criteria were applied to the six sealants as shown in Figure 5.15.

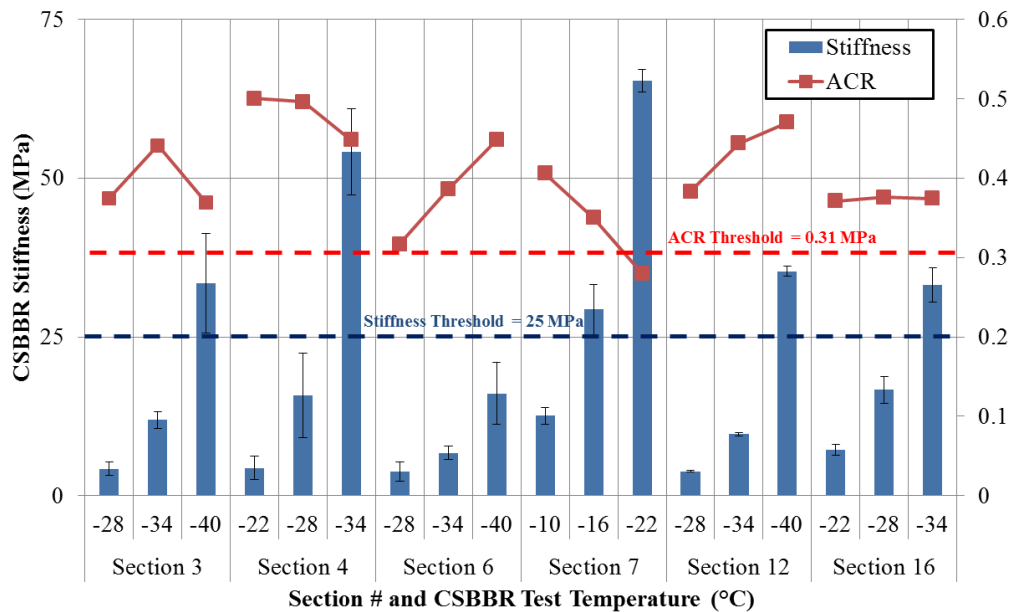


Figure 5.15. Summary of CSBBR results of selected sealants at 240s.

Five sealants showed less than 25MPa at 240s and passed the threshold at -28°C , with the exception of Section 7, which showed the highest stiffness. At the same temperature, the average creep rate for six sealants was above 0.31mm/mm/s, except for Section 7. Figure 5.15 clearly shows that Section 7 had the stiffest material with a low SG of -16, and Section 6 had the softest material with a low SG of -46. The sealants in Sections 3 and 12 had almost the same stiffness level. The sealant in Section 7 was also tested at -28°C to compare the average creep rate and stiffness for all sealants at the same temperature.

To better characterize sealants performance, test results at three different temperatures were used to develop a master curves for all materials. The stiffness master curve was obtained for each sealant at a reference temperature of -28°C (Figure 5.16). CSBBR results indicated a wide range of low-temperature stiffness for the materials used in the MI test site. Based on the CSBBR master curves, the sealant in Section 7 had the highest stiffness followed by the sealants in Sections 4 and 16. The stiffness curves for the other three sealants (sections 3, 6, and 12) exhibited similar characteristics.

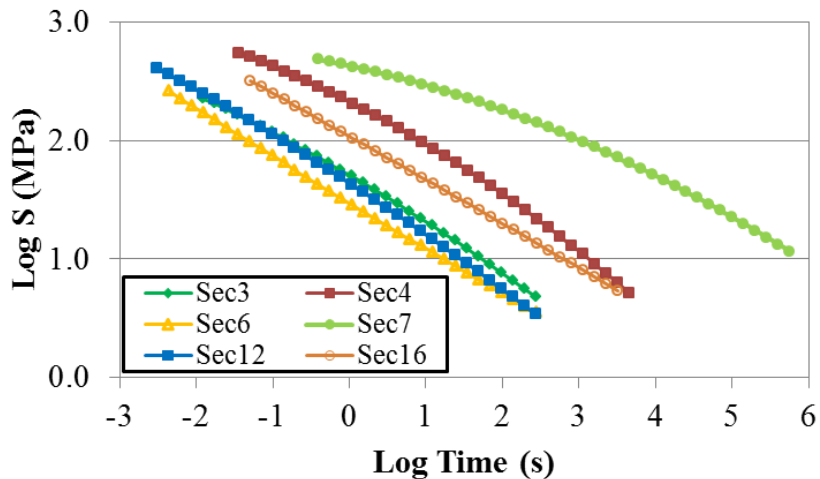


Figure 5.16. Stiffness master curves obtained from CSBBR test results at -28°C .

The field and lab performance of six sealants installed in the MI test site is presented in Table 5.8 and

Table 5.9. The table of correlation between low-temperature stiffness and plow damage (Table 5.8) shows that three out of four sealants with low stiffness values (Subset “A” in stiffness) are placed in the same subset (subset “A”) in the field with poor performance ($\text{PI} < 50\%$). It is, therefore, concluded that sealants with low stiffness have low resistance to shear loading applied during plowing operation. A similar observation was made for the performance

of sealants using the rout and seal techniques where it was noted that overband resistance is even more significant for clean and seal technique. Therefore, the need for defining a minimum threshold for low-temperature stiffness, especially for overband application, is justified based on field observations.

Similar to plow damage, the CSBBR stiffness was also correlated to cohesive failure, as shown in

Table 5.9. All sealants with low stiffness (subset “A”) are placed in the same subset (subset “A”) based on cohesive failure with a good field PI (PI>90%). Sealants with average stiffness (sections 4 and 16 in subset “B”) also appear in the same field subset (subset “B”) with a fair PI (80%<PI<90%). Among these sealants, Section 7 had the highest stiffness and the lowest and poor PI (PI<80%). This important observation is later used to validate maximum stiffness threshold to ensure field performance.

It should be mentioned that the field performance of sealants is related to several factors, including low-temperature stiffness, cohesive, and shear resistance. Therefore, it is not expected to achieve high correlation between field and CSBBR data at this point. However, the preliminary trends achieved using the CSBBR stiffness parameters appear to group sealants in two major categories of “too soft” and “too stiff” with generally low performance characteristics. A holistic analysis of laboratory results is performed using all laboratory test parameters.

Table 5.8. Statistical Grouping of the Sealants Based on CSBBR Stiffness at 240s and Plow Damage.

Sealant ID	Stiffness at -28°C			Field Performance		
	MPa	Statistical Subset	Prediction due to Min. Stiffness	Plow Damage		
				PI (%)	Subset	performance
6	3.8	A	Fail	29.1	A, B	Poor
12	3.9	A	Fail	87.4	C	Good
3	5.4	A	Fail	23	A	Poor
16	14.1	A, B	Pass/Fail	41.7	A, B	Poor
4	23	B	Pass	77	C	Good
7	139	C	Pass	50.1	B	Fair

Table 5.9. Statistical Grouping of the Sealants based on CSBBR Stiffness at 240s and Cohesive Failure.

Sealant ID	Stiffness at -28°C			Field Performance		
	MPa	Statistical Subset	Status	Cohesive Failure		
				PI (%)	Subset	performance
6	3.8	A	Pass	98.3	A	Good
12	3.9	A	Pass	97.9	A, B	Good
3	5.4	A	Pass	90.3	A	Good
16	14.1	A, B	Pass	80.5	B	Fair
4	23	B	Pass	88.8	B	Fair
7	139	C	Fail	74.9	B	Poor

Correlation of field and lab results is also presented in Figure 5.17. The PI values decrease with the increase in stiffness and load values.

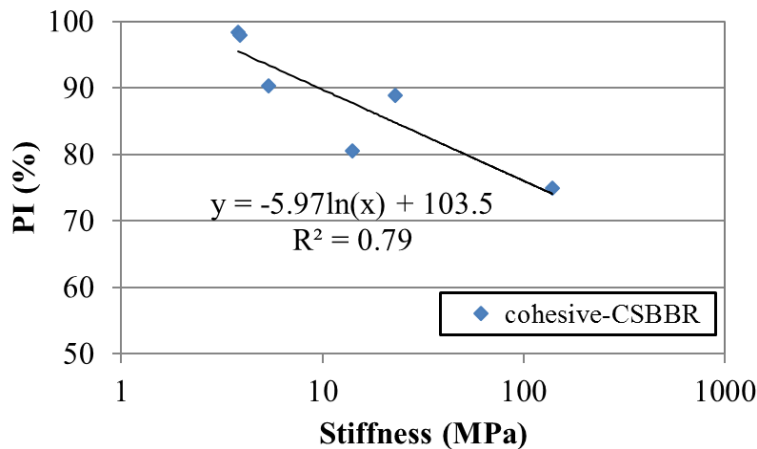


Figure 5.17. Correlation of performance index based on cohesive failure with CSBBR stiffness.

5.3.2 Crack Sealant Direct Tension Test Validation

Crack Sealant Direct Tension Test (CSDTT) has been adopted as an AASHTO standard (AASHTO T369). Extendibility at the test temperature is suggested as a performance parameter. Similar to the CSBBR test method, sealants with distinct lab results were expected to be grouped in the same field performance subsets to validate the CSDTT test method.

Michigan Test Site (Case Study)

Following AASHTO T369 Standard, selected sealants were aged and tested in the laboratory to obtain their CSDTT parameter as shown in Table 5.10. The low-temperature sealant grade was obtained for the selected crack sealants in the MI test site. Five out of six crack sealants had an extensibility higher than 89% at the grading temperature.

Table 5.10. Summary of CSDTT Test Parameters for the Selected Sealants in Michigan Test Site.

Section (ID)	Test Temperature (°C)	Max. Load (N)	Extensibility	AASHTO Extensibility Threshold	SG (°C)	Confirmed SG (°C)
3	-34	31.8	97%	85%	≥-40	-40
4	-22	24.6	95%	55%	≥-28	-28
6	-34	19.4	95%	85%	≥-40	-40
7	-4	13.7	15%	10%	≥-10	-10
12	-34	31	92%	85%	≥-40	-40
16	-22	17.1	89%	55%	≥-28	-28

In addition, boxplots were generated for all sealants tested at -28 °C and shown in Figure 5.18, which highlights the variation in the overall values of maximum load and extensibility.

Figure 5.18 also shows that the sealants in Section 3, 6 and 12 had more than 98% extensibility at -28 °C. The sealant in Section 7 exhibited the least extensibility while reaching the highest maximum load at failure. Sealants in Sections 3, 6 and 12 with maximum loads less than 20 N showed more than 98% of extensibility, while the sealant in Sections 4, 7 and 16 with loads more than 30 N significantly showed low extensibility.

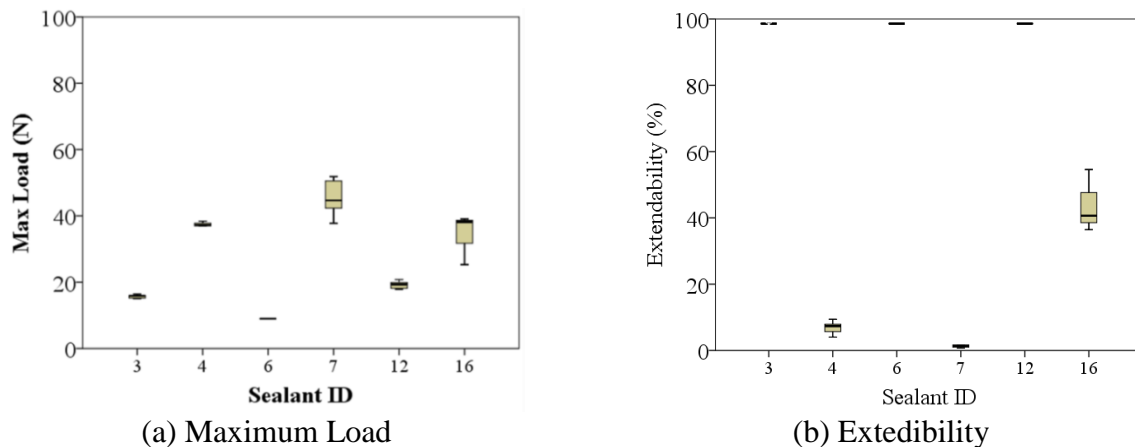


Figure 5.18. Boxplots of CSDTT results illustrating variation in the maximum load and extensibility.

CSDTT results were further analyzed using the Tukey test to categorize the sealants in different subsets based on extendibility and maximum load as reported in Table 5.11 and Table 5.12. Different subsets of sealants were obtained for maximum load and extendibility. The correlation table between low-temperature extendibility and cohesive failure (Table 5.11) shows that the three sealants with maximum extendibility (98%) were placed in the same statistical group and had good field performance based on cohesive failure. The other three sealants with extendibility lower than threshold (75% at -28 °C) had fair (80% < PI < 90%) or poor performance (PI < 80%). CSDTT maximum load was also correlated to the cohesive failure as shown in Table 5.12, which indicates sealants ductile or brittle behavior. All sealants in laboratory subsets “A” and “B” with low load (less than 20 N) were in field subset “A,” indicating good performance. On the other hand, sealants with greater maximum load at failure demonstrated fair or poor field performance. Therefore, it was concluded that sealants with greater maximum loads tend to be more brittle. Figure 5.19 shows PI change with CSDTT loads; the value of PI decreases with the load’s increase.

Table 5.11. Statistical Grouping of the Sealants Based on CSDTT Extendibility and Cohesive Failure

Sealant ID	Extendibility at -28 °C			Field Performance		
	%	Statistical Subset	Status	Cohesive Failure		
				PI (%)	Subset	Performance
3	98.6	A	Pass	90.3	A	Good
6	98.6	A	Pass	98.3	A, B	Good
12	98.6	A	Pass	97.9	A	Good
16	43.9	B	Fail	80.5	B	Fair
4	6.9	C	Fail	88.8	B	Fair
7	1.3	C	Fail	74.9	B	Poor

Table 5.12. Statistical Grouping of the Sealants Based on CSDTT Maximum Load and Cohesive Failure

Sealant ID	Maximum Load at -28 °C			Field Performance		
	N	Statistical Subset	Status	Cohesive Failure		
				PI (%)	Subset	Performance
6	9	A	Pass	98.3	A	Good
3	15.7	A, B	Pass	90.3	A, B	Good
12	19.2	B	Pass	97.9	A	Good
16	34.2	C	Fail	80.5	B	Fair
4	36.3	C	Fail	88.8	B	Fair
7	45.4	D	Fail	74.9	B	Poor

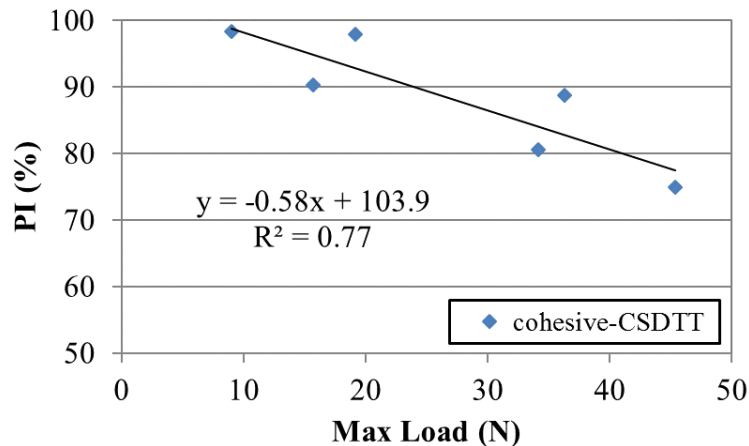


Figure 5.19. Performance index based on cohesive failure and CSDTT stiffness.

New York Test Site

The field-aged samples collected during the second survey from the NY test site were tested using the CSDTT test method. Similar to the MI test site, PI of clean and seal sections from the NY test site was correlated with the laboratory performance data in Table 5.13 through Table 5.15. The sealants Jd and Ob, belonging to the same subset for having low tensile load and high extensibility (greater than 70%), demonstrated good field performance in 2013. On the other hand, sealants Ca and Ib, belonging to the same statistical groups, failed in 2013 just after a winter season due to high tensile load and low extensibility. However, sealants Kc and Da had either high tensile load or low extensibility, and both demonstrated good field performance. The tensile failure energy, which considers the effect of both load and extensibility, is calculated and presented in Table 5.15. The table shows that sealants in laboratory subset “C” with low tensile energy (less than 5 N.mm) were the only ones that did not survive the first winter (sealant Ca and Ib).

Table 5.13. Statistical Grouping of the Sealants Based on CSDTT Maximum Load and Performance Index in New York Test Site.

Sealant ID	Maximum Load			Field Performance (2013)			Field Performance (2014)		
	N	Statistical Subset	Status	PI (%)	Subset	Performance	PI (%)	Subset	Performance
Ob	16.8	A	Pass	71.5	A	Good	14.3	B	Poor
Da	17.2	A	Pass	84.4	A, B	Good	13.9	B	Poor
Jd	20.5	A	Pass	76.3	A, B	Good	14.3	A, B	Poor
Ib	34.9	B	Fail	32.2	A	Poor	0	A	Poor
Kc	38	B	Fail	90.3	B	Good	24	B	Poor
Ca	38.1	B	Fail	50.8	A	Poor	5.4	A, B	Poor

Table 5.14. Statistical Grouping of the Sealants Based on CSDTT Extendibility and Performance Index in New York Test Site.

Sealant ID	Extendibility			Field Performance (2013)			Field Performance (2014)		
	%	Statistical Subset	Status	PI (%)	Subset	Performance	PI (%)	Subset	Performance
Ca	2.4	A	Fail	50.8	A	Poor	5.4	A, B	Poor
Ib	2.7	A	Fail	32.2	A	Poor	0	A	Poor
Da	13.4	A, B	Fail	84.4	A, B	Good	13.9	B	Poor
Kc	27.5	B	Fail	90.3	B	Good	24	B	Poor
Jd	72	C	Pass	76.3	A, B	Good	14.3	A, B	Poor
Ob	91.2	C	Pass	71.5	A	Good	14.3	B	Poor

Table 5.15. Statistical Grouping of the Sealants Based on CSDTT Energy and Performance Index in New York Test Site.

Sealant ID	Energy			Field Performance (2013)			Field Performance (2014)		
	N.mm	Statistical Subset	Status	PI (%)	Subset	Performance	PI (%)	Subset	Performance
Ob	275.9	A	Pass	71.5	A	Good	14.3	B	Poor
Jd	245	A	Pass	76.3	A, B	Good	14.3	A, B	Poor
Kc	156.7	A	Pass	90.3	B	Good	24	B	Poor
Da	32	B	Pass	84.4	A, B	Good	13.9	B	Poor
Ib	4.7	C	Fail	32.2	A	Poor	0	A	Poor
Ca	2.7	C	Fail	50.8	A	Poor	5.4	A, B	Poor

Summary of Lab-to-Field Comparison

Based on observations of two test sites, each including six clean and seal sections, tensile load and extendibility are well-correlated with field performance. The New York test site showed that using tensile energy renders better correlation between lab and field performance. Using extendibility as a threshold, however, would be a conservative approach.

5.4 Validation of High-Temperature Tests Methods

5.4.1 Crack Sealant Tracking Test Validation

Tracking failure is a crack sealant failure that results from vehicles shear loading. This type of failure is attributed to improper selection of sealant type, early traffic opening, or high temperatures. In the performance grading system, the tests performed to predict tracking failure are also used to determine high-temperature grades. In previous study (Al-Qadi et. al. 2009), a multiple-step creep recovery (MSCR) test was developed using dynamic shear rheometer (DSR)

to determine high-temperature grading and tracking resistance. The MSCR test is a well-developed test for this purpose, but needs to be validated using field performance data. However, the MSCR test procedures are extremely complex and time consuming. Therefore, there was a need to refine the MSCR test procedures or find a more practical test that would address the same need as MSCR. This test should simulate sealant tracking failure because of shearing at high temperatures.

An experimental procedure was developed to evaluate tracking resistance of crack sealants. This procedure can also be a candidate for determining the high-temperature grade of sealants to indicate safe installation without any tracking failure potential. A test procedure using DSR was implemented for simulating this phenomenon. A test with the following attributes is proposed for this purpose:

- Monotonic increase of shear strain at a constant shear rate until complete failure to observe yield point for sealants (shear strains will go up to 600%);
- A shear rate of 0.01 1/s;
- Test temperatures from 46 to 82 °C with 6 °C increments;
- A threshold value as a cut-off value for high-temperature grading. The threshold value will initially be determined based on MSCR results. For good tracking resistance, a higher shear stress than the recommended threshold is desired.

The testing protocol summarized in Table 5.16 was applied for ten selected sealants for grading and evaluation. The specimens were prepared according to ASTM D5167 procedures (1 hr melting and homogenization at recommended installation temperature). Unaged samples were selected to find the high-temperature grade. Most of the tracking failures was reported at the installation stage due to early opening to the traffic when the sealant was still hot.

Table 5.16. The Experimental Program for High-Temperature Grading.

Test	Parameter	Objective
MSCR	C and P values	To find high-temperature grade with respect to the previous procedure
Yield	Yield stress at a specific strain	A potential new approach for high-temperature grading

Crack Sealants Laboratory Performance at High Temperature

The sealants selected to be tested at high temperature are summarized in Table 5.1. The MSCR test results for these sealant were used to find the high-temperature grade presented in Table 5.1. According to the MSCR procedure, the sealant high-temperature grade was selected where C-value (flow coefficient) was higher than 4.0 kPa.s and P-value (thinning coefficient) was higher than 0.7. MSCR coefficients also show that the C-value is more critical for defining the high-temperature grade than the P-value.

Table 5.17. Summary of High-Temperature Grade for Selected Sealants Used in This Study

Sealant ID		MSCR Parameters		High-Temperature Sealant Grade (°C)
		C-value (kPa.s)	P-value	
1	Ad	4.4	0.91	70
2	Bb	4.8	0.92	64
3	Ca	4.6	0.96	70
4	Da	4.7	0.91	76
5	Ed	4.2	0.86	76
6	Gd	5.2	0.86	76
7	Jd	5.5	0.86	70
8	Ob	4.5	0.79	82
9	Pd ¹	NA	NA	64
10	Sd	6.3	0.85	76

¹The grade for sealant Pd is predicted based on coefficients at 70 °C.

On the other hand, the results of a sample yield test (for sealant Ad) conducted at different temperatures are presented in Figure 5.20. These tests were conducted at three different temperatures initially based on the grade defined by the MSCR test. As temperature increases, the capacity of the material sustaining shear loads decreases. Since the sealants do not exhibit a clear yielding point, yield stress is selected at specific strain levels (50%, 100%, and 200%).

The shear stresses of three different strain levels for sealants failing or passing temperatures are presented in Figure 5.21. A threshold value can only be determined after the yield tests are conducted at high-temperature grade. It can be seen that the yield test is a good alternative for grouping sealants in a stress range of 180-200 Pa at the expected grade of each material. Based on the strain level (50, 100, or 200%), a threshold value for shear stress can be selected. For example, if a sealant is tested at a specific temperature, and it has a shear stress higher than 160 Pa at 200% strain level, then the sealant will pass the criteria for that temperature.

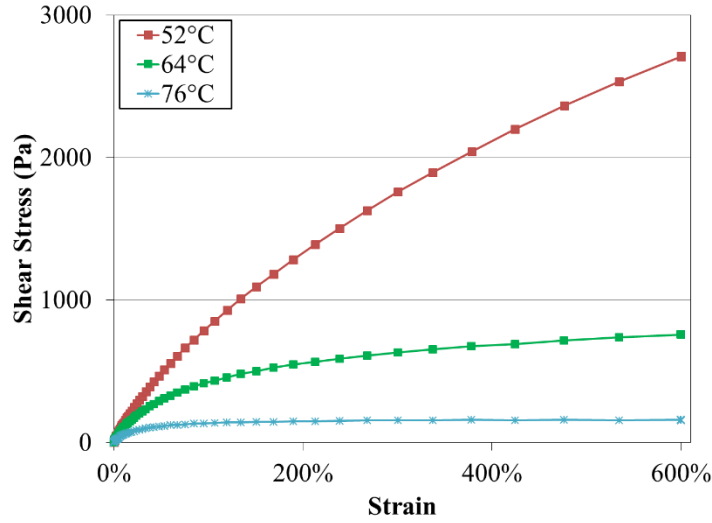


Figure 5.20. Shear stress vs. strain for sealants Ad at three different temperatures.

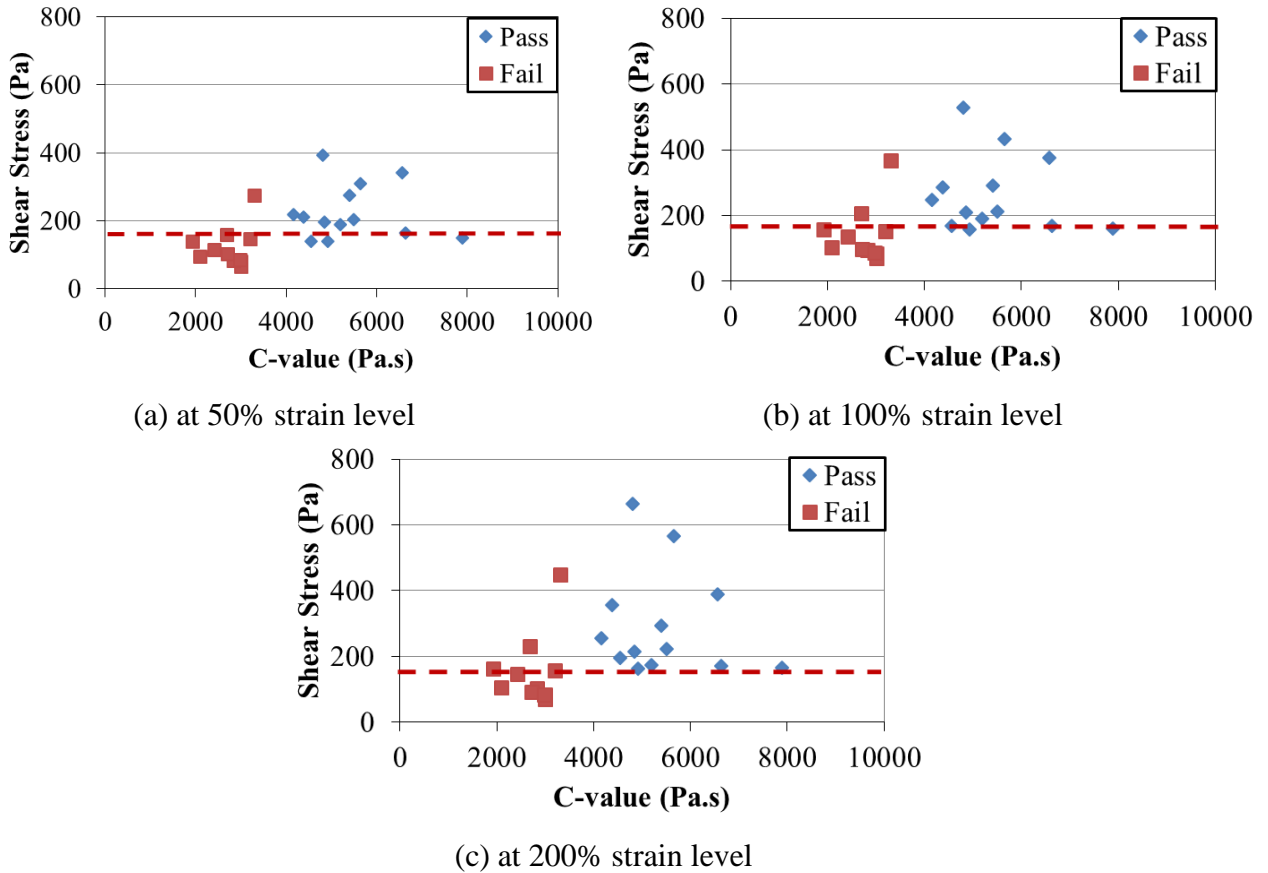


Figure 5.21. Shear stress threshold for yield testing at different strain levels.

Using the 180 kPa threshold at 200% strain, sealants are graded again for high temperature and correlated with the grade defined by MSCR test (Table 5.18). It can be seen there is a good correlation between two tests. Eight sealants have the same grade defined by both test methods.

Table 5.18. Crack Sealant High-Temperature Grads Using Yield Test and Correlating to MSCR Test.

ID		MSCR Grade (°C)	Yield Grade (°C)	Agreement
1	Ad	70	70	Yes
2	Bb	64	76	No
3	Ca	70	70	Yes
4	Da	76	76	Yes
5	Ed	76	76	Yes
6	Gd	76	76	Yes
7	Jd	70	70	Yes
8	Ob	82	82	Yes
9	Pd	64	76	No
10	Sd	76	76	Yes

Michigan Test Site

Six out of 16 sealants installed and evaluated by MDOT were selected for correlating field and laboratory performance. The main difference between Michigan test site evaluations and other test sites evaluations lies in the field surveys frequency which were conducted twice every year (winter and summer) as opposed to once a year for other test sites (after winter). This helps evaluate the overband failure separately for hot and cold seasons and correlate it with corresponding laboratory performance. Overband failure of sealants during the summer season happens as a result of insufficient tracking resistance at high in-service temperature. During hot seasons, the shear strength of sealants is reduced significantly so they may be picked up or tracked.

The ambient air temperature was continuously monitored using a data acquisition system installed on the site to collect and store temperature data. Table 5.19 shows the five maximum site temperatures for several years.

Table 5.19. Summary of Maximum Temperatures for the Five Hottest Days at Michigan Test Site.

Year	Temperature (°C)					Average
	1	2	3	4	5	
2011	35.2	35.0	34.8	34.8	34.5	34.9
2012	46.0	43.0	42.5	42.2	42.2	43.2
2013	29.5	28.5	26.5	24.8	24.8	26.8

Overband Performance of Selected Sealants During Summer

The PI of selected crack sealants installed in Michigan test site was calculated from 2010 onward, as presented in Figure 4.71, based on overband and cohesive failure.

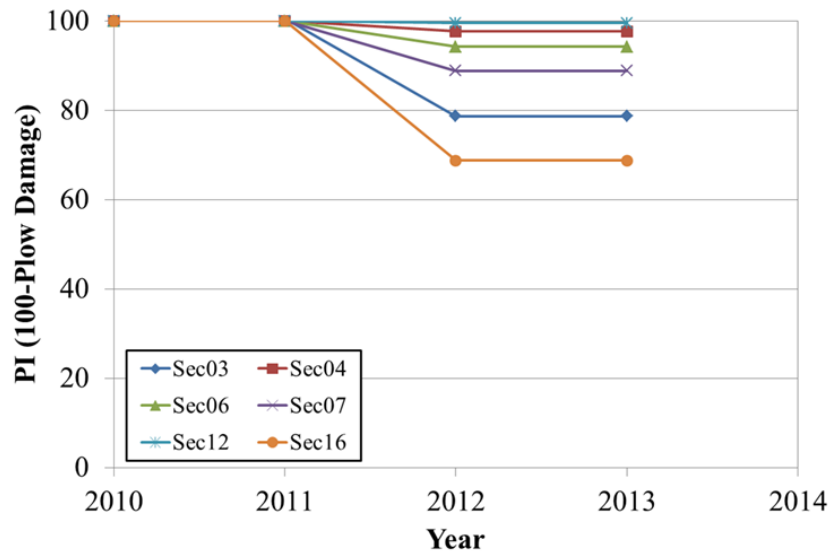


Figure 5.22. Performance index of all sealants based on overband failure.

Figure 4.71 presents the PI of sealants based on sealant tracking. Most sealants failures resulting from tracking occurred during summer 2012. Sections 12 and 4 are the best performers among the selected sealants while Section 16 is the worst performer followed by Section 3.

Overband and Laboratory Performance Correlation

Michigan sealants were also graded using both test methods (Table 5.20). For five out of six sealants, both tests rendered the same high temperature. The grade can also be correlated to the field performance presented earlier in Figure 4.71. Similar to the PI for cohesive failure, a PI lower than 80% reflects poor performance. Based on Table 5.20, Section 3 has the lowest grade with poor field performance. However, Section 16 had the lowest performance. The MSCR test shows a high grade for this section while the yield test grades it lower.

Table 5.20. Field and Lab Performance Correlation for Selected Sealants at Michigan Test Site.

Test Section	PI (%)	Field Performance	High-Temperature Grade (°C)	
			MSCR Test	Yield Test
3	78.7	Poor	64	64
4	97.8	Good	76	76
6	94.3	Good	70	70
7	88.9	Good	82	82
12	99.6	Good	70	70
16	68.8	Poor	76	70

Hamburg Wheel Test for Laboratory Validation of Tracking Test

The other approach for evaluating tracking resistance and validating laboratory tests (MSCR and Yield tests) is to use the Hamburg wheel test (HWT). A cyclic shear loading was applied on the specimen with true overband thickness by a steel tire. The number of cycles to complete failure, or a specific tracking length, was counted for evaluating the tracking potential of sealants (Figure 5.23). Four sealants with various high-temperature stiffness were selected for testing and validation (Ca and Bb as stiff sealants and sealants Ob and Ed as soft sealants). Specimens were prepared from the homogenized unaged samples.

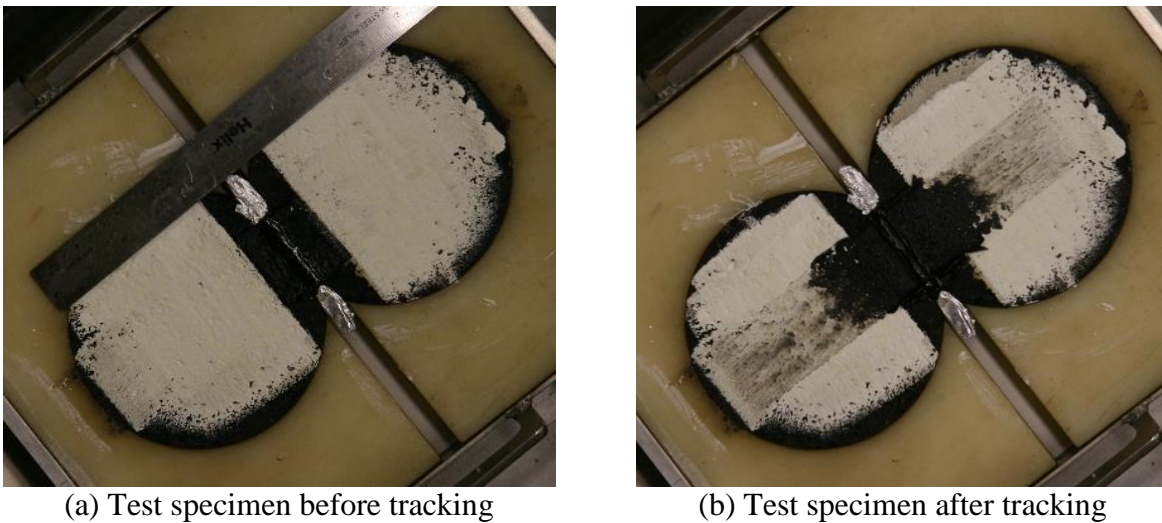


Figure 5.23. Hamburg wheel test.

The test results for four sealants are presented in Figure 5.24. Sealants with shorter tracking length are supposed to have a higher grade. However, looking at the MSCR results in Table 5.18, Sealant Ca and Bb had a low grades even with a low tracking length (around 10 mm). On the other hand, despite having a high tracking length, Sealants Ob and Ed had the highest grade among the sealants (Table 5.18). Results for HWT showed no correlation with the sealant grade defined by DSR.

Comparing the two different tests for high-temperature grade determination, the yield test is recommended for detecting tracking potential in a simplified approach.

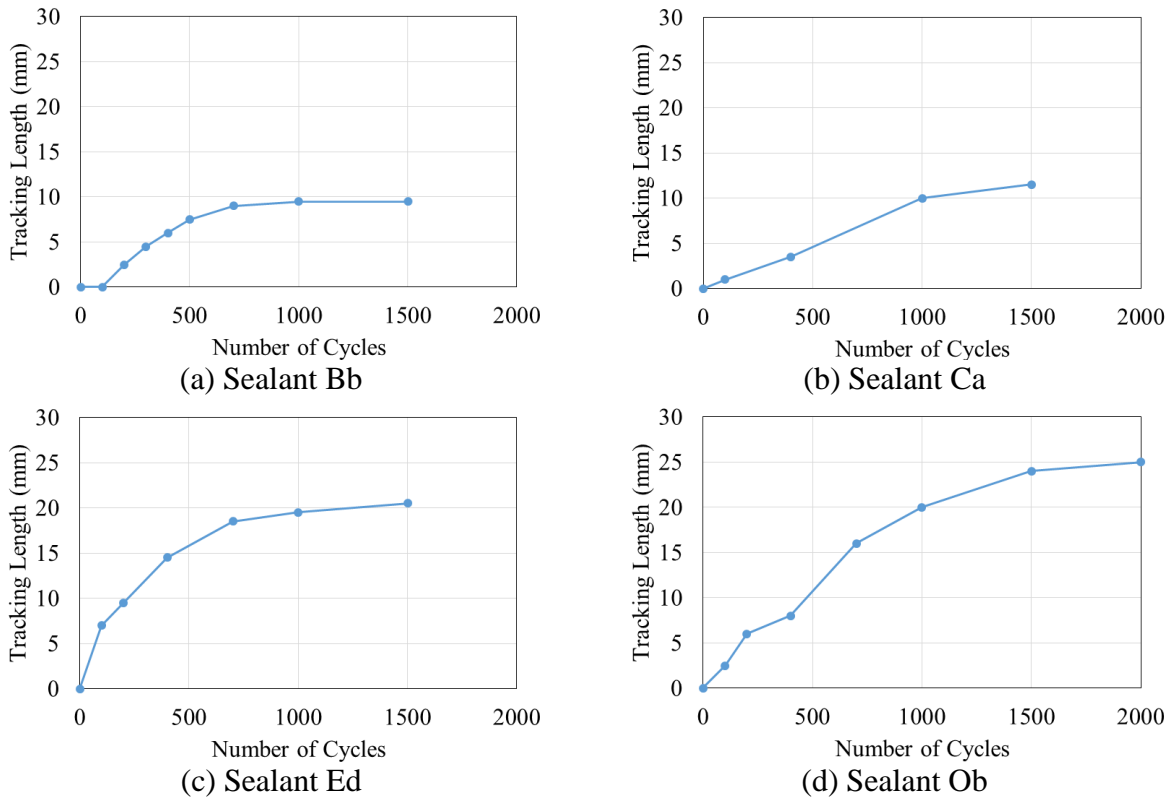


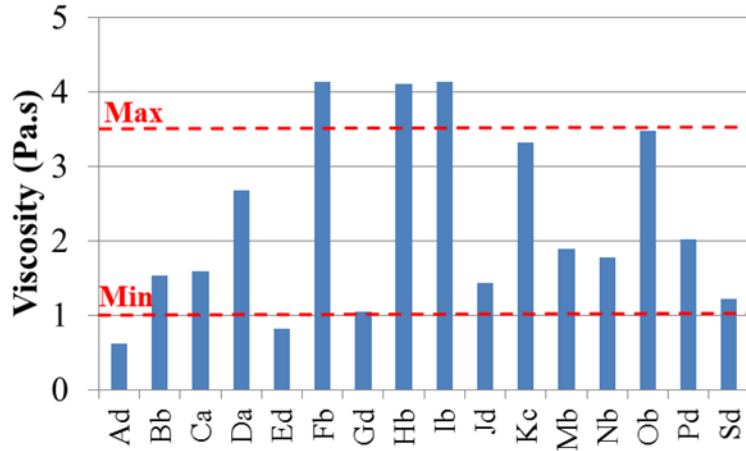
Figure 5.24. Tracking length by number of cycles for four selected sealants.

5.4.2 Rotational Viscosity Test

A Brookfield rotational viscometer was used to measure the apparent viscosity of hot-poured crack sealants (Figure 5.25a). This procedure was modified from the one adopted by SuperPave™ for asphalt binders (AASHTO T366). The main difference is the change in spindle and hook configuration along with some changes in testing procedures. The viscosity test was designed to simulate installation conditions. Since viscosity plays an essential role in predicting the field performance of hot-poured crack sealants, upper and lower viscosity limits were recommended. The upper limit ensures that the material is sufficiently liquid so it can be poured; the lower limit helps avoid excessively liquid sealants which create problems in filling cracks during installation. The tests were run in accordance with AASHTO T366 at 60 rpm at the installation temperatures recommended by the manufacturers. Test results for all sealants are presented in Figure 5.25b. Based on the field observations during installation, the thresholds showed reliability for ensuring sufficient workability during installation at the recommended pouring temperature. However, it is very important not to overheat or underheat sealants as will be discussed hereafter.



(a) Rotational Viscometer



(b) Test Results

Figure 5.25. Viscosity test and results

5.5 Thresholds Selection and Fine-Tuning

This section presents the methodology used in performing a holistic evaluation of field and laboratory results supported by statistical methods. The ultimate goal was to validate or fine-tune the performance thresholds to ensure the right selection of sealants based on test site requirements. Test method validation was performed by seeking positive correlation between test method criterion and field results. It was concluded that the test methods are providing satisfactory positive correlations.

In this section, sealants will be grouped based on their field performance. All test parameters were scored to find the strength of correlation between the test parameter and field performance. This score would help determine which test parameter was critical and should be selected to define the field performance.

After validating the test method and scoring the parameters, laboratory data were recalculated at the actual test site temperature and the required test site grading temperature during the service life using the collected temperature log and LTTPbind data. At the end, the thresholds would be selected by comparing the accurate test parameters at the performance temperature with the field performance index regarding the failure mechanism and corresponding test parameter.

5.5.1 Evaluation of Field Performance in Relation to Laboratory Test Results

Low-temperature test parameters and their expected trend with field performance are summarized in Table 5.21. Cohesive failure was the main failure type observed in clean and seal

treatment, while adhesive failure was the main failure type observed in rout and seal treatment. Field correlation results showed that the crack sealant bending beam rheometer (CSBBR) parameters (especially stiffness) play an important role in ensuring good sealant durability for types of treatment applications. Thus, a higher relaxation potential (represented by high ACR values) is required to ensure good flexibility rate of the material against deformation. Stiffness reduces the stress built up during crack movements within the material as well as at the interface of the material and rout wall. The parameters obtained from the CSBBR test can be related to adhesive and cohesive failures as stiffness was also shown to reflect the overall characteristics of sealants as related to formulation and field performance.

Table 5.21. Test Parameters and Expected Trends with Field Performance.

Test Method	Test Parameter	Expected Trend with Field Performance	Mechanism	Application
CSBBR (AASHTO T368)	Stiffness at 240 s	Inverse	Increasing stiffness and higher stresses in the sealant	Required for both rout and seal and clean and seal
	Average Creep Rate	Proportional	Lower ACR and higher stresses in the sealant	Required for both rout and seal and clean and seal
CSAT (AASHTO TP 370)	Peak Load	Proportional	Increasing adhesive load and stronger bond between sealant and rout's wall	Required for rout and seal
	Interfacial Energy	Proportional	Increasing energy and work of adhesion	Required for rout and seal
CSDTT (AASHTO T369)	Extendibility	Proportional	High elongations and large crack openings	Required for clean and seal
	Dissipated Energy	Proportional	Increasing energy and better tensile work	Required for clean and seal

The CSAT simulates adhesion performance in the rout and seal configurations. The parameters that can be obtained are maximum adhesion load and interfacial energy. Higher peak loads as well as higher adhesive energy are desired for good bonding between the sealant and rout wall. The crack sealant direct tension test (CSDTT) method is required to ensure good cohesive properties of the sealants for clean and seal treatment. Therefore, high extendibility and tensile energy should result in better field performance. Based on the field observations, the following grading scheme is recommended for the two sealing applications:

- Rout and Seal (R&S): CSBBR is the primary test (stiffness and ACR parameters) and adhesion (the CSAT and maximum adhesion load parameter) is the secondary test.
- Clean and Seal (C&S): CSBBR is the primary test (stiffness and ACR parameters) and the direct tension test (the CSDTT and extendibility parameter) is the secondary test.

Based on the laboratory performance and correlation with field performance, sealants can be categorized into three general groups (Table 5.22). The first group represents sealants with poor field performance ($PI < 50\%$). Compared to the site they are installed in, the sealants in this group possessed too stiffness and low adhesive properties.

The majority of sealants belong to the second group which represents fair field performance ($50\% < PI < 70\%$). Most of these sealants have low stiffness (except F_b and E_d) with respect to test site requirements. In addition, except for Sealant Pd, all other sealants in this group have an acceptable adhesive load at the test site temperature and, therefore, their fair performance can be related to the low stiffness and resistance to wear and abrasion, as discussed earlier in this chapter. Low CSBBR stiffness means low resistance against plows and early failure of the overband which will expose the sealant and rout interface to the adhesive failure. It is important to note that the performance of some sealants in this category could be lower or higher depending on the on-site conditions such as crack length, pavement and initial crack condition as well as the installation quality.

The third group includes sealants that have moderate stiffness and good adhesive performance at the test site low temperature. This is the ideal combination for longer field performance. Subsequently, these sealants also have good field performance ($PI > 70\%$).

Table 5.22 presents the average climatic conditions observed in the majority of test site installations to illustrate the most critical testing parameters that have a defining role in the field performance. It appears that adhesion and stiffness are the two critical parameters. In general, it was observed that when adhesion capacity is low, the risk of premature failures is high accompanied by crack openings as well as excessive stiff characteristics of sealants (two or more grades warmer) in this performing group. The best performing sealants are the ones with high adhesion capacity and moderate stiffness as compared with the climate they are installed in. The medium performing group are those with soft sealants (one or two grades colder) and moderate adhesion. Mobility is observed in this group indicating moving upward and downwards in the

ranks depending on the installation quality and on-site conditions affecting crack movements such as crack length, pavement type and materials. Another observation from the information provided in the table is the correlation between adhesion and stiffness property. As sealant stiffness increases or decreases, adhesion capacity drops indicating an optimum adhesion performance that can be obtained from a sealant formulation.

Table 5.22. Overall Sealant Grouping Based on Expected Field Performance for Sites at Moderately Cold Climate Regions (-28 to -34°C) .

Sealant ID	Test Site	Field Performance	Adhesion Load	Stiffness Property	Remarks
Bb	ON, MN, WI	Group 1: Poor (PI less than 50%)	Low	High	Sealants having high stiffness AND low adhesive capacity. Failure mechanism could be due to low adhesion or excessive stiffness with respect to the climate they are installed in.
Ca	NY		Low	High	
Hb	MN		Low	High	
Ib	NY		Low	High	
Kc	NY, NH		Low	High	
Ad	MN, WI	Group 2: Fair (PI between 50% and 70%)	Medium	Low	Sealants with low stiffness AND moderate adhesion capacity. Overband failure common in those sealants. Some mobility upwards or downwards is expected with installation quality and on-site conditions (i.e., Ed and Fb)
Ed ¹	NH, WI		Medium	Low	
Fb ¹	MN, NH, WI		Medium	Medium	
Gd	MN, ON, NH		Medium	Low	
Mb	MN, ON		Medium	Low	
Nb	MN		Medium	Low	
Ob	NH, NY		Medium	Low	
Pd ²	ON, WI		Low	Low	
Sd	ON	Group 3: Good (PI higher than 70%)	High	Medium	Sealants with moderate stiffness AND good adhesion capacity. Candidates for the best performance for this climate.
Da	ON, NY		High	Medium	
Jd	NY		High	Medium	
Rb	ON		High	Medium	

¹ Sealant Pd can switch to a low performing type depending on the on-site conditions and installation quality

² Sealants Fb and Ed were among the relatively high performing subset of medium performing sealants. Depending on the on-site conditions and installation quality, these two sealants can switch to high performing group.

5.5.2 Correlation Score between Field and Laboratory Performance

A holistic evaluation method is required to evaluate which laboratory test method has the best correlation to field performance and determine where to draw boundaries of performance thresholds to improve the strength of correlation. Composite score was used to establish a

quantitative correlation based on lab-to-field correlation of sealants utilizing the parameters obtained from different test methods. Different statistical tests were used to develop a composite score and to establish a quantitative correlation based on the field performance of sealants (PI) compared with different parameters, such as flexural stiffness and ACR from the CSBBR method, peak load from CSAT method, and peak load and extendibility from CSDTT method. Two different statistical correlation techniques were used: Kendall's tau-b and regression (linear or quadratic). Kendall's tau-b is an independence test that correlates PI with test parameters based on ranking; the regression method correlates field and lab results based on their values.

The composite score is developed based on Gibson et al. (2012) as follows:

$$CS = \frac{|R|+(1-P_R)+|\tau_K|+(1-P_K)}{4} \quad (5.1)$$

where,

CS = Composite score, (0 for no correlation and 1 for complete correlation)

R = Regression coefficient

τ_K = Kendall's tau-b measure of association score, $-1 < \tau_K < 1$

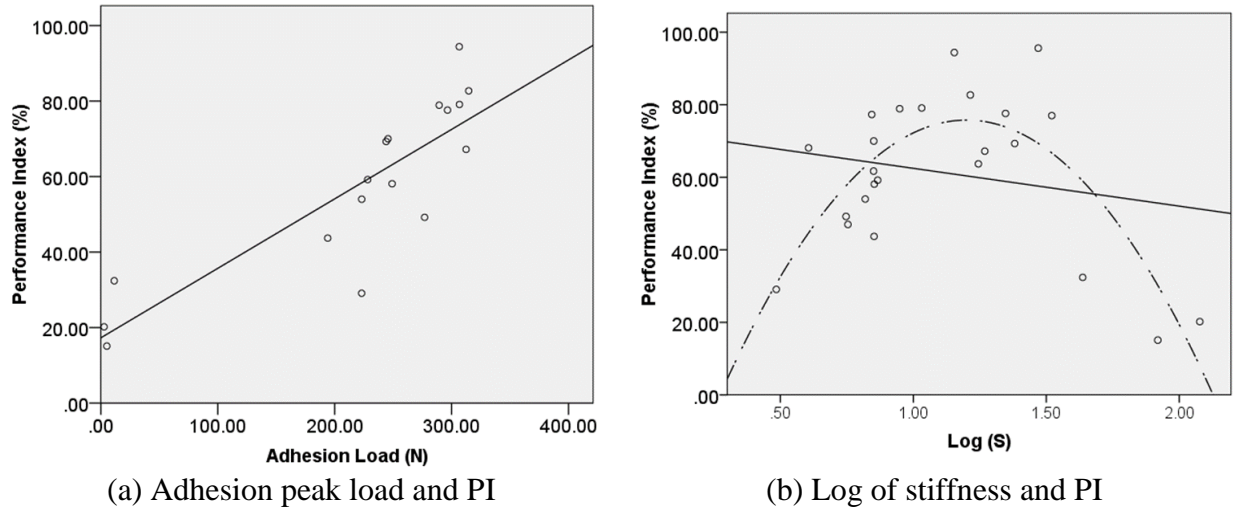
P_R = ANOVA significance of the regression slope

P_K = Significance of the Kendall's tau-b association

Kendall's tau-b measure of association is a distribution-free, or non-parametric, rank correlation parameter. Kendall's parameter is better suited to small datasets than the correlation coefficient, R , or the coefficient of determination, R^2 , which are more appropriate for larger datasets. First, it is important to find the type of regression between the PI and test parameters. Figure 5.26 shows that there is a linear regression between PI and adhesion peak load whereas the relationship between the PI and stiffness is quadratic.

The statistical significance for regression and Kendall's parameters are obtained using SPSS statistical tool. Using these parameters, the composite score was calculated for clean and seal as well as rout and seal sections. For the rout and seal sections, the scores of CSAT and CSBBR parameters were evaluated, while for clean and seal sections the scores were calculated for CSDTT and CSBBR parameters. The following thresholds were used to identify satisfactory levels of correlation. A score higher than 0.60 was considered acceptable and a score higher than 0.80 indicated a strong correlation between the parameters. Composite scores using stiffness and

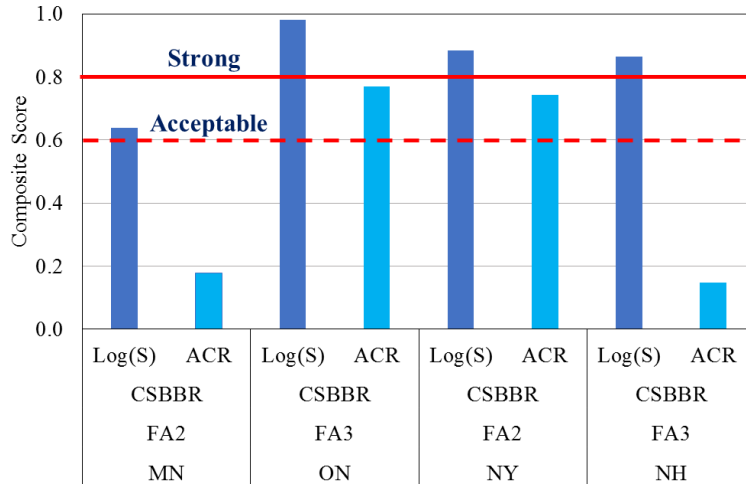
adhesion criteria are shown in Figure 5.27. Low-temperature stiffness parameter obtained from the CSBBR test (Figure 5.27a) had a strong correlation with the field performance (except Minnesota test site which has an acceptable correlation score). However, the score for ACR was either acceptable or very poor. Adhesion peak load and energy, except for the sealants in the Minnesota test site, had an acceptable or a strong correlation score with the field performance (Figure 5.27b).



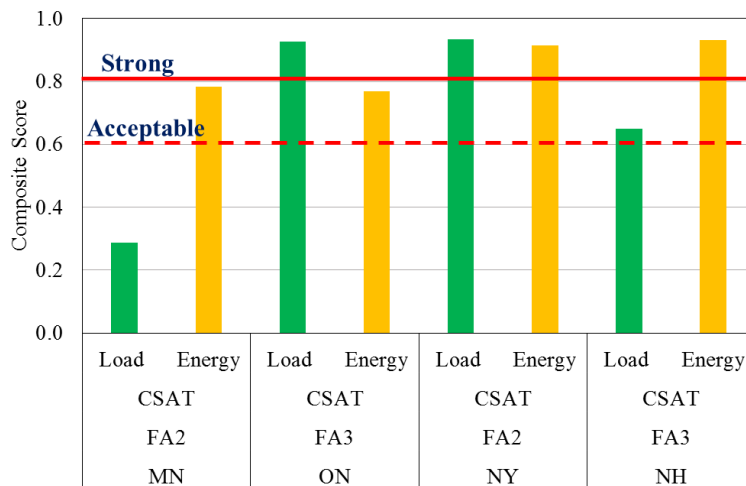
(a) Adhesion peak load and PI (b) Log of stiffness and PI
 Figure 5.26. Type of regression between test parameters and performance index (PI).

To calculate the composite score for clean and seal treatment, New York and Michigan test sites were selected. The number of sections treated as clean and seal at these two test site were sufficient to run an acceptable statistical test. For the clean and seal sections, the correlation score was calculated for the parameters obtained from CSDTT and CSBBR methods. The scores presented in Figure 5.28 show that, similar to the rout and seal sections, stiffness had a strong correlation with field performance. However, ACR either resulted in a strong or very poor score. For the CSDTT test parameters, both peak load and extendibility had an acceptable or strong score.

In addition to the field and lab correlation, the relationship and strength of correlation between the main test parameters with each other was also investigated. The correlation score between CSBBR stiffness and CSAT peak load is presented in Figure 5.29a. It can be concluded that these two parameters had a strong correlation for most cases, except Minnesota, which could be considered an acceptable correlation. Similarly, for CSBBR stiffness and CSDTT peak load, a strong correlation was observed for both New York and Michigan test sites (Figure 5.29b).



(a) CSBBR test parameters



(b) CSAT test parameters

Figure 5.27. Composite score correlating test parameters with PI for rout and seal sections.

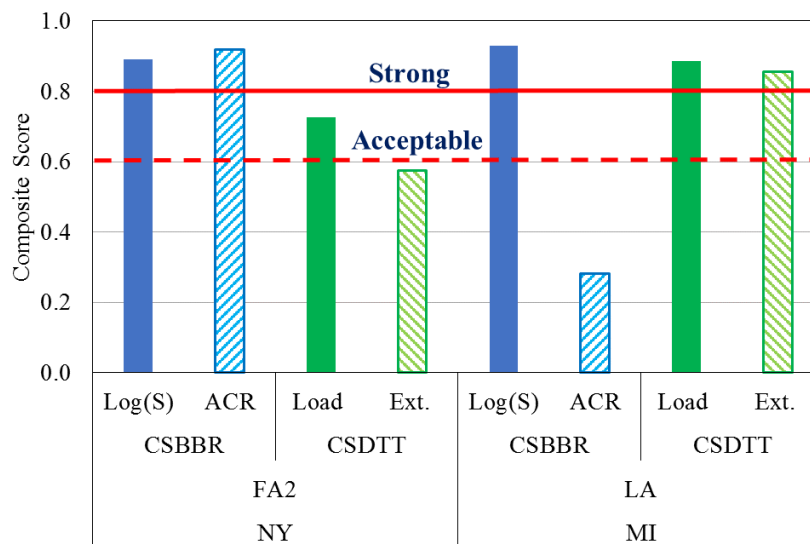
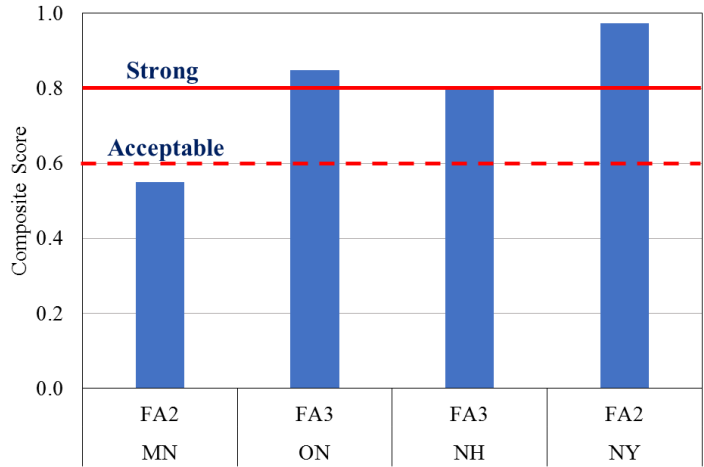
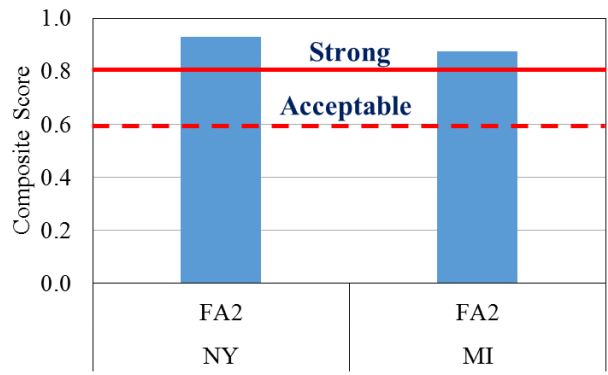


Figure 5.28. Composite score correlating test parameters with PI for clean and seal sections.



(a) CSBBR stiffness and CSAT peak load



(b) CSBBR stiffness and CSDTT peak load

Figure 5.29. Composite score correlating different test parameters with each other.

5.5.3 CSBBR Test Performance Thresholds Fine-Tuning

The CSBBR test was validated using the correlation of field and lab performance of 17 different sealants in five test sites with diverse climates. In the following section, the parameters and thresholds were fine-tuned using the same field and laboratory performance data.

Validation of Maximum Stiffness Threshold

A maximum threshold for stiffness must be set to ensure the flexibility of crack sealants at low temperature due to thermal loading caused by crack opening. Thermal loading is simulated by the creep test and measuring stiffness after 240s which represents five hrs of crack continued opening. During test development, the five-hr loading time was obtained based on the data collected from the two different sites. During field installation, a wireless temperature node was installed at each test site to monitor air temperature during the evaluation period (Figure 4.46). The ambient temperature data was used to validate or adjust the time of creep loading. A

maximum threshold was defined for each test site. Then, based on all of the threshold value measured for each test site, final threshold for maximum allowable stiffness was selected.

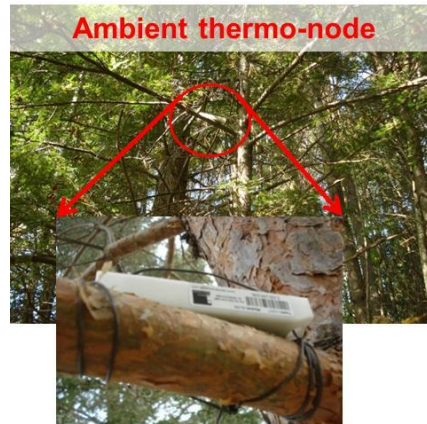


Figure 5.30. Wireless temperature node for ambient temperature.

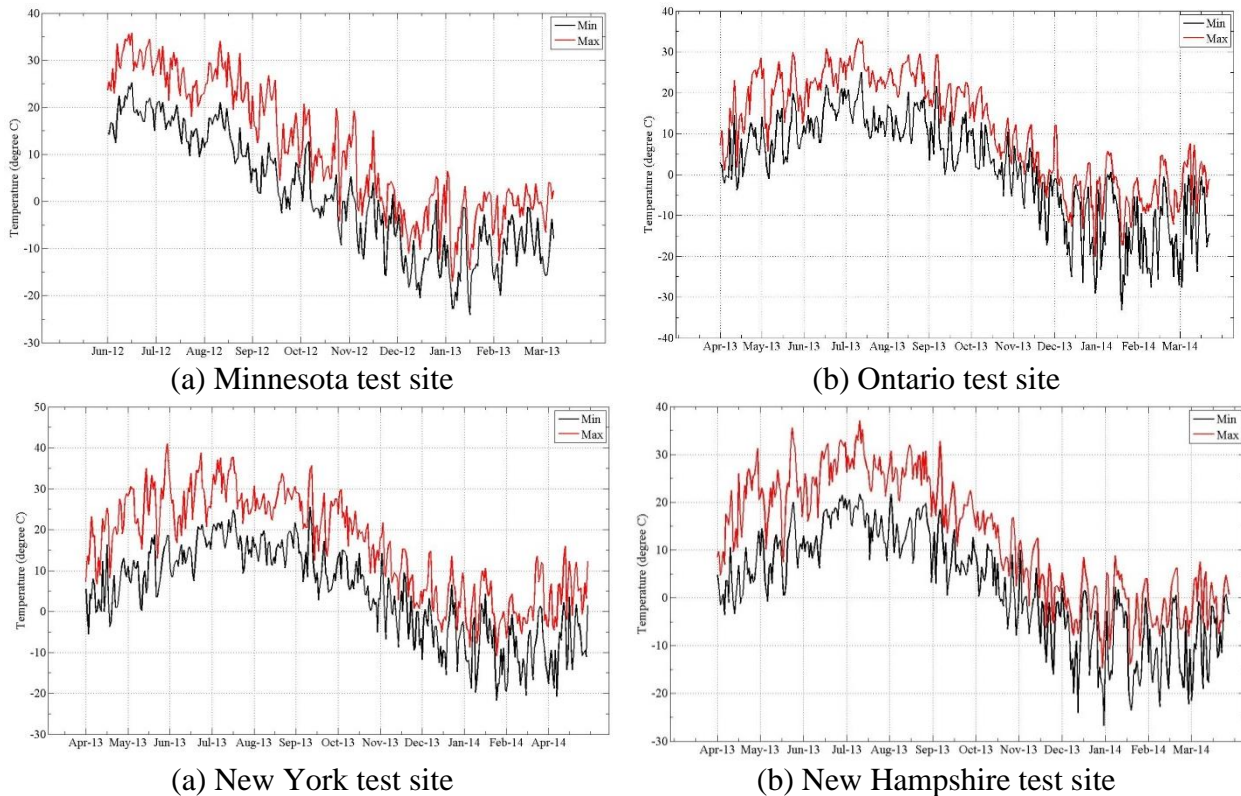


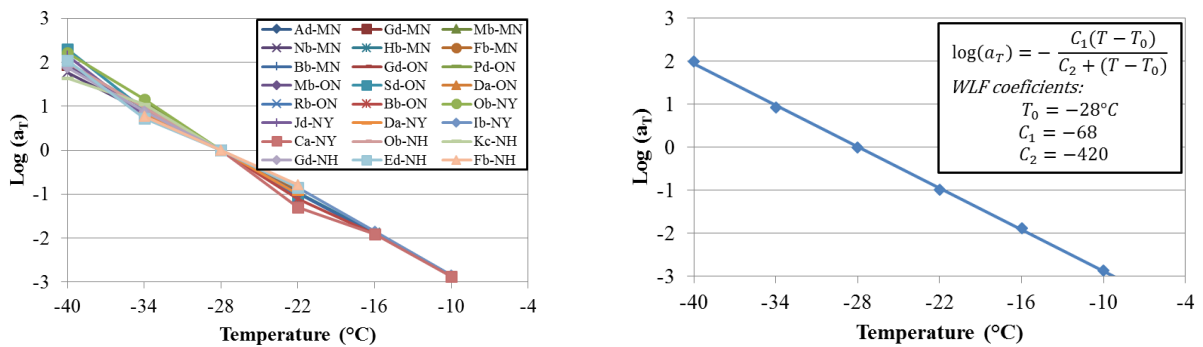
Figure 5.31. Ambient temperature for all test sites during the second year after the installation.

The temperature log obtained from all four test sites in the second (Minnesota and New York sites) and third (New Hampshire and Ontario sites) years after installation is plotted in Figure 5.31. Based on the temperature log, the minimum temperatures for the five coldest days in the second winter are summarized in Table 5.23 for each test site. The average of these five days was used to obtain the thresholds.

Table 5.23. Summary of Minimum Temperatures for the Five Coldest Days at All Test Sites

Test Site	Temperature (°C)					
	1	2	3	4	5	Average
Minnesota	-24.0	-22.8	-22.8	-21.0	-20.5	-22.2
Ontario	-33.2	-29.0	-28.8	-27.5	-27.5	-29.2
New York	-21.7	-20.7	-20.5	-19.7	-19.0	-20.3
New Hampshire	-26.7	-24.0	-23.5	-22.8	-22.2	-23.8

To fine-tune the maximum threshold, sealants properties should be measured or calculated at the actual field low temperature. Stiffness master curves were shifted to the low test site temperature and the stiffness was extracted at proper thermal loading time. All shift factors used to calculate the master curves for field-aged samples are presented in Figure 5.32a. Based on the average shift factors, considering all sealants tested herein, it was observed that almost every 6 °C in temperature shifting is equal to a decade of shifting in loading time (Figure 5.32b). Based on the CSBBR test method, sealants should be tested to determine stiffness at 240s at a temperature 6 °C higher than their sealant grade. Therefore, the stiffness at 240s at the testing temperature would be equivalent to the stiffness of the same sealant at 2400s at grading temperature. Hence, stiffness values for the sealants with highest stiffness at different test sites were calculated from the master curves at 2400s at the average test site low temperature and correlated with the field PI in Table 5.24.



(a) All shift factors to obtain master curves

(b) Average shift factors

Figure 5.32. Shift factors for all field-aged sealants to obtain master curve at -28 °C.

A sealant with a PI less than 70% was considered as failed. For specific test sites, such as Minnesota and New Hampshire, none of the sealants failed due to high stiffness value. In these test sites, there could be other reasons for the sealants poor field performance. For example, the failure could be attributed to poor adhesion bonding, installation quality, or softness of the sealants at low temperatures.

Three sealants demonstrated poor performance as a result of high stiffness (Ib and Ca at New York test site and Bb at Ontario test site). Stiffness data obtained from the CSBBR test and PI for these sealants are summarized in Table 5.24. Based on lab and field correlation, high stiffness threshold can be selected as 15 MPa at the testing temperature (6 °C below grading temperature), which is lower than the initial threshold (25 MPa) selected during the test development.

Table 5.24. Field and Lab Correlation for Sealants Failing due to High Stiffness

Sealant ID	Test Site	CSBBR Stiffness at Real Test Temperature (MPa) ¹	CSBBR Stiffness at Test Site Low Temperature (MPa) ²	Performance Index (PI)	Status
Ib	NY	19.1	14.4	15.1	Fail
Ca	NY	22.0	14.8	20.2	Fail
Bb	ON	18.2	22.7	32.4	Fail
Da	ON	10.7	10.9	77.6	Pass
Rb	ON	8.96	12.0	69.3	Pass

¹ Stiffness is obtained from stiffness master curve by shifting to the actual test site temperature

² Stiffness is obtained from the test temperature based on the test site sealant grade

Minimum Stiffness Threshold

Based on field results, it was observed that some sealants could have failed because of their low stiffness. In winter, snow plowing combined with traffic shear loading may cause damage to sealants by applying high amounts of shear stresses at low speeds. Vehicular loading can also contribute to wearing of sealants. Sealants with low stiffness would not have enough resistance against the applied shear loading, thus leading to overband loss. In a study by Ozer et al. (2014), it was observed that overband has a significant effect on the performance of sealants. Therefore, a minimum stiffness threshold should be identified for sealants to assure their resistance to plow damage.

To determine the minimum threshold, the shear rate applied to the sealants by plow must first be calculated. Shear rate is the ratio of loading speed to thickness of the material:

$$\dot{\gamma} = V/h \quad (5.2)$$

Assuming a plow speed of 8.94 m/s (20 mph) and a typical rout depth of 20 mm, the shear rate would be 447 1/s. Hence, loading time would equal 0.0022s. The minimum threshold is, therefore, obtained by correlating the stiffness values identified from the CSBBR master curves at low temperature with the PI. The summary of field and lab data for the sealants failing due to their low stiffness in all test sites is presented in Table 5.25. Based on these results, the minimum

stiffness can be defined as 210 MPa at real loading time (0.0022s). Stiffness of sealants to withstand loading rate applied by plows was extracted from the master curves developed using the CSBBR test. A practical loading time in the CSBBR test is then needed to correlate with relatively fast loading rates applied in the field and resulting in overband wear. Thus, the corresponding stiffness in the CSBBR is also calculated during the first second at the testing temperature, which represents sealants resistance to faster loading rates (Table 5.25). Based on the lab and field correlation, it is concluded that the low stiffness threshold should be more than 40 MPa at the testing temperature.

Table 5.25. Field and Lab Correlation for Sealants Failing due to Low Stiffness.

Sealant ID	Test Site	PI (%)	CSBBR Stiffness (MPa) at 0.0022s at real temperature ¹	CSBBR Stiffness (MPa) at 1s at test temperature ²	Status
Ob	NY	54.0	128.8	18	Fail
Gd	MN	47.0	194.0	39	Fail
Nb	MN	61.7	168.8	21	Fail
Ad	MN	68.1	157.0	< 40	Fail
Sd	ON	79.1	> 750	92	Pass
Mb	MN	77.3	244.4	74	Pass
Da	NY	82.7	266.2	69	Pass

¹ Stiffness is obtained from stiffness master curve by shifting to the actual test site temperature

² Stiffness is obtained from the test temperature based on the test site sealant grade

5.5.4 CSDTT Test Performance Thresholds Fine-Tuning

The recommended thresholds for minimum extendibility at testing temperature (6 °C higher than grading temperature) are summarized in Table 5.26. Similar to the CSBBR test method, CSDTT was validated using the correlation of field and lab performance. The parameters and thresholds were fine-tuned using the same field performance data and laboratory performance of sealants.

Table 5.26. Extendibility Thresholds for CSDTT Method.

Temperature (°C)	-4	-10	-16	-22	-28	-34	-40
Extendibility (%)	10	25	40	55	70	85	85

Field and lab correlation showed that sealants passing the extendibility threshold also performed well in the field. However, field and lab correlation showed that some sealants might fail the extendibility threshold, but had acceptable field performance (sealant Kc and Da in New York test site). In this case, load is defined as a secondary threshold. CSDTT tensile load indicates

sealants brittleness; the higher the tensile load, the more brittle the sealant can be. Brittle sealants are not appropriate for clean and seal treatment. The peak tensile load for sealants treated as clean and seal is plotted based on their PI in Figure 5.33. This plot shows that sealants with a peak tensile load higher than 25 N have poor field performance and, therefore, this value can be selected as a secondary threshold for the CSDTT method.

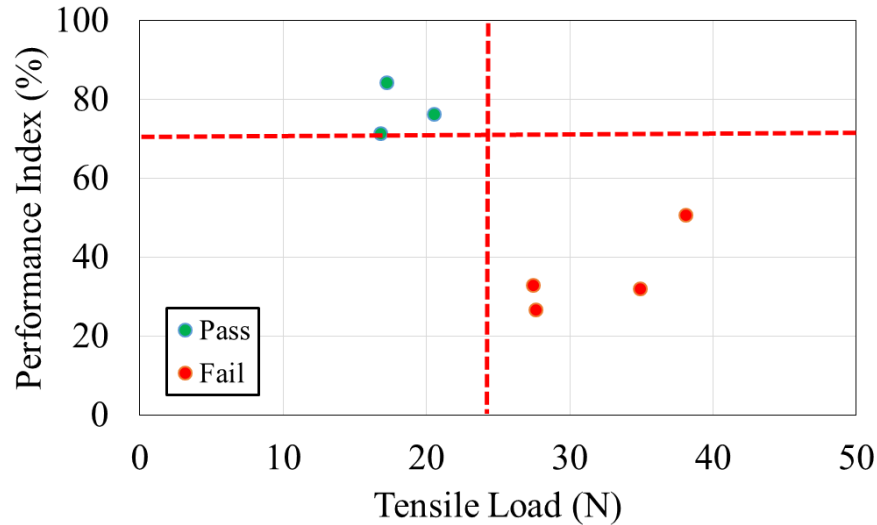


Figure 5.33. Sealants CSDTT tensile load vs. performance index.

5.6 Sealant Laboratory Performance and Grading Based on New Thresholds

A summary of fine-tuned thresholds and grading scheme is presented in Table 5.27. Based on the performance correlations, new thresholds are proposed. The new low-temperature grading scheme also suggests a different testing protocol for the sealing techniques. The CSBBR test is used for both techniques. The CSAT follows the CSBBR for the rout and seal technique while the CSDTT is required for the clean and fill technique. All sealants in the test matrix are graded again using low-temperature tests based on the new thresholds summarized in Table 5.28.

The required SG based on LTPPbind for different test sites is listed in Table 5.29. These grades are based on ambient temperature rather than pavement temperature. Most of failures in crack sealants were initiated at the top of sealant exposed to weathering effects and overband wear. Therefore, using the ambient temperature for grading represents a conservative approach.

Table 5.27. Summary of the New and Old Thresholds for Low-Temperature Tests.

Test Methods	Test Parameter	Treatment Type	Criteria	Threshold	
				Preliminary	Fine-tuned or New
CSBBR	Max. Stiffness	C&S R&S	@ 240s @Temp 6°C Higher Than Grade	25MPa	15MPa
	Min. Stiffness	C&S R&S	@ 1s @ Temp 6°C Higher Than Grade	N.A.	40MPa
	ACR	C&S R&S	@Temp 6°C Higher Than Grade	0.31	0.31
CSDTT	Extendibility	C&S	@ Max/Failure Load @Temp 6°C Higher Than Grade	Diff. % at Diff. Grade	Kept Same
	Load	C&S	Maximum/Failure Load	N.A.	25 N
CSAT	Min. Load	R&S	@Temp 6°C Higher Than Grade	50N	50N (@ - 4°C) + 25/- 6°C

Table 5.28. Low SG based on Fine-Tuned Thresholds.

ID		Rout and Seal (R&S)			Clean and Seal (C&S)			Initial SG (°C)
		Low-Temperature Grade (°C)			Low-Temperature Grade (°C)			
		CSBBR	CSAT	Overall	CSBBR	CSDTT	Overall	
1	Ad	-40	-46	-40	-40	-46	-40	-40
2	Bb	-22	-22	-22	-22	-16	-16	-16
3	Ca	-16	-22	-16	-16	-10	-10	-10
4	Da	-28	-40	-28	-28	-34	-28	-34
5	Ed	-34	-46	-34	-34	-40	-34	-40
6	Fb	-34	-40	-34	-34	-34	-34	-34
7	Gd	-40	-40	-40	-40	-46	-40	-34
8	Hb	-28	-22	-22	-28	-22	-22	-22
9	Ib	-16	-10	-10	-16	-10	-10	-10
10	Lb ¹	NA	NA	NA	NA	NA	NA	NA
11	Jd	-46	-40	-40	-46	-46	-46	-46
12	Kc	-34	-22	-22	-34	-28	-28	-28
13	Mb	-34	-40	-40	-34	-40	-40	-34
14	Nb	-40	-40	-40	-40	-40	-40	-34
15	Ob	-40	-40	-40	-40	-40	-40	-40
16	Pd	-40	-40	-40	-40	-28	-28	-28
17	Rb ¹	NA	NA	NA	NA	NA	NA	NA
18	Sd	-34	-40	-34	-34	-34	-34	-34

¹ Virgin samples was not available to be aged and graded in the laboratory.

Table 5.29. Required SG for Test Sites based on LTTPbind.

Test Site Location	Ambient (°C)		Low SG (°C)
	Min	Max	
Belleville, Wisconsin	-28.9	32	-34
St Charles, Minnesota	-31	31.1	-34
Lindsay, Ontario, CA	-28.7	29.7	-34
Grantham, New Hampshire	-29.1	31.9	-34
Canandaigua, New York	-24	30.9	-28

Based on the sealants SG and required grade for the test sites, the grade difference was calculated separately for two different treatments (clean and seal and rout and seal):

$$SG_{diff} = SG_S - SG_T \quad (5.3)$$

where, SG_S is the sealant grade and SG_T is the required grade for the test site. The statistical boxplots are generated based on the grade difference (Table 5.30) for each sealant and its PI. For rout and seal sections, Figure 5.34a shows that sealants at the right grade (with no-grade-difference) performed well at the test sites. Sealants at a grade higher than the required grade for the test site (positive grade difference) failed in the lab due to high stiffness, low adhesion load, or both and were eventually graded with a higher grade. These sealants (to the right of no-grade-difference) showed declining performance in the field. On the other hand, sealants with a grade lower than test site grade (negative grade difference) had much lower stiffness than required and were graded accordingly. These sealants (to the left of no-grade-difference) demonstrated poor performance possibly due to low stiffness and early overband failure, which may have accelerated other types of failures such as the adhesive failure.

Similar observations, but not as clear as the rout and seal case, can also be seen for the clean and seal treatment. Sealants with a higher grade (positive grade difference) have an insufficient cohesive capacity (failing either of the thresholds for maximum stiffness or minimum extendibility) leading to poor field performance. On the other hand, sealants with a lower grade (negative grade difference) could be too soft for the test site. These sealants could suffer from overband wear due to low stiffness.

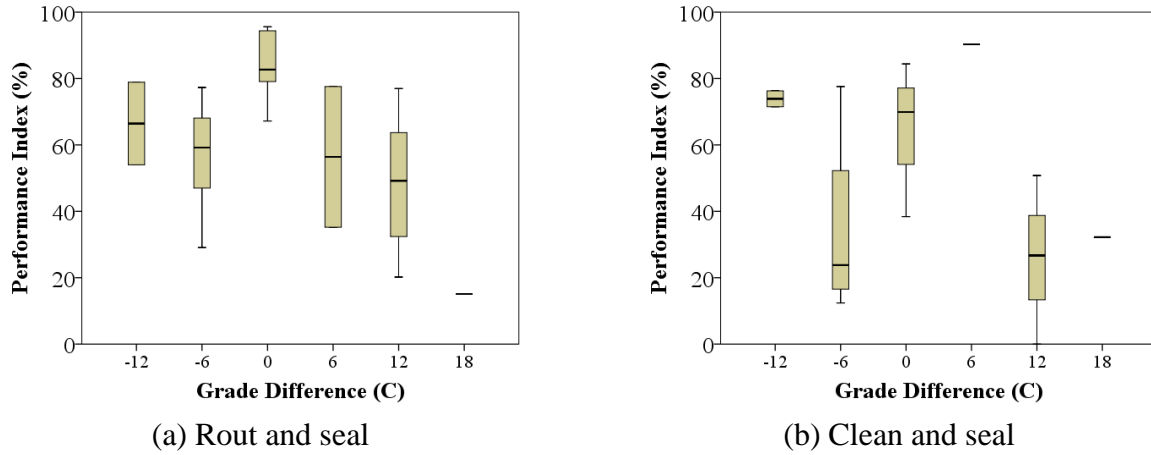


Figure 5.34. Boxplots of the relationship between sealants grade difference with test site and their field performance.

Table 5.30. SG Difference for the Sealants Installed at Different Test Sites.

Sealant ID	Low SG (°C)	Test Site SG (°C)			
	R&S/C&S	Minnesota	Ontario	New Hampshire	New York
		-34	-34	-34	-28
Ad	-40/-40	-6/-6	-	-	-
Bb	-22/-16	12/18	12/18	-	-
Ca	-16/-10	-	-	-	12/18
Da	-28/-28	-	6/6	-	0/0
Ed	-34/-34	-	-	0/0	-
Fb	-34/-34	0/0	-	0/0	-
Gd	-40/-40	-6/-6	-6/-6	-6/-6	-
Hb	-22/-22	12/12	-	-	-
Ib	-10/-10	-	-	-	18/18
Jd	-40/-46	-	-	-	-12/-18
Kc	-22/-28	-	-	12/6	6/0
Mb	-40/-40	-6/-6	-6/-6	-	-
Nb	-40/-40	-6/-6	-	-	-
Ob	-40/-40	-	-	-6/-6	-12/-12
Pd	-40/-28	-	-6/6	-	-
Sd	-34/-34	-	0/0	-	-

5.7 Summary

This chapter provides a holistic evaluation of sealants field and laboratory performance. Critical test methods and associated criteria were identified based on correlation to field performance. The governing and key laboratory performance criteria were stiffness and adhesion capacity. The worst performing sealants were the ones with low adhesion capacity and high stiffness for the climatic regions they were installed in. The best performing sealants were those with the highest adhesion capacity and moderate stiffness. The remainder sealants were in the medium performing category with moderate adhesion capacity and very low modulus. The importance of selecting a sealant with optimum low-temperature grade for the climatic region was highlighted. Following the grouping of sealants with respect to their field performance and potential causes of failures, a statistical method was used to validate the selected test method criteria.

A composite score approach combining ranking and correlation was used to develop a quantitative scale to determine the level of acceptance. Based on the composite score, for most of the test sites, a strong or acceptable correlation between field performance and laboratory test parameters were obtained. CSBBR stiffness had the strongest correlation followed by adhesion energy and load for rout and seal treatment. However, ACR from CSBBR test had either good or poor correlation with the PI. Similarly, for clean and seal treatment, CSBBR stiffness had the best score followed by tensile load and extendibility. A good correlation was observed between CSBBR stiffness and adhesion load as well as CSBBR stiffness and tensile load.

Based on laboratory testing and field validation, thresholds for different test methods were selected or fine-tuned as follow:

- Two separate low-temperature grading schemes were suggested for rout and seal and clean and fill techniques depending on the failure modes. The CSBBR and CSDDT methods are required for clean and fill treatment; whereas, the rout and seal treatment requires the use of CSBBR and CSAT methods.
- For CSBBR test method, the maximum stiffness threshold is 15MPa at 240s at 6°C higher than grading temperature. The minimum stiffness threshold is 40MPa at 1s at 6°C higher than grading temperature. The minimum ACR remains at 0.31.

- For the CSDTT test method, the extendibility thresholds are presented in Table 3.4. A secondary threshold, as a maximum tensile load, is 25 N to avoid the use of less ductile sealants.

Table 5.31. Thresholds for CSDTT at Various Temperatures.

Temperature (°C)	-4	-10	-16	-22	-28	-34	-40
Extendibility (%)	10	25	40	55	70	85	85

- For CSAT, the minimum adhesion load is 50 N at -4 °C and 25 N for every 6 °C reduction at the test temperature.

Sealant performance was maximized when there was no-grade-difference, meaning that test site temperature was equivalent to the sealant grade testing temperature (perfect match). In the case of a negative (too soft) or positive (too stiff) grade difference, a decline in sealant performance was observed. This shows the importance and validity of using a sealant grade as a performance criteria.

CHAPTER 6. FIELD AND LABORATORY AGING OF CRACK SEALANTS

Three main modes of failure for crack sealant treatments were identified: Cohesive, adhesive, and overband failures. The cohesive and adhesive capacity of a sealant may be significantly altered by heating during installation and weathering during its service life. Aging may differ for each of sealant's component: Oxidation and loss of oils may affect the binder phase; whereas, cross-linking, degradation, and oxidation may define the aging for the polymer phase.

Installation activities, weathering, and trafficking during the service life of a sealant may alter its characteristics by triggering a combination of the aforementioned aging mechanisms.

The effect of aging on sealants was studied extensively in the past two decades (Masson et. al 2003, Al-Qadi et. al. 2003). An accelerated laboratory aging procedure was proposed to simulate short-term installation and long-term weathering effects. Laboratory-aged and field-aged samples were compared to fine-tune an accelerated aging procedure. Field samples were collected from several field sections where sealants exposed to up to nine-year aging. The accelerated laboratory aging procedure considers the sealant complex moduli and viscosity values.

Development of a short-term aging was a challenge and delayed the development a performance-based specification for bituminous crack sealants. Therefore, procedures were developed to simulate different crack sealant aging states. Vacuum oven aging (VOA) was introduced to simulate crack sealant aging and weathering during installation and life service. To verify the effectiveness of the VOA method, several laboratory-aged crack sealants were tested and compared to results from field samples. A variation between VOA laboratory-aged (LA) sealants and field-aged (FA) samples was observed.

Sealant aging may be divided into two categories: Short-term aging, which refers to aging during installation; and long-term aging, which reflects the changes in the material characteristics because of weathering and vehicular loading. Short-term aging, include degradation of elastomers in sealants, loss of volatile oils, and degradation of mechanical properties.

Additionally, crack sealants undergo field aging through weathering, oxidation, exposure to UV rays, and loading (Masson et. al. 2003). Hence, a study on field aging mechanism of crack sealants was needed.

The collection of field samples from routed and sealed cracks presented significant challenges. The samples collected from routed and sealed cracks are subject to weathering and traffic effects

during sealants service life; especially when sealants are contaminated by de-icing chemicals, dust, and debris. Cleaning the field samples from these particles to obtain a representative sample for laboratory testing was a challenge. In addition, the thickness of a typical crack-extracted sample ranges from 10-20 mm. The crust layer of the sample, where most of the aging occurs, may be mixed during the sample cleaning from the contamination.

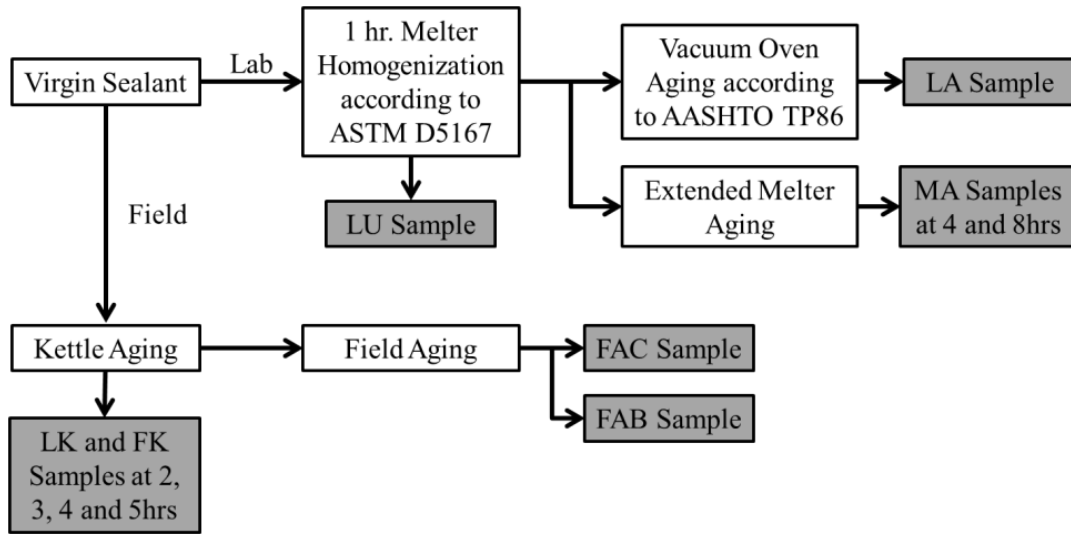
The effects of aging during installation and weathering, on sealants critical rheological and mechanical properties, are discussed in this chapter. A wide array of crack sealants, exposed to several aging protocols, was studied and evaluated using series of laboratory tests; developed as part of the performance-based specifications of hot-poured sealants.

A detailed summary of the aging study is presented in this chapter. This includes a summary of different aging methods. The test results, of each crack sealant collected from five various test sites, were compared to VOA laboratory-aged sample results (AASHTO T367). An aging prediction model, based on BBR test results at low temperatures and DSR test results at intermediate and high temperatures, was developed. The effect of aging on binder's chemical composition was studied using Fourier-transform infrared spectroscopy (FTIR) test.

6.1 Aging Methods

The test samples used in the experiment program are prepared to represent various aging stages occurring during the lifetime of a sealant. Figure 6.1 illustrates the sample preparation. Sealants were grouped into two categories: laboratory and field samples. Details of sample preparation at each aging stage are discussed in the next section. The aged samples prepared at each stage were obtained from the same sealant lot.

Table 6.1 illustrates different aging conditions and the nomenclature used in this thesis. The results for two low-temperature tests: Bending beam rheometer (CSBBR) and adhesion test (CSAT) are presented. The test results obtained for the field-aged sealants (FA2 and FA3) are also compared with results for lab-aged sealants.



*Note: LU = Lab Unaged, LA = Lab Aged, MA = Melter Aged, LK = Lab Kettle aged, FK = Field Kettle aged, FAC = Crust portion of Field Aged, and FAB = Bottom portion of Field Aged.

Figure 6.1. Sealant sample preparation pathways to represent various stages for sealant aging.

Table 6.1. Aging Procedures for Sealants Used in Performance Characterization.

Aging Condition	Label	Remarks
Lab Unaged	LU	Lab homogenized sealants using ASTM D5167
Lab Aged	LA	Lab long-term aging using VOA (AASHTO T86)
Lab Kettle Aged	LK	Short-term kettle aging using a rental kettle
Field Kettle Aged	FK	Short-term kettle aging obtained from kettles during test site installations
Melter Aged	MA	Extensive aging time in the melter used to homogenize sealants
6-month Field Aged	FA1	Field-aged samples collected during the first test site evaluation
1.5 Year Field Aged	FA2	Field-aged samples collected during the second test site evaluation
2.5 Year Field Aged	FA3	Field-aged samples collected during the third test site evaluation

6.2 Collection of Field-Aged Samples

During field installation, two to three samples were obtained from each material at different times. The first sample was collected right before installation when the material was at the recommended temperature. The second and third samples were collected during installation. These samples were used to study the effect of kettle aging (short-term aging) on the rheological properties of crack sealants (Figure 6.2a). Also during the annual field surveys, field-aged

(referred to as FA2 and FA3) samples were collected from Minnesota, Wisconsin, Ontario, New Hampshire, and New York test sites during the second and third evaluation periods (Figure 6.2b).



(a) Field kettle (FK) sampling



(b) Field-aged (FA) sampling

Figure 6.2. Collection of field-aged samples.

6.3 Laboratory Aging

The sealants were homogenized and melted for one hr in lab melter, in accordance with ASTM D5167 standard. These samples are considered laboratory-unaged samples. This is a standard procedure used to prepare sealants for laboratory tests. The unaged sealants are then aged per the VOA procedure: 35g sealant was kept at 115°C in vacuumed air for 16hrs (Figure 6.3). The last set of laboratory-aged samples was prepared using the melter by heating and stirring the sealants for extended 4 and 8hrs to represent aging during installation.



Figure 6.3. Vacuum oven aging to simulate long-term aging for crack sealants.

6.3.1 Effect of Laboratory Aging Procedures

Three different aging methods were practiced in the laboratory: Extended melter aging (MA) per ASTM D5167, kettle aging (LK) using a rental kettle, and vacuum oven aging (LA) in accordance with AASHTO T367. Test results are expressed in terms of an Aging Index (AI); defined by a relative change in the rheological property of aged and unaged sealants.

$$\text{Aging Index (AI)} = \frac{S_{aged}}{S_{unaged}} \quad (6.1)$$

where, S is the CSBBR stiffness at 240s of creep loading. An AI higher than unity indicates an increase in low-temperature stiffness and an AI lower than unity indicates sealants softening and degrading.

Starting with kettle aging, the AI presented in Figure 6.4a for half of the sealants (five out of ten) shows an increase in stiffness, while the remaining sealants show softening and degradation. The effect of the duration of kettle aging was also investigated. LK samples were taken from the kettle at 2, 3, 4 and 5hrs after adding and heating the samples. The results for 2 and 5hrs aging are presented in Figure 6.4b. It was noted that increasing aging time in the kettle, the change in AI was not significant, except for two sealants (Fb and Kc).

The second aging method was melter (MA); used for sealant homogenization according to ASTM D5167. In this method, sealants were kept in the melter for extended aging time, 4 to 8 hrs. Similar to kettle aging, MA has two different effects on sealants low-temperature stiffness. Figure 6.4b shows an increase in stiffness for half of the sealants and softening of the other half. The effect of MA does not change significantly with aging time (except for Sealant Ad).

The third aging method developed to simulate long-term sealant aging in laboratory is vacuum oven aging (VOA) according to AASHTO T367. Laboratory aging (LA) results for CSBBR stiffness are presented in Figure 6.4c, which shows, except for Sealant Ob, all sealants become stiffer. However, the increments in AI for sealants were not the same. This might be caused by sealants aging potential. Therefore, VOA may increase sealants stiffness (AI higher than 1 for CSBBR stiffness), however, the aging effect can be minimal on maximum adhesion load obtained from the CSAT method (Figure 6.5). For most sealants, at different temperatures, AI was almost equal 1, thus indicating that adhesion load does not change during the aging process.

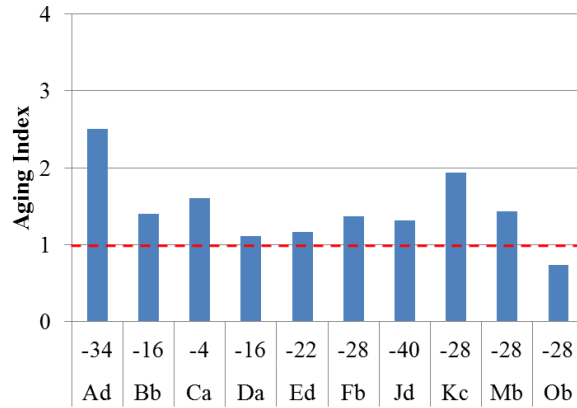
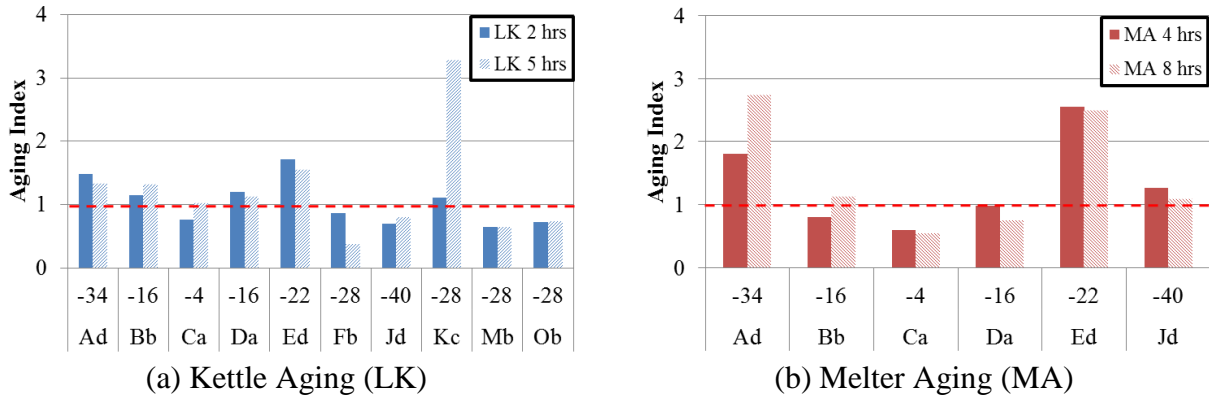


Figure 6.4. Aging index (AI) for sealants using various laboratory aging methods, based on CSBBR stiffness at 240s.

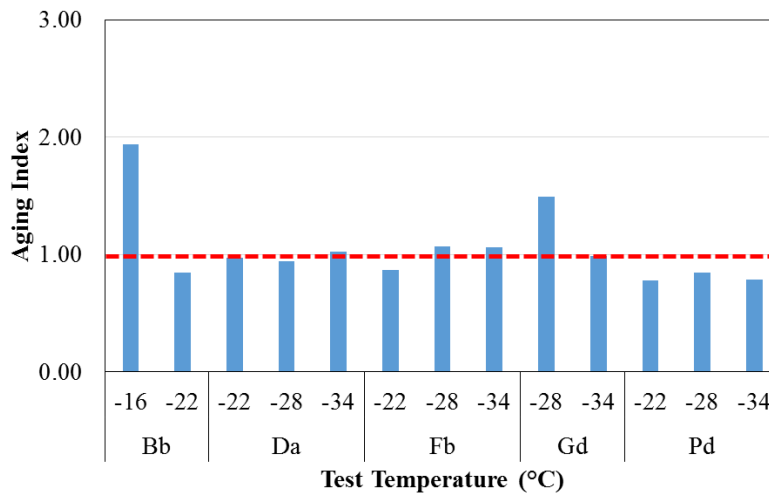


Figure 6.5. Aging index for vacuum oven aging method based on maximum adhesion load.

6.4 Validation of Laboratory Aging Method

The results from the low-temperature tests were discussed separately for each material in the previous chapters. In this chapter, CSBBR test results of various aged samples were compared. The information collected from lab- and field-aged samples was used to establish possible

correlations between laboratory and field aging. Low-temperature stiffness and average creep ratio (ACR) at 240s at various aging conditions, laboratory-aged and field-aged samples collected after the second and third winter (FA2 and FA3), are compared in Figure 6.6 for three sealants at three different temperatures. Plots for all other sealants are presented in Appendix E. For most sealants (except sealant Mb and Nb), sealant stiffness increased with field aging. Comparing FAs with LA samples, no specific trend could be observed at this point. This will be further investigated in the following sections.

Stiffness master curves obtained from test data at three different temperatures, are used instead of the single stiffness value at 240s. Figure 6.7 illustrated the master curves for three sealants at different aging conditions; other sealants are presented in Appendix F. Three different trends could be observed:

- Laboratory-aging (VOA) resulted in stiffer sealant than field-aging; VOA could over age sealants (e.g., sealants Ca and Da).
- Field- and laboratory-aging results in same stiffness sealants; VOA appropriately represents field aging (e.g., sealants Bb, Gd, Hb, Mb, and Pd).
- Field-aging (VOA) resulted in stiffer sealant than laboratory-aging; VOA could under age sealants (e.g., sealants Ad, Nb, Ob, and Sd).

To summarize the comparison between field-aged and lab-aged sealants based on stiffness master curves, presented in Figure 6.7, the average difference between the curves was calculated as follows:

$$S_{dif} = (\sum_{i=1}^n \frac{(S_i^{LA} - S_i^{FA})}{S_i^{LA}}) / n \times 100 \quad (6.2)$$

where;

S_i^{LA} = Stiffness at a specific creep loading time for laboratory-aged sample

S_i^{FA} = Stiffness at a specific creep loading time for field-aged sample

n = number of data points

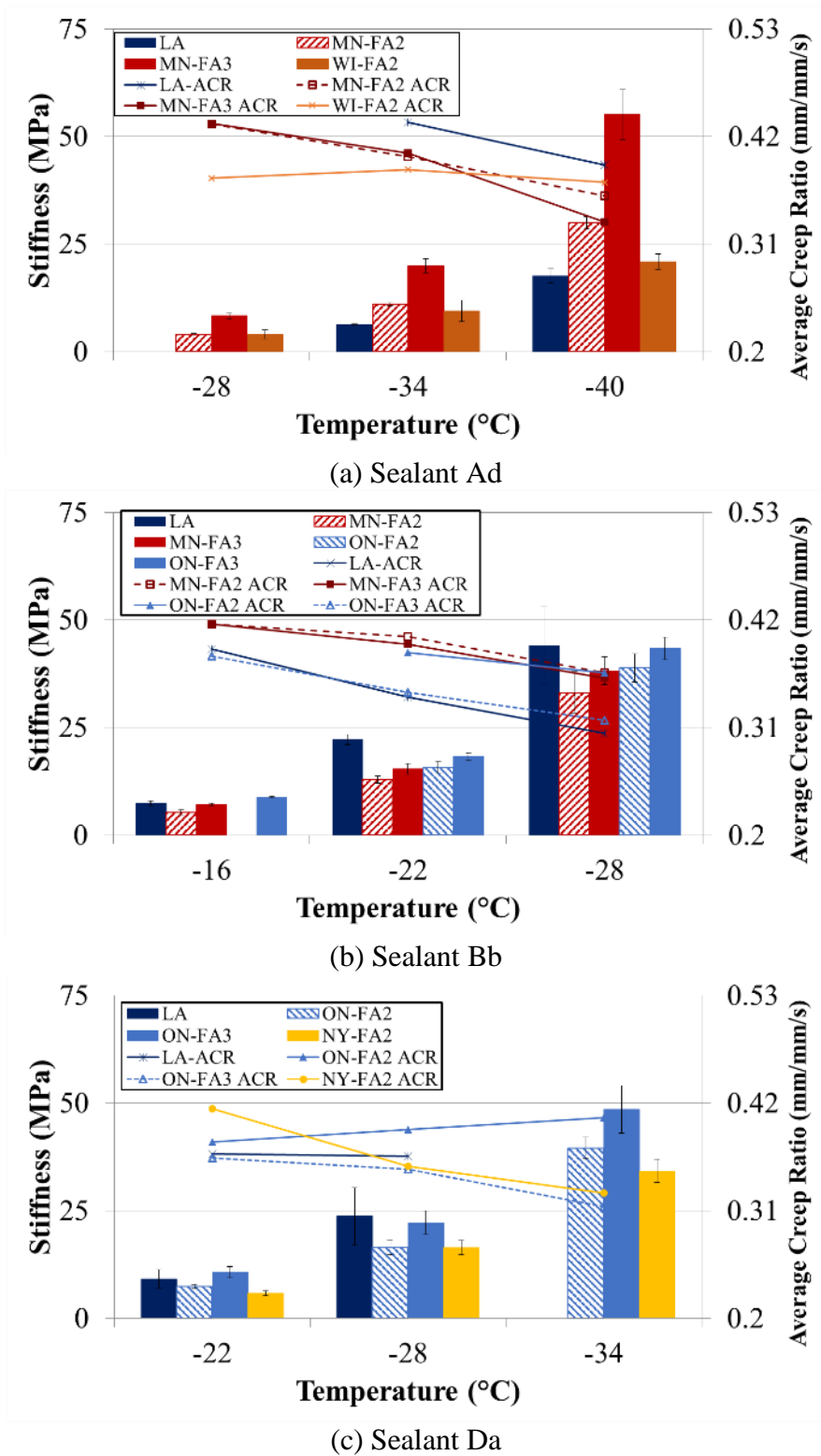
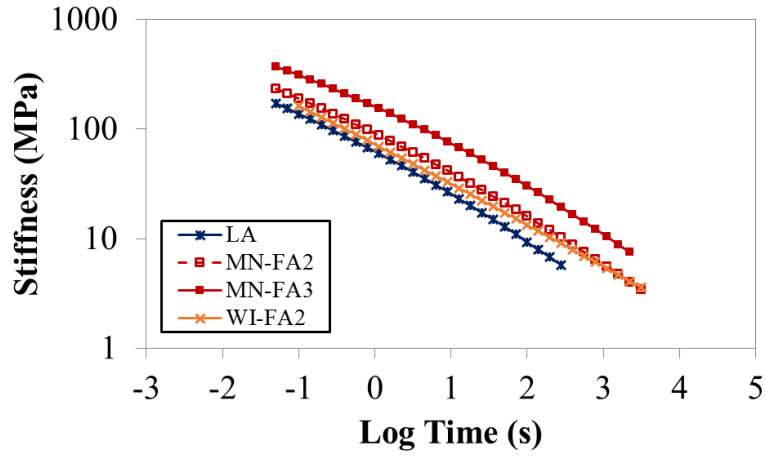
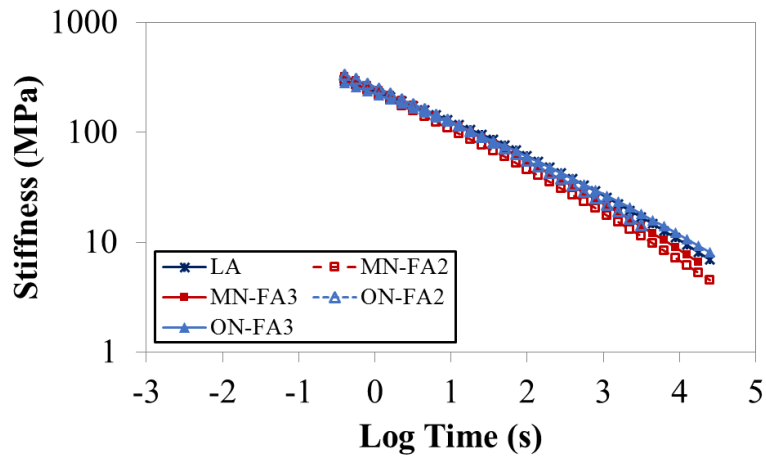


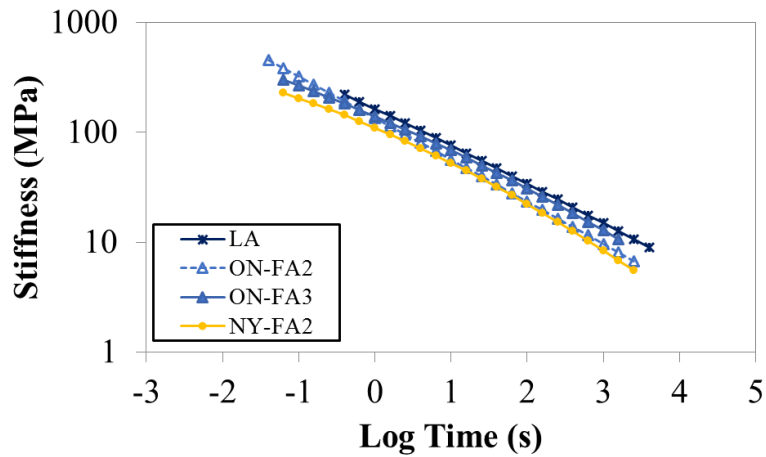
Figure 6.6. CSBBR stiffness and average creep ratio (ACR) at 240s at different aging conditions tested at three temperatures.



(a) Sealant Ad



(b) Sealant Bb



(c) Sealant Da

Figure 6.7. Stiffness master curves for laboratory-aged and three field-aged (FAs) CSBBR samples.

The average difference in stiffness between field-aged samples and lab-aged sample is summarized in Table 6.2. The table illustrates the feasibility of predicting sealant field aging using lab aging results. The gap variation in field-aged and laboratory-aged sealant stiffness is approximately $\pm 30\%$; the majority of samples were within $\pm 10\%$. The table's cells shaded with green represent stiffness differences within $\pm 10\%$, LA stiffness higher than field-aged samples and are considered conservatively acceptable. The aging of some sealants was underestimated by lab aging. Based on the number of acceptable cases, the VOA procedure satisfactorily represented field aging at a rate higher than 70%.

The differences in laboratory- and field-aged sealants could be attributed to several factors. First, the samples collected from the routs were homogenized in the lab, resulting in blended properties of sealants, in spite of different aging gradient with depth profile. The properties of the bottom portion of the sealant may remain unchanged or weakened because of moisture infiltration. Second, field aging only covers a time period of two and a half years. As the materials continue to age in the field, these properties will change. Third, deicing chemicals and salts, applied in the field, may affect sealant stiffness and adhesion.

Table 6.2. Comparison between Field- and Lab-aged Sealants Using Sealant Stiffness Master Curves.

Sealant	Test Sites						
	Minnesota		Ontario		Wisconsin	New York	New Hampshire
	2 nd yr.	3 rd yr.	2 nd yr.	3 rd yr.	2 nd yr.	2 nd yr.	3 rd yr.
Ad	-13.10%	-32%	-	-	-6.80%	-	-
Bb	5.90%	2.00%	1.60%	0.20%	27.40%	-	-
Ca	-	-	-	-	-	6.50%	-
Da	-	-	8.90%	3.30%	-	11.80%	-
Ed	-	-	-	-	11.30%	-	-16.60%
Fb	-14.00%	-3.80%	-	-	0.10%	-	-2.70%
Gd	-1.50%	2.70%	1.60%	-9.00%	-	-	-7.10%
Hb	3.40%	0.20%	-	-	-	-	-
Mb	-2.70%	6.10%	3.20%	3.00%	-	-	-
Nb	-32.50%	-17.30%	-	-	-	-	-
Ob	-	-	-	-	-	-45.20%	-13.00%
Pd	-	-	-2.70%	-6.20%	-11.80%	-	-
Sd	-	-	-10.50%	-12.50%	-	-	-

6.5 Field Aging Evaluation and Modeling for a Non-Trafficked Test Section

A test section was installed to evaluate field aging mechanisms of various types of sealants. An asphalt surfaced section at the Advanced Transportation and Research Laboratory (ATREL) was used to install eight different types of sealants using the rout and seal technique. The section provided valuable information on field samples exposed to all weathering conditions from 2011 to 2015. Eight sealants were installed, from various manufacturers spanning low and high modulus materials. The list of materials is presented in Table 3.3. The research is divided into two stages: Short-term kettle aging and long-term field aging. A comprehensive experimental program was applied for samples collected at each stage.

Two types of materials were obtained during the course of the study: Kettle-aged materials collected during heating and sealant application, and samples collected every six months after installation.

Table 6.3. Crack Sealant Material Used in the Study.

Sealant ID		ASTM Type
1	Ca	I
2	Da	I
3	Ed	IV
4	Fb	II
5	Jd	IV
6	Kc	III
7	Mb	II
8	Ob	II

6.5.1 Kettle-aged Materials

For this part of the investigation, each product was heated inside a small kettle. A double boiler kettle with 475L capacity was used to melt the sealants. Sealant temperatures were adjusted according to manufacturer recommendations. The procedure followed in this phase is as follows:

- **Kettle cleaning** – Before using new material, the kettle was carefully cleaned to ensure that the kettle container was completely free of contamination. The residual material was fully drained using the drain valve. Then, the kettle was flushed out using 20 to 40L of the new product to create a residue of the same product.

- **Placing sealant blocks** – The quantity of material placed in the kettle was 230L. This amount represents almost half of the kettle capacity and would maintain a uniform temperature inside the kettle.
- **Kettle temperature control** – Using recommended heating temperatures is critical to maximize sealants adhesive bonding properties. Kettle temperatures were monitored using two thermostats to record materials temperature in the kettle and the nozzle. In addition, a thermal probe was used to measure the temperature of the material inside the kettle. This probe was equipped with thermo couples 25, 125, and 255mm in above the tip of the probe. Temperature readings were taken at hourly intervals inside the kettle at several spots.
- **Sampling** – After the material reached recommended temperatures, samples were collected every hour until the 5th hr.

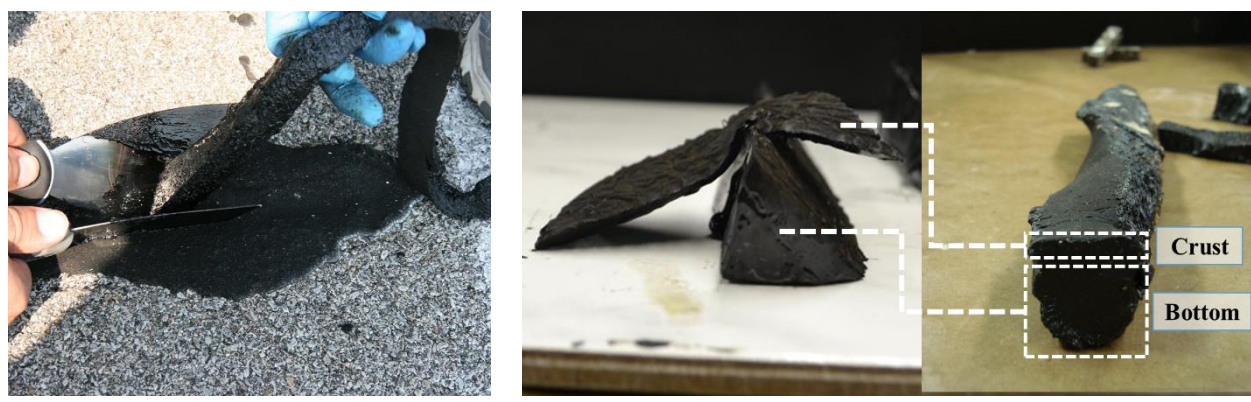
6.5.2 Field-aged Materials

After obtaining the last sample from the kettle, previously prepared routs were filled by kettle-sealant; eight sealants were used. A router machine was used to create 25x25 mm reservoirs. Eight to twelve routs were created for each sealant product. The routs were cleaned with an air compressor; debris and loose particles were removed from the surface of the pavement; and the sealant was applied with an overband using a disk-shaped finisher attached to the end of the nozzle. Every time a new product was installed, the existing sealed routs were covered with an impermeable plastic sheet to avoid dust contamination from the new routing process. Figure 6.8 illustrates the entire process of sampling from kettles to sealant application in the routs.

Sampling from the routs was planned every six months. Once the sealant was extracted from the rout, it was cleaned to remove any dust or particles. Since the area was protected from any vehicle use, the surface of the collected samples was fairly clean. Following the cleaning process, the remaining thickness of the sealant was approximately 20 mm. For evaluation of differential aging, the specimens were cut further into two parts. The first 5 mm from the top of the sample is designated as “crust” whereas the remaining 15 mm is designated as “bottom”. These two parts were tested independently and compared to evaluate the apparent viscosity, flexural stiffness, and adhesion strength.



Figure 6.8. Sealant installation process: (a) Sealant heating and temperature monitoring; (b) routing; (c) rout cleaning with high-pressure air; and (d) finishing the installation in the routs.



(a) Field sampling (b) Crust (FAC) and Bottom (FAB)

Figure 6.9. Separating field-aged samples to crust and bottom.

6.5.3 Differential Aging of Sealants due to Weathering

Sealants were subjected to weathering effects after installation in a traffic-free section. Figure 6.10 shows photos taken approximately 1-4 years after installation; the effect of aging can be clearly seen. Several sealants exhibited significantly different aging patterns. Most sealants developed block cracking style surface deformations; while the surface pattern of the two

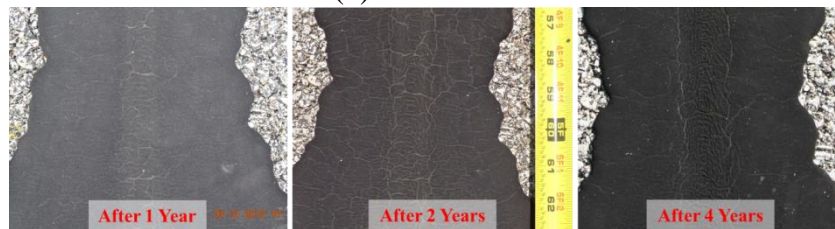
materials (Jd and Kc) was quite distinctive. These two materials were obtained from the same manufacturer and both are intended for cold climates. For the majority of sealants, the amount of surficial cracks increased after one year of aging.



(a) Sealant Ca



(b) Sealant Da



(c) Sealant Ed



(d) Sealant Fb

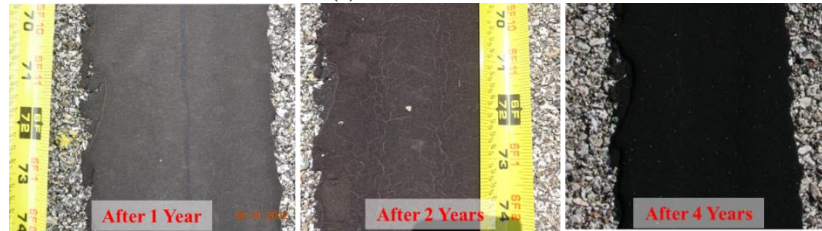


(e) Sealant Jd

Figure 6.10. Pictures taken from routed and sealed cracks to illustrate surface aging of various sealants under the same weathering conditions.



(f) Sealant Mb



(g) Sealant Ob



(h) Sealant Kc

Figure 6.10 (continued)

6.5.4 Viscosity Development with Aging

The viscosity tests were performed in accordance with AASHTO T366 at 30 and 60 rpm at the installation temperatures recommended by the manufacturers. A minimum of four replicates was used for each material. The results from 30 rpm only are presented herein; results from 60 rpm tests were showing the same trend as 30 rpm presented in Figure 6.11. Samples from the installation stage (labeled as kettle) were compared with six-month field-aged samples (FAC and FAB). A clear trend of viscosity increase was observed from kettle aged to field samples with the crust part showing the highest viscosity. This behavior is attributed to sealant exposure directly weathering conditions.

Viscosity test results for FAC and FAB demonstrate significant viscosity increase for the samples exposed to direct weathering without any exception. Viscosity increases under short- and long-term aging. At high temperature, the composite structure (polymer + filler + binder) of sealants disappears. The material can be described as polymer chains and fillers suspended in viscous asphalt binder matrix. It is, therefore, expected that the viscosity test will only capture the aging effect of the asphalt binder component of sealants, which is mostly oxidation.

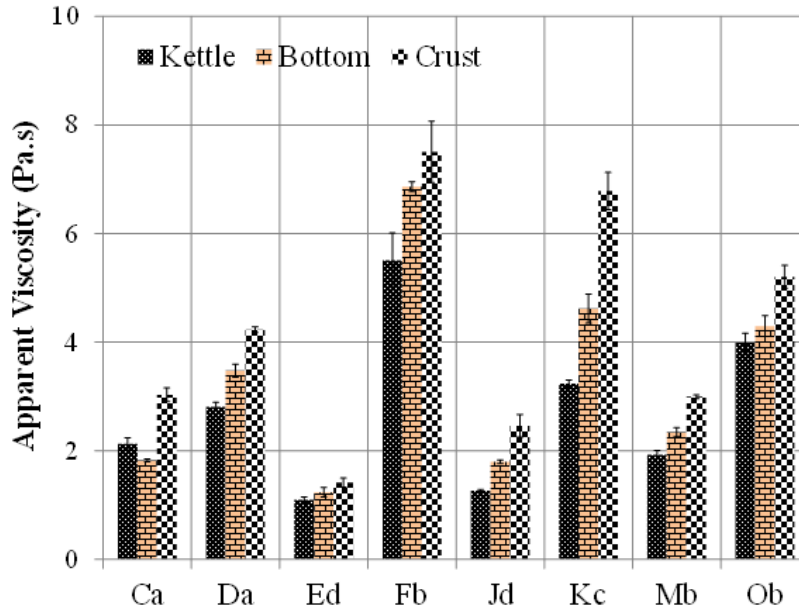


Figure 6.11. Apparent viscosity results for 5-hr heated sealants in a small kettle (lk-5h) and field-aged sealants.

6.5.5 Flexural Stiffness Development with Aging

Similar to the viscosity tests, FAC and FAB segments of sealants extracted from the routes were tested separately to evaluate differential aging. Figure 6.12 illustrates the stiffness and average creep ratio at 240s at various temperatures for two sealants (Ca and Ob) tested at different aging times. CSBBR stiffness and ACR variation with aging for all other sealants can be found in Appendix G. Of all tested sealants, these two materials exhibited extreme aging potential. Stiffness either increased significantly or remained constant in the FAC for most aging periods. In general, a significant stiffness increase was observed in the FAC sealant samples with respect to that of FAB sealant samples. FAB sealant samples experienced softening according to CSBBR stiffness results. This might be an indication of a competition between multiple aging mechanisms (scission, oxidation, and cross-linking). Moisture is yet another factor influencing the stiffness of sealants as most sealants have equal or lower modulus after installation. The same trend was observed with the samples collected after each winter period, thus indicating the effect of precipitation.

Figure 6.13 shows the change of stiffness with rout depth; FAC samples are always stiffer than those of FAB samples for the same sealant. Some sealants, such as Ca (Figure 6.13a), initially experienced softening in the first winter after installation for both FAC and FAB. For this type of sealants, the effect of moisture on stiffness may overcome the effect of oxidation in winter time.

The increase in stiffness was observed in the samples collected after the first summer cycle and continued to increase. On the other hand, the stiffness of other sealants, such as Ob, continued to increase, albeit at a slower rate (Figure 6.13b). Appendix H includes the figures for six other sealants.

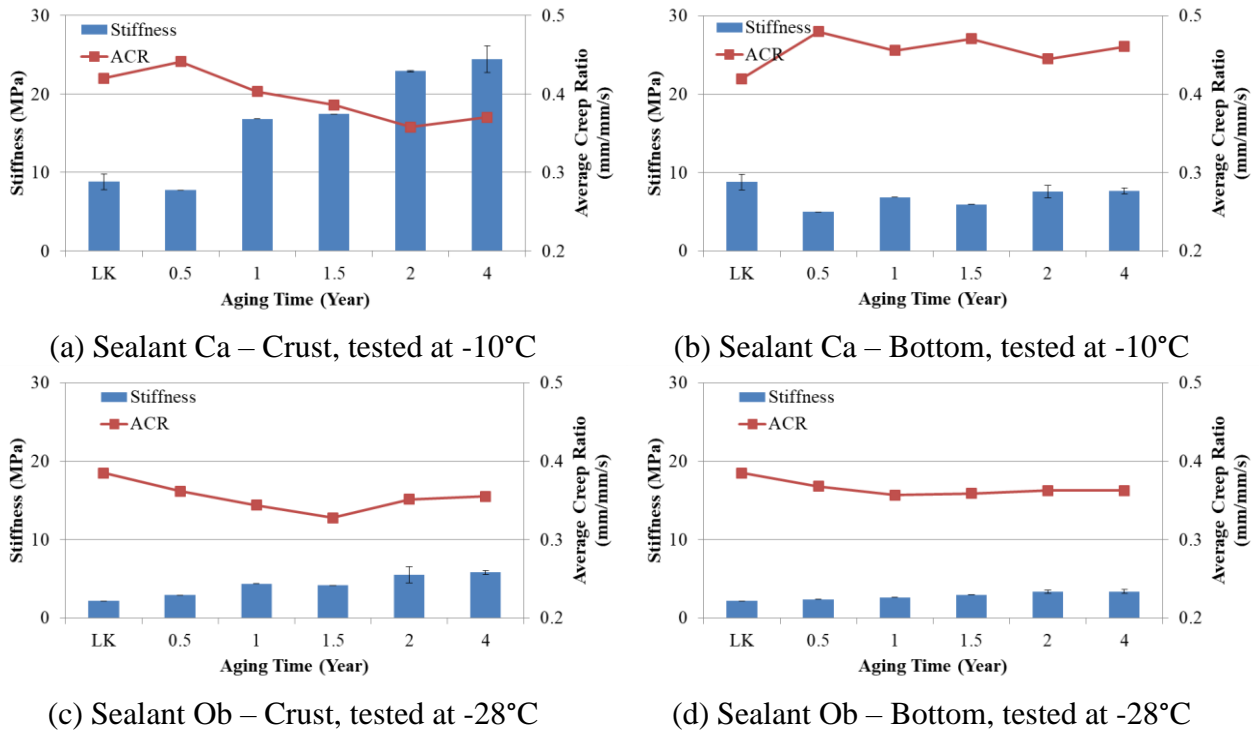


Figure 6.12. Stiffness and ACR at 240s at various test temperatures for two sealants sampled from the kettle at 4hrs and routes after 6 months, 1 year, 1.5 year, 2 years, and 4 years.

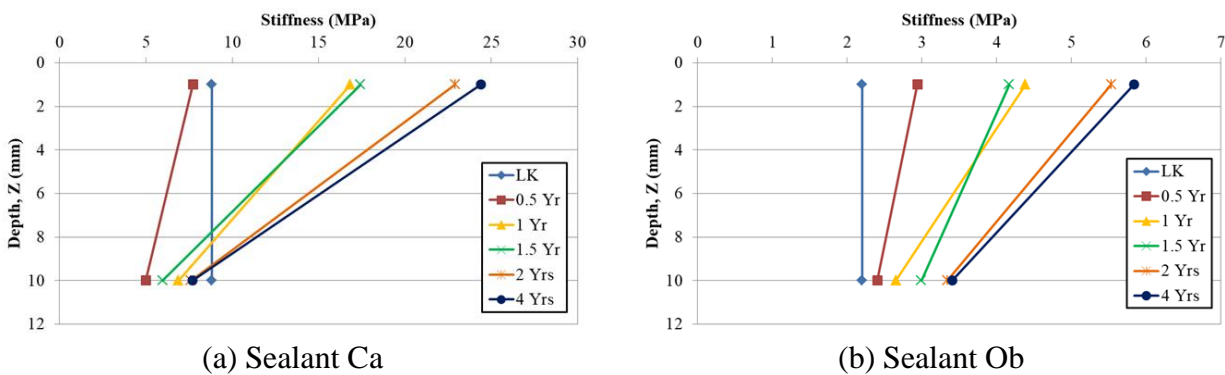


Figure 6.13. Stiffness change within the sealant; illustrating differential aging for two different types of sealants.

6.5.6 Aging Model Development Based on Low-Temperature Stiffness

To assess the aging mechanisms of sealants, an aging prediction model was developed using the results obtained from the laboratory tests. The objective of the model was to categorize aging

potential of sealants and provide guidance on how much aging can be predicted for each category at the laboratory characterization stage. Superposition rule was applied to the low-temperature stiffness results in the same way time and temperature superposition was used to develop master curves. The procedure is based on the global aging model used in Superpave binder specifications (Mirza and Witczak, 1995).

It is well documented that modulus and strength properties of viscoelastic materials, such as polymer, asphalt binder and sealants, are sensitive to temperature and time of loading. Hence, master curves were developed for each sealant's FAC and FAB parts. Development of a master curve for Sealant Jd is shown in Figure 6.14a to Figure 6.14c. The following steps are followed to construct master curves. Using the CSBBR creep curves (AASHTO T368), each curve representing a field-aged state was shifted to the LK condition, which is considered the original state (aging time is equal to zero) (Figure 6.14c). Shift factors used to develop the aging master curves are shown in Figure 6.14d for FAC and FAB of Sealant Jd. The same procedure was followed for all tested sealants.

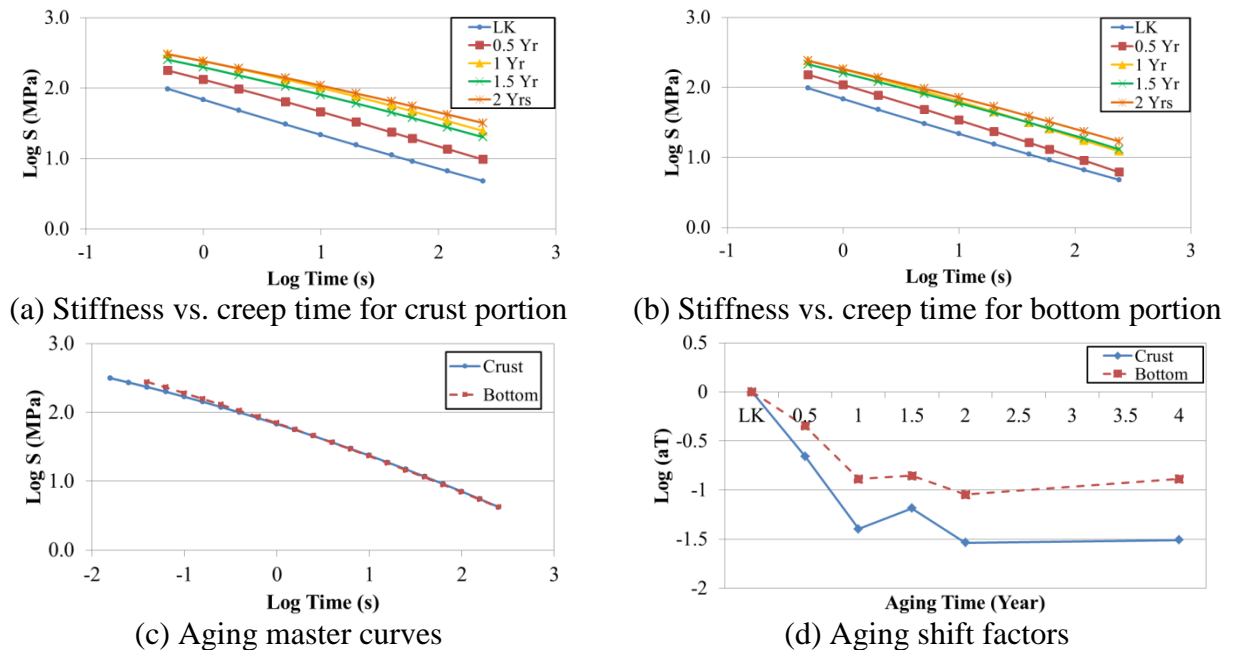


Figure 6.14. An illustration of aging master curve development based on CSBBR results.

Aging shift factors used to develop the master curves for FAC and FAB parts of eight sealants are presented in Figure 6.15 for four-year field aging. A positive shift factor indicates a decrease in the modulus of sealant with time, while a negative shift factor indicates an increase in the modulus. The greater the shift factor, the higher the change in modulus. Aging-related shift

factors can be compared to time and temperature shifting. A 6 °C change in temperature is generally equivalent to one decade of shifting (logarithm of shift factor a_T is equal to one). For example, the decade of shifting can be achieved after about 1.5 years of aging for the crust portion of Sealant Jd.

The difference between the shift factors for FAC and FAB samples is evident. The shift factors for FAC are lower than those for FAB at each stage of aging, indicating a relatively smaller stiffness. This suggests that the stiffness change (due to aging) is slower for FAB compared to FAC. In general, both sealant parts experienced similar aging mechanisms, but the effect is at different magnitude.

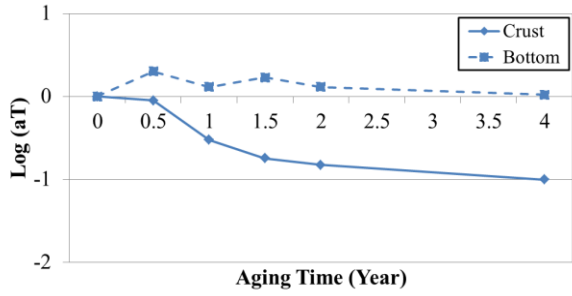
The competition between multiple aging mechanisms can be clearly seen in shifting factors. Sealant stiffness (e.g., K_c) increased with aging over four years. However, aging softening may occur for most sealants, such as Da and Ed, at 0.5 year of aging, or Jd, Kc and Mb after 1.5 year. The aging periods (0.5 year and 1.5 year) correspond to the sampling time following a winter season. In general, during winter, sealants could be affected by moisture more than oxidation. On the other hand, stiffness increases during the summer time (one, two and four years of aging). Finally, the crust and bottom portions of most sealants, except for Kc, converged to an asymptotic value of shift factor after two years; indicating reaching aging limit.

These observations allow us to generalize the findings of this study and characterize the aging potential of sealants and, more importantly, to develop an aging model that can be used to predict the sealants field performance.

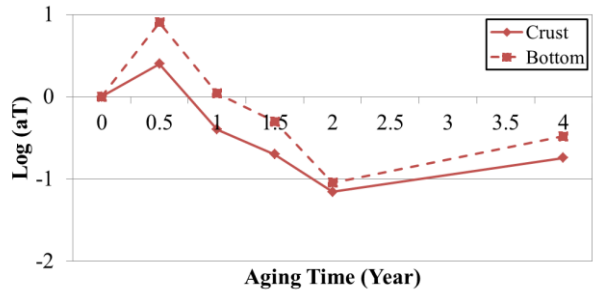
A simple aging shift factor model is proposed to allow evaluating sealant aging potential. The shift factor equation is chosen with two asymptotes representing little-to-no aging at the beginning of service life (after installation) and long-term aging saturation. For this purpose, an S-shaped curve is used to fit the aging curves.

$$\text{Log}(a_T) = -A(1 - e^{-bt})^c \quad (6.3)$$

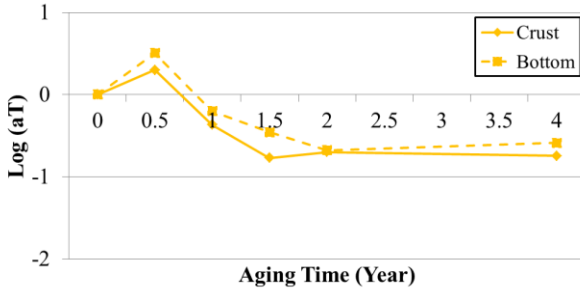
where, a_T is the shifting factor; constant A is the long-term aging potential; t is the aging time in years; and b and c are factors relate to size and shape of the curve. Only data for LK, one, two and four years of aging are used in fitting to include the aggregated effect of winter and summer aging.



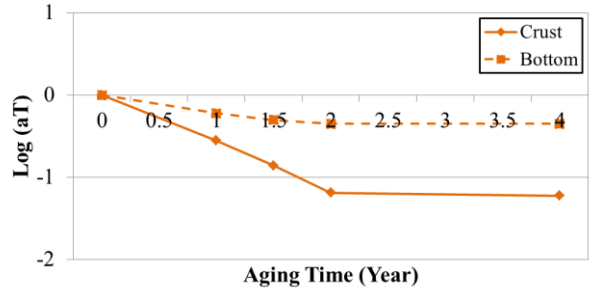
(a) Sealant Ca



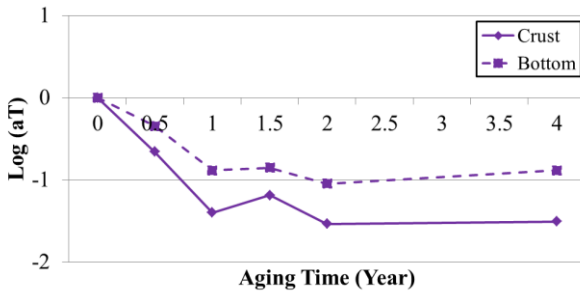
(b) Sealant Da



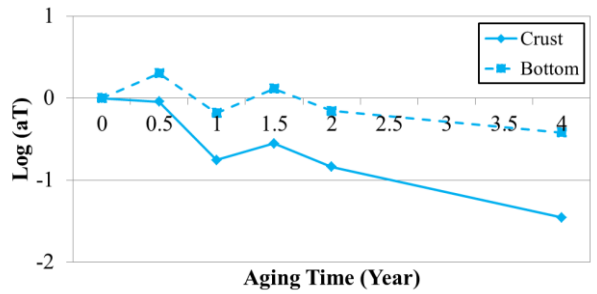
(c) Sealant Ed



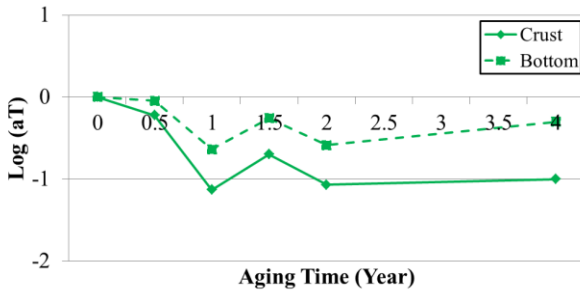
(d) Sealant Fb



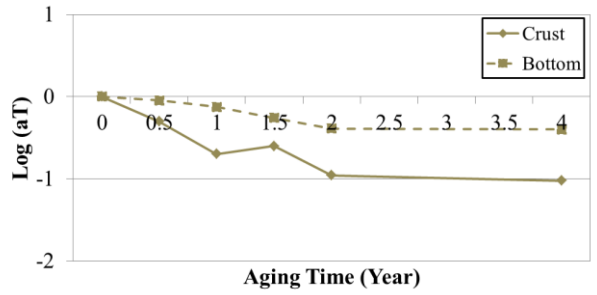
(e) Sealant Jd



(f) Sealant Kc

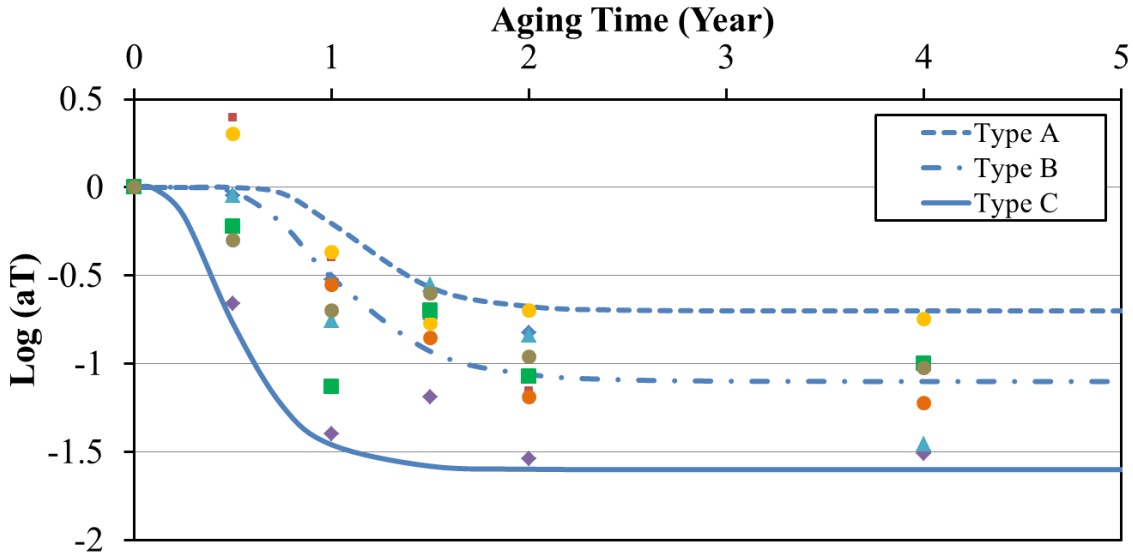


(g) Sealant Mb

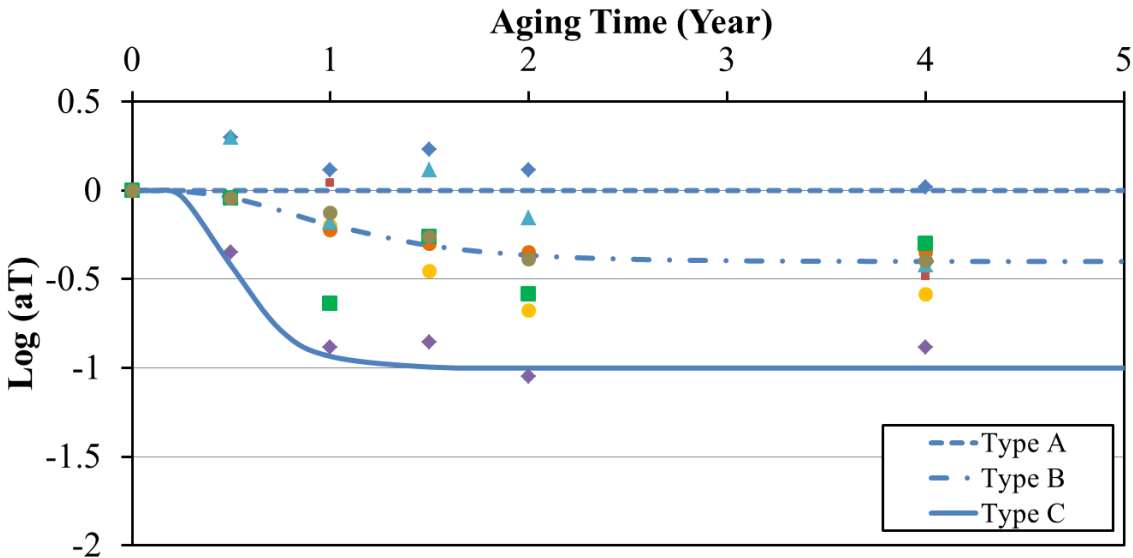


(h) Sealant Ob

Figure 6.15. Shifting factors for eight sealants along four years of aging.



(a) Crust



(b) Bottom

Figure 6.16. Typical sealant types classified based on field-aged low-temperature stiffness.

The sealants were grouped into three categories based on their aging potential: Type A includes sealants with the lowest aging potential; sealants with medium aging potential are categorized under Type B; and sealants with the highest aging potential are considered Type C. The coefficients of proposed shift function are chosen to capture the aging potential of all sealants. Figure 6.16 shows that most sealants are in the range of Type B. Based on the proposed model, suggested values were developed and summarized in Table 6.4. Coefficient A, indicating aging potential, ranges between 0.7-1.6 with increasing aging magnitude for the FAC. The A coefficient varies from 0-1.0 for the FAB.

Table 6.4. Typical Aging Potential Values for Low-Temperature Model for Asphalt Crack Sealants.

Sealant Aging Type	Portion	Aging Potential	A	b	c	Sealants in This Category
A	Crust	Low	0.7	3.5	40	Ed
	Bottom		0	0	1	Ca
B	Crust	Medium	1.1	3	15	Ob, Fb, Mb, Ca, Da
	Bottom		0.4	2	5	Ob, Fb, Mb, Ed, Da Kc
C	Crust	High	1.6	4	5	Jd, Kc
	Bottom		1.0	5	10	Jd

6.5.7 Shear Strength and Modulus Development with Aging

The DSR was used to evaluate shear stress at high shear strain for field-aged sealants at high temperatures. An experimental procedure was originally developed to evaluate tracking resistance of crack sealants. A test with the following attributes was proposed for this purpose:

- Shear strain was monotonically increased at a constant shear rate until complete failure to observe the yield point for sealants (shear strains goes up to 600%).
- A shear rate of 0.01 1/s was selected.
- Test temperatures ranged from 46-82°C with 6°C increments. For evaluating one year aging effect on shear stress, a test temperature is selected as 76°C.

The increase in shear stress by strain and field aging shows a trend similar to complex modulus. Except for Fb and Ed sealants, the results show that shear strength increased and the rate was higher for field-aged crust samples than that of the bottom part (Figure 6.17).

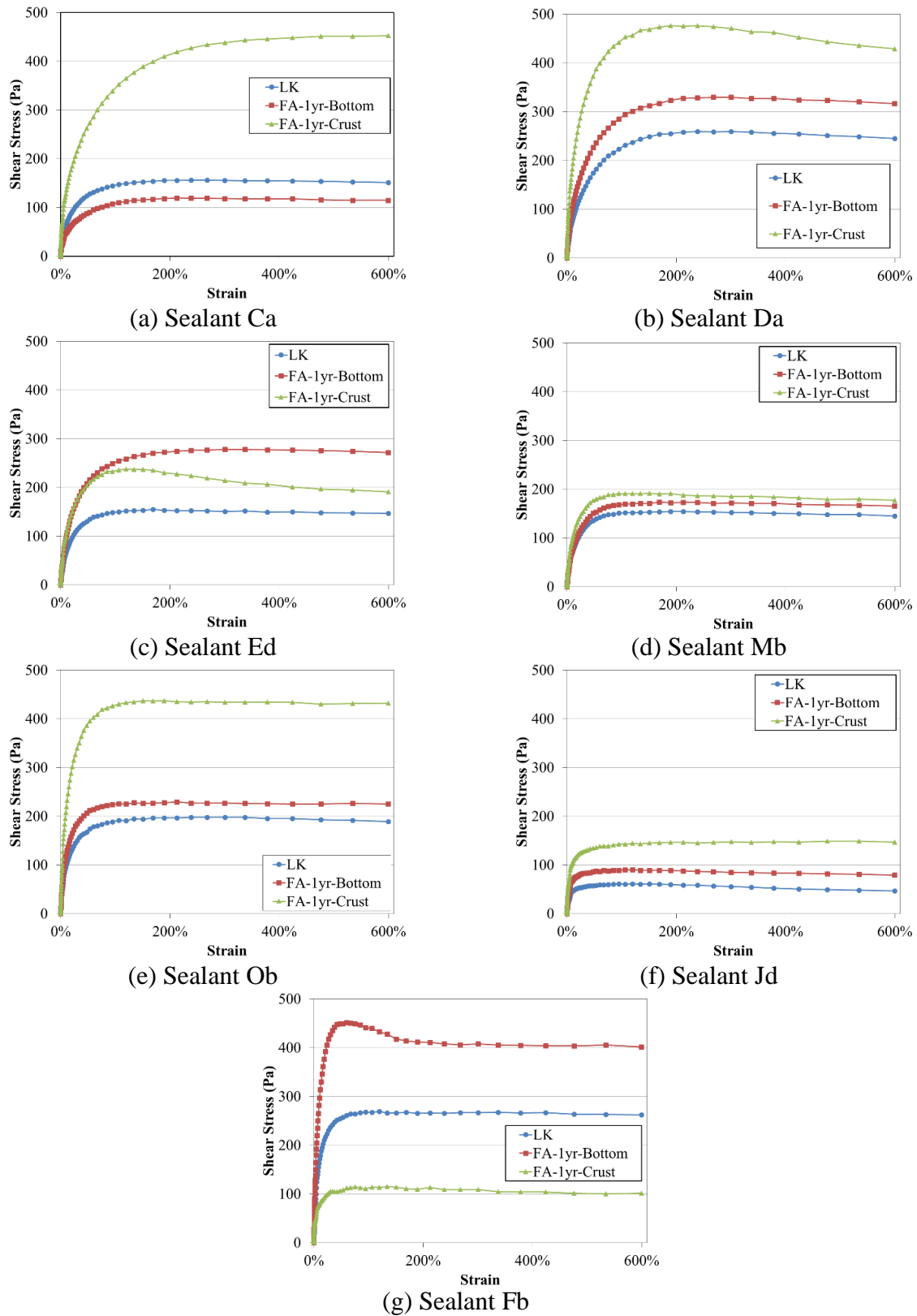


Figure 6.17. Variation of shear stress at high shear strain for sealants under different field-aged conditions at 76°C.

6.5.8 Aging Model Development Based on High-Temperature Shear Modulus

To develop an aging model based on high-temperature shear modulus, field-aged crack sealants were tested using a dynamic shear rheometer (DSR). A frequency sweep test was conducted to measure complex shear modulus at different loading frequencies. The samples were tested at an angular frequency range of 0.1-100 rad/s. To cover intermediate and high-temperature properties, the test was conducted at temperatures ranging from 30°C to 82°C.

Similar to low-temperature model, another aging prediction model was developed for high temperatures. Using time and temperature superposition concept, the superposition rule was applied to complex shear modulus at high temperature in the same way was used to develop master curves. Although at high temperatures due to high amount of modification crack sealant is not a linear viscoelastic material it was assume to be linear to be able to adopt aging-time-temperature superposition. Following the same procedure for CSBBR stiffness, master curves were developed for each sealant's part: FAC and FAB. A sample procedure and master curves for sealant Fb is presented in Figure 6.18. Using the DSR frequency sweep test results, each field-aged curve was shifted to the LK condition, which is considered the original state (aging time is equal to zero). Shift factors used to develop the aging master curves are shown in Figure 6.18d for sealant Fb FAC and FAB. The same procedure was followed for all tested sealants.

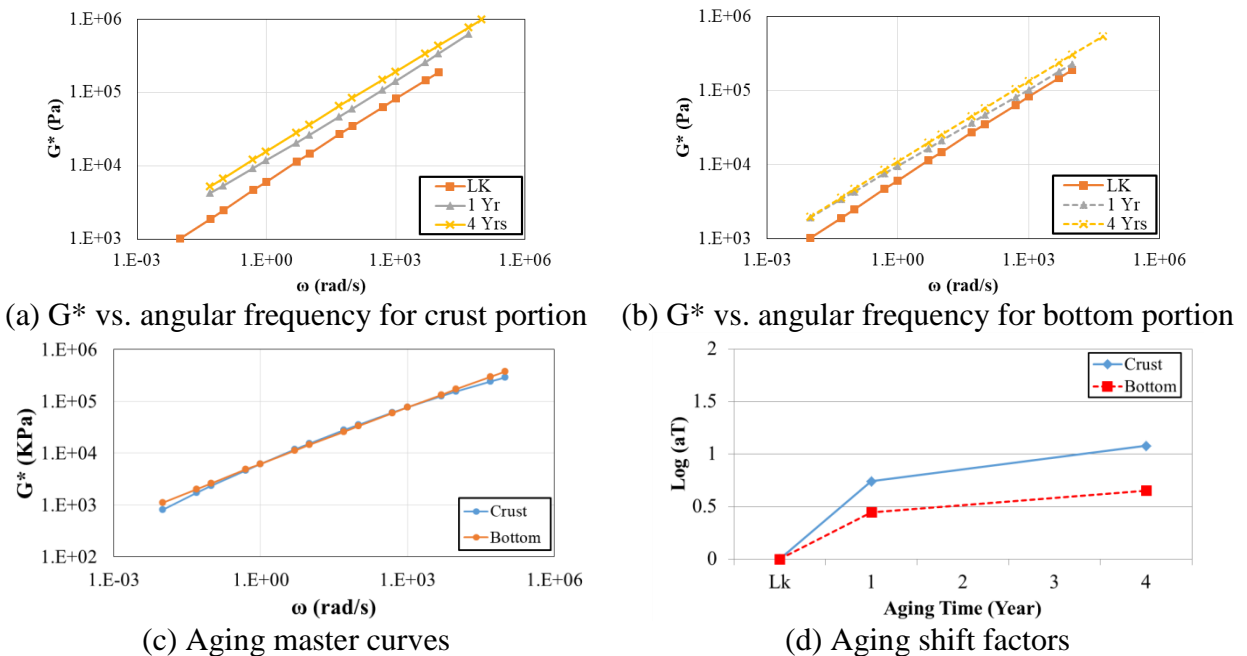


Figure 6.18. Aging master curve development based on DSR results for Sealant Fb.

Figure 6.19 presents the aging shift factors used to develop the master curves for FAC and FAB parts for the eight sealants. A positive shift factor indicates an increase in the modulus with time. The higher the shift factor, the greater the change is in modulus. The difference between the shift factors for FAC and FAB samples is evident. The shift factors for FAC are higher than FAB at each stage of aging indicating higher modulus. This means that the change for shear modulus (indicating the effect of aging) is slower in FAB than in FAC. Similar trends for both FAB and FAC parts were observed. This indicates that both parts of sealant were subject to similar aging mechanisms, but the impact is different. Figure 6.20 shows the change of complex shear modulus with rout depth; FAC is always stiffer than FAB for the same sealant.

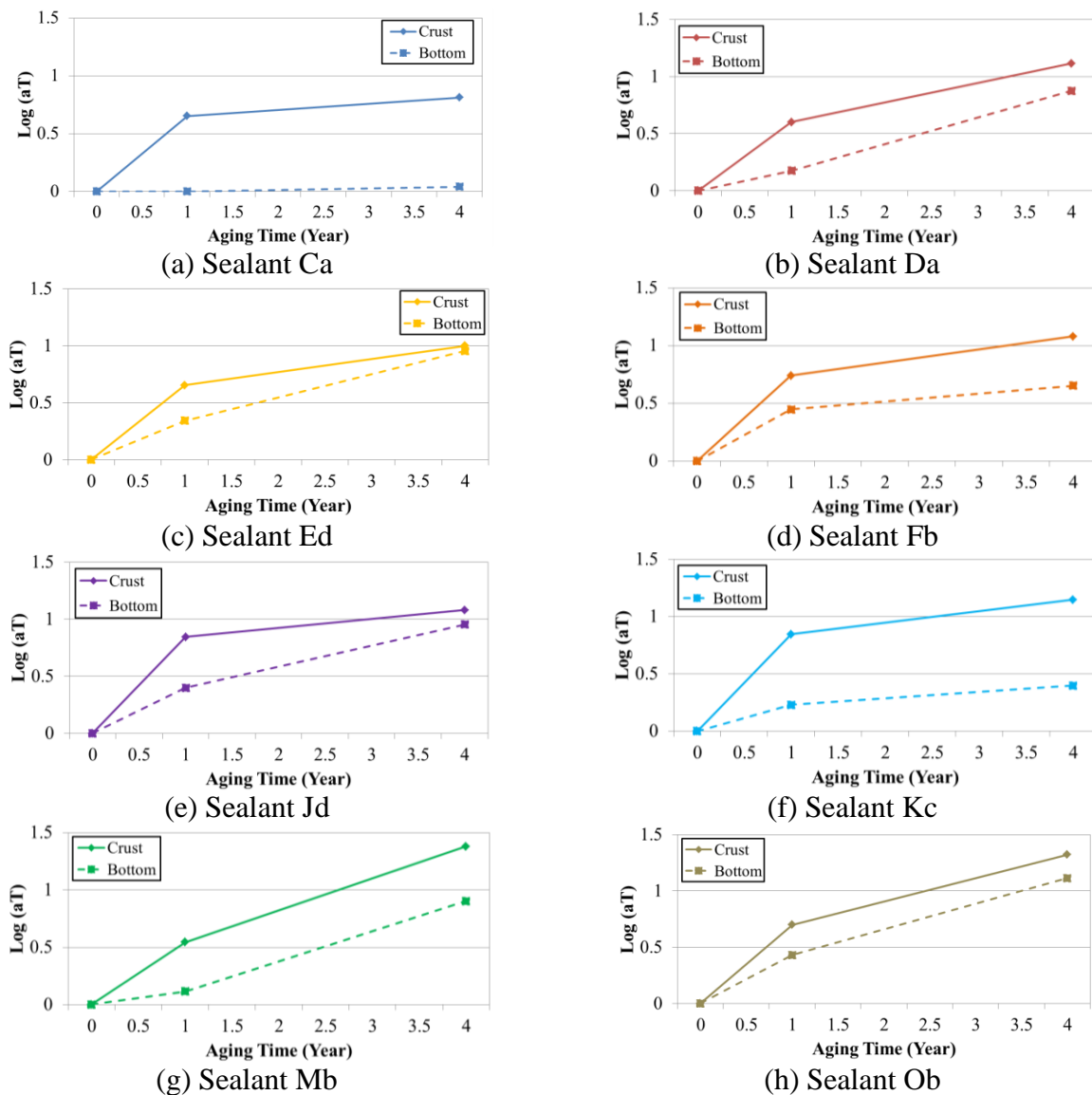
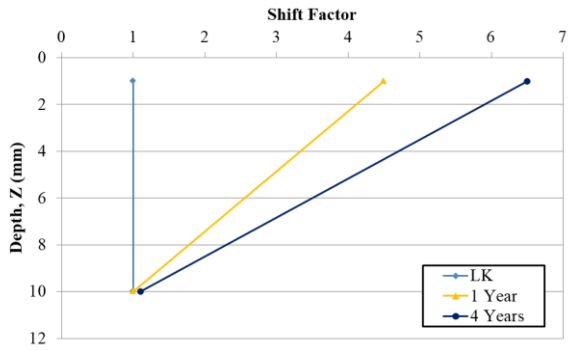
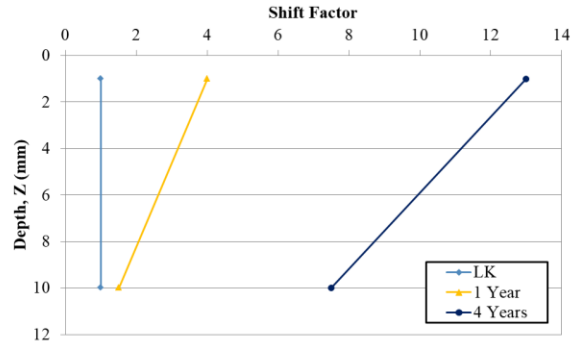


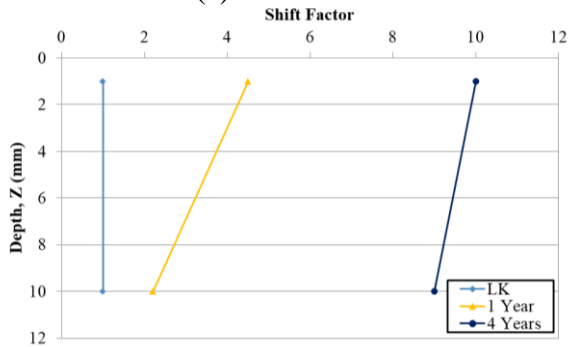
Figure 6.19. Shifting factors for eight sealants over four years of aging.



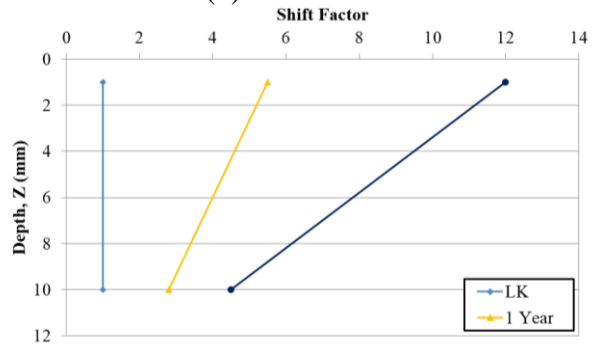
(a) Sealant Ca



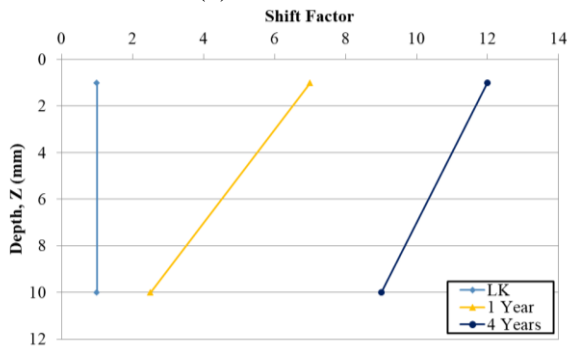
(b) Sealant Da



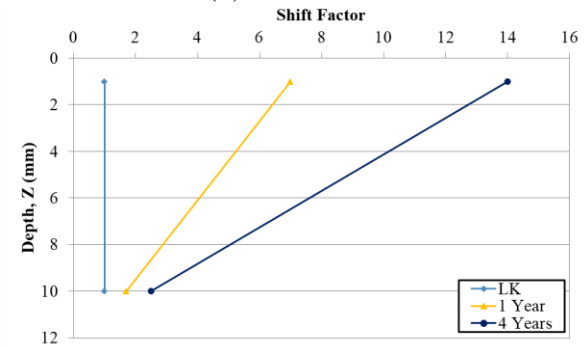
(c) Sealant Ed



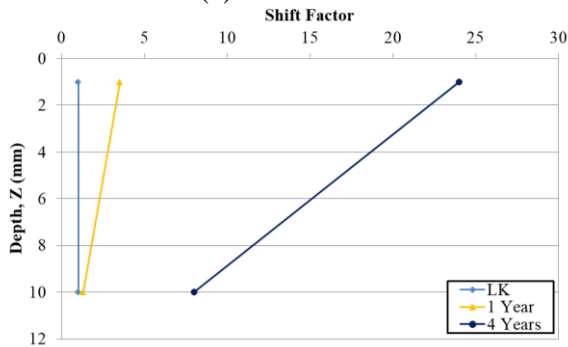
(d) Sealant Fb



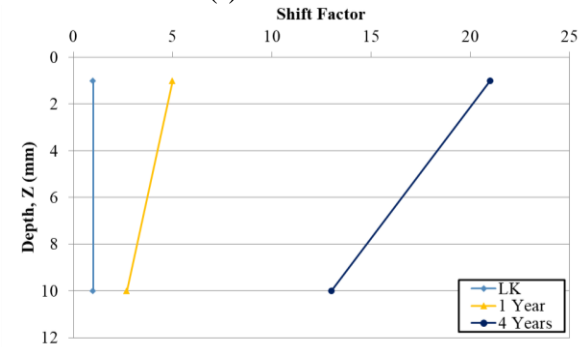
(e) Sealant Jd



(f) Sealant Kc



(g) Sealant Mb



(h) Sealant Ob

Figure 6.20. Complex shear modulus change within the sealant illustrating differential aging as a function of aging time.

Based on the pattern of aging similar to the low-temperature stiffness within a four-year timeframe, a similar form of equation for aging shift factor is proposed for high-temperature shear modulus. The shift factor represents aging rate. Similar to the low-temperature model, the shift factor equation is chosen with two asymptotes representing little-to-no aging at the beginning of service life and long-term aging limit. Hence, an S-shaped curve is used to fit the aging curves.

$$\text{Log}(a_T) = A(1 - e^{-bt})^c \quad (6.4)$$

where, a_T is the shifting factor; constant A is the long-term aging potential; t is the aging time in years; and b and c are factors relate to the size and shape of the curve.

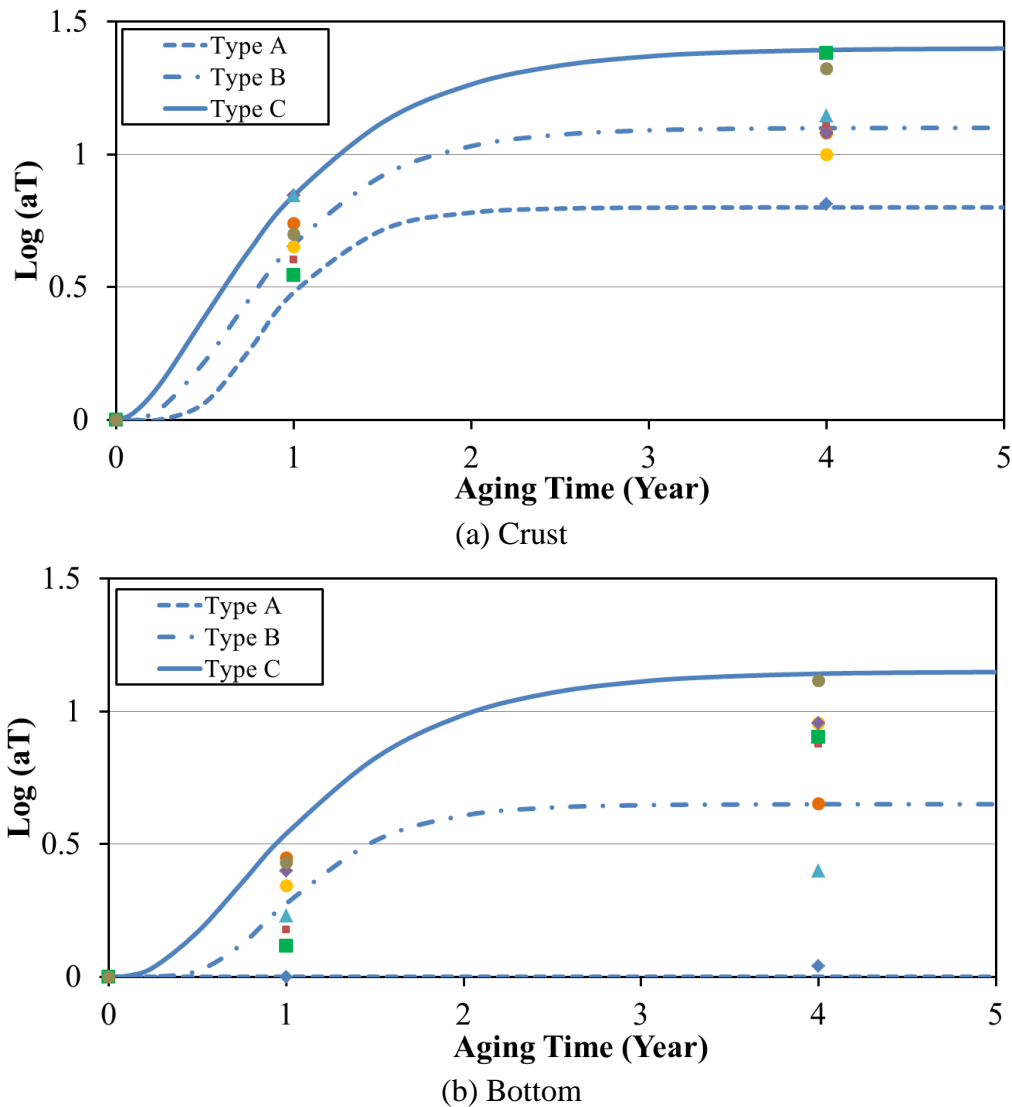


Figure 6.21. Typical sealant types classified based on high-temperature field-aged sealant modulus.

The sealants were grouped into three categories based on their aging potential: Type A includes sealants with the lowest aging potential; sealants with medium aging potential are categorized under Type B; and sealants with the highest aging potential are considered Type C. The coefficients of proposed shift function are chosen to capture the aging potential of all sealants. Figure 6.21 shows that most sealants are in the range of Type B and Type C. Based on the proposed model, values were suggested and summarized in Table 6.5. Coefficient A, indicating aging potential, ranges between 0.8-1.4 with increasing aging magnitude for the FAC. The same coefficient for the bottom portion varies from 0-1.15.

Table 6.5. Typical Aging Potential Values for High-Temperature Model for Asphalt Crack Sealants.

Sealant Aging Type	Portion	Aging Potential	A	b	c	Sealants in This Category
A	Crust	Low	0.8	3	10	Ca
	Bottom		0	0	1	Ca
B	Crust	Medium	1.1	2	3.5	Da, Ed, Fb, Jd, Kc
	Bottom		0.65	2.5	10	Da, Fb, Kc, Mb
C	Crust	High	1.4	1.5	2	Mb, Ob
	Bottom		1.15	1.5	3	Ed, Jd, Ob

6.5.9 Effect of Climate on Aging Model Parameters

In this study, sealants were subjected to weather conditions in central Illinois and may not predict effect of aging at other locations in the U.S. accurately. To address this limitation, field-aged samples were collected from test sites at different locations. However, the following variations from tested section sealant data used in the models development must be considered. First, the sections were open to traffic and significant small particles intruded into the crack sealants crust. Second, field sections are subjected to salt and other chemicals during cold seasons, which may affect sealant stiffness. Third, sealant reservoir (rout size) is usually not consistent; hence, crust to bottom parts ratio varies.

In the global aging system developed by Mirza and Witczak (1995), asphalt binders are characterized by their “expected hardening resistance” regardless of climate effects. However, temperature and mean annual temperature are included in that model. In this study, if it is assumed that parameter A (aging potential of crack sealant) only relate to type and content of raw material (formulation), climate would affect the parameters b and c, which are related to

shape and size of the aging curve. Climate parameters such as UV index, mean annual temperature, as well as latitude and air density at a site play important role in sealant aging path. For example, A is constant for a specific product at different locations, a higher parameter b would indicate a faster aging development and a higher parameter c would suggest longer time to initiate the aging process.

6.5.10 Chemical Evaluation of Aged Sealant Using Fourier-Transform Infrared (FTIR) Spectroscopy

Fourier-Transform Infrared (FTIR) is one of the most popular chemical testing methods to track bituminous material aging (Zofka et. al. 2010). A small sample is required to fingerprint the crack sealant and to identify functional groups that may form during aging. The functional groups change the mechanical properties and affect crack sealant performance during its service life. Examples of functional groups developed during asphalt binder oxidative aging are ketons, dicarboxylic anhydrides, carboxylic acids, and sulfoxides (Peterson 2009). In addition to oxidative aging, polymer degradation may occur during the service life of crack sealant because of heat and solar UV lights. Most types of crack sealants are considered highly polymer modified; SB-based polymers are the most common modifiers used in their formation. FTIR fingerprint may also identify the polymer degradation by measuring changes in polybutadiene and polystyrene indices (Mason et. al. 2001).

In this study, crack sealants were sampled for FTIR testing after kettle heating (LK) and four years of service. Since a relatively small sample of crack sealant is required for FTIR testing, four replicates for each crust and bottom parts were tested and averaged. This avoids bias measurement if large rubber particles are in some tested samples. One to two grams of crack sealant sample was used to collect the infrared spectra. Sixty four scans were averaged for each sample at a resolution of 2 cm^{-1} . Each spectrum covers the wavenumbers from 4000 to 640 cm^{-1} . An analytical approach, recommended by Yut and Zofka (2011), was used to analyze all spectra from FTIR test. A sample spectrum focused to wavenumbers from 2000 to 640 cm^{-1} for the bottom part of Jd sealant is presented in Figure 6.22. This figure identifies the areas related to indices for the aromatic, oxygen containing, and polymer-related abortion bands; they were measure as follows:

$$\text{Aromaticity Index: } I_{AR} = AR_{1600} / \sum AR_{\bar{\nu}} \quad (6.5)$$

$$\text{Carbonyl Index: } I_{CO} = AR_{1700} / \sum AR_{\bar{\nu}} \quad (6.6)$$

$$\text{Sulfoxide Index: } I_{SO} = AR_{1030} / \sum AR_{\bar{\nu}} \quad (6.7)$$

$$\text{Polybutadiene Index: } I_{PB} = AR_{968} / \sum AR_{\bar{\nu}} \quad (6.8)$$

$$\text{Polystyrene Index: } I_{PS} = AR_{700} / \sum AR_{\bar{\nu}} \quad (6.9)$$

where, AR_{ν} is the valley to valley area next to the wavenumber and indices were calculated by dividing the AR_{ν} to the total sum of all band areas ($\sum AR_{\nu}$). Band area was used rather than peak absorbance to reduce the variability of the measurements especially for the crack sealant samples with large rubber particle size.

To measure the changes in the indices, an aging index was introduced at four-year aging for both crust and bottom parts.

$$\text{Aging Index (AI)} = \frac{FTIR \text{ Index}_{Aged}}{FTIR \text{ Index}_{LK}} \quad (6.10)$$

All five indices mentioned above are presented in Figure 6.23 in addition to the ratio of the indices for the crust-to-bottom portion of the aged crack sealant. Among the five indices calculated from FTIR spectra, the main field aging products related to bitumen portion of the crack sealant are carbonyls and sulfoxides. No specific trend was observed for polybutadiene and polystyrene. Previous studies such as the one by Mason et al. (2001) suggested that at high level of polymer concentration changes in SB-based polymers are significant. Unfortunately in this study the amount of polymer used in crack sealants was not available to characterize sealants per level of modification.

The aging index was not calculated for carbonyls since there was no or little amount of I_{CO} at LK (lab kettle) stage (Figure 6.23i). I_{CO} was developed during field aging, and comparing the crust to the bottom portion, the difference was observed to be significant. For all sealants, the I_{CO} for the crust portion was at least double that of bottom part. For the I_{SO} , however, the bottom part is higher than the crust part, except for Fb and Ed (Figure 6.23d). Considering the aging index for I_{SO} in Figure 6.23c, the bottom part developed I_{SO} during the field aging for all sealant except Fb and Ed, while the aging index dropped for the crust portion after 4 years of installation for five out of eight sealants. For some hot-poured crack sealants sulfur is added as a disperser agent for polymers. The amount of added sulfur may be significantly higher than the sulfur in the bitumen

crude, which could impact the I_{SO} developed during field aging. The effect of initial sulfur content on I_{SO} could not be determined in this study because of unknown sealant formulation.

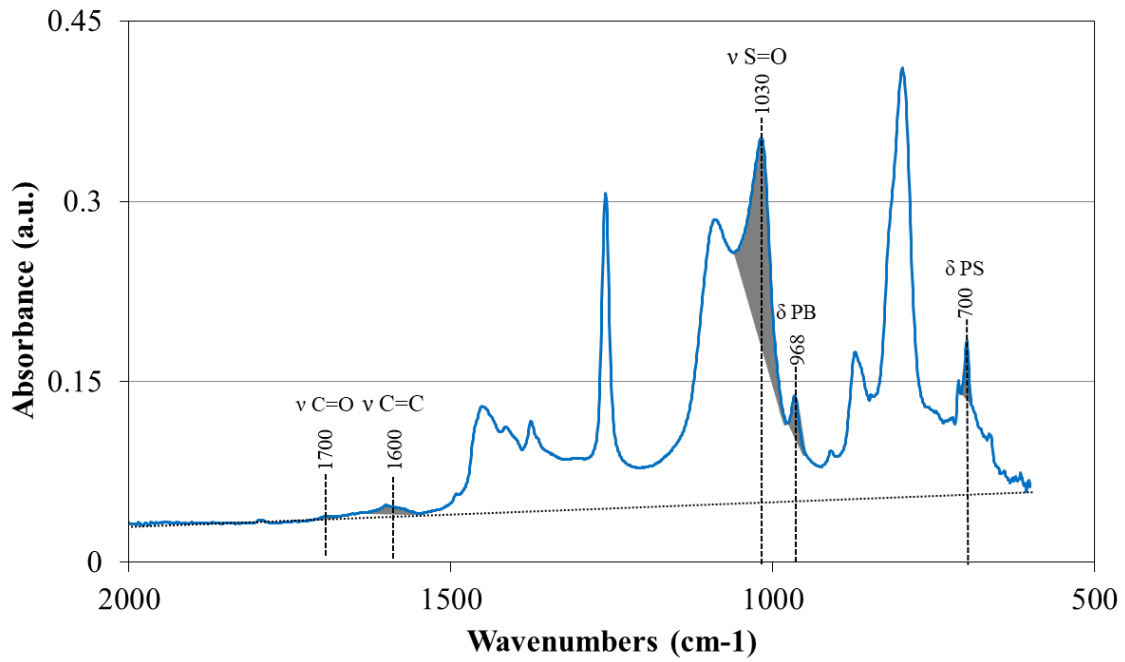
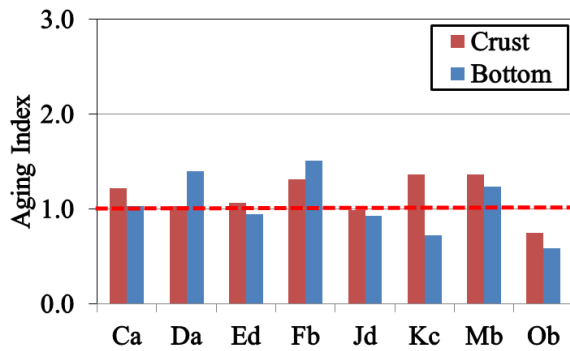
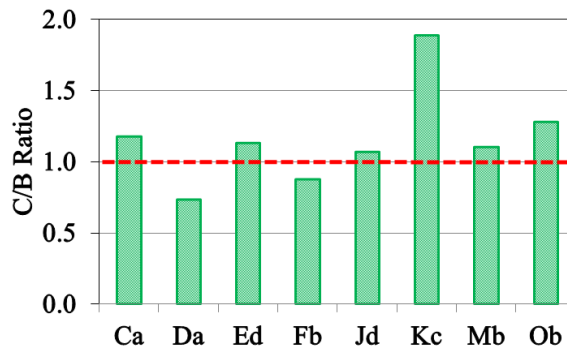


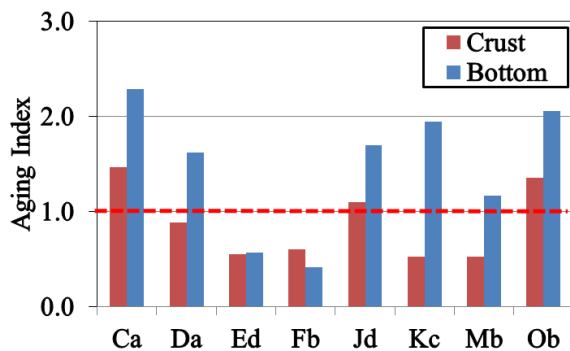
Figure 6.22. Identification of crack sealant components on FTIR spectrum for fingerprinting region between 200 and 600cm-1.



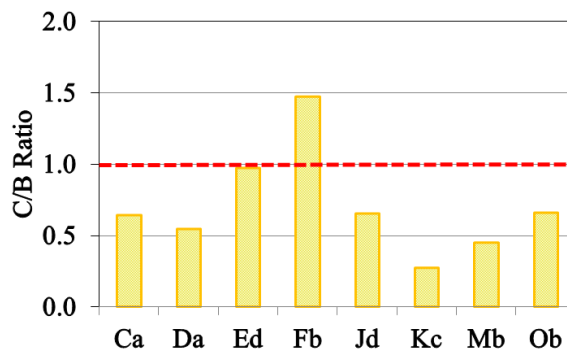
(a) Aging index for I_{AR}



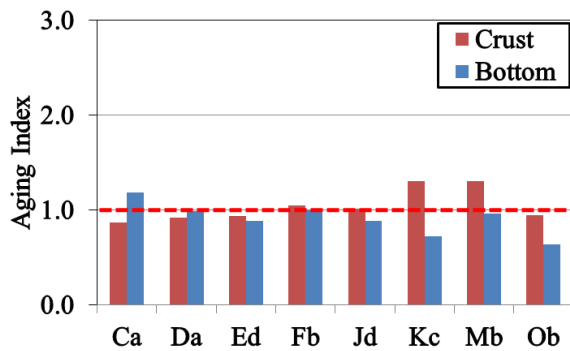
(b) I_{AR} ratio of crust to bottom portion



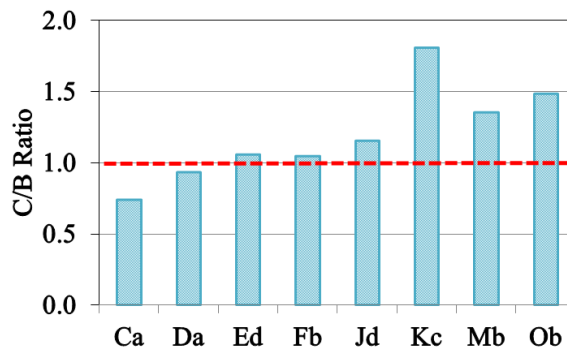
(c) Aging index for I_{SO}



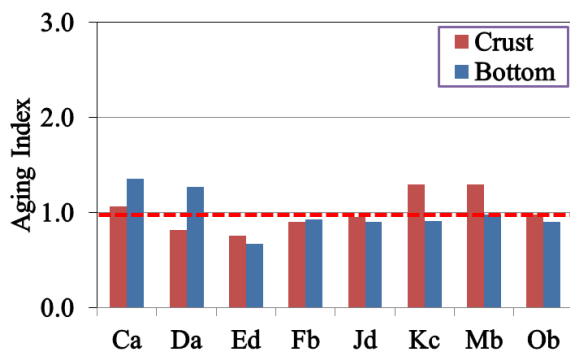
(d) I_{SO} ratio of crust to bottom portion



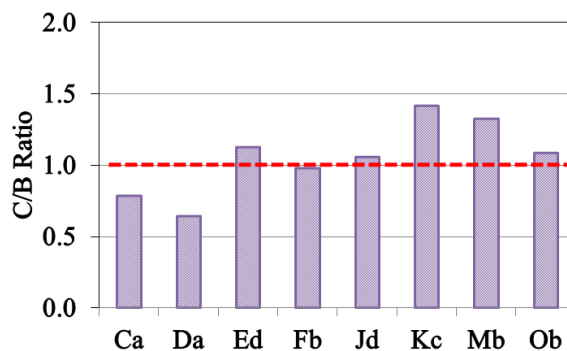
(e) Aging index for I_{PB}



(f) I_{PB} ratio of crust to bottom portion

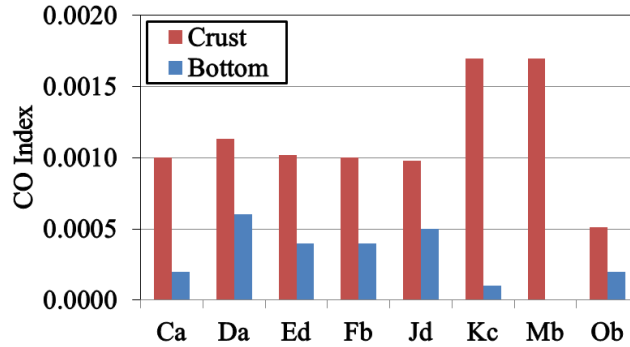


(g) Aging index for I_{PS}



(h) I_{PS} ratio of crust to bottom portion

Figure 6.23. Summary of FTIR indices for the eight sealants' crust and bottom parts.



(i) I_{CO} for bottom and crust

Figure 6.23 (continued)

6.6 Summary

Short- and long-term aging effects on hot-poured crack sealants were evaluated. Sealants were rheologically, mechanically, and chemically characterized at various age stages. Sealants were laboratory-aged (LA) using three methods: Kettle aging, melter aging, and vacuum oven aging (VOA). An aging index was introduced to evaluate the effect of each aging method. Results show that aging in the kettle or melter occurs in the first two hrs of heating. After that, most sealants did not show consistent pattern in their low-temperature stiffness until after approximately 5 hrs of kettle-heating. For most sealants, however, LA increased low-temperature stiffness. In general, based on CSBBR stiffness master curves, VOA was found to be a reasonable aging method to simulate 2-5 years of field aging.

To investigate the effect of weather-related aging only, eight crack sealants were exposed to four years of weathering at a controlled test section without traffic. A field-aging model was developed.

The effect of field aging on sealants properties at low and high temperature was consistent. The following observations summarize findings from the field aging study:

- An overall increase was observed in low-temperature stiffness, high-temperature shear strength and modulus, and viscosity at the installation temperature for both crust and bottom parts most sealants because of weathering.
- Most sealants experienced softening or no change in stiffness following a winter season, possibly due to moisture effect.
- Similar aging patterns were observed for the bottom and crust parts -- converging to a plateau value after two years.

- Aging effects are more pronounced in the mechanical and rheological properties of the crust part of the sealant because of the aging gradient effect.
- Sulfoxide and carbonyl were the main groups among the chemical groups developed during field aging. Sulfoxide index was higher for the bottom part, while carbonyl index indicated greater content in the crust.

Aging models were developed based on time–temperature superposition principle. The sealants were designated as Type A, B, and C with respect to aging. Model coefficients allow predicting changes in sealant low- and high-temperature modulus after installation for each category. Based on developed models, it is recommended to install crack sealants in the fall to avoid summer aging after installation.

CHAPTER 7. SUMMARY, CONCLUSIONS, FINDINGS, AND RECOMMENDATIONS

The standards and specifications currently used to select crack sealants were established based on material properties that are generally empirical. The specification limits vary from one state to another. These differences create difficulties for crack sealant suppliers because many states with the same environmental conditions specify different limits for the measured properties. These standard tests, because do not measure sealant fundamental properties, were reported to poorly characterize the rheological properties of bituminous-based crack sealants and often fail to predict sealant performance in the field.

Therefore, performance-based guidelines were developed as a systematic procedure to select hot-poured bituminous crack sealants. The work proposed a “Sealant Grade” (SG) system to select hot-poured crack sealants based on environmental conditions. A special effort was made to use the equipment originally developed by the Strategic Highway Research Program, used to measure binder rheological behavior as part of the Performance Grade system. The equipment, specimen preparation, and testing procedure were modified in accordance with crack sealant behavior. In addition, new tests for sealant aging and sealant evaluation were introduced. These developed laboratory tests allow for measuring hot-poured bituminous-based crack sealants rheological and mechanical properties over a wide range of service temperatures. Preliminary thresholds for each test were identified to ensure desirable field performance.

Because preliminary SG thresholds were determined based on limited field data, an extensive field study was required to validate and fine-tune the threshold values. The study was designed to validate and fine-tune the threshold values. The scope of this study included installation of test sites, evaluation of field data, and correlation of laboratory results and field performance. Finally, new guidelines were developed and validated for full implementation as AASHTO specifications.

Seven sections were selected in collaboration with participating state departments of transportation in different environmental regions in North America. A wide spectrum of materials was installed in these test sites. Test sites are all wet-freeze climatic zone with some variations in temperature fluctuations. Two commonly used sealing techniques were implemented: (1) *Rout and seal*, and (2) *clean and seal*. Rout and seal treatments were applied

with varying reservoir geometry. Clean and seal treatments were also applied at the same locations to compare with two sealing techniques.

Field inspection of crack sealant performance was conducted annually during the project duration, immediately after crack sealant installation and every winter season during the February-March months. Performance data were routinely collected, including visual distress identification, crack opening displacement, temperature measurements, and sampling for laboratory evaluation. Based on the discussions of this study, followings are the main conclusions:

- Mechanical performance-based tests, developed for sealant selection in an earlier study, were validated. Test thresholds were fine-tuned using field-measured data and a new sealant grading system is introduced (Table 7.1).
- An aging model was developed using aging–time–temperature superposition. The model allows for prediction of changes in the low-temperature and high-temperature modulus properties of a sealant after installation.
- For the same sealant, rout and seal treatment preforms better than clean and seal treatment. Hence, for longer treatment life, rout and seal treatment is recommended.

The other findings of this study are the following:

- Most sealants failed below the performance index (PI) threshold of 70% after three years. The severe temperature drops in 2013-2014 winters affected the performance of sealants significantly.
- Rout and seal sections performed better than clean and seal sections. Most of clean and seal sections failed within two years, except for the Michigan test site. This shows the importance of test site selection for clean and seal application. It was noted that transverse reflective cracks are not suitable candidates for clean and seal applications.
- Adhesive failure was the predominant type of failure for rout and seal section; whereas, the clean and seal section failed due to either complete loss of overband or cohesive failure.
- In general, spalling occurred at the rout walls when crack and reservoir were not properly aligned. This was considered a pavement failure affecting sealants capacity and efficiency to perform their primary function, i.e., sealing cracks.

- Although reservoir geometry may affect sealant performance, no clear trend between reservoir size and performance. Reservoir narrow geometry is not recommended because of construction difficulties. On the other hand, wide routs may have greater exposure to weathering. Shallow depths are also not recommended as they may increase the probability of adhesive failure due to insufficient bonding.
- Overband application had a clear and positive impact on the performance of sealants.
- Overall, a good correlation was observed for CSBBR and CSDTT test parameters and field performance.
- Field PI and sealants stiffness (from CSBBR test method) exhibited three distinctive zones:
 - Zone 1: Sealants with fair field performance ($50\% < PI < 70\%$) and low stiffness
 - Zone 2: Sealants with acceptable field performance ($PI > 70\%$) with moderate stiffness
 - Zone 3: Sealants with poor field performance ($PI < 70\%$) and high stiffness
- For clean and seal, PI was reduced as stiffness and/or tensile load increase.
- Two-tiered thresholds were recommended for CSBBR test to avoid using sealants that are either too soft or too stiff. When sealant stiffness is too soft, premature overband failure could accelerate adhesive failure. On the other hand, stiff sealant is not a good candidate in low-temperature climate because of excessive stresses accumulating in the sealant.
- Energy obtained from CSDTT correlated with PI better than tensile load or extendibility.
- A good correlation was generally observed for MSCR, obtained by dynamic shear rheometer, and yield test parameters. Yield test was recommended for detecting tracking potential in a simplified approach.
- It is important not to overheat or underheat sealants. Based on field observations during installation, viscosity thresholds were identified to insure sufficient workability during installation at the recommended pouring temperature.
- Laboratory aging (LA) of sealants was simulated using three aging methods: Kettle aging, melter aging, and vacuum oven aging (VOA). An aging index was introduced to evaluate the

effect of these aging methods. Results showed that aging in the kettle or melter occurs in the first two hrs of heating; thereafter, most sealants did not show a consistent pattern in their low temperature stiffness until approximately five hrs of heating in the kettle. For most sealants, however, LA increased the low-temperature stiffness. Eventually, by comparing stiffness master curves obtained from CSBBR test for field-aged samples and laboratory-aged samples, it was concluded that VOA is a reasonable aging method for simulating 2-5 years of field aging.

- The effect of field aging on sealants low temperature was consistent. The following observations summarize the findings of the field aging experiments:
 - An overall increase was observed in the low temperature stiffness, high temperature shear strength and modulus, and viscosity at installation temperature for both crust and bottom portion of most of the sealants due to weathering.
 - Some sealants experienced softening or no change in stiffness after a cold season, possibly due to moisture effects compensating oxidation.
 - Similar aging patterns were observed for bottom and crust portions of most sealant converging to a plateau value after two or three years.
 - Aging effects were more pronounced in the crust, as expected. Aging effect has a gradient from surface of the material through the sealant thickness.
 - Sulfoxide is higher in the bottom part, while carbonyl has higher content in crust.
- Worst performing sealants were the ones with low adhesion capacity and high stiffness for the climatic regions they are installed in. On the other hand, best performing sealants were those with the highest adhesion capacity and moderate stiffness. Moderate adhesion capacity and very low modulus sealant performed moderately.
- A composite score, combining ranking and correlation, was used to develop a quantitative scale to determine the level of acceptance. For most of the test sites, a strong or acceptable correlation between field performance and laboratory test parameters was obtained. CSBBR stiffness has the strongest correlation followed by adhesion energy and load for rout and seal treatment. However, average creep ratio (ACR) from CSBBR test had either good or poor correlation with the PI. Similarly, for clean and seal treatment, CSBBR stiffness had the best

score followed by tensile load and extendibility. Also, a good correlation was observed between CSBBR stiffness and adhesion load as well as CSBBR stiffness and tensile load.

- Two separate low-temperature grading schemes were suggested for rout and seal and clean and fill techniques depending on the failure mode. The CSBBR and CSDTT tests are required for clean and fill treatment; whereas, the rout and seal treatment requires CSBBR and CSAT tests.
- For the CSBBR test, the maximum stiffness threshold was reduced from 25 MPa to 15 MPa at 240s at 6°C higher than grading temperature.
- To control tracking wear, a minimum stiffness threshold was introduced and selected as 40 MPa at 1s at 6°C higher than grading temperature. The ACR was kept a minimum of 0.31.
- The extendibility thresholds were not changed from the provisional standard. However, a secondary threshold as a maximum tensile load was introduced and selected as 25N to avoid the use of less ductile sealants.
- In the case of a soft or stiff grade sealant, a decline in sealant performance was observed. This shows the importance and validity of using SG as a performance criterion.
- Based on the aging models, it is recommended to install crack sealants in the fall to avoid summer aging after installation.
- Based on the sealants' field performance, overband application is recommended to increase the sealant treatment life.
- Crew members should be well trained on routing the cracks to avoid spalling during the construction. Spalling negates the effect of crack treatment.

Based on the outcome of this study, the followings are recommended for future studies:

- Effect of geographical parameters such as latitude, UV index, elevation and maximum, minimum and annual air temperature on the aging path of sealants. Hence, the developed aging model can be extended to cover various environments.
- The effect of polymer type and content, rubber type and content as well as sulfur content in the original formulation on crack sealant aging need to be investigated.

- Shift factors, used to develop the aging model at low temperatures, showed that moisture damage may play an important role than oxidation during the cold season. Low temperature affects bonding between sealant and rout walls and lead to adhesion loss.

Table 7.1 Crack Sealant Performance Grade

Crack Sealant Performance Grade	SG 46					SG 52					SG 58					SG 64					SG 70					SG 76					SG 82															
	-46	-40	-34	-28	-22	-16	-10	-4	-40	-34	-28	-22	-16	-10	-4	-40	-34	-28	-22	-16	-10	-4	-40	-34	-28	-22	-16	-10	-4	-40	-34	-28	-22	-16	-10	-4	-40	-34	-28	-22	-16	-10	-4	-40	-34	-28
Apparent Viscosity, T 366	Installation Temperature																																													
Maximum Viscosity (Pa.s)	3.5																																													
Minimum Viscosity (Pa.s)	1.0																																													
Dynamic Shear (MSCR) TP 126	46					52					58					64					70					76					82															
Minimum Flow Coeff. (kPa.s)	4.0																																													
Minimum Shear Thinning	0.7																																													
Dynamic Shear (Yield) TP XX-XX	46					52					58					64					70					76					82															
Minimum Shear Stress at 200% Strain (Pa)	160																																													
Vacuum Oven Residue (T 367)																																														
Crack Sealant BBR, T 368	-40	-34	-28	-22	-16	-10	-4	-40	-34	-28	-22	-16	-10	-4	-40	-34	-28	-22	-16	-10	-4	-40	-34	-28	-22	-16	-10	-4	-40	-34	-28	-22	-16	-10	-4	-40	-34	-28	-22	-16	-10	-4				
Maximum Stiffness at 240 s (MPa)	15																																													
Minimum Stiffness at 1 s (MPa)	40																																													
Minimum Avg. Creep Rate	0.31																																													
Clean and Seal Treatment																																														
Crack Sealant DTT, T 369	-40	-34	-28	-22	-16	-10	-4	-40	-34	-28	-22	-16	-10	-4	-40	-34	-28	-22	-16	-10	-4	-40	-34	-28	-22	-16	-10	-4	-40	-34	-28	-22	-16	-10	-4	-40	-34	-28	-22	-16	-10	-4				
Minimum Extensibility (%)	85	85	70	55	40	25	10	85	85	70	55	40	25	10	85	85	70	55	40	25	10	85	85	70	55	40	25	10	85	85	70	55	40	25	10	85	85	70	55	40	25	10				
Maximum Tensile Load (N)	25																																													
Rout and Seal Treatment																																														
Crack Sealant AT, T 370	-40	-34	-28	-22	-16	-10	-4	-40	-34	-28	-22	-16	-10	-4	-40	-34	-28	-22	-16	-10	-4	-40	-34	-28	-22	-16	-10	-4	-40	-34	-28	-22	-16	-10	-4	-40	-34	-28	-22	-16	-10	-4				
Minimum Load (N)	200	175	150	125	100	75	50	200	175	150	125	100	75	50	200	175	150	125	100	75	50	200	175	150	125	100	75	50	200	175	150	125	100	75	50	200	175	150	125	100	75	50				

REFERENCES

1. Al-Qadi, I.L., Fini, E., and Masson, J-F. Effect of Bituminous Material Rheology on Its Adhesion. In Proceedings of the 87th Transportation Research Board Annual Meeting 08-2331, Washington, DC, 2008.
2. Al-Qadi, I.L., Yang, S., Elseifi, M., Masson, J-F., and McGhee, K. Specifications of Bituminous-Based Crack Sealants Using Modified Bending Beam Rheometer. In Proceedings of the 85th Transportation Research Board Annual Meeting, Washington, DC, 2006.
3. Al-Qadi I.L., J.-F. Masson, A. Loulizi, P. Collins, K. K. McGhee, J.R. Woods, and S. Bundalo-Perc. *Long-Term Accelerated Aging and Low Temperature Testing*, Report No. B5508-5. In National Research Council, Ottawa, Canada, 2003.
4. Al-Qadi, I. L., Fini, E., Elseifi, M., Masson, J-F, and McGhee, K. (2006), "Procedure for Viscosity Determination of Hot-Poured Bituminous Sealants," *Transportation Research Record: Journal of the Transportation Research Board*, No. 1958, pp. 74–81.
5. Al-Qadi, I. L., Fini, E., Figueroa, H. D. Masson, J-F, and McGhee, K. M. (2008a), *Development of Adhesion Tests for Hot-Poured Crack Sealants*, Final Report, Submitted to Virginia Transportation Research Council, VDOT, Charlottesville, VA.
6. Al-Qadi, I. L., Fini, E., Masson, J-F, Loulizi A., Elseifi, M., and McGhee, K. M. (2008b), *Development of Apparent Viscosity Test for Hot-Poured Crack Sealants*, Final Report, Submitted to Virginia Transportation Research Council, VDOT, Charlottesville, VA.
7. Al-Qadi, I. L., Yang, S-H, Masson, J-F, Dessouky, S., Loulizi, A., Elseifi, M., and McGhee, K. M. (2008c), *Characterization of Low Temperature Mechanical Properties of Crack Sealants Utilizing Direct Tension Test*, Final Report, Submitted to Virginia Transportation Research Council, VDOT, Charlottesville, VA.
8. Al-Qadi, I. L., Yang, S-H, Masson, J-F, Elseifi, M., Dessouky, S., Loulizi, A., and McGhee, K. M. (2008d), *Characterization of Low Temperature Creep Properties of Crack Sealants Using Bending Beam Rheometry*, Final Report, Submitted to Virginia Transportation Research Council, VDOT, Charlottesville, VA.
9. Al-Qadi, I., Loulizi, A., Aref, S., Masson, J-F, and McGhee, K. M. (2005), "Modification of Bending Beam Rheometer Specimen for Low-temperature Evaluation of Bituminous Crack Sealants," *Transportation Research Record: Journal of the Transportation Research Board*, No. 1933, pp. 97–106.
10. Al-Qadi, I. L., Yang, S-H., Dessouky, S., Masson, J-F, Loulizi, A., and Elseifi, M. (2007), "Development of Crack Sealant Bending Beam Rheometer (CSBBR) Testing to Characterize Hot-Poured Bituminous Crack Sealant at Low Temperature," *The Journal of AAPT*, Vol. 76, pp. 85–122.

11. Al-Qadi, I. L., Masson, J-F, Dessouky, S., Collins, P., Yang, S-H, Bundalo-Perc, S., Fini, E., Elseifi, M., and McGhee, K. M., *Development of Performance Guidelines for Selection of Hot-Poured Crack Sealants*, Interim Report No. B5508-7, National Research Council of Canada, Sep 2005, 142 p.
12. Al-Qadi, I. L., Masson, J-F, Loulizi, A., Collins, P., Woods, J. R., Bundalo-Perc, S., and McGhee, K. M. (2004), *Long-Term Accelerated Aging and Low Temperature BBR Testing of Sealants*, Interim Report No. B5508-7, National Research Council of Canada, 262 p.
13. Al-Qadi, I. L., Masson, J-F, Yang, S-H, and Fini, E. (2008), *Towards Performance-Based Selection Guidelines for Roadway Crack Sealant*, Submitted to International ISAP Symposium on Asphalt Pavements and Environment, Zurich, Switzerland, August, 2008.
14. Al-Qadi, I. L., Yang, S-H, Dessouky, S., Masson, J-F, “Low Temperature Characterization of Hot-Poured Crack Sealant Using Modified SHRP Direct Tensile Tester,” *Transportation Research Record: Journal of the Transportation Research Board*, No. 1991, Oct 2007, pp. 109–118.
15. Al-Qadi, I., Masson, J.-F., Fini, E., Yang, S.-H., & McGhee, K. K. (2009). *Development of Performance-Based Guidelines for Selection Of Bituminous-Based Hot-Poured Pavement Crack Sealant: An Executive Summary Report*. Springfield: Illinois Center for Transportation.
16. American Association of State Highway and Transportation Officials, MP 25. Performance-Graded Hot-Poured Asphalt Crack Sealant AASHTO, Washington, DC, 2018.
17. American Association of State Highway and Transportation Officials, PP 85. Grading or Verifying the Sealant Grade (SG) of a Hot-Poured Asphalt Crack Sealants, AASHTO, Washington, DC, 2018.
18. American Association of State Highway and Transportation Officials, T366. Apparent Viscosity of Hot-Poured Asphalt Crack Sealant Using Rotational Viscometer, AASHTO, Washington, DC, 2018.
19. American Association of State Highway and Transportation Officials, T367. Accelerated Aging of Hot-Poured Asphalt Crack Sealants Using a Vacuum Oven, AASHTO, Washington, DC, 2018.
20. American Association of State Highway and Transportation Officials, T368. Measure Low-Temperature Flexural Creep Stiffness of Hot-Poured Asphalt Crack Sealants by BBR, AASHTO, Washington, DC, 2018.

21. American Association of State Highway and Transportation Officials, T369. Evaluation of the Low-Temperature Tensile Property of Hot-Poured Asphalt Crack Sealants by Direct Tension Test AASHTO, Washington, DC, 2018.
22. American Association of State Highway and Transportation Officials, T370. Measuring Adhesion of Hot-Poured Asphalt Crack Sealant Using Direct Adhesion Tester AASHTO, Washington, DC, 2018.
23. American Association of State Highway and Transportation Officials, T371. Measuring Interfacial Fracture Energy of Hot-Poured Crack Sealant Using a Blister Test, AASHTO, Washington, DC, 2018.
24. American Association of State Highway and Transportation Officials, T126. Evaluation of the Tracking Resistance of Hot-Poured Asphalt Crack Sealants by Dynamic Shear Rheometer (DSR), AASHTO, Washington, DC, 2018.
25. Anderson, D.A., Christensen, H.U., Bahia, R., Dongre, R., Sharma, M.G., and Button, J.J. Binder Characterization and Evaluation. Vol. 3: Physical Characterization, SHRP-A-369, Strategic Highway Research Program, Washington, DC, 1994.
26. ASTM D6690. Standard Specification for Joint and Crack Sealants, Hot Applied, for Concrete and Asphalt Pavements. *American Society of Testing and Material*, Philadelphia, Pennsylvania, 2006.
27. ASTM D5167. Standard Practice for Melting of Hot-Applied Joint and Crack Sealant and Filler for Evaluation. *American Society of Testing and Material*, Philadelphia, Pennsylvania, www.astm.org.
28. ASTM D5329, *Standard Test Methods for Sealants and Fillers, Hot-Applied, for Joints and Cracks in Asphaltic and Portland Cement Concrete Pavements*, American Society of Testing and Material, Philadelphia, PA, 2004, www.astm.org.
29. Belangie, M.C., and Anderson, D.I. Crack Sealing Methods and Materials for Flexible Pavements. Final Report, No. FHWA-UT-85-1. 74 p., Utah Department of Transportation, Salt Lake City, Utah, 1985.
30. Bennett, S.J., Devries, K.L., and Williams, M.L. Adhesion Fracture Mechanics. *International Journal of Fracture*, Vol. 10, No. 1, 1974, pp. 33-43.
31. Bhasin, A., Masad, E., Little, D., and Lytton, R. Limits on Adhesive Bond Energy for Improved Resistance of Hot Mix Asphalt to Moisture Damage. In Proceedings of the 85th Transportation Research Board Annual Meetings, Washington, DC, 2006.
32. Cheng, D.X., Little, D., Lytton, R., and Holste, J.C. Surface Free Energy Measurement of Aggregates and Its Application to Adhesion and Moisture Damage of Asphalt Aggregate

Systems. International Center for Aggregates Research, 9th Annual Symposium, Austin, Texas, 2001.

33. Chong, G. J. and Phang, W. A. (1987), *Consequences of Deferred Maintenance Treatment on Transverse Cracks in Cold Regions*, Proceedings of Paving in Cold Areas Mini-Workshop, Ottawa, Ontario, Canada, pp. 638–686.
34. Chong, G. J. and Phang, W. A. (1987), “Improved Preventive Maintenance: Sealing Cracks in Flexible Pavements in Cold Regions,” Final Report, PAV-87-01, Ontario Ministry of Transportation, Downsview, ON.
35. Chong, G. J. (1990), “Rout and Seal Cracks in Flexible Pavements—A Cost-Effective Preventive Maintenance Procedure,” *Transportation Research Record: Journal of the Transportation Research Board*, TRR, No. 1268, National Research Council, Washington DC, pp. 8–16.
36. Christensen, D.W., Anderson, D.A. Chemical-Physical Property Relationships for Asphalt Cements and the Dispersed Polar Fluid Model. Vol. 37, No. 3 & 4, Division of Fuel Chemistry, American Chemical Society, Preprints of Papers, 204th ACS National Meeting, Washington, D. C., pp. 1279–1291, August 1992.
37. Collins, P., Veitch, M., Masson, J-F, Al-Qadi, I., “Deformation and Tracking of Bituminous Sealants in Summer Temperatures: Pseudo-Field Behavior,” *International Journal of Pavement Engineering*, in print.
38. Cook, J.P., Weisgerber, F.E., and Minkarah, I.A. Evaluation of Joint and Crack Sealants. FHWA/OH-91/007. University of Cincinnati, Cincinnati, Ohio, 1990.
39. Cortizo, M. S., Larsen, Do. O., Bianchetto, H., Alessandrini, J. L., (2004). Effect of the Thermal Degradation of SBS Copolymers During the Ageing of Modified Asphalts. *Journal of Polymer Degradation and Stability*, Vol. 86 (2), pp. 275–282.
40. Cuelho, E., Johnson, D. R., and Freeman, R. B. (2002), “*Cost-Effectiveness of Crack Sealing Materials and Techniques for Asphalt Pavements*,” Final Report, FHWA/MT-02-002/8127, Montana Department of Transportation, Helena, MT, 247 pp.
41. Cuelho, E., Ganeshan, S. K., Johnson, D. R., Freeman, R. B., and Schillings, P. L. (2003), “Relative Performance of Crack Sealing Materials and Techniques for Asphalt Pavements,” Third International Symposium on Maintenance and Rehabilitation of Pavements and Technological Control, Guimarães, Portugal, pp. 327–337.
42. Cuelho, E., & Freeman, R. B. (2004). *Cost-Effectiveness of Crack sealing Materials and Techniques for Asphalt Pavements*. Helena: NTIS, Springfield, Virginia 22161.
43. Curtis, C.W. Investigation of Asphalt-Aggregate Interaction in Asphalt Pavements. *American Chemical Society* (Fuel section), Vol. 37, 1992, pp. 1292–1297.

44. Elseifi, M., Dessouky, S., Al-Qadi, I. L., Yang, S-H (2006), "A Viscoelastic Model to Describe the Mechanical Response of Bituminous Sealants at Low Temperature," *Transportation Research Record: Journal of the Transportation Research Board*, No. 1958, pp. 82–89.
45. Fang, C., Galal, K. A., Ward, D. R., Haddock, J. E., and Kuczek, T. (2003), "Cost-Effectiveness of Joint and Crack Sealing," Presented at the 82nd Annual Meeting of the Transportation Research Board, Washington, DC.
46. Fang, C., Haddock, J., Galal, K., & Ward, D. (2003). *Initial Study for Cost-Effectiveness of Joint/Crack Sealing*. Indianapolis: National Technical Information Service, Springfield, VA 22161.
47. Fini, E., Al-Qadi, I. L., and Dessouky, S. H. (2006), *Adhesion of Hot-Poured Crack Sealant to Aggregate*, TRB Paper No. 06-2888, The 85th Annual Meeting of the Transportation Research Board, National Research Council, Washington, D. C.
48. Jiang, K.R., and Penn, L.S. Use of the Blister Test to Study the Adhesion of Brittle Materials, Test Modification and Validation. *Journal of Adhesion*, Vol. 32, 1990, pp. 203–216.
49. Lamontagne, J., Dumas, P., Mouillet, V., Kister, J. (2001), "Comparison by Fourier Transform Infrared (FTIR) Spectroscopy of Different Ageing Techniques: Application to Road Bitumens" *Fuel*, No. 80, pp. 483–488.
50. Malyshev, B.M., and Salganik, R.L. The Strength of Adhesive Joints Using the Theory of Cracks. *International Journal of Fracture Mechanics*, Vol. 1, 1965, pp. 114–128.
51. Masson, J-F., Collins, P., Wood, J.R., and Bundalo-Perc, S. Degradation of Bituminous Sealants Due to Extended Heating before Installation. In Proceedings of the 85th Transportation Research Board Annual Meeting, Washington, DC, 2006.
52. Masson, J-F., and Al-Qadi, I.L. Long-Term Accelerated Aging and Low Temperature BBR Testing of Sealants. Internal Report, National Research Council of Canada, No. B5508.5, 2004.
53. Masson, J-F., and Lacasse, M.A. A Review of Adhesion Mechanisms at the Crack Sealant/Asphalt Concrete Interface. In Proceedings of the 3rd International Symposium on Durability of Building and Construction Sealants, Fort Lauderdale, Florida, 2000.
54. Masson, J. F., Collins, P., and Légaré, P.P. Performance of Pavement Crack Sealants in Cold Urban Conditions. *Canadian Journal of Civil Engineering*, Vol. 26, No. 4, 1999, pp. 395–401.

55. Masson, J. F., Pelletier, L., Collins, P., (2000). Rapid FTIR Method for Quantification of Styrene-Butadiene Type Copolymers in Bitumen. *Journal of Applied Polymer Science*, Vol. 79, No. 6, pp. 1034–1041.
56. Masson, J-F., and Lacasse, M.A. Effect of the Hot-Aired Lance on Crack Sealant Adhesion, *Journal of Transportation Engineering*, Vol. 125, 1999.
57. Masson, J-F., Polomark, G., and Collins, P. Glass Transitions and Amorphous Phases in SBS-Bitumen Blends. *Thermochimica Acta*, Vol. 435, 2005, pp. 96–100.
58. Masson, J-F, Collins, P., Perraton, D., Al-Qadi, I. L. (2007), “Rapid Assessment of the Tracking Resistance of Bituminous Crack Sealants,” *Canadian Journal of Civil Engineering*, Vol. 34, pp. 126–131.
59. Masson, J.-F. (2000), “Bituminous Sealants for Pavement Joints and Cracks: Building the Basis for a Performance-Based Specification,” In *Durability of Building and Construction Sealants*, A. Wolf, Ed., RILEM, Paris, pp. 315–328.
60. Mirza, M. W., Witzak, M. W., (1995). Development of a Global Aging System for Short and Long Term Aging of Asphalt Cements (with Discussion). *Journal of the Association of Asphalt Paving Technologists*, Vol. 64, pp. 393–430.
61. Ozer, H., P. Solanki, S. S. Yousefi, and I. L. Al-Qadi. Field Validation of Laboratory-Predicted Low-Temperature Performance of Hot-Poured Crack Sealants. *Transportation Research Record: Journal of the Transportation Research Board*. No. 2431, pp.57–66.
62. Ozer, H, S. S. Yousefi, I. L. Al-Qadi, and G. Elizalde. Field Aging and Development of Aging Model for Hot-Poured Crack Sealants. *Transportation Research Record: Journal of the Transportation Research Board*. No. 2481, pp.90–99.
63. Panea, J. (1990), “*Field Evaluation of Rout and Seal Crack Treatment in Flexible Pavement*,” Final Report, PAV-90-03, Ministry of Transportation of Ontario, Downsview, ON, Canada.
64. Penn, L.S., and Defex, E. (2002). Relation between Work of Adhesion and Work of Fracture for Simple Interfaces. *Journal of Material Science*, Vol. 37, pp. 505–513.
65. Peshkin, D., Smith, K. L., Wolters, A., Krstulovich, J., Moulthrop, J., & Alvarado, C. (2011). *Guidelines for the Preservation of High-Traffic-Volume Roadways*. Washington: Transportation Research Board.
66. Petersen, J. C., (2009), *A Review of the Fundamentals of Asphalt Oxidation: Chemical, Physicochemical, Physical Property, and Durability Relationships*. E-C140, Transportation Research Circular, Transportation Research Board, Washington, D. C., 78p.

67. Petersen, J. C., Harnsberger, P. M., (1988). Asphalt Aging: Dual Oxidation Mechanism and Its Interrelationships with Asphalt Composition and Oxidative Age Hardening. *Transportation Research Record: Journal of the Transportation Research*, Vol. 1638 (1).
68. Ponniah, J. E., & Kennepohl, G. (1996). Crack Sealing in Flexible Pavements: A Life-Cycle Cost Analysis. *Transportation Research Record*, Vol. 1529 (1), pp. 86–94.
69. Sawalha, M., H. Ozer, I. L. Al-Qadi. *Cost-Effectiveness for Hot-Poured Asphalt Crack Sealants*. Presented at 97th Annual Meeting of the Transportation Research Board, Washington, D.C., 2018.
70. Smith, K. L., and Romine, A. R. (1993), *Innovative Materials Development and Testing Volume 3: Treatment of Cracks in Asphalt Concrete-Surfaced Pavements*, SHRP-H-354. Strategic Highway Research Program, National Research Council, Washington, D. C.
71. Smith, K. L., and Romine, A. R. (1999), *LTPP Pavement Maintenance Materials: SHRP Crack Treatment Experiment*. FHWA-RD-99-143, Final Report, FHWA, Washington, D. C.
72. Solanki, P., H. Ozer, S. S. Yousefi, and I. L. Al-Qadi. Effect of Installation Parameters on Performance of Hot-Poured Crack Sealants. *Proceeding of T&DI Congress*. ASCE, Orlando, FL, pp. 142–152.
73. Sugano, M., Kajita, J., Ochiai, M., Takagi, N., Iwai, S., and Hirano, K. Mechanisms for Chemical Reactivity of Two Kinds of Polymer Modified Asphalts during Thermal Degradation. *Chemical Engineering Journal*, 2011, pp. 231–236.
74. Thelen, E. Surface Energy and Adhesion Properties in Asphalt-Aggregate Systems. In *Proceedings of the 37th Annual Meeting of the Highway Research Board; Rheological and Adhesion Characteristics of Asphalt*, Bulletin 192, 1958.
75. Tschoegl, N.W. *The Phenomenological Theory of Linear Viscoelastic Behavior*. Springer-Verlag, 1989, New York.
76. Van Oss, C.J., Chaudhury, M.K., and Good, R.J. Interfacial Lifshitz-van der Waals and Polar Interactions in Macroscopic Systems. *Chemical Reviews*, Vol. 88, No. 6, 1988, pp. 927-941.
77. Wang, Y., Wang, G., & Mastin, N. (2012). Costs and Effectiveness of Flexible Pavement Treatments: Experience and Evidence. *American Society of Civil Engineering*, 516–525.
78. Ward, D. R. (2001), “Evaluation of the Implementation of Hot-Pour Sealants and Equipment for Crack Sealing in Indiana,” Final Report, FHWA/IN/JTRP-2000/27, FHWA, Washington, DC.

79. Williams, M.L. (1969). The Continuum Interpretation for Fracture and Adhesion. *Journal of Applied Polymer Science*, Vol. 13, pp. 20–40.
80. Williams, M.L., and Kelley, F.N. The Interaction between Polymeric Structure, Deformation and Fracture, in *Polymer Networks: Structural and Mechanical Properties*. A.J. Chompff, (Ed), New York: Plenum Press, 1971, pp. 193–218.
81. Yang, X., You, Z., Mills-Beale, J., (2015). Asphalt Binders Blended with a High Percentage of Biobinders: Aging Mechanism Using FTIR and Rheology. *Journal of Materials in Civil Engineering*, Vol. 17 (4).
82. Yang, S-H and Al-Qadi, I. (2008), “A Modified Direct Tension Test (DTT) for Bituminous Crack Sealant Characterization at Low Temperature.” *The Journal of AAPT*, Vol. 77.
83. Yousefi, S. S., H. Ozer, I. L. Al-Qadi. Identification of Low Temperature Stiffness Thresholds for Hot-Poured Sealants Using the Crack Sealant Bending Beam Rheometer Test Method. Presented at 95th Annual Meeting of the Transportation Research Board, Washington, D.C., 2016.
84. Yousefi, S. S., H. Ozer, I. Hafeez, I. L. Al-Qadi. *Field and Laboratory Low Temperature Performance of Hot-Poured Crack Sealants in Michigan*. Presented at 95th Annual Meeting of the Transportation Research Board, Washington, D.C., 2016.
85. Yut, I. Zofka, A., (2011). Attenuated Total Reflection (ATR) Fourier Transform Infrared (FT-IR) Spectroscopy of Oxidized Polymer-Modified Bitumens. *Applied Spectroscopy*, Vol. 66 (7).
86. Zanzotto, L. *Laboratory Testing of Crack Sealing Materials for Flexible Pavement*. Transportation Association of Canada, Ottawa, Canada, 1996.
87. Zofka, A., Chrysochoou, M., Yut, I., Johnston, C., Shaw, M., Sun, Sh., Mahoney, J., Farquharson, S., Donahue, M., (2013), *Evaluating Applications of Field Spectroscopy Devices to Fingerprint Commonly Used Construction Materials*. S2-R06B-RR-1, Final Report, Transportation Research Board, Washington, D. C.
88. Zollinger, C.J. *Application of Surface Energy Measurements to Evaluate Moisture Susceptibility of Asphalt and Aggregates*. MSc dissertation, Texas A&M University, Texas, 2005.

APPENDIX A. TEST SITES TEMPERATURE VARIATION

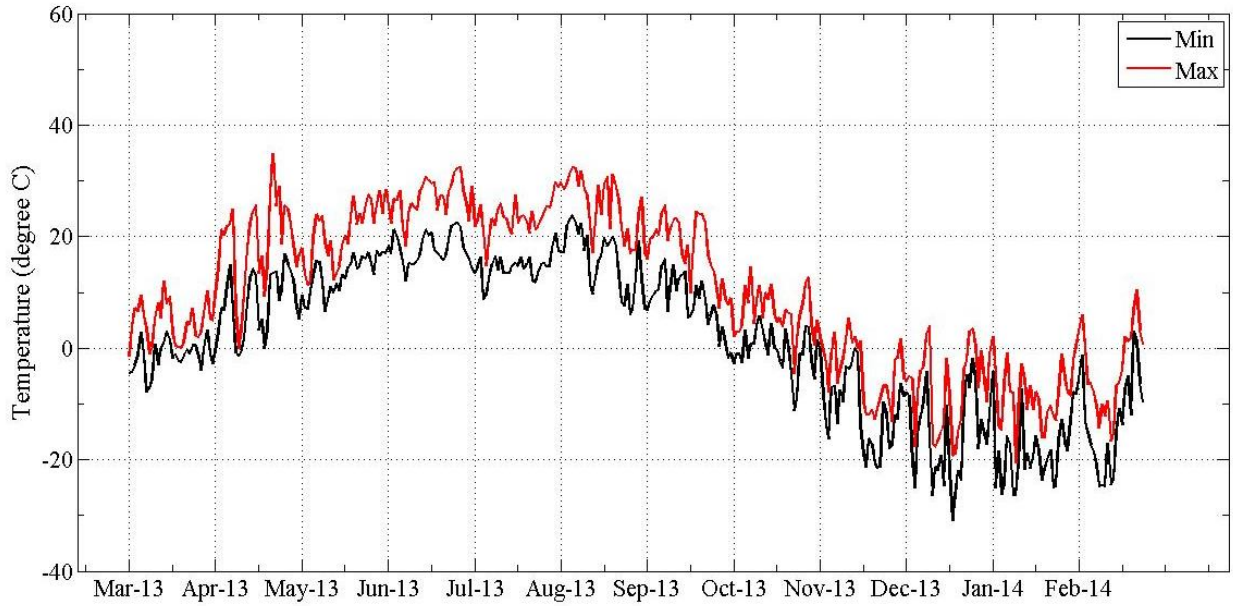


Figure A.1. Ambient temperature for Minnesota test site during the third year after installation.

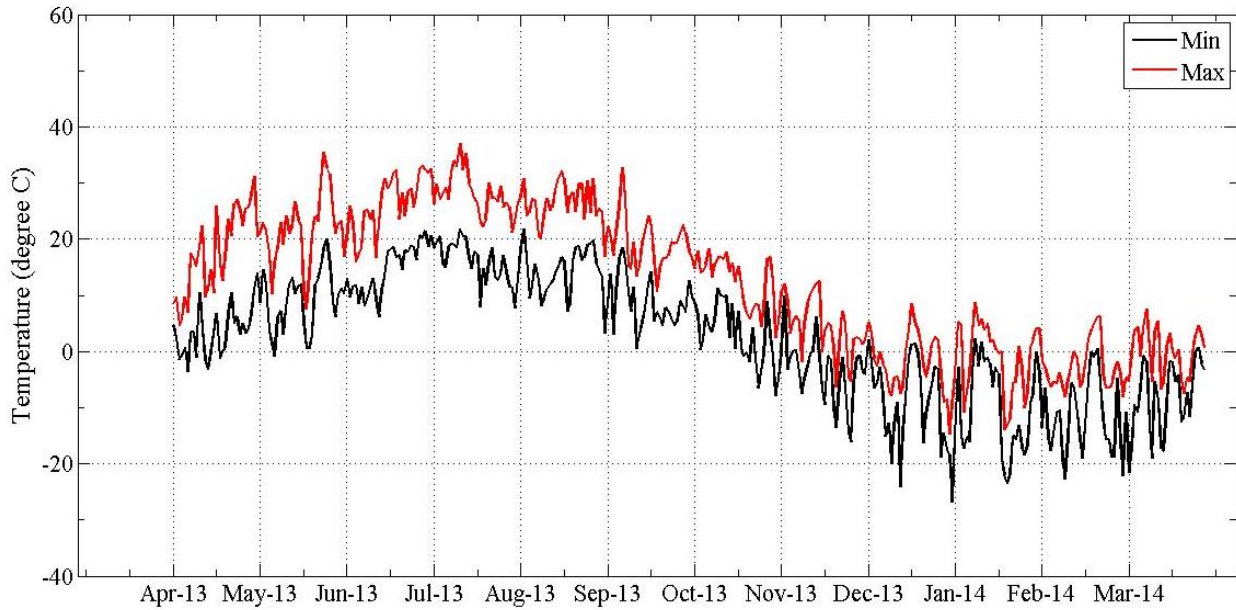


Figure A.2. Ambient temperature for New Hampshire test site during the third year after installation.

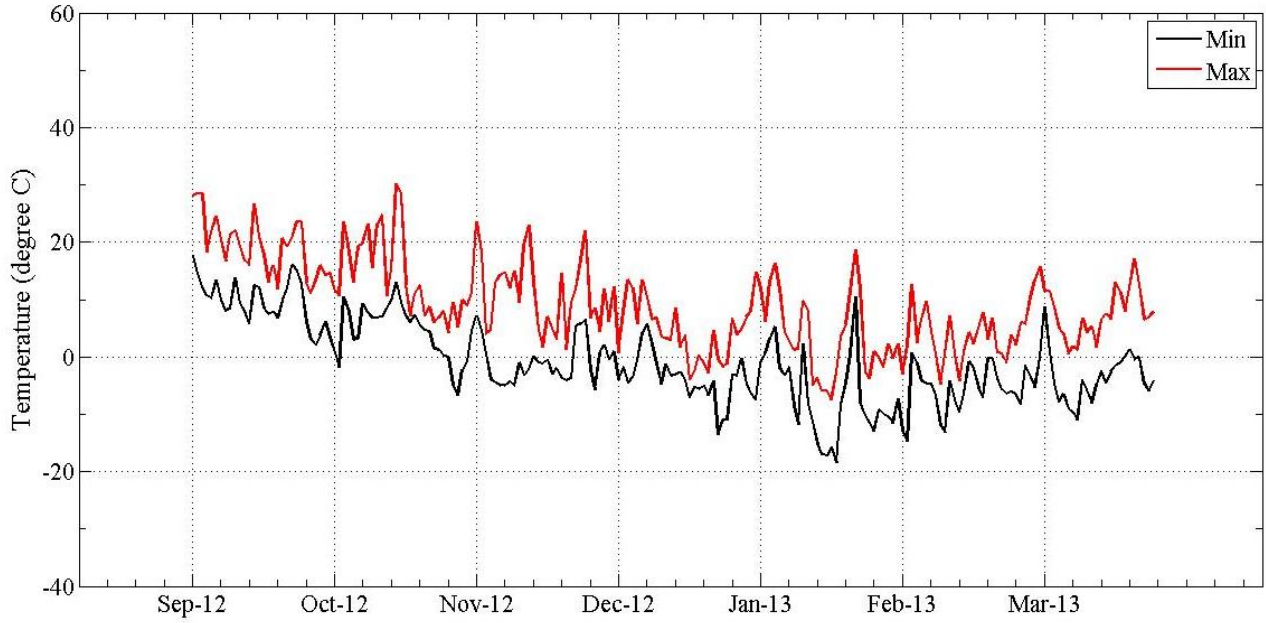


Figure A.3. Ambient temperature for New York test site during the first year after installation.

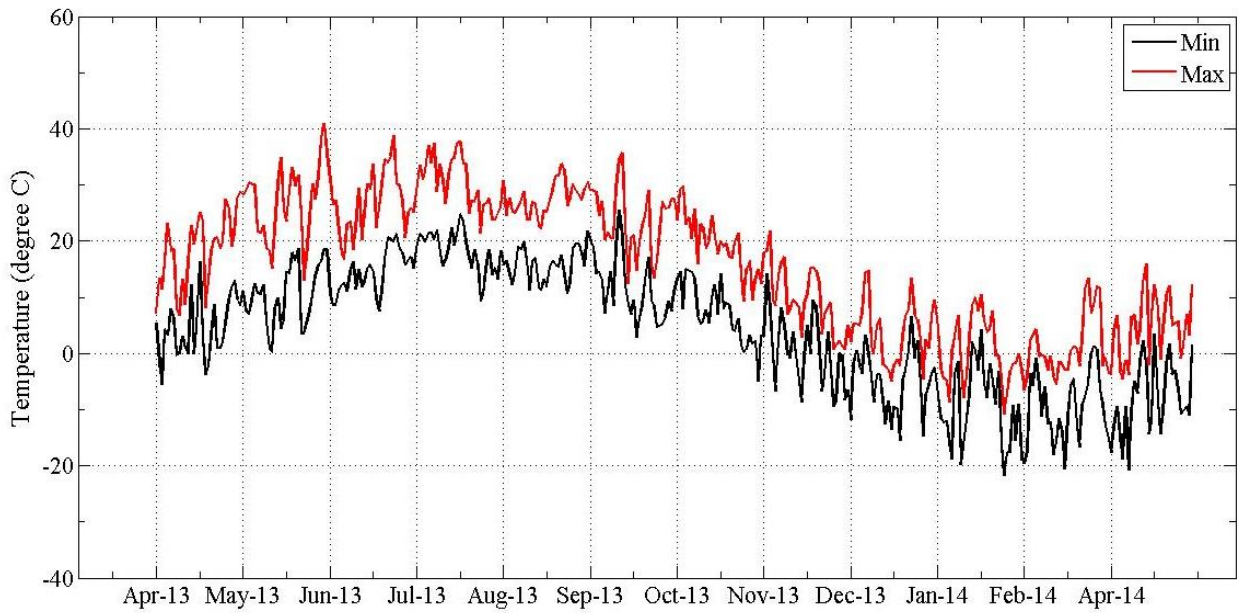


Figure A.4. Ambient temperature for New York test site during the second year after installation.

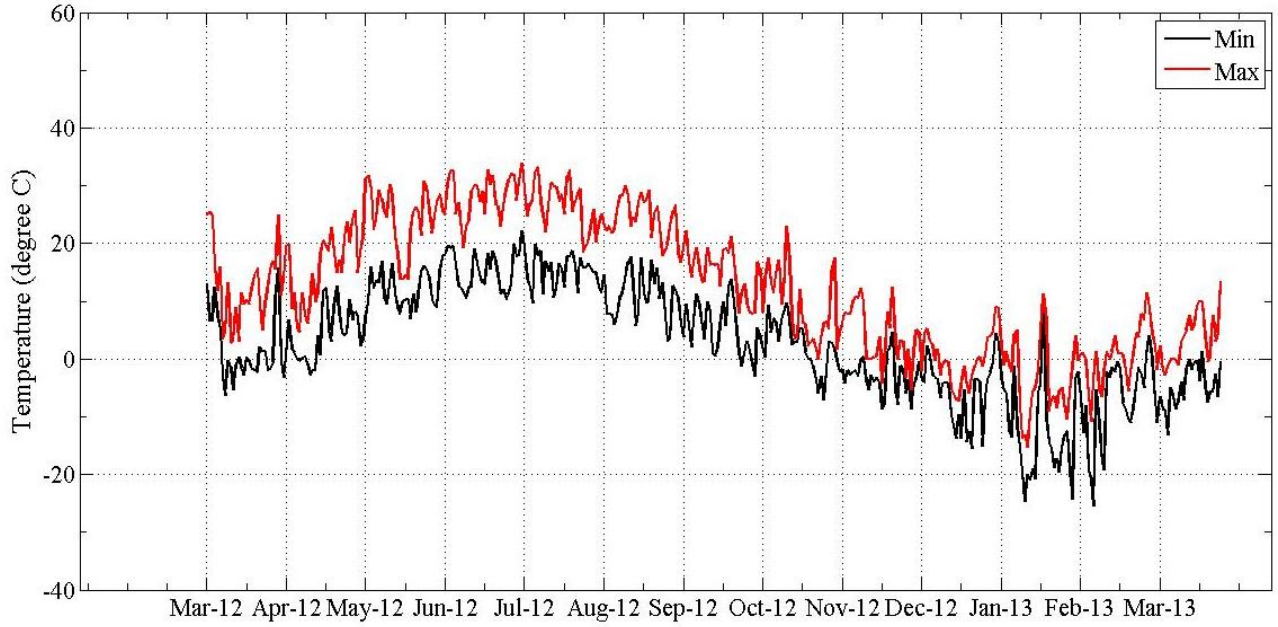


Figure A.5. Ambient temperature for Ontario test site during the second year after installation.

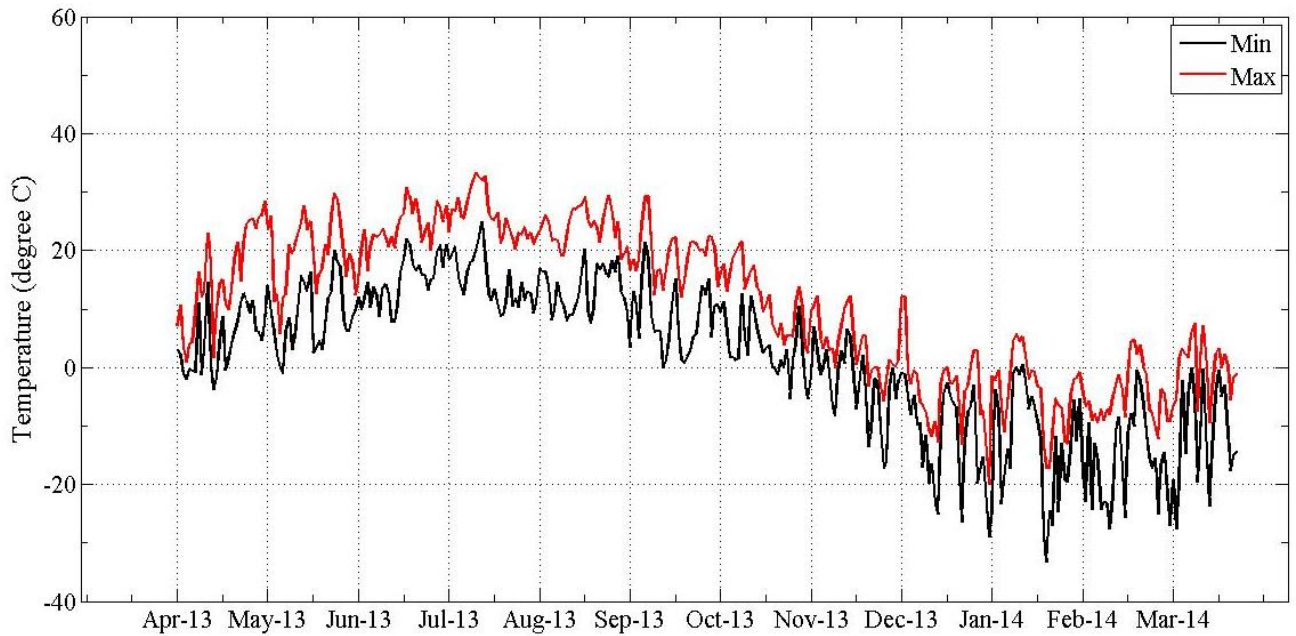


Figure A.6. Ambient temperature for Ontario test site during the third year after installation.

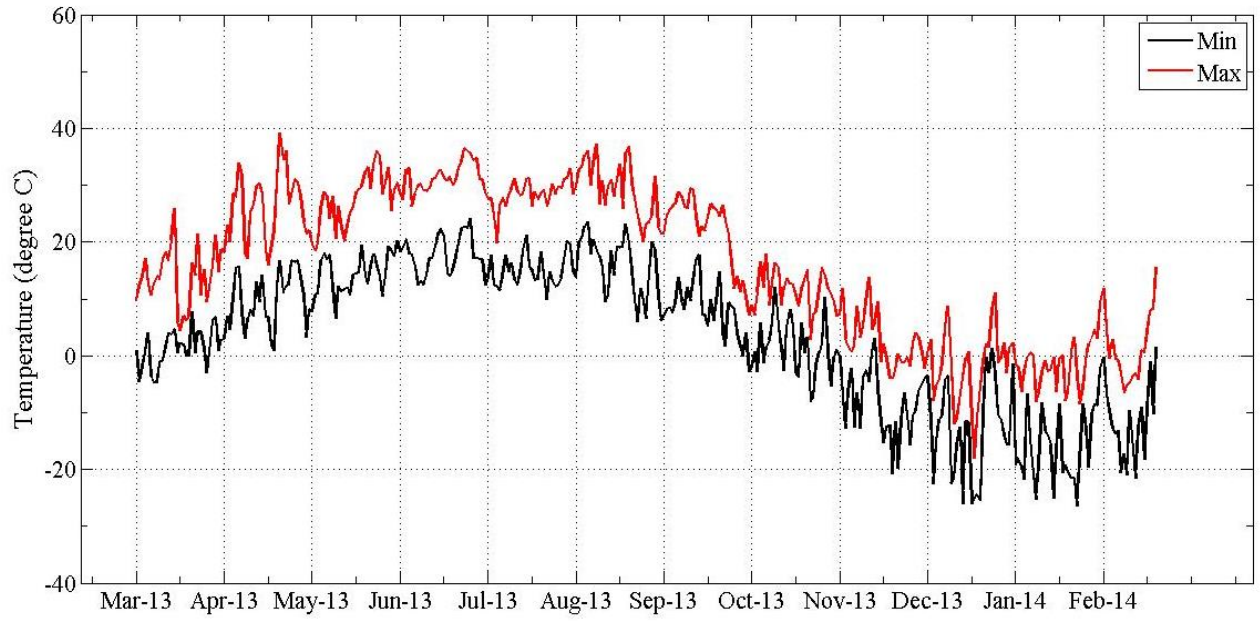
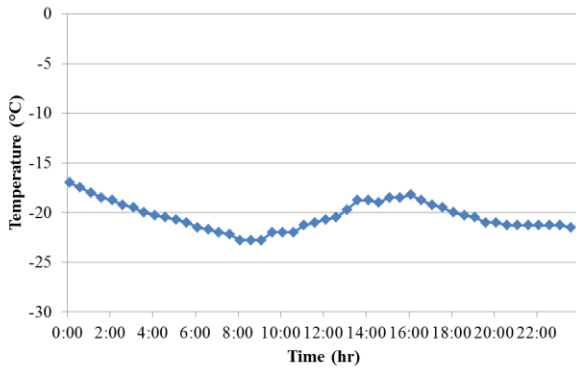
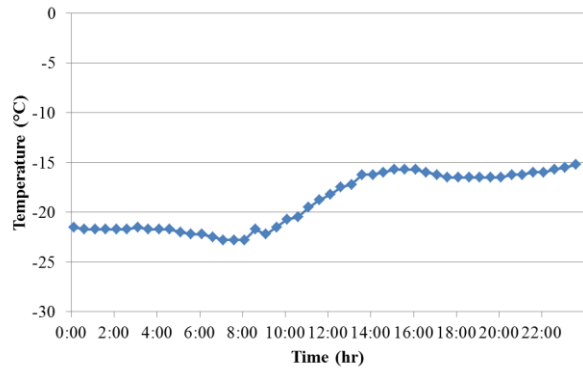


Figure A.7. Ambient temperature for Wisconsin test site during the third year after installation.

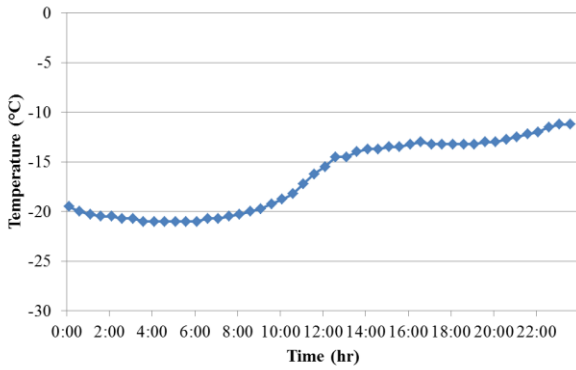
APPENDIX B. DAILY LOW TEMPERATURE VARIATION



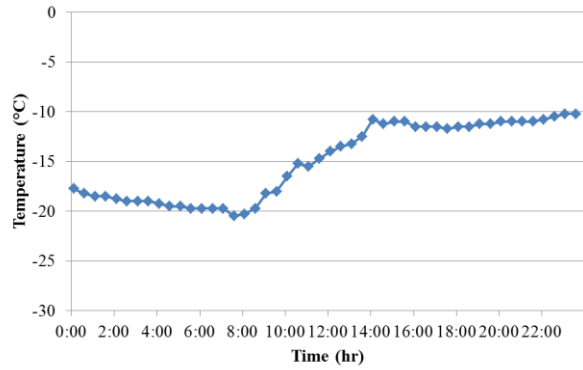
(a) 21st of February 2013



(b) 22nd of January 2013

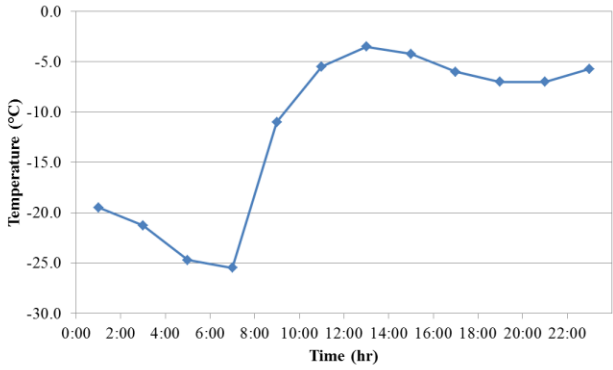


(c) 24th of January 2013

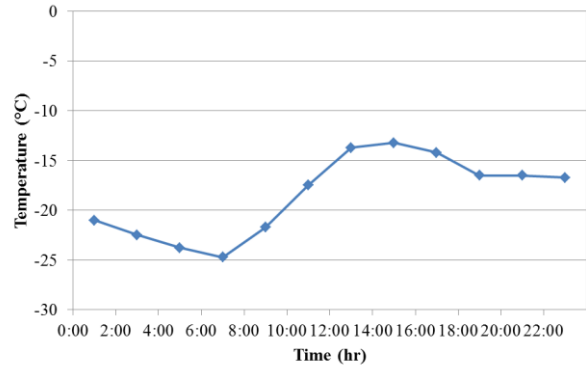


(d) 1st of January 2013

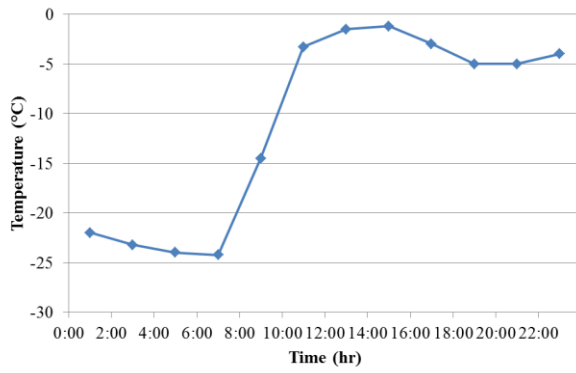
Figure B.1. Daily variation of next four lowest ambient temperatures for Minnesota test site from March 2012 to March 2013.



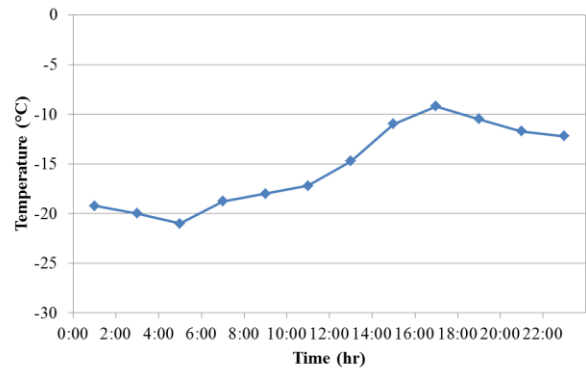
(a) 18th of February 2013



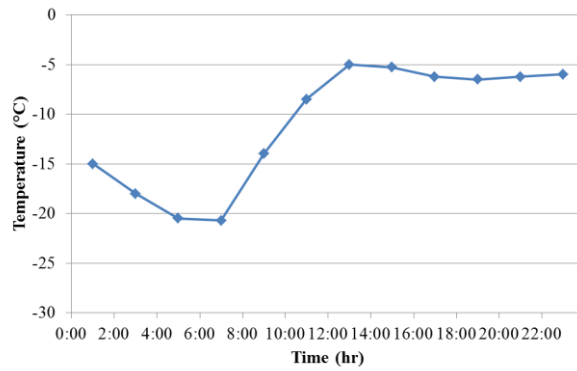
(b) 23rd of January 2013



(c) 10th of February 2013

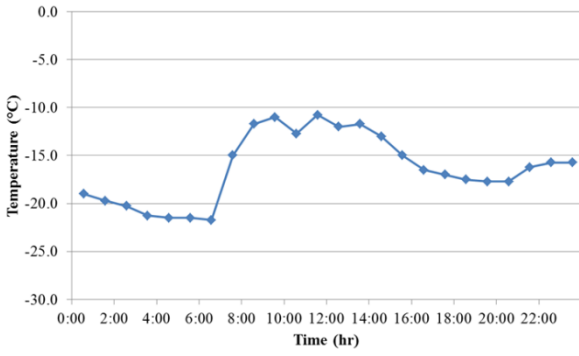


(d) 25th of January 2013

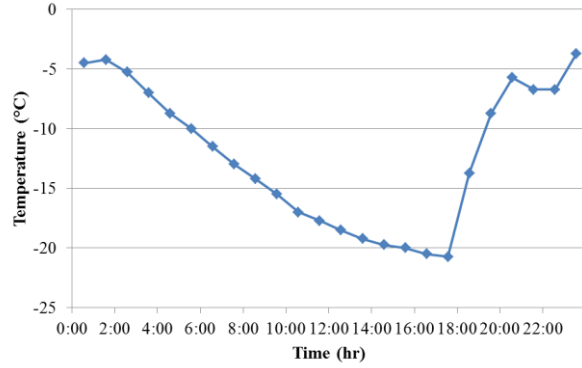


(e) 27th of January 2013

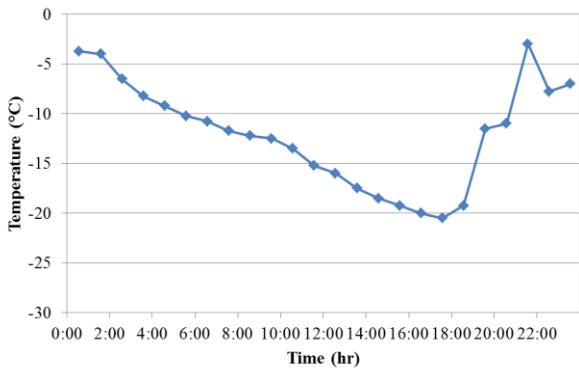
Figure B.2. Daily variation of five lowest ambient temperatures for Ontario test site from March 2012 to March 2013.



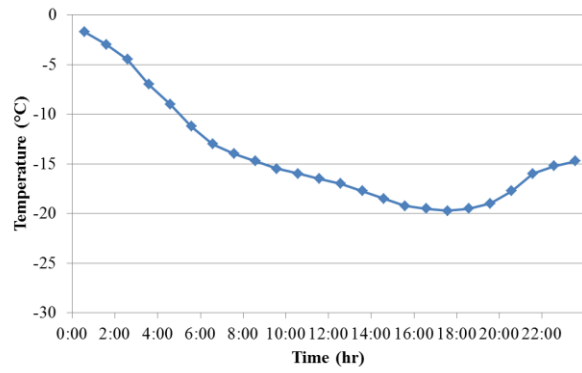
(a) 21st of January 2014



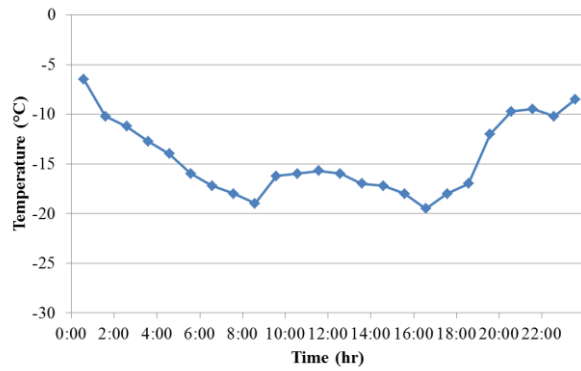
(b) 5th of March 2014



(c) 11th of February 2014

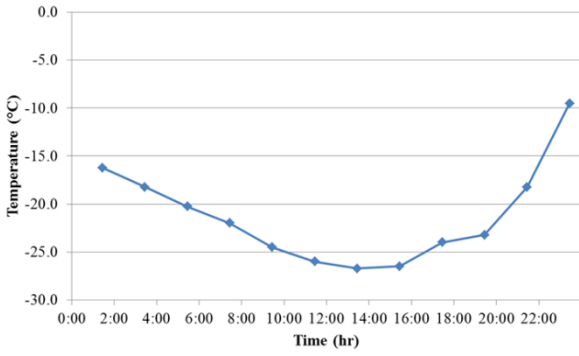


(d) 6th of January 2014

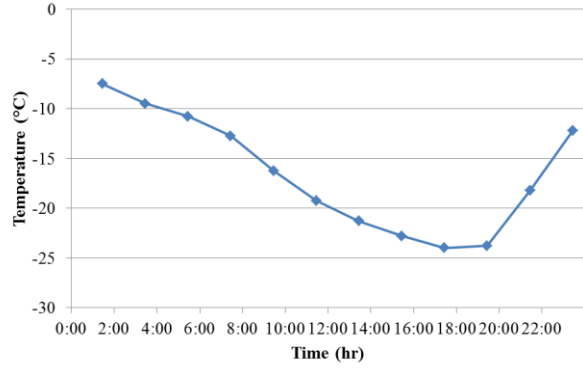


(e) 28th of January 2014

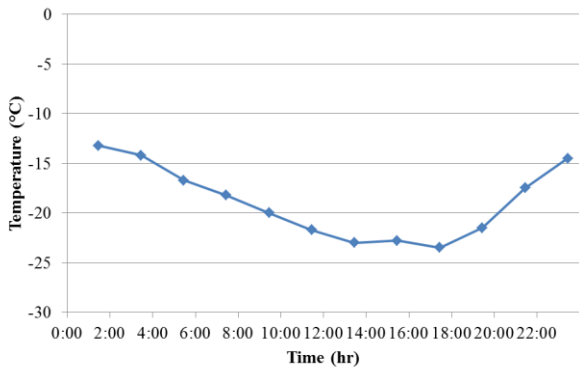
Figure B.3. Daily variation of five lowest ambient temperatures for New York test site from March 2013 to March 2014.



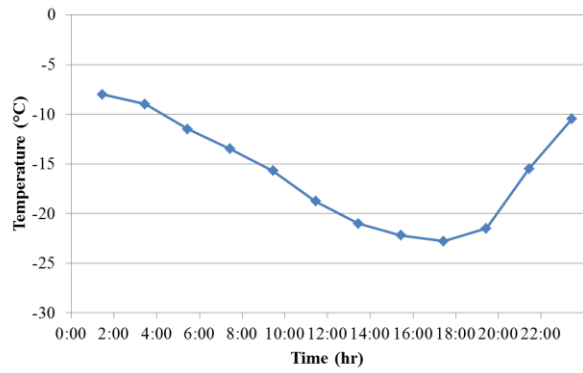
(a) 3rd of January 2014



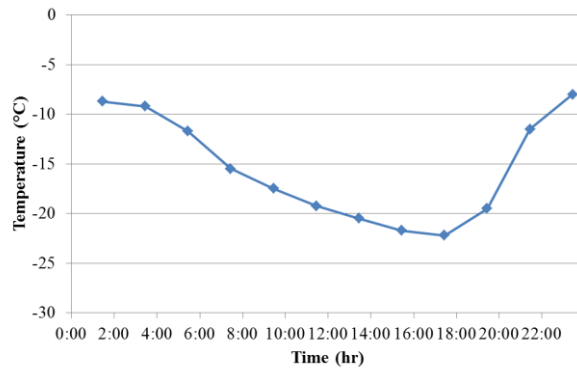
(b) 16th of December 2013



(c) 22nd of January 2014



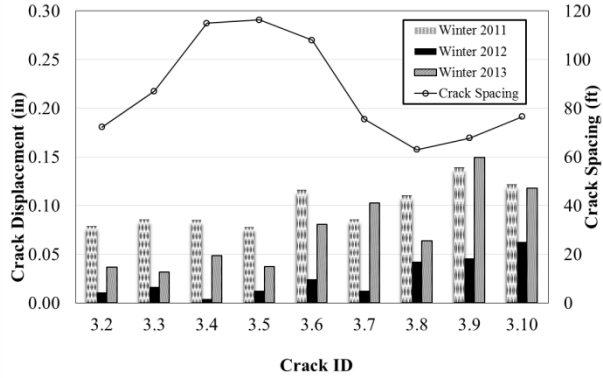
(d) 11th of February 2014



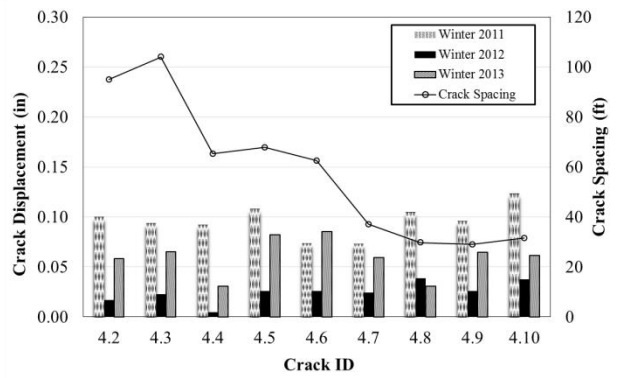
(e) 3rd of March 2014

Figure B.4. Daily variation of five lowest ambient temperatures for New Hampshire test site from March 2013 to March 2014.

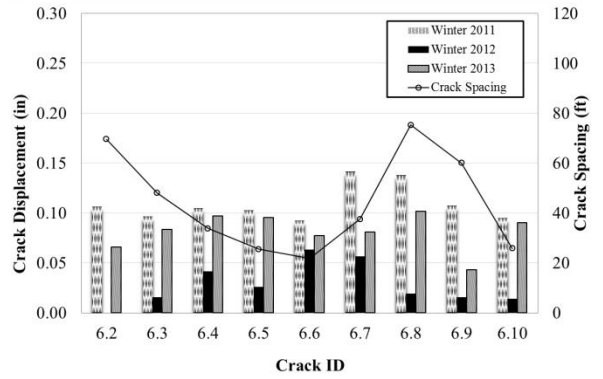
APPENDIX C. CRACK DISPLACEMENT AND SPACING



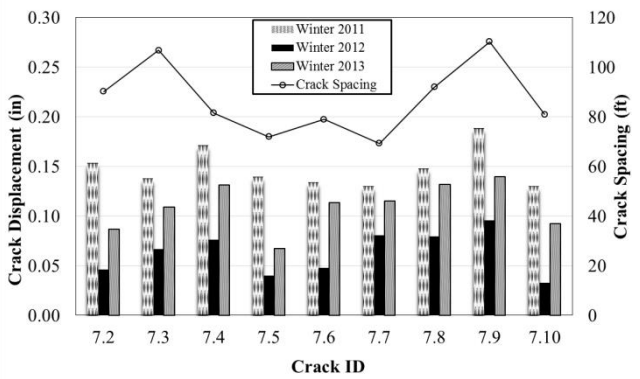
(a) Section 3



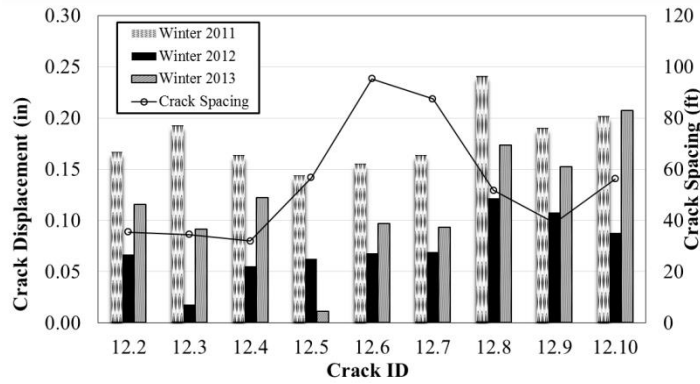
(b) Section 4



(c) Section 6



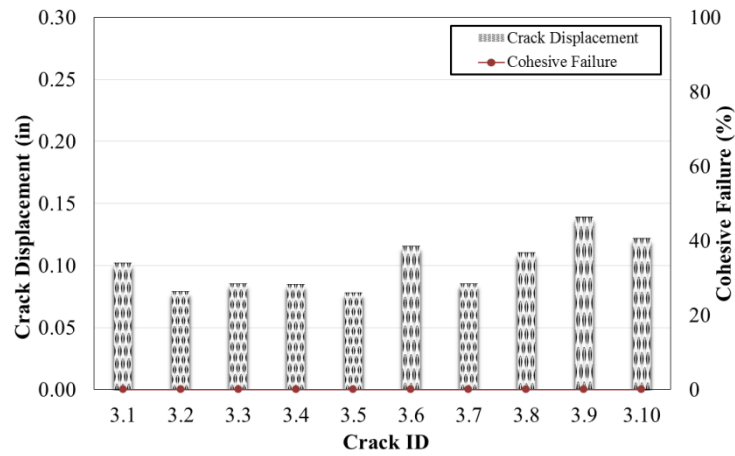
(d) Section 7



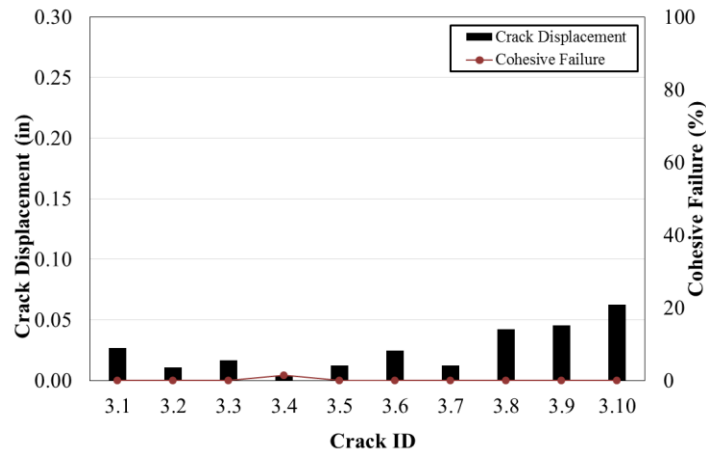
(e) Section 12

Figure C.1. Crack movement and crack spacing.

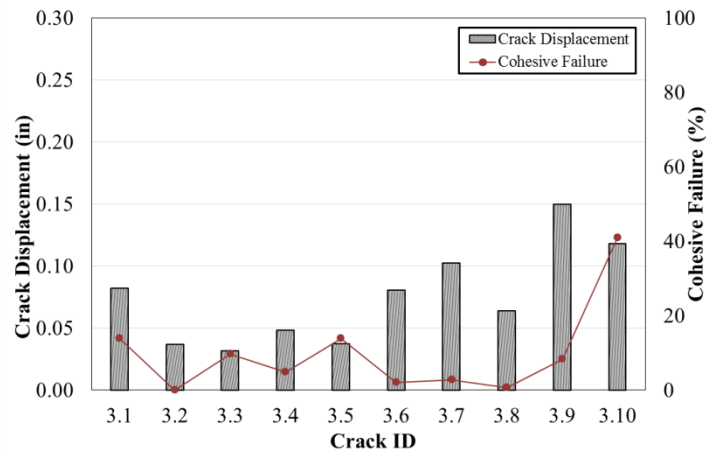
APPENDIX D. CRACK DISPLACEMENT AND COHESIVE FAILURE



(a) Winter 2011

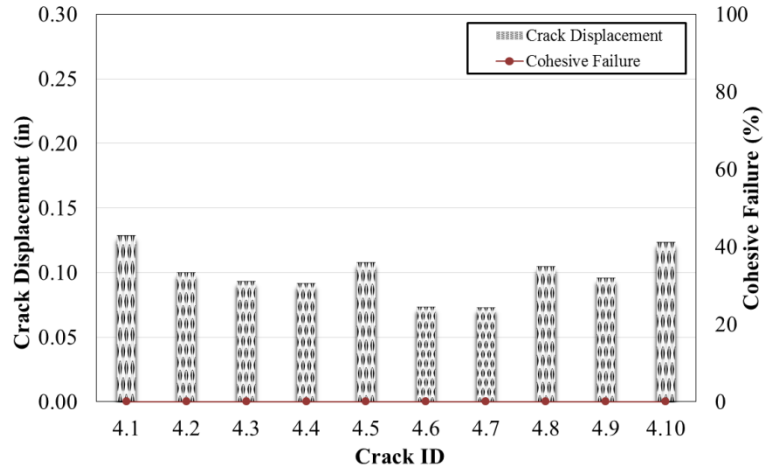


(b) Winter 2012

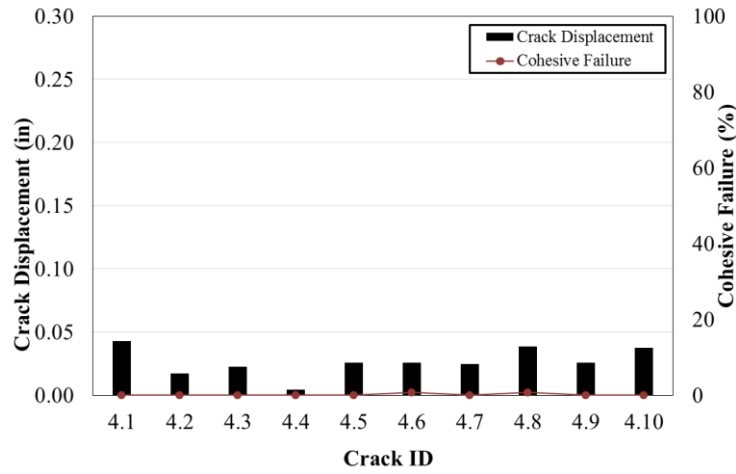


(c) Winter 2013

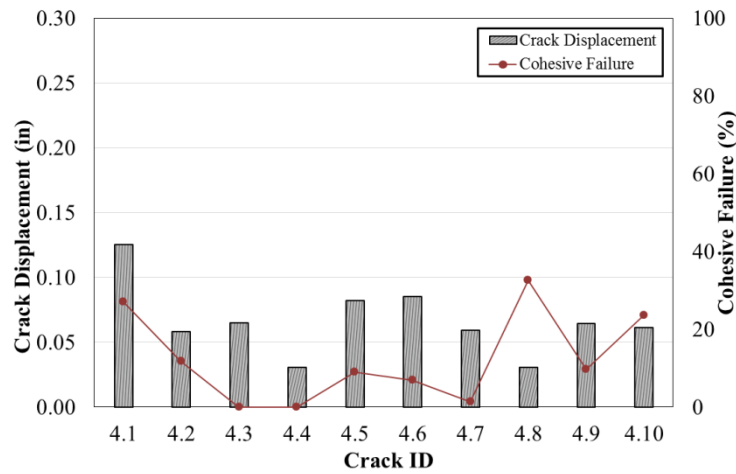
Figure D.1. Cohesive failure for each crack of Section 3 for different years.



(a) Winter 2011

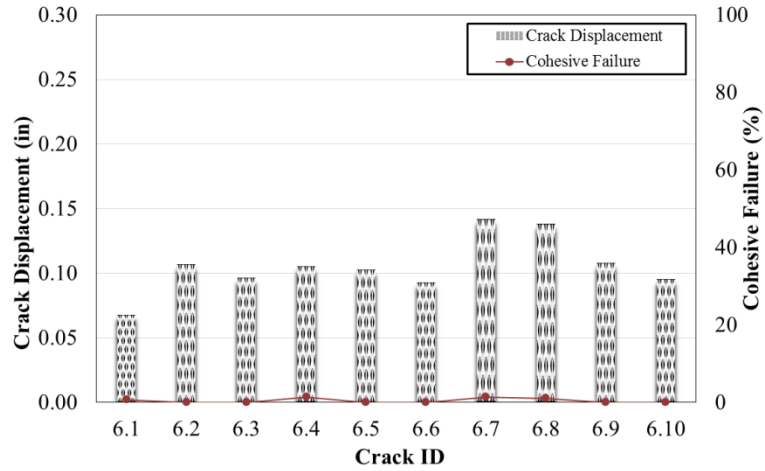


(b) Winter 2012

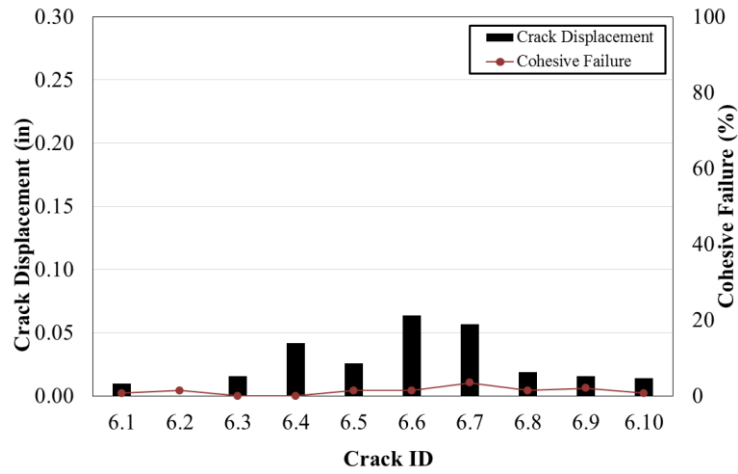


(c) Winter 2013

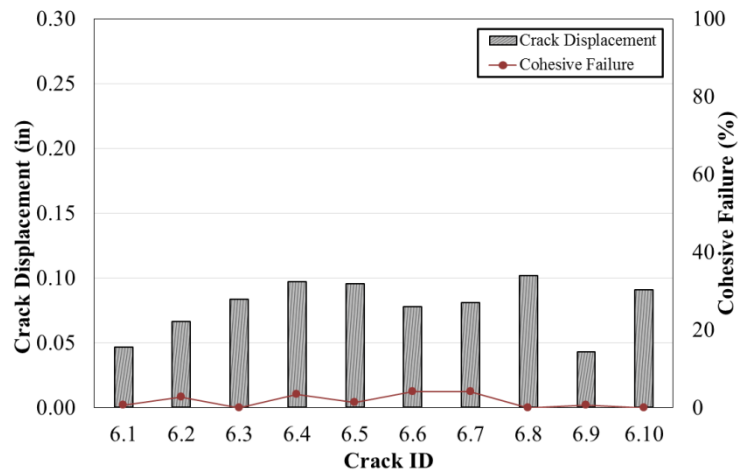
Figure D.2. Cohesive failure for each crack of Section 4 for different years.



(a) Winter 2011

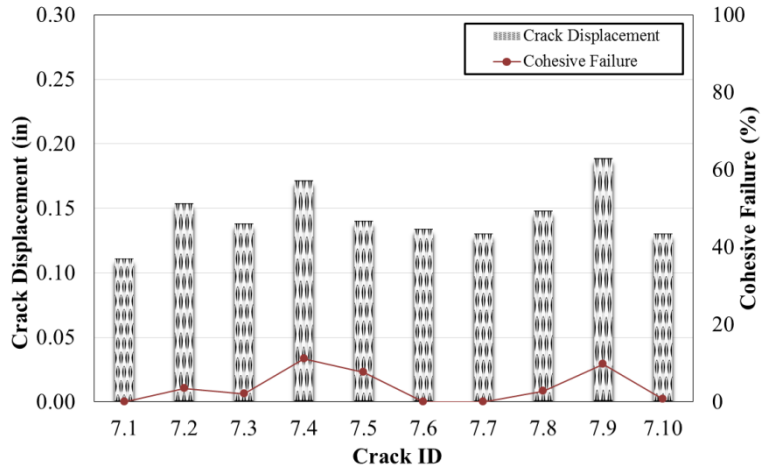


(b) Winter 2012

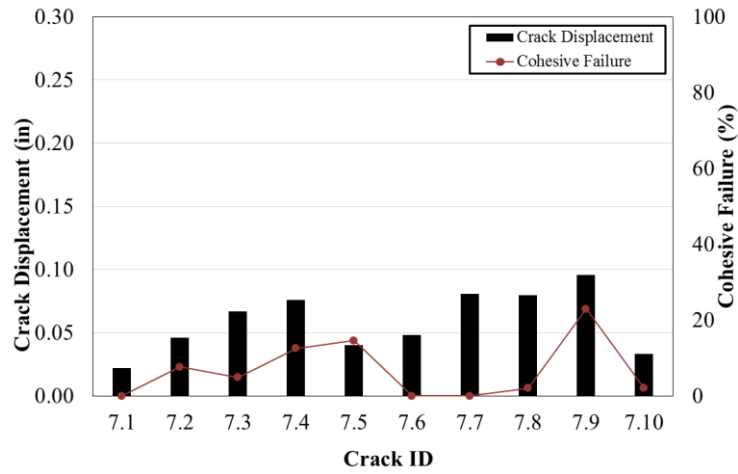


(c) Winter 2013

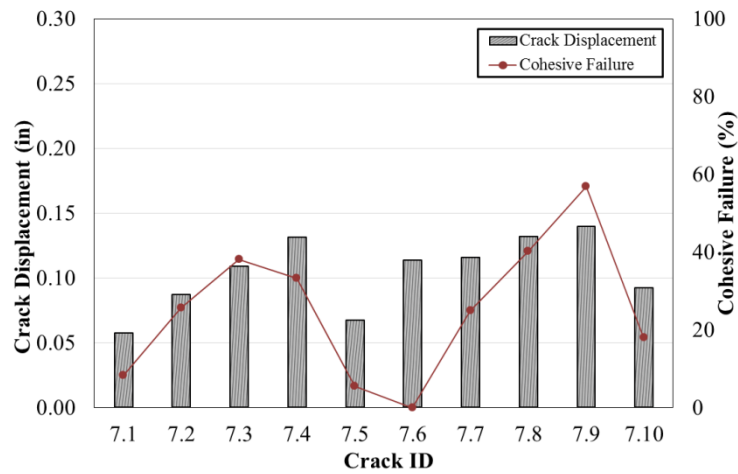
Figure D.3. Cohesive failure for each crack of Section 6 for different years.



(a) Winter 2011

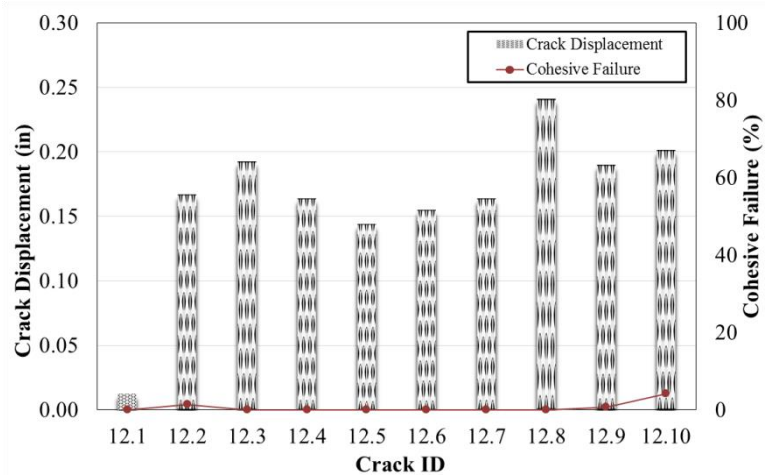


(b) Winter 2012

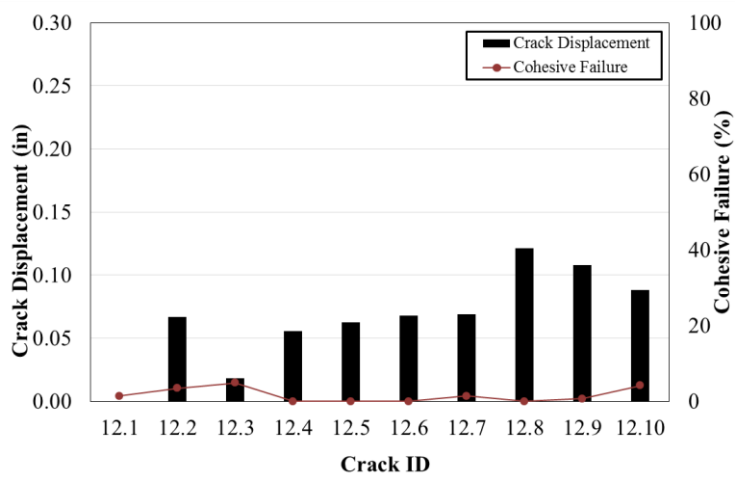


(c) Winter 2013

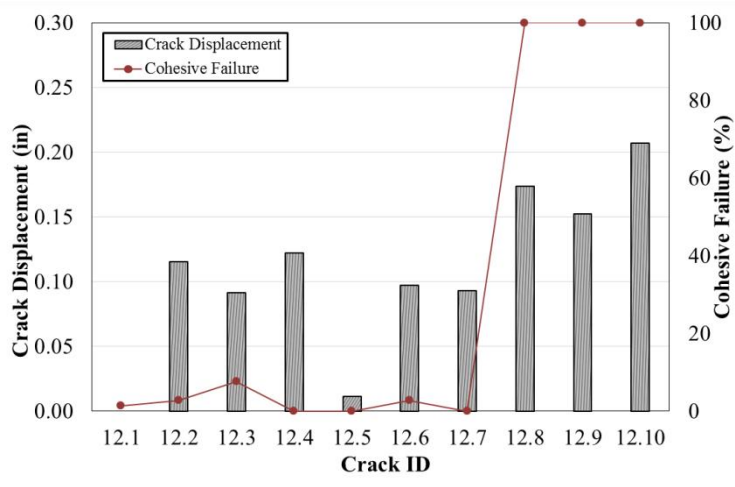
Figure D.4. Cohesive failure for each crack of Section 7 for different years.



(a) Winter 2011



(b) Winter 2012



(c) Winter 2013

Figure D.5. Cohesive failure for each crack of Section 4 for different years.

APPENDIX E. CSBRR STIFFNESS AND ACR AT 240S AT DIFFERENT AGING CONDITIONS

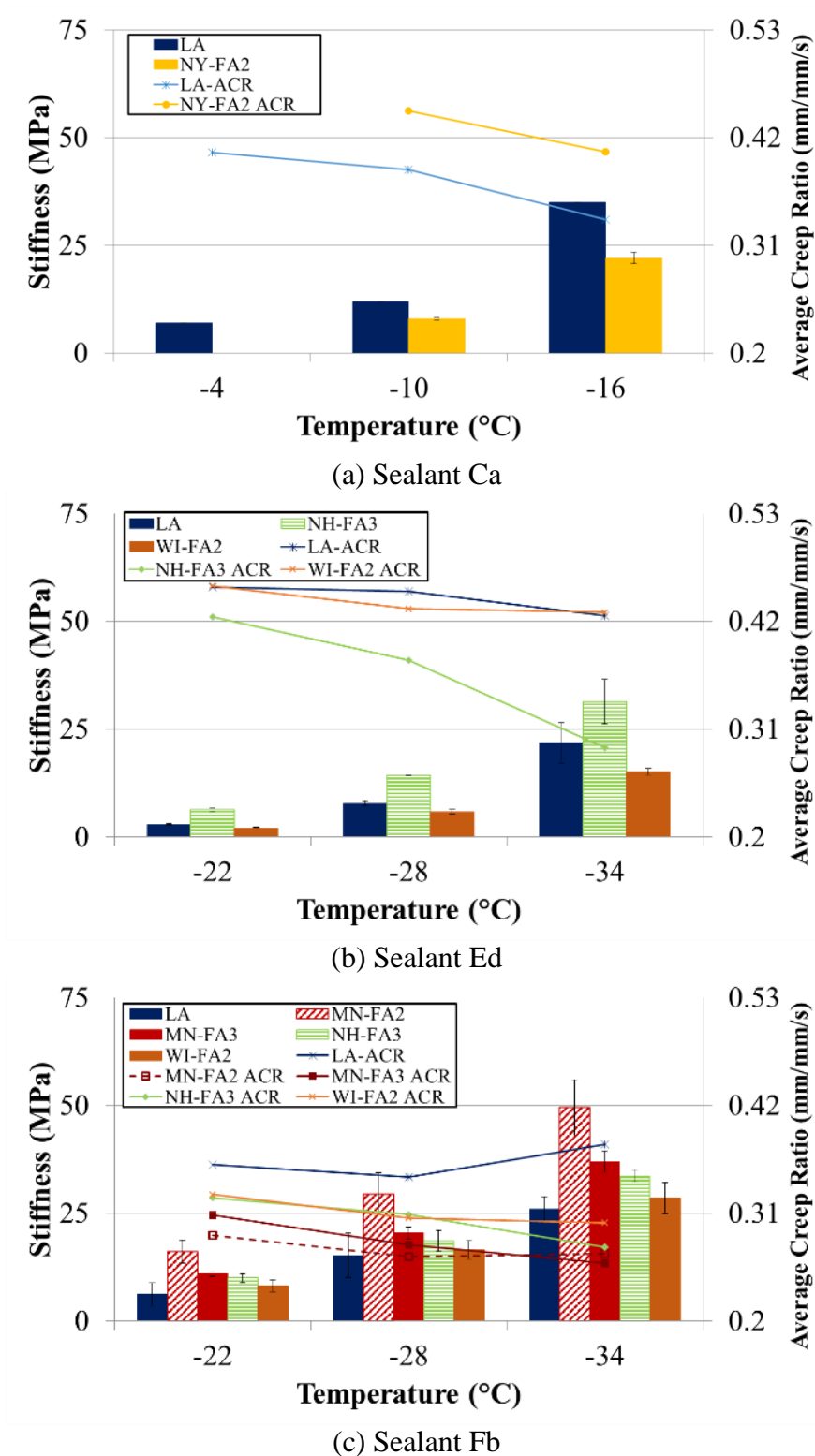
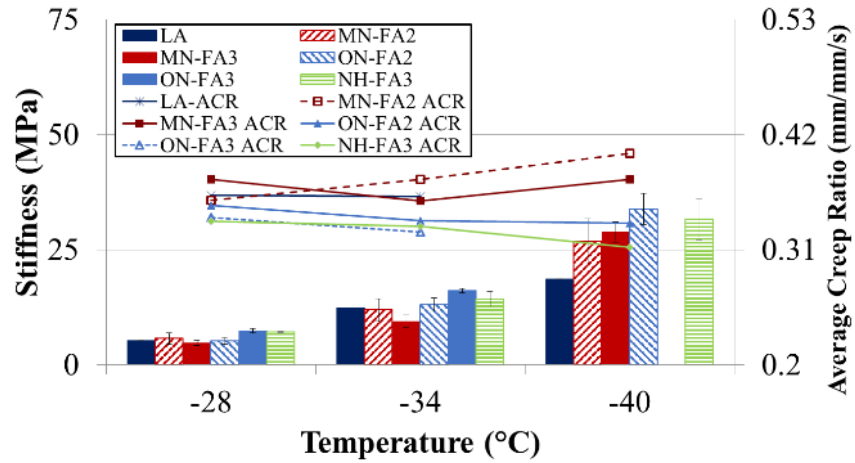
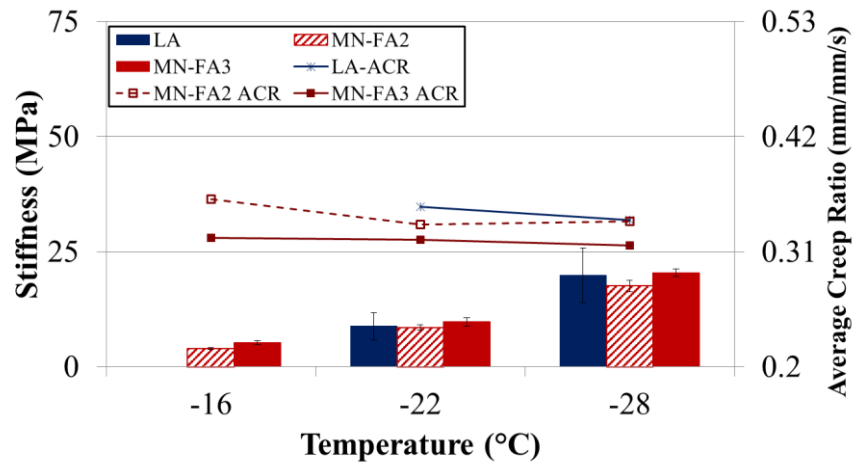


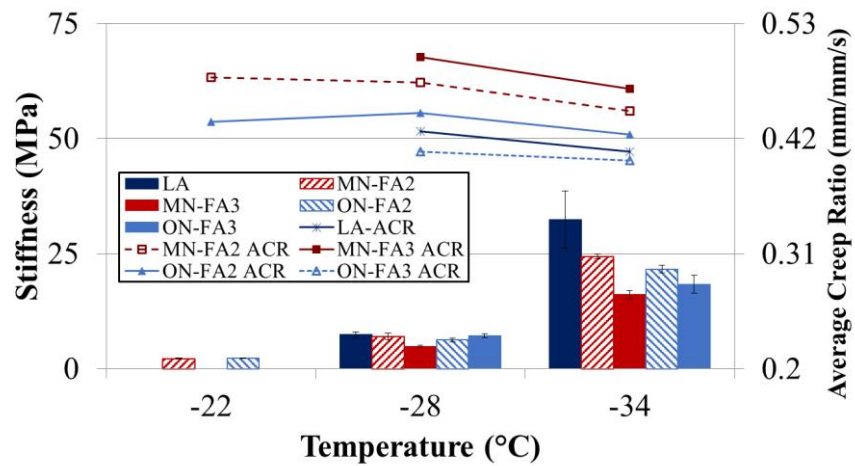
Figure E.1. CSBRR stiffness and average creep ratio (ACR) at 240 seconds at different aging conditions tested at three different temperatures.



(d) Sealant Gd

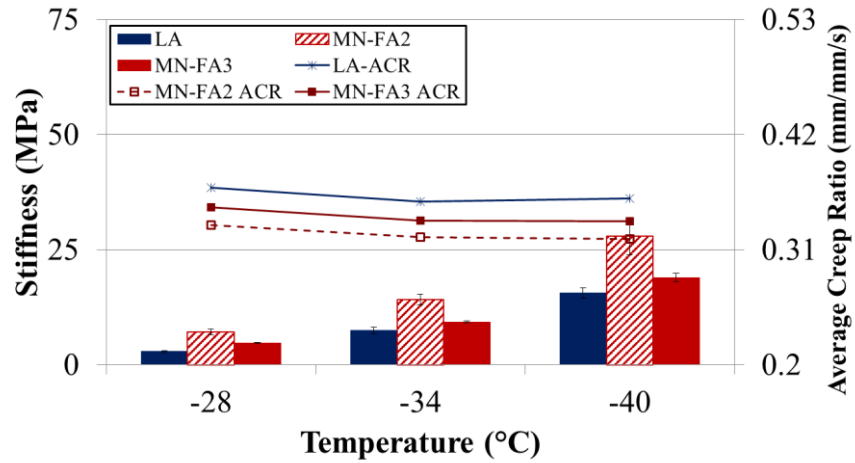


(e) Sealant Hb

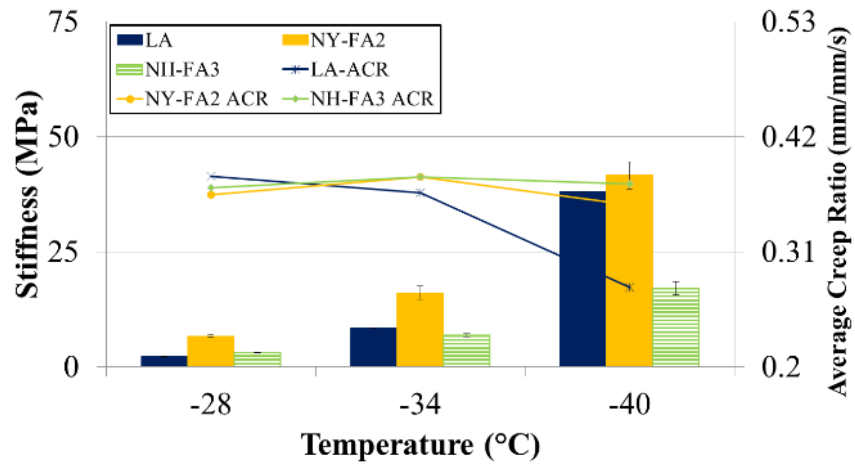


(f) Sealant Mb

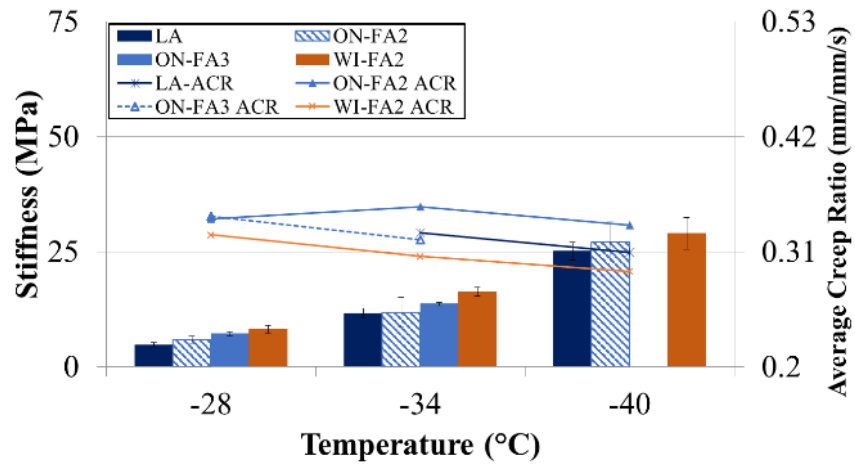
Figure E.1 (continued)



(g) Sealant Nb

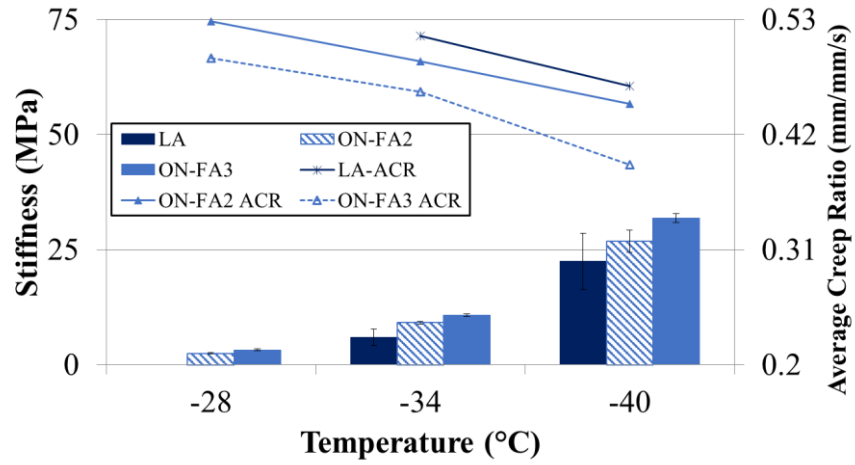


(h) Sealant Ob



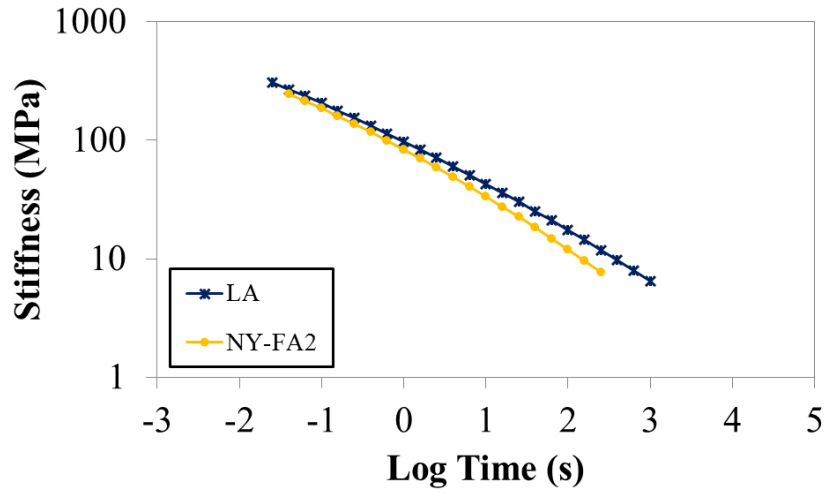
(i) Sealant Pd

Figure E.1 (continued)

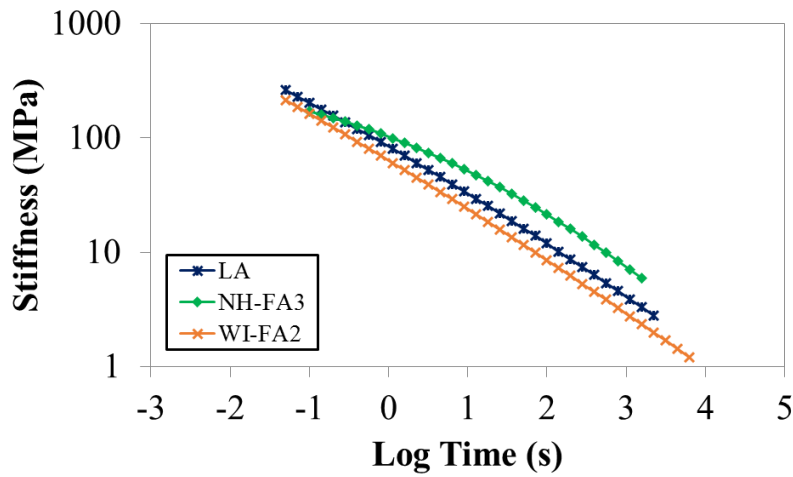


(j) Sealant Sd
Figure E.1 (continued)

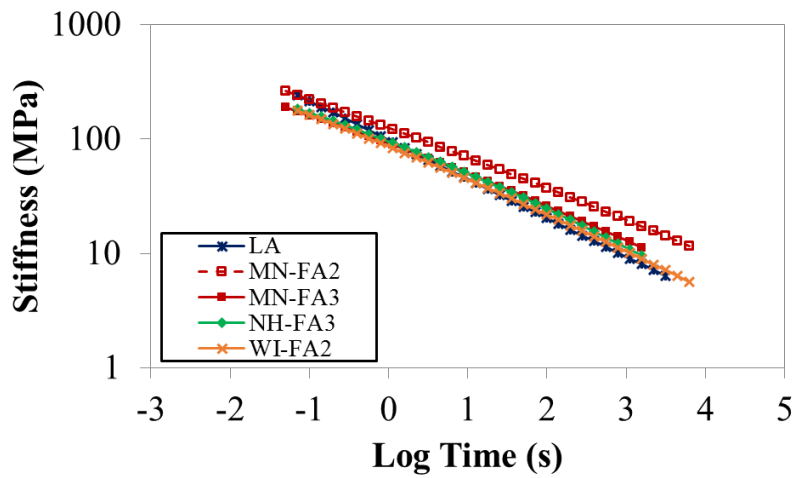
APPENDIX F. CSBBR STIFFNESS MASTER CURVES



(a) Sealant Ca

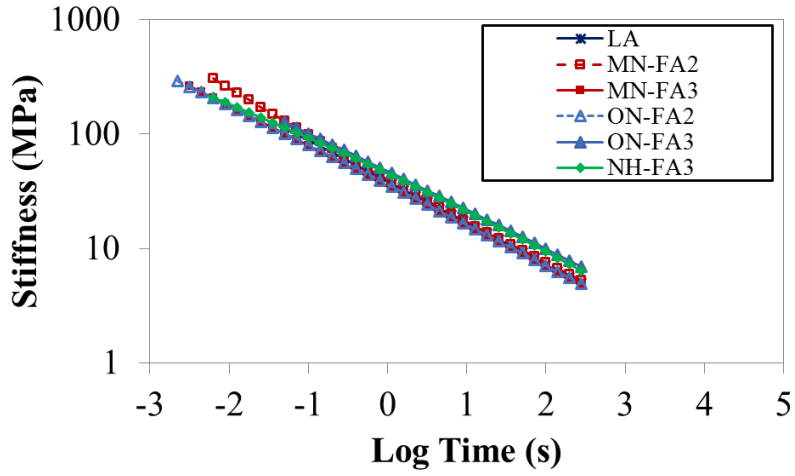


(b) Sealant Ed

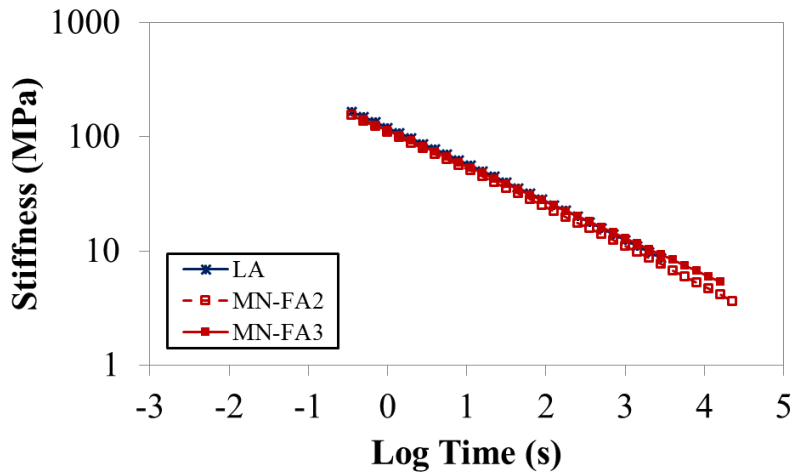


(c) Sealant Fb

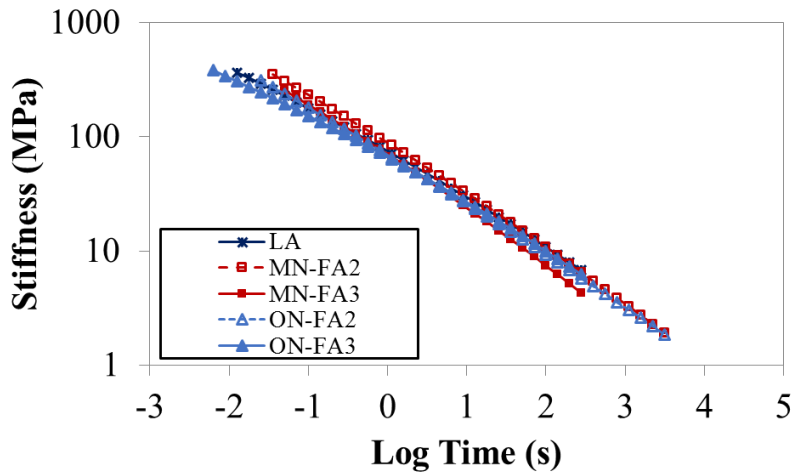
Figure F.1. CSBBR stiffness master curves comparing laboratory-aged samples with field-aged (FAs) samples.



(d) Sealant Gd

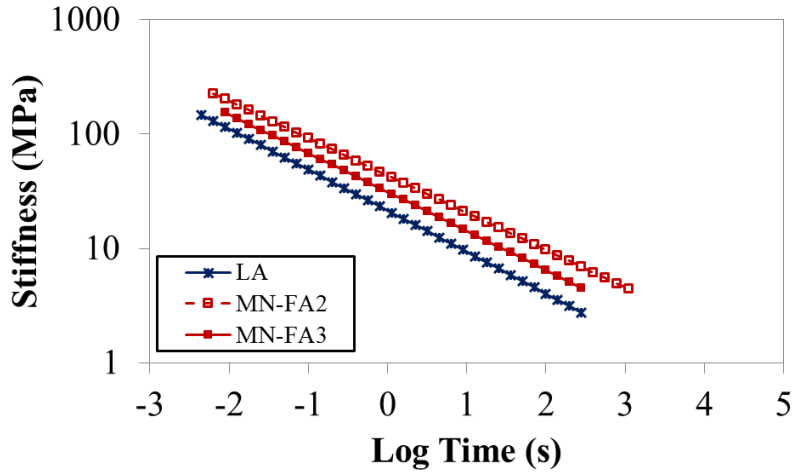


(e) Sealant Hb

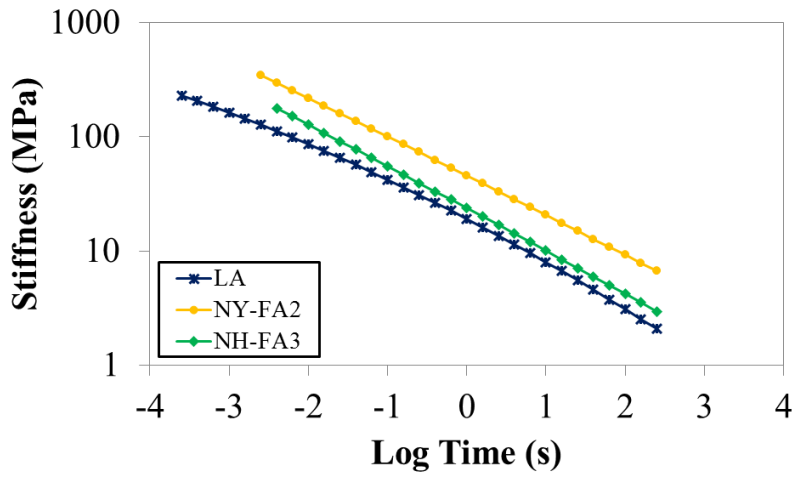


(f) Sealant Mb

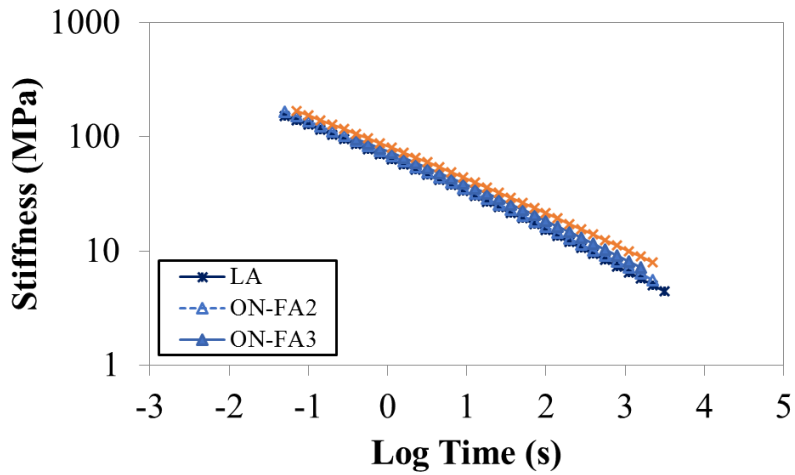
Figure F.1 (continued)



(g) Sealant Nb

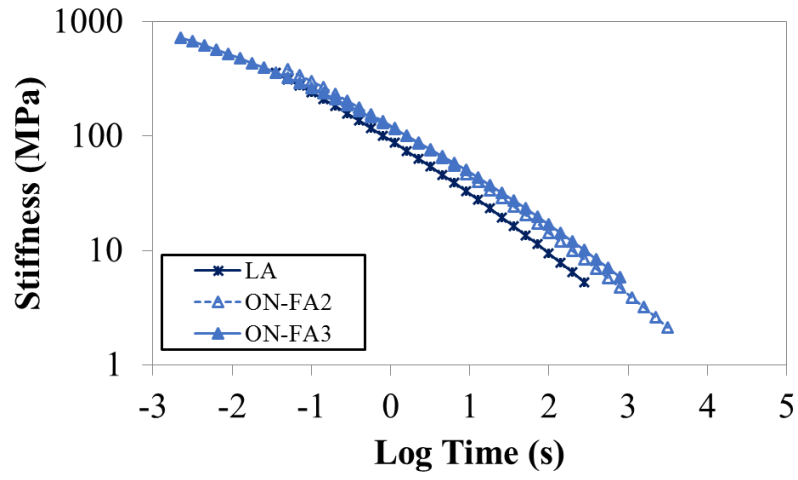


(h) Sealant Ob



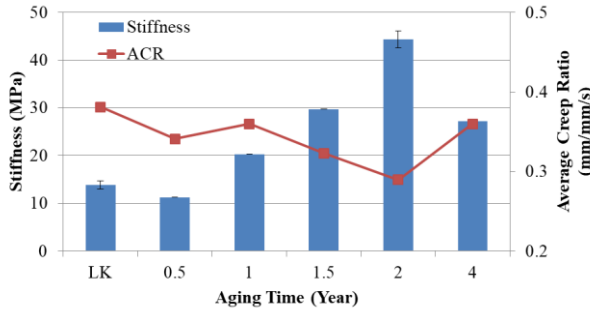
(i) Sealant Pd

Figure F.1 (continued)

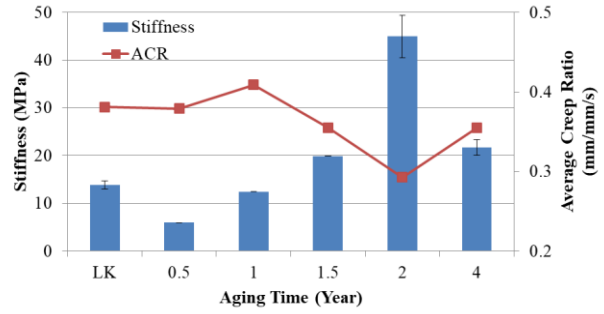


(j) Sealant Sd
Figure F.1 (continued)

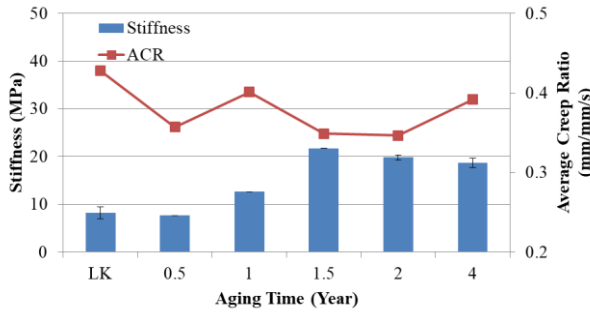
APPENDIX G. CSBBR STIFFNESS AND ACR VARIATION WITH AGING TIME



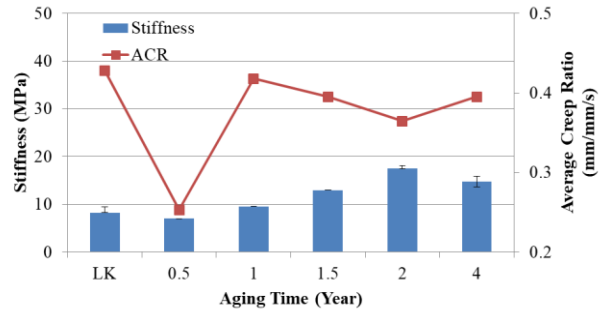
(a) Sealant Da – Crust , tested at -28°C



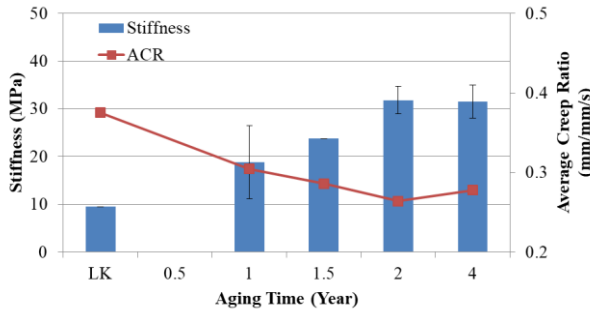
(b) Sealant Da – Bottom , tested at -28°C



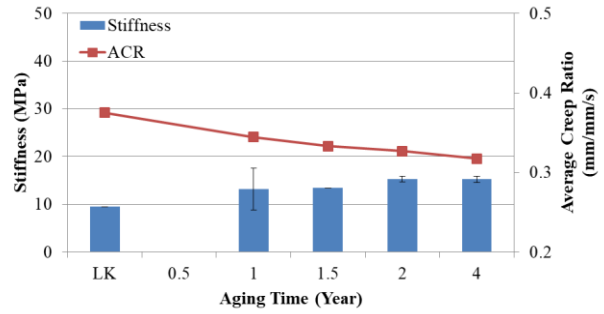
(c) Sealant Ed – Crust , tested at -28°C



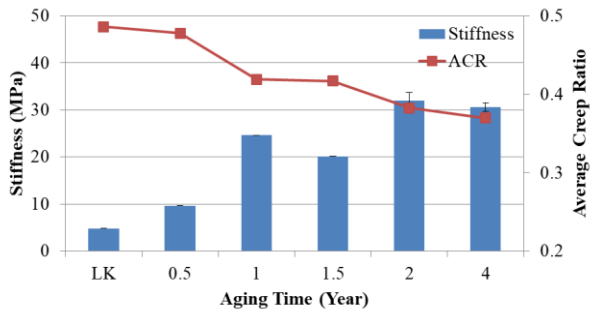
(d) Sealant Ed – Bottom , tested at -28°C



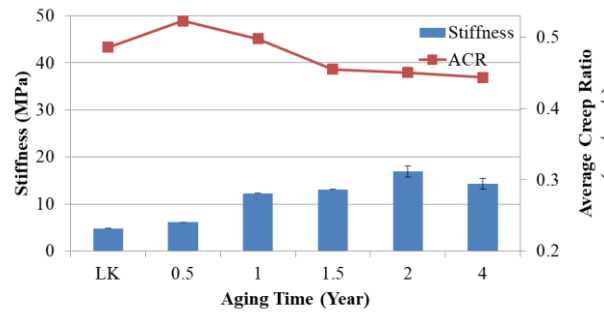
(e) Sealant Fb – Crust , tested at -28°C



(f) Sealant Fb – Bottom , tested at -28°C

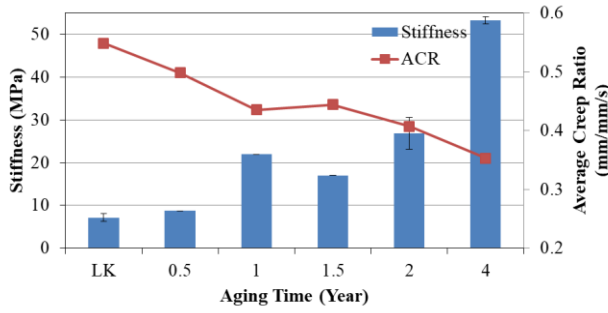


(g) Sealant Jd – Crust , tested at -40°C

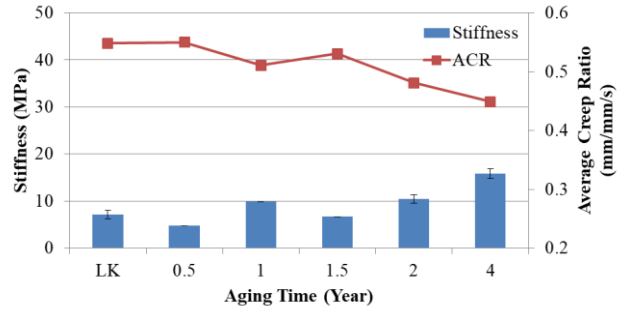


(h) Sealant Jd – Bottom , tested at -40°C

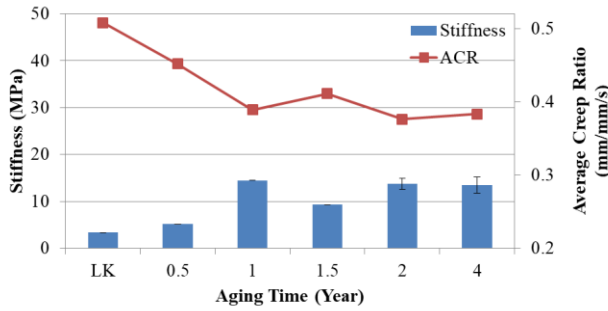
Figure G.1. Stiffness and ACR at 240 seconds at various test temperatures changing with aging.



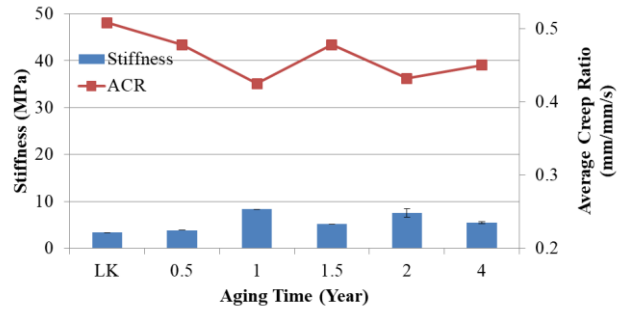
(i) Sealant Kc – Crust , tested at -34°C



(j) Sealant Kc – Bottom , tested at -34°C



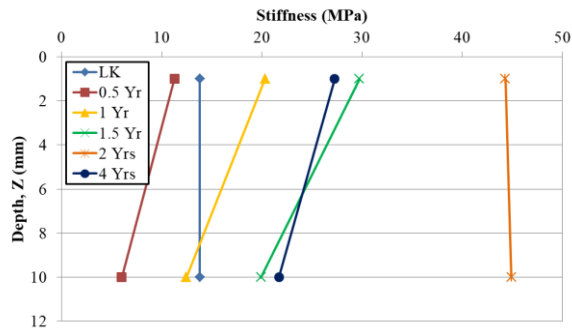
(k) Sealant Mb – Crust , tested at -28°C



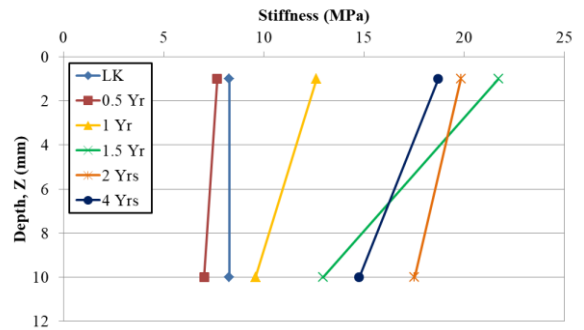
(l) Sealant Mb – Bottom , tested at -28°C

Figure G.1 (continued)

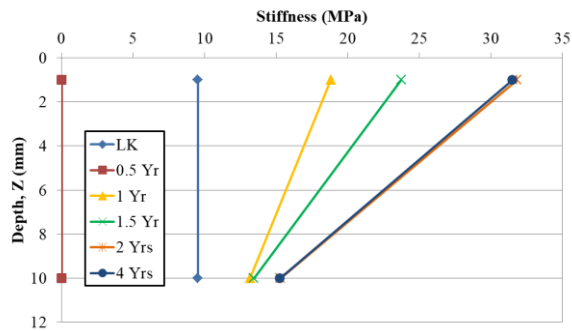
APPENDIX H. CSBBR STIFFNESS CHANGING WITH THE SEALANT DEPTH



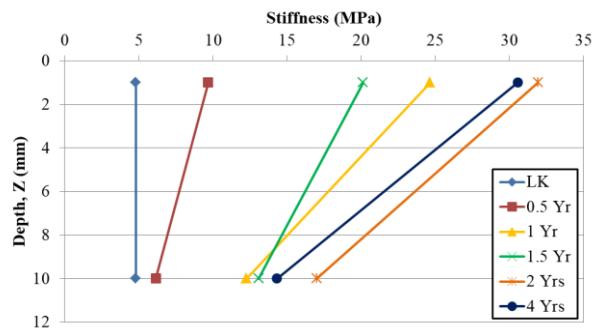
(a) Sealant Da tested at -28°C



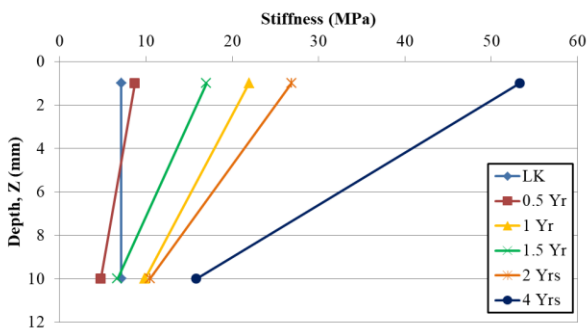
(c) Sealant Ed tested at -28°C



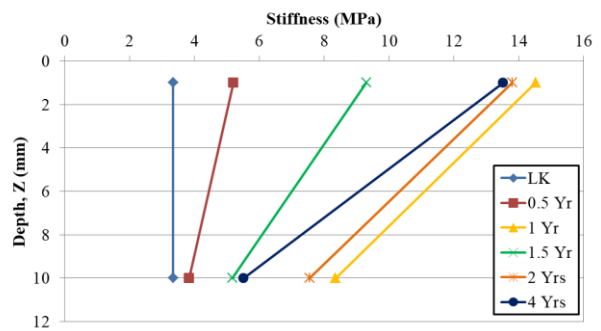
(e) Sealant Fb tested at -28°C



(g) Sealant Jd tested at -40°C



(i) Sealant Kc tested at -34°C



(k) Sealant Mb tested at -28°C

Figure H.1. Stiffness profile at 240 seconds at various aging condition.